frontiers | Research Topics

Case reports in pulmonary medicine 2023

Edited by
Talat Kilic and Santi Nolasco

Published in
Frontiers in Medicine

ISSN 1664-8714
ISBN 978-2-8325-6029-7
DOI 10.3389/978-2-8325-6029-7

About Frontiers

Frontiers is more than just an open access publisher of scholarly articles: it is a pioneering approach to the world of academia, radically improving the way scholarly research is managed. The grand vision of Frontiers is a world where all people have an equal opportunity to seek, share and generate knowledge. Frontiers provides immediate and permanent online open access to all its publications, but this alone is not enough to realize our grand goals.

Frontiers journal series

The Frontiers journal series is a multi-tier and interdisciplinary set of open-access, online journals, promising a paradigm shift from the current review, selection and dissemination processes in academic publishing. All Frontiers journals are driven by researchers for researchers; therefore, they constitute a service to the scholarly community. At the same time, the *Frontiers journal series* operates on a revolutionary invention, the tiered publishing system, initially addressing specific communities of scholars, and gradually climbing up to broader public understanding, thus serving the interests of the lay society, too.

Dedication to quality

Each Frontiers article is a landmark of the highest quality, thanks to genuinely collaborative interactions between authors and review editors, who include some of the world's best academicians. Research must be certified by peers before entering a stream of knowledge that may eventually reach the public - and shape society; therefore, Frontiers only applies the most rigorous and unbiased reviews. Frontiers revolutionizes research publishing by freely delivering the most outstanding research, evaluated with no bias from both the academic and social point of view. By applying the most advanced information technologies, Frontiers is catapulting scholarly publishing into a new generation.

What are Frontiers Research Topics?

Frontiers Research Topics are very popular trademarks of the *Frontiers journals series*: they are collections of at least ten articles, all centered on a particular subject. With their unique mix of varied contributions from Original Research to Review Articles, Frontiers Research Topics unify the most influential researchers, the latest key findings and historical advances in a hot research area.

Find out more on how to host your own Frontiers Research Topic or contribute to one as an author by contacting the Frontiers editorial office: frontiersin.org/about/contact

Case reports in pulmonary medicine 2023

Topic editors
Talat Kilic — İnönü University, Türkiye
Santi Nolasco — University of Catania, Italy

Citation
Kilic, T., Nolasco, S., eds. (2025). *Case reports in pulmonary medicine 2023*. Lausanne: Frontiers Media SA. doi: 10.3389/978-2-8325-6029-7

Table of contents

05 Rare case of pulmonary fat embolism and acute respiratory distress syndrome after liposuction and fat grafting: a case report
Xiaoyan Gai, Xiaoyan Sun, Xiang Zhu, Qingtao Zhou and Yongchang Sun

10 Diagnosis of *mycobacterium avium* complex infection utilizing metagenomics next-generation sequencing: a case report
Hongli Li, Luqing Wei and Fenge Li

17 Selective bronchial occlusion for the prevention of pneumothorax after transbronchial lung cryobiopsy in a pulmonary alveolar proteinosis patient: a case report
Hua-Man Wu, You-Li Wen, Xiao-Yu He and Zhi-Ping Deng

21 Sinus metastasis of lung adenocarcinoma: a case report
Mingyuan Xu, Qi Sun, Xin Lv, Fangjun Chen, Shu Su and Lifeng Wang

28 Case report: VEXAS as an example of autoinflammatory syndrome in pulmonology clinical practice
Ewa Więsik-Szewczyk, Arkadiusz Zegadło, Agnieszka Sobczyńska-Tomaszewska, Marcelina Korzeniowska and Karina Jahnz-Rózyk

35 Case report: The first account of undifferentiated sarcoma with epithelioid features originating in the pleura
Ling-Xi Xiao, Li Liu and Wang Deng

44 Bronchopulmonary foregut malformation with severe hemoptysis in advanced age: a case report and literature review
Cheng-Sen Cai, Bin Li, Yu-chun Yuan, Li-na Fu, Xiao-ye Zhang and Jun Wang

49 Case report: If it is not asthma—think of lymphangioleiomyomatosis in younger female patients
Malene Helligsø Kirkeby, Elisabeth Bendstrup and Hanne Krogh Rose

55 Multiple pulmonary cavities in an immunocompetent patient: a case report and literature review
Zihan Guo, Anli Zuo, Xinyi Liu, Yunxiu Jiang, Shuran Yang and Degan Lu

63 Diagnosis of pulmonary hemorrhagic leptospirosis complicated by invasive pulmonary aspergillosis complemented by metagenomic next-generation sequencing: a case report
Qiong-Fang Yang, Cai-Min Shu and Qiao-Ying Ji

69 Effects of inhaled beclomethasone dipropionate/formoterol fumarate/glycopyrronium on diaphragmatic workload and lung function in uncontrolled asthma: a case report
Antonio Maiorano, Chiara Lupia, Nicola Montenegro, Giuseppe Neri, Andrea Bruni, Eugenio Garofalo, Federico Longhini, Claudia Crimi, Angelantonio Maglio, Alessandro Vatrella, Girolamo Pelaia and Corrado Pelaia

75 Pulmonary infection with *Aeromonas dhakensis* in a patient with acute T lymphoblastic leukemia: a case report and review of the literature
Chaoyang Wang, Nan Wei, Moyuan Zhang and Xiaoju Zhang

82 Pulmonary alveolar microlithiasis combined with gastric mucosal calcification: a case report
Wen-Zhuo Li, Shuo Liu, Ji-Li Luo and Jing Xia

88 Pulmonary granulomas confirmed in Blau syndrome using TBLC specimens: Case report
Yasuo Shimizu, Yoshitomo Kushima, Ayae Tanaka, Akihiro Takemasa, Kazuyuki Ishida and Seiji Niho

93 Combining high-flow nasal cannula oxygen therapy with repeated toilet bronchoscopies for respiratory failure due to excessive infected airway secretions: a case report and series from a non-intensive hospital ward
Filippo Luca Fimognari, Francesco Baffa Bellucci, Flavio Fedele, Simone Scarlata, Giuseppe Armentaro and Angela Sciacqua

frontiers | Frontiers in Medicine

TYPE Case Report
PUBLISHED 23 May 2023
DOI 10.3389/fmed.2023.1202709

OPEN ACCESS

EDITED BY
Santi Nolasco,
University of Catania, Italy

REVIEWED BY
Giuseppe Muscato,
University of Catania, Italy
Joseph Shiber,
UF COM - Jacksonville, United States

*CORRESPONDENCE
Qingtao Zhou
✉ qtzhou75@163.com

†These authors have contributed equally to this work

RECEIVED 09 April 2023
ACCEPTED 09 May 2023
PUBLISHED 23 May 2023

CITATION
Gai X, Sun X, Zhu X, Zhou Q and Sun Y (2023) Rare case of pulmonary fat embolism and acute respiratory distress syndrome after liposuction and fat grafting: a case report. *Front. Med.* 10:1202709. doi: 10.3389/fmed.2023.1202709

Rare case of pulmonary fat embolism and acute respiratory distress syndrome after liposuction and fat grafting: a case report

Xiaoyan Gai[1†], Xiaoyan Sun[1†], Xiang Zhu[2], Qingtao Zhou[1*] and Yongchang Sun[1]

[1]Department of Respiratory and Critical Care Medicine, University Third Hospital, Beijing, China, [2]Department of Pathology, Peking University Third Hospital, Beijing, China

Background: Pulmonary fat embolism usually occurs after fracture, yet rarely observed after liposuction and fat grafting.

Case presentation: We describe a 19-year-old female patient who presented with acute respiratory failure and diffuse pulmonary opacities on chest radiographic image shortly after liposuction and fat grafting. Bronchoalveolar lavage was performed and lipid content in alveolar cells contribute to the diagnosis of the fat embolism syndrome. The patient was successfully treated with noninvasive mechanical ventilation and a short course of glucocorticoids.

Conclusions: Early recognition and appropriate treatment are very important to improve the outcome of pulmonary fat embolism. Considering that liposuction and fat grafting are increasingly common cosmetic surgeries, our aim is to raise awareness for this rare adverse event.

KEYWORDS

acute respiratory distress syndrome, fat grafting, liposuction, pulmonary fat embolism, bronchoalveolar lavage (BAL)

Background

Fat embolism syndrome (FES) often occurs after trauma, such as long bone fractures (1). Fat embolism following liposuction is a rare complication with few cases reported worldwide (2). The common clinical manifestations of FES include lung, central nervous system, and skin symptoms, which usually occur 12–72 h after trauma. The most typical triple sign is hypoxemia, decreased level of consciousness, and petechial rash. There is no standardized validated diagnostic test for FES. The diagnosis is challenging and often achieved in most cases based on clinical manifestations, imaging, and risk factors. We report a patient presenting with acute hypoxemia, respiratory distress, and typical blizzard-like changes on chest computed tomography (CT) hours after liposuction.

Case presentation

A 19-year-old woman was admitted to the emergency department with chest tightness persisting for 2 h. She had a six-year history of unhealthy habits including fasting and self-induced vomiting to control weight and was diagnosed with an eating disorder in

a psychiatric hospital. In the past 2 years, she had undergone zygomatic plastic surgery with subsequent rhinoplasty. Ten h before presentation, she underwent liposuction and fat grafting (liposuction of the limbs and hips and fat grafting in the face and chest), lasting for 3 h under general anesthesia. Approximately 8 h after the operation, she experienced chest tightness and palpitations in the ward, with a heart rate of 120 beats/min, and her peripheral blood oxygen saturation decreased to 80% on room air. She had a fever of 37.4°C and coughed up a small amount of yellow phlegm. No shivering, headache, dizziness, systemic rash and other clinical signs were noted. She was immediately treated with non-invasive mechanical ventilation and transferred to the Respiratory Intensive Care Unit (RICU).

Vital signs at the entrance of RICU revealed a temperature of 37.2°C, blood pressure of 97/62 mmHg, heart rate of 120 beats/min, respiratory rate of 18 breaths/min, and blood oxygen saturation level of 96% (non-invasive mechanical ventilation at FiO_2 of 50%). Height of 162 cm, weight of 48 kg. The whole body was wrapped in compression bandages. Breathing sounds in both lungs were decreased, with no wheezing, crackles, or rhonchi. Cardiovascular examination revealed normal heart sounds without murmur or rubs. There was no swelling of the upper limbs; both lower limbs were wrapped in elastic bandages and exhibited mild tenderness.

Complete blood examination revealed the following: white blood cell count, 10.52×10^9/L; neutrophils, 88.9%, hemoglobin, 99 g/L; rapid C-reactive protein level, 11.9 mg/L; serum procalcitonin, 0.08 ng/mL; albumin, 22.2 g/L; total cholesterol, 0.03 mmol/L; triglyceride, 0.01 mmol/L; high-density lipoprotein cholesterol, 0.02 mmol/L; low-density lipoprotein cholesterol, 0.02 mmol/L; D-dimer, 0.28 μg/mL; and brain natriuretic peptide, 1,104 pg/mL. Liver and renal functions and cardiac enzyme and troponin T levels were normal. Arterial blood gas analysis (on room air) showed a pH of 7.32, $PaCO_2$ of 31 mmHg, PaO_2 of 53 mmHg, HCO3- of 15.90 mmol/L, and lactic acid level of 2.37 mmol/L. Arterial blood gases on admission (under 5 cm H_2O of positive end-expiratory pressure and FiO_2 45%) showed a pH of 7.39, PaO_2 of 76 mmHg, with a PaO_2/FiO_2 ratio of 168.

Chest CT scan (Figure 1) revealed diffuse mixed ground-glass and consolidative opacities involving both lungs, thickening of the interlobular septa, bilateral pleural effusion, and subcutaneous soft tissue edema of the chest and back. CT pulmonary angiography (CTPA) showed no filling defect in the pulmonary artery. Echocardiography revealed an estimated pulmonary arterial systolic pressure of 36 mmHg, left ventricular ejection fraction of 70%, normal right ventricular systolic function, and normal inferior vena cava diameter. Brain CT showed no obvious abnormality. Given the suspicion of FES, bedside bronchoscopy performed within 24 h showed "mild inflammation". Bronchoalveolar lavage was performed, and differential cell counts in the bronchoalveolar lavage fluid (BALF) sample showed macrophages, 10.8%; lymphocytes, 7.2%; and neutrophils, 82%. Cytopathologic evaluation of BALF revealed a multitude of tissue cells in the smear, with oil red O-positive bodies of different sizes and numbers in the cytoplasm of some cells, representing lipid droplets (Figure 2).

Noninvasive ventilation was initiated. Methylprednisolone 80 mg daily and moxifloxacin 400 mg daily were given intravenously. Additionally, she received nutritional support and intravenous infusion of human albumin for 3 days. Her respiratory failure gradually improved. On day 5 of admission, her peripheral oxygen saturation was maintained >95% under air condition; subsequently, oxygen support was withdrawn, and methylprednisolone dosage was reduced to 40 mg daily for 2 days. She was discharged from the hospital on day 7 and was treated with prednisone acetate (40 mg qd followed by 20 mg qd for 5 days each). On reexamination 10 days after discharge, the patient's condition had improved. Her heart rate and peripheral SpO_2 were 70–80 bpm and 98–99% on room air, respectively. Chest CT was normal (Figure 3), and prednisone was tapered to 10 mg daily for 3 days and then halted.

Discussion and conclusions

Although the diagnosis of FES is challenging, researchers have tried to define diagnostic criteria. In 1974, Gurd and Wilson established the diagnostic criteria for FES (3), which are the most widely used in clinical practice, and Schonfeld developed a scoring scale for diagnosis in 1983 (4).

Our patient presented with acute hypoxemia, respiratory distress, and typical blizzard-like changes on chest CT hours after liposuction and a seriously low PaO_2/FiO_2 of 168, which were in accordance with acute respiratory distress syndrome (ARDS) diagnosis, graded as moderate based on Berlin Criteria of PaO^2/FiO^2 ratio 100–200 (5). The positive oil red O staining of BALF supported the diagnosis of pulmonary fat embolism; however, the patient did not show any skin or nervous system symptoms. Pulmonary fat embolism can lead to ARDS, which is one of the most serious complications and the main cause of death in such patients (6). ARDS is a kind of high permeability pulmonary edema, which is caused by many factors, and eventually results in diffuse alveolar injury (i.e., edema, inflammation, transparent membrane, atelectasis, or hemorrhage). Its clinical features are hypoxemia and double-lung infiltration shadows, accompanied by increased flow, increased physiological dead space, and decreased lung compliance.

Supportive care is the main therapy in the management of pulmonary fat embolism, with respiratory support being crucial. According to the severity of hypoxemia, the appropriate oxygen supply and respiratory support treatment should be determined to ensure oxygenation and minimize further lung damage. Corticosteroids are considered applicable and effective in cases of fulminant pulmonary fat embolism and ARDS, which can help reduce inflammation and fatty acid levels and improve oxygenation (2, 7). In a recent meta-analysis, the total mortality of FES was found to be 30.2%, and corticosteroid therapy was significantly associated with reduced mortality (7). There is a lack of enough evidence or recommendation about the appropriate dosage of corticosteroids. A low-dose regimen of glucocorticoids was administered in this case, in the form of methylprednisolone 80 mg daily for 5 days. Subsequently, the patient's respiratory failure

Abbreviations: ARDS, acute respiratory distress syndrome; BALF, bronchoalveolar lavage fluid; CT, computed tomography; CTPA, CT pulmonary angiography; FES, fat embolism syndrome.

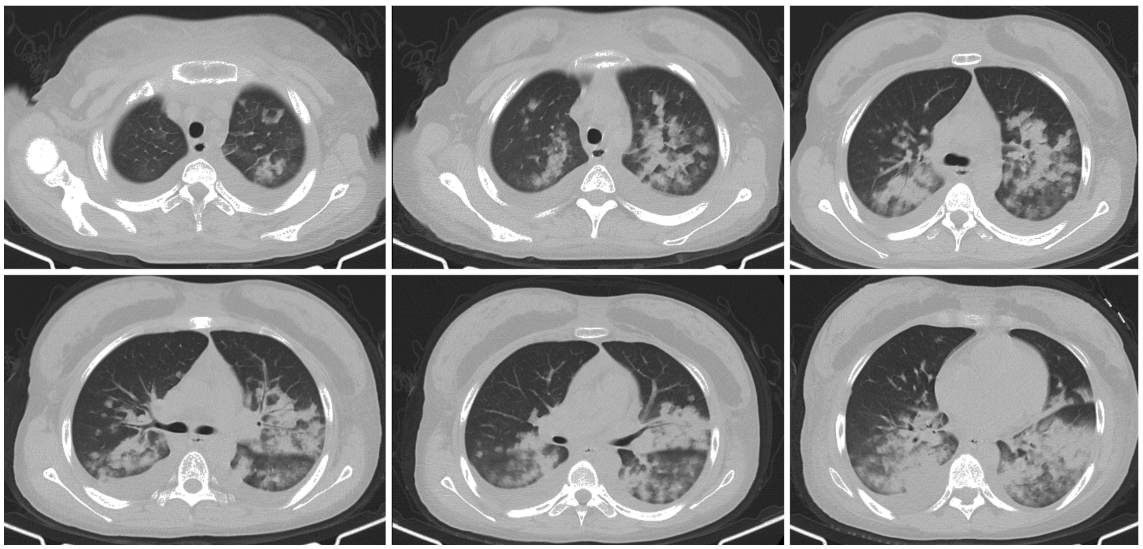

FIGURE 1
Chest computed tomography scan 1 day before admission. The lung window shows diffuse mixed ground-glass and consolidative opacities involving both lungs and small bilateral pleural effusion.

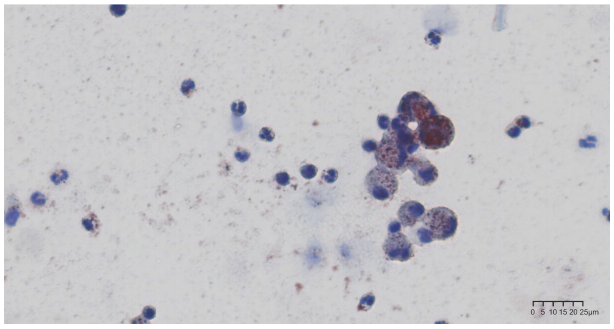

FIGURE 2
Oil red O staining of bronchoalveolar lavage fluid specimen. Alveolar macrophages with multiple prominent red- or brown-staining cytoplasmic inclusions seen under light microscopy.

was significantly relieved, and methylprednisolone was tapered. By contrast, the use of heparin is still controversial (1).

The most common CT features of pulmonary fat embolism are patchy ground-glass or nodular opacities, lobular septal thickening, or diffuse bilateral infiltrates consistent with ARDS (2, 8). The extent of ground-glass opacities and presence of consolidation correlates with disease severity (9). A retrospective review of radiological features on CTPA images of 15 patients diagnosed clinically with pulmonary fat embolism reported pulmonary opacity in 14 (93.3%) patients, ground-glass opacities in 9 (64.3%), alveolar opacities in 6 (42.9%), interlobular septal thickening in 10 (66.7%), and pleural effusions in 7 (46.7%) (9). Pulmonary artery filling defects were observed on CTPA only in 3 (20%) patients, suggesting that pulmonary artery filling defects are not commonly seen in patients with pulmonary fat embolism (10). In our case, the chest image showed diffuse exudation and consolidation in both lungs—considered to be a manifestation of ARDS secondary to pulmonary fat embolism—that was absorbed completely in 2 weeks, which is consistent with a previous report (10).

Another effective method for the diagnosis of pulmonary fat embolism is lung biopsy, although it is not the first choice because of its invasiveness. Round or oval negative staining observed in the blood vessels of the lung tissue section suggests potential fat emboli (1, 5). The lung tissue sections fixed in formalin can be stained with osmium tetraoxide solution and then embedded in paraffin. Round, uniform black droplets in the blood vessels indicate fat emboli. In addition, oil red O staining helps detect the presence of lipids in frozen sections and BALF, which appear red when visualized under light microscopy. The presence of lipid droplets in macrophages in BALF, especially if the number of cells positive for the staining is >30%, supports an FES diagnosis (11) and helps identify ARDS caused by other factors.

In the BALF pathological examination, routine processed pathological specimens (paraffin embedding, xylene dewaxing, and alcohol solvent dissolution) and cytospin specimens made from fresh cell suspension were examined separately in this case. Both specimens were stained with oil red O; the routine pathological specimens were negative for the staining, whereas the fresh cell slice was positive (Figure 2). During the processing of conventional pathological specimens, xylene and alcohol solvents lead to lipid dissolution, which may produce a false-negative result.

Pulmonary fat embolism is a serious complication after liposuction that can develop suddenly and progress rapidly. Early diagnosis and appropriate treatment are essential to reduce mortality and improve prognosis. Oil red O staining of BALF is helpful in the diagnosis of pulmonary fat embolism. Xylene and alcohol solvents should be avoided during the processing of specimens. Respiratory support and corticosteroid therapy are key in treating pulmonary fat embolism and ARDS.

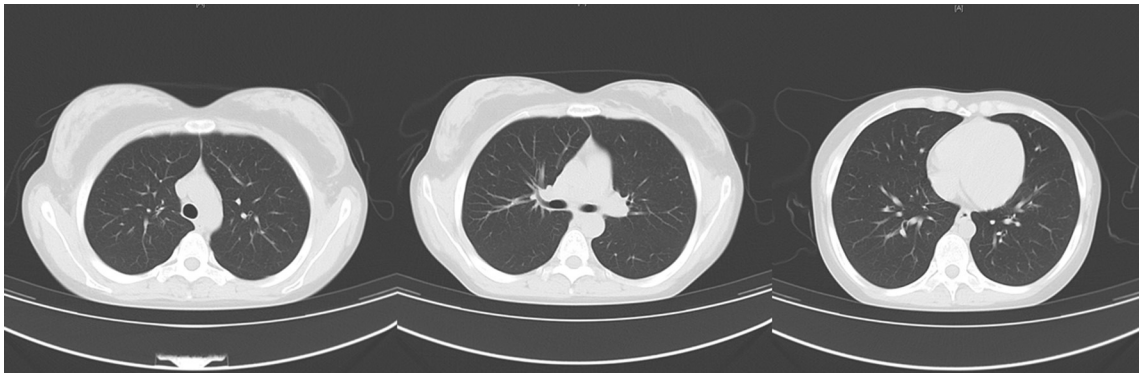

FIGURE 3
Chest computed tomography scan after discharge. There was no pulmonary infiltrates or pleural effusion.

Data availability statement

The original contributions presented in the study are included in the article/supplementary material, further inquiries can be directed to the corresponding author.

Ethics statement

The studies involving human participants were reviewed and approved by Peking University Third Hospital. The Ethics Committee waived the requirement of written informed consent for participation. Written informed consent was obtained from the patient for the publication of this manuscript and of potentially identifiable images or data included in this article.

Author contributions

XG, XS, and QZ performed the study. XZ performed the histological examination and provided the photos. XG and QZ were major contributors in writing the manuscript. All authors analyzed and interpreted the patient data. All authors read and approved the final manuscript.

Funding

This study was supported by the Capital's funds for Health Improvement and Research (Grant No. 2022-2G-40910) and the National Natural Science Foundation of China (Grant No. 81800038).

Conflict of interest

The authors declare that the research was conducted in the absence of any commercial or financial relationships that could be construed as a potential conflict of interest.

Publisher's note

All claims expressed in this article are solely those of the authors and do not necessarily represent those of their affiliated organizations, or those of the publisher, the editors and the reviewers. Any product that may be evaluated in this article, or claim that may be made by its manufacturer, is not guaranteed or endorsed by the publisher.

References

1. Rothberg DL, Makarewich CA. Fat embolism and fat embolism syndrome. *J Am Acad Orthop Surg.* (2019) 27:e346–55. doi: 10.5435/JAAOS-D-17-00571

2. Kadar A, Shah VS, Mendoza DP, Lai PS, Aghajan Y, Piazza G, et al. Case 39-2021: A 26-year-old woman with respiratory failure and altered mental status. *N Engl J Med.* (2021) 385:2464–74. doi: 10.1056/NEJMcpc2107355

3. Gurd AR, Wilson RI. The fat embolism syndrome. *J Bone Joint Surg Br.* (1974) 56B:408–16. doi: 10.1302/0301-620X.56B3.408

4. Schonfeld SA, Ploysongsang Y, DiLisio R, Crissman JD, Miller E, Hammerschmidt DE, et al. Fat embolism prophylaxis with corticosteroids. A prospective study in high-risk patients. *Ann Intern Med.* (1983) 99:438–43. doi: 10.7326/0003-4819-99-4-438

5. ARDS Definition Task Force, Ranieri VM, Rubenfeld GD, Thompson BT, Ferguson ND, Caldwell E, et al. Acute respiratory distress syndrome: the Berlin Definition. *JAMA.* (2012) 307:2526–33. doi: 10.1001/jama.2012.5669

6. Kao SJ, Yeh DY, Chen HI. Clinical and pathological features of fat embolism with acute respiratory distress syndrome. *Clin Sci (Lond).* (2007) 113:279–85. doi: 10.1042/CS20070011

7. He Z, Shi Z, Li C, Ni L, Sun Y, Arioli F, et al. Single-case metanalysis of fat embolism syndrome. *Int J Cardiol.* (2021) 345:111–7. doi: 10.1016/j.ijcard.2021.10.151

8. Newbigin K, Souza CA, Torres C, Marchiori E, Gupta A, Inacio J, et al. Fat embolism syndrome: state-of-the-art review focused on pulmonary imaging findings. *Respir Med.* (2016) 113:93–100. doi: 10.1016/j.rmed.2016.01.018

9. Newbigin K, Souza CA, Armstrong M, Pena E, Inacio J, Gupta A, et al. Fat embolism syndrome: do the CT findings correlate with clinical course and severity of symptoms? A clinical-radiological study. *Eur J Radiol.* (2016) 85:422–7. doi: 10.1016/j.ejrad.2015.11.037

10. Dwivedi S, Kimmel LA, Kirk A, Varma D. Radiological features of pulmonary fat embolism in trauma patients: a case series. *Emerg Radiol.* (2022) 29:41–7. doi: 10.1007/s10140-021-01969-4

11. Mimoz O, Edouard A, Beydon L, Quillard J, Verra F, Fleury J, et al. Contribution of bronchoalveolar lavage to the diagnosis of posttraumatic pulmonary fat embolism. *Intensive Care Med.* (1995) 21:973–80. doi: 10.1007/BF01700658

frontiers | Frontiers in Medicine

TYPE Case Report
PUBLISHED 18 October 2023
DOI 10.3389/fmed.2023.1247034

OPEN ACCESS

EDITED BY
Santi Nolasco,
University of Catania, Italy

REVIEWED BY
Octavio Rivero-Lezcano,
Complejo Asistencial Universitario de León (CHLeon), Spain
Bingqing Zhao,
Stanford University, United States

*CORRESPONDENCE
Luqing Wei
luqingwei@163.com
Fenge Li
rosetea85@163.com

RECEIVED 25 June 2023
ACCEPTED 25 September 2023
PUBLISHED 18 October 2023

CITATION
Li H, Wei L and Li F (2023) Diagnosis of *mycobacterium avium* complex infection utilizing metagenomics next-generation sequencing: a case report.
Front. Med. 10:1247034.
doi: 10.3389/fmed.2023.1247034

Diagnosis of *mycobacterium avium* complex infection utilizing metagenomics next-generation sequencing: a case report

Hongli Li[1], Luqing Wei[1]* and Fenge Li[1,2]*

[1]Department of Respiratory, Tianjin Beichen Hospital, Tianjin, China, [2]Core Laboratory, Tianjin Beichen Hospital, Tianjin, China

Mycobacterium avium-intracellulare complex (MAC) is a type of nontuberculous mycobacteria (NTM) and is associated with underlying pulmonary diseases, such as chronic obstructive pulmonary disease, bronchiectasis, chronic aspiration or recurrent pneumonia, inactive or active tuberculosis, pneumoconiosis, and bronchogenic carcinoma. The risk factors for NTM-PD include host, drug, and environmental factors. In this report, we present the case of a 61-year-old man who developed bilateral lung nodules and was experiencing severe hemoptysis. The repeat acid-fast bacilli test performed on both sputum and bronchoalveolar lavage fluid (BALF) samples showed a negative result, as did the GeneXpert test. We employed metagenomic next-generation sequencing (mNGS) to analyze the lung nodule and BALF samples collected from the patient. Both samples tested positive for MAC within 3 days. In addition, traditional MAC culture, conducted for 2 months, confirmed the growth of MAC in the patient's BALF. Then, the patient was treated accordingly. Following treatment, a high-resolution chest computed tomography scan revealed a significant reduction in lung nodules of the patient after 2 months. These results indicate that MAC-associated lung nodules were responsible for the patient's symptoms, emphasizing the need for vigilance in diagnosing MAC infection in the patient without predisposing conditions. Furthermore, these results highlight the potential utility of mNGS as a promising rapid diagnostic tool for MAC infection and its potential role in the diagnosis of NTM disease.

KEYWORDS

nontuberculous mycobacterium, *Mycobacterium avium*, pulmonary disease, metagenomics next-generation sequencing, diagnosis

Introduction

Nontuberculous mycobacteria (NTM) refer to species of mycobacterium that do not belong to *Mycobacterium tuberculosis* complex or *Mycobacterium leprae*. NTM are known to cause both pulmonary and extrapulmonary illnesses in humans of all ages (1), with *Mycobacterium avium* complex (MAC) being the most common type. MAC consists of a growing number of species, including *M. arosiense*, *M. bouchedurbonense*, *M. timonense*, *M. vulneris*, and *M. yongonense*. NTM-related pulmonary disease (NTM-PD) is a common type of NTM infection (2–5). Predisposing conditions such as chronic obstructive pulmonary disease, bronchiectasis, chronic aspiration or recurrent pneumonia, inactive or active tuberculosis, pneumoconiosis, and bronchogenic carcinoma are present in 54–77% of the patients with pulmonary MAC disease.

Risk factors for NTM-PD include host, drug, and environmental factors (6). Few studies have investigated the value of metagenomic next-generation sequencing (mNGS) for diagnosing MAC infection. Here, we report a case of a man with pulmonary disease caused by MAC that was promptly and effectively diagnosed using metagenomic next-generation sequencing (mNGS), leading to a timely and precise treatment for the patient following the diagnosis.

Case presentation

A 61-year-old man presented with bilateral lung nodules in chest roentgenograms (Figure 1A) during his routine health examination in January 2019. The bilateral lung nodules remained stable during subsequent regular outpatient reexaminations in February 2019, December 2019, and December 2020. Particularly, this patient showed no clinical symptoms throughout this period. However, in July 2021, the patient was admitted to our hospital due to hemoptysis. He did not display symptoms commonly associated with infection, such as fever, dyspnea, pyrosis, night sweats, or weight loss at that time. Additionally, the physical examination results were also normal. All laboratory tests of the patient, including peripheral blood count, renal and liver functions, indirect immunofluorescence test for antinuclear (ANA) antibodies, rheumatoid factor test, anti-cyclic citrullinated peptide test, anti-extractable nuclear antigen test, lymphocyte subtype test, urine test, and stool test showed normal results. The patient underwent a chest computed tomography (CT) scan, revealing multiple small nodules in both upper lobes and ground glass opacity in the right upper lobe (Figure 1B). The nodules were found to be similar in size to the ones found in the original CT scan from January 2019, but ground glass opacity was observed. Subsequently, the patient underwent bronchoscopy examination, and bronchoalveolar lavage fluid (BALF) samples were collected for further pathogen analysis. The results of the acid-fast bacilli (AFB) test and GeneXpert MTB/RIF test for sputum and BALF were all negative. The patient then received antibiotics treatment with moxifloxacin, while he did not show hemoptysis during his stay at the hospital. The patient did not

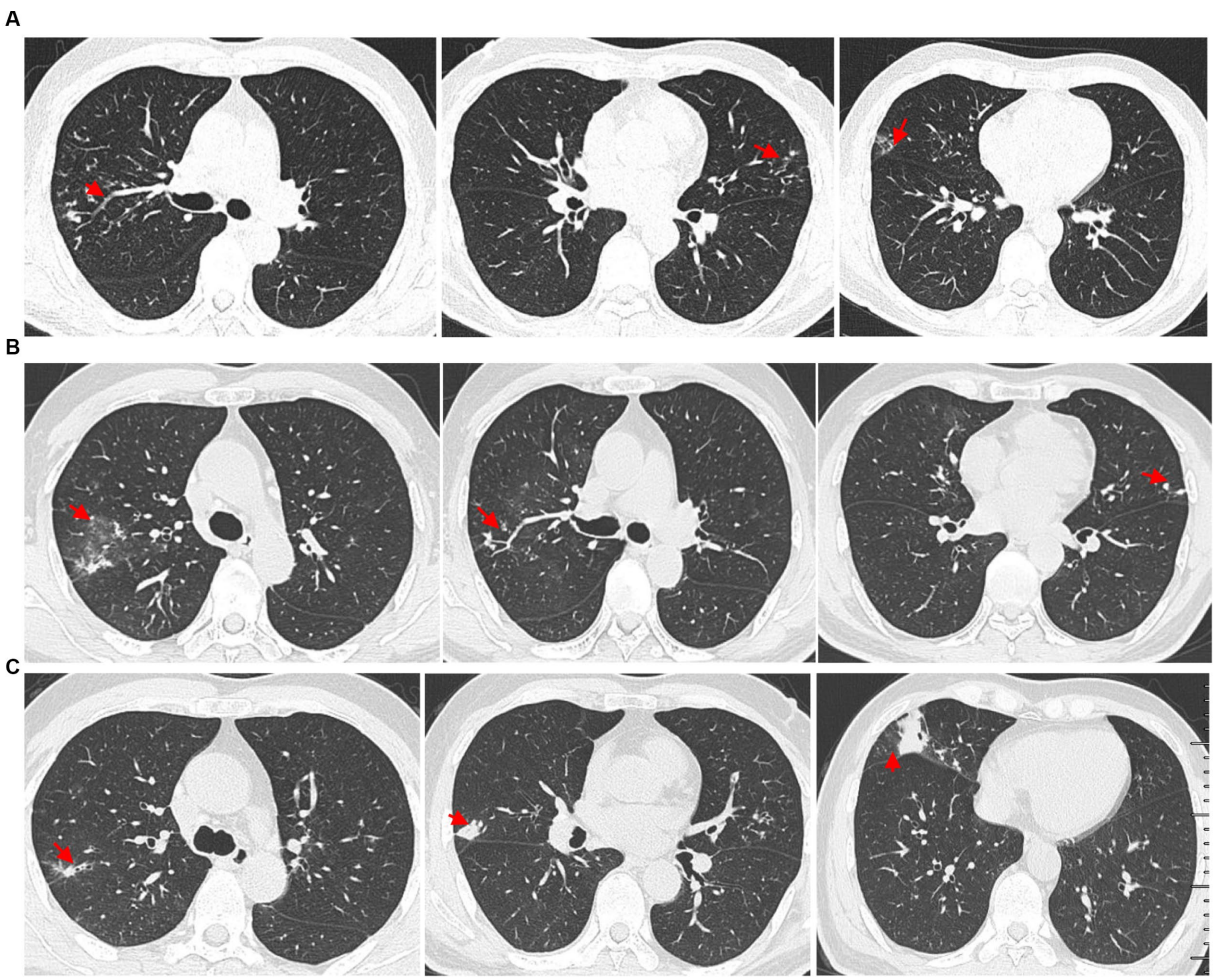

FIGURE 1
High-resolution chest computed tomography (CT) scan results from different periods. **(A)** CT scan results from different layers taken on 14 January 2019. The multiple small nodules (red arrow) in the right upper lobe, left upper lobe, and right middle lobe. **(B)** The patient underwent a CT scan of the chest on 7 July 2021, which showed ground glass opacity in the right upper lobe (red arrow) and multiple small nodules in both upper lobes (red arrow). **(C)** Outpatient reexaminations using a repeat CT scan on 19 August 2021 revealed an increase in the size of multiple small nodules in the upper and middle lobes (red arrow).

show any symptoms throughout the 5-day course of antibiotics treatment and was subsequently discharged from the hospital.

Another outpatient reexamination on 19 August 2021 using a repeat high-resolution chest CT scan revealed a noticeable increase in the size of the multiple small nodules in the upper and middle lobes of the lung (red arrow) (Figure 1C). A chest CT-guided lung biopsy was performed. The histopathology (right lung biopsy) showed the alveolar tissue, local lymphocyte infiltration, granulomatous lesions, scattered Langerhans giant cells, some fibrinoid exudates along with no caseous necrosis. The result of the tissue acid-fast staining was negative (Figure 2). As such, a second bronchoscopy was performed, and BALF was collected for pathogen testing. However, both acid-fast bacilli test and GeneXpert MTB/RIF test results for BALF were negative. Particularly, this patient still experienced no clinical symptoms of infection during this time. On 24 August 2021, the lung tissue and BALF of the patient were subjected to mNGS testing, and 23 reads (Figures 3A,B) and 11,948 reads (Figures 3D–F) of MAC were identified within 3 days. Moreover, the MAC infection was confirmed again through a BALF culture test conducted 20 days later. The patient was then treated with a combination of ethambutol (25 mg/kg three times per week), rifampicin (600 mg three times per week), and azithromycin (500 mg three times per week) after breakfast for 6 months. Notably, the patient did not experience any additional symptoms during these drug treatments. It is also worth noting that no drug-related adverse reactions were observed throughout the treatment period. Moreover, a significant decrease in nodule size was observed in a high-resolution chest CT scan which was performed 2 months after the aforementioned combination therapy (Figure 4).

Method of metagenomic next-generation sequencing

Bronchoalveolar lavage fluid (BALF, 3–5 mL) was collected from patients in sterile tubes with anticoagulant, following standard procedures. The samples were then transported at hypothermia at 4–8°C after collection. Subsequently, DNA extraction was performed using PathoXtract® Basic Pathogen Nucleic Acid Kit (WYXM03211S, WillingMedCorp, Beijing, China), following the manufacturer's protocol. Then, DNA libraries were constructed using the Illumina® DNA Prep, (M) Tagmentation kit (20018705, Illumina) according to the manufacturer's protocol. DNA libraries were sequenced on NextSeq™ 550Dx system using a 75 bp, single-end sequencing kit (Illumina), and at least 20 million sequencing reads were acquired for each sample. A negative control sample (nuclease-free water) was processed and sequenced in parallel in each sequencing run for quality control. Finally, the raw FASTQ-format data were subjected to Trimmomatic v0.40 for quality control and evaluation, whereby low-quality or undetected sequences, sequences contaminated by splices, high-coverage repeats, and short-read-length sequences were filtered out. High-quality sequencing data were compared with the human reference genome GRCh37 (hg19) using Bowtie2 v2.4.3, enabling the removal of human host sequences. Using Kraken2 v2.1.0 software, the remaining sequences were aligned to four databases downloaded from NCBI, including bacteria, fungi, viruses, and parasites, for classification. For identification of the pathogens, a RPTM value, which defined as a detected number of pathogen specific reads per 10 million was used. RPTM ≥3 was used as an empirical threshold for virus detection. For bacteria and fungi, positive pathogens were required to meet a RPTM threshold of ≥20. Special pathogens (including *Cryptococcus* and *Mycobacterium*) with RPTM ≥1 was identified as positive.

Discussion

MAC is the most common microbe for nontuberculous mycobacterial associated pulmonary disease (2–5). It contains two major microbe species, *Mycobacterium avium* and *Mycobacterium intracellulare* (7). MAC are commonly isolated from water, house dust, and soil. Patients become infected with MAC primarily through inhalation, ingestion, invasive procedures, or trauma (8). Host-environment interactions are the main cause of MAC-PD (9), and the following are risk factors that contribute to the development of MAC-PD: (1) patients with smoking and alcoholism history (8, 10); (2) elderly white men with underlying pulmonary diseases, such as active tuberculosis, bronchiectasis, pneumoconiosis, chronic aspiration pneumonia, lung cancer, and chronic obstructive pulmonary disease (COPD) (11); (3) non-smoking women over the age of 50 with a normal immune system and no underlying lung disease (12); (4) cystic fibrosis carriers (13); and (5) patients with immunosuppression, such as acquired immunodeficiency syndrome (AIDS) (12–14). Clinical symptoms of MAC-PD, including chronic cough, expectoration, fatigue, dyspnea, hemoptysis, and chest pain,

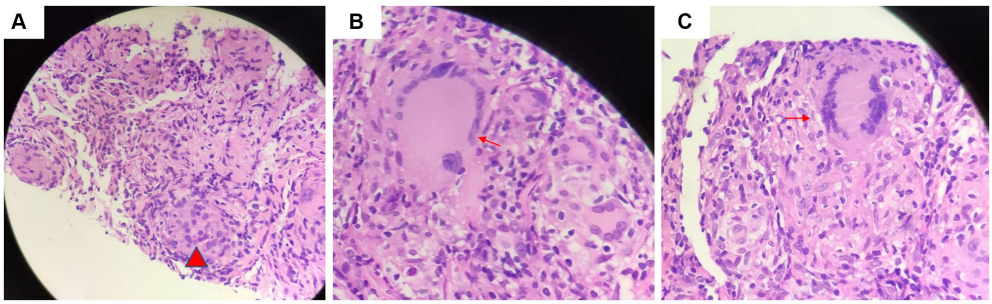

FIGURE 2
Tissue acid-fast staining indicated the presence of **(A)** granulomatous lesions (red arrow) and **(B)** scattered giant multinucleated giant cell (red arrow). **(C)** There was no caseous necrosis observed (red arrow).

10.3389/fmed.2023.1247034

A

Species	Reads number (RPTM)	Reference Ranges
Mycobacterium avium complex	23	≥1

B

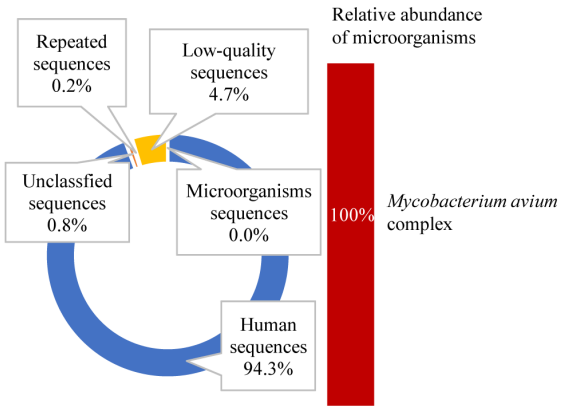

C

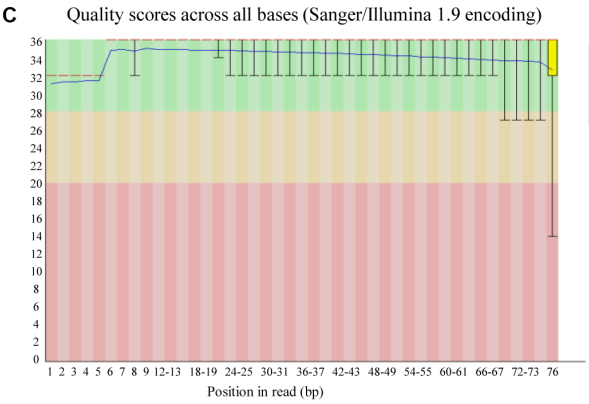

D

Species	Reads number (RPTM)	Reference Ranges
Mycobacterium avium complex	11948	≥1
Acinetobacter baumannii	27	≥20
Lelliottia amnigena	16	≥20
Rothia mucilaginosa	549	≥20
Lactobacillus salivarius	53	≥20
Peptoniphilus lacrimalis	29	≥20
Corynebacterium matruchotii	24	≥20
Peptostreptococcus stomatis	24	≥20
Atopobium parvulum	21	≥20
Streptococcus infantis	20	≥20
Parvimonas micra	20	≥20

E

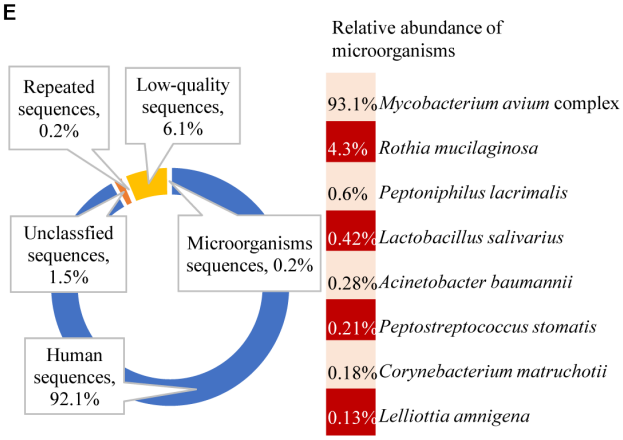

F

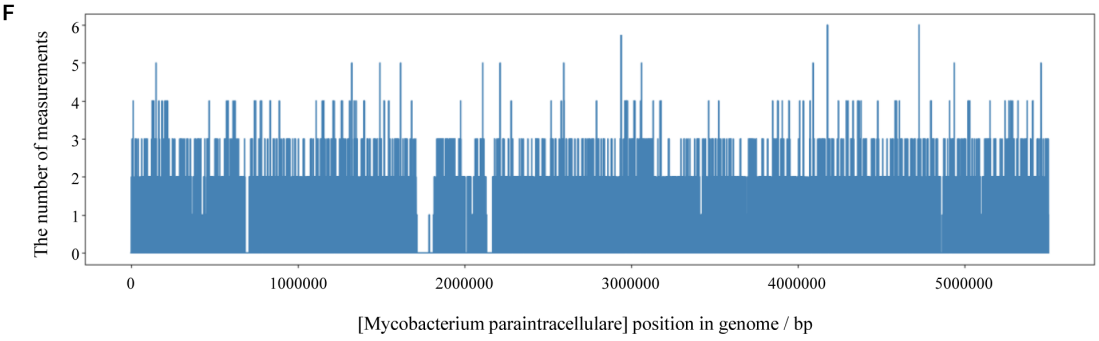

FIGURE 3
The mNGS results of the patient's tissue and BALF. **(A)** The identified pathogen in the tissue was *Mycobacterium avium* complex (MAC). **(B)** The relative abundance of MAC accounts for 100% of the identified microorganisms in tissue. **(C)** The results of single base quality distribution in the tissue sample. **(D)** MAC was also identified in the BALF sample. **(E)** 93.1% of the reads of microorganisms were identified in BALF that belongs to MAC. **(F)** Coverage of MAC detected by BALF mNGS.

are non-specific. Patients with MAC-PD less frequently exhibit fever and weight loss than patients with typical tuberculosis (12). It has been reported recently that a 65-year-old man with NTM presented with recurrent fever and cough, and the CT scan of the chest revealed a lung infection. The patient's clinical condition did not improve because they received an incorrect diagnosis and treatment previously. With the help of mNGS, the pathogen was identified as MAC. Subsequently, he received accurate antibiotics treatment, resulting in significant improvements in clinical symptoms and CT scan performance (15). Further, Liu et al. (16) have also reported the effectiveness of mNGS in facilitating and improving the clinical diagnosis of NTM infections.

In this case report, we present the case of a man with a smoking history and no underlying lung-related diseases who experienced only a short-term hemoptysis. The patient's MAC-PD infection was diagnosed using mNGS technology in only 3 days, which emphasizes the importance of rapid and accurate recognition of MAC infection for timely initiation of effective treatment and symptom alleviation.

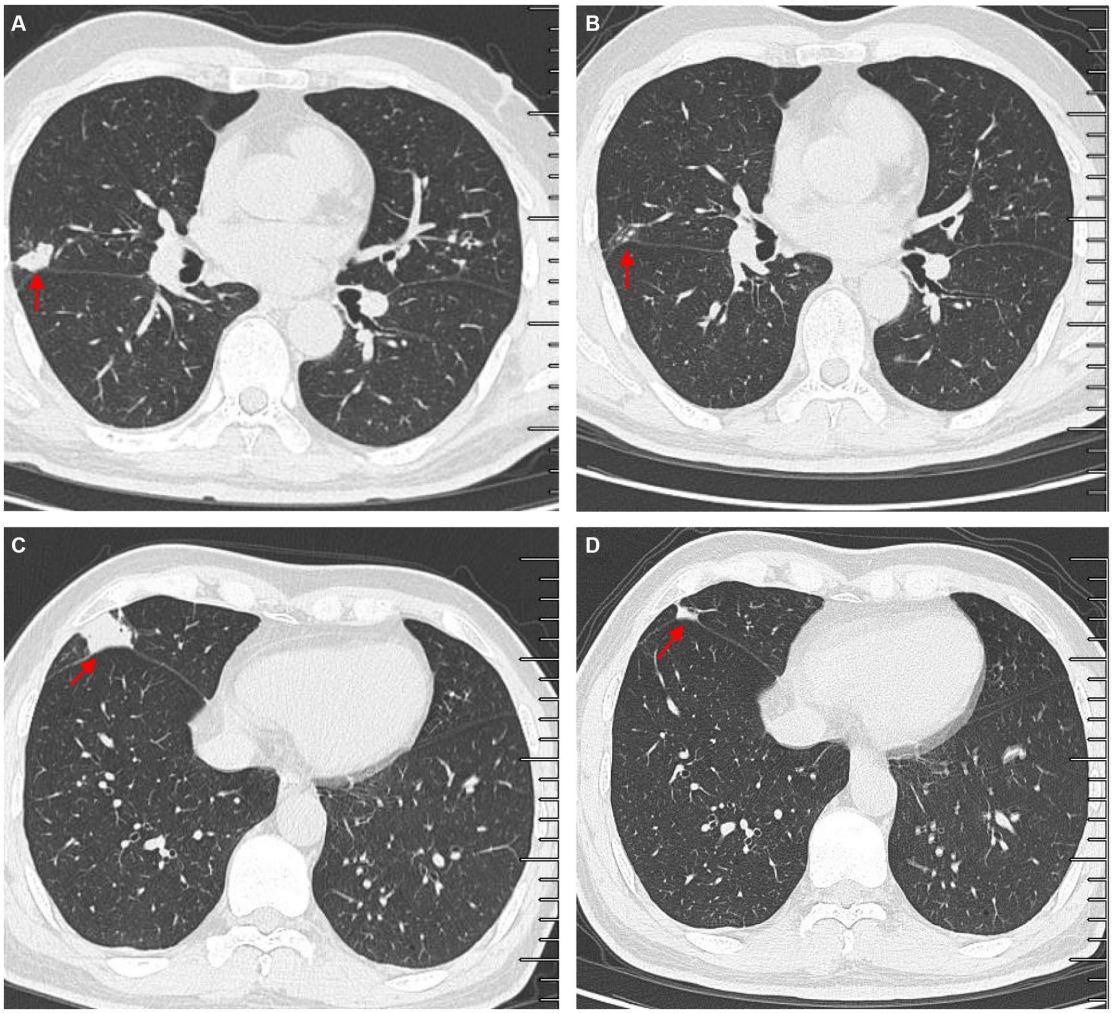

FIGURE 4
Comparisons of outpatient reexaminations of chest computed tomography (CT) scan on 19 August 2021 and 21 October 2021. The results showed that the nodules in the middle lobes observed on 21 October 2021 **(A,C)** became much smaller than those observed on 19 August 2021 **(B,D)**. Red arrow–lung nodules.

Therefore, mNGS diagnosis can be precise and rapid when compared to conventional bacteria culture testing. It is worth noting that the patient's MAC infection was diagnosed rapidly using mNGS, as the patient transitioned from asymptomatic to symptomatic. This led to successful treatment for the patient. This case study can provide valuable clinical experiences for the doctors in the field. Further, the clinical symptoms of this patient were mild and minimal with increasing lung nodules, which was very different from the cases reported previously (15, 16), indicating that clinical symptoms may not be easily noticeable in healthy populations infected with MAC.

Most researchers contend that the histopathology of MAC-PD is comparable to that of TB. Key features of pathology of MAC-PD include (1) the presence of necrotizing granulomas characterized by a central zone of necrosis surrounded by a variably thick rim of epithelioid histiocytes, including pink ("caseating") necrosis, dirty necrosis (basophilic, rich in nuclear debris), and suppurative necrosis; (2) granulomatous rims that may contain Langhans-type giant cells that are multinucleated; and (3) the presence of atypical lesions with tissue cell aggregation granulomas that are absent or poorly formed, which is normally described as a characteristic reaction in patients with AIDS. Because of these similarities, it is difficult to distinguish TB-and MAC-infected tissue (6, 17, 18). Jing et al. found that pulmonary TB exhibits more pink necrosis and basophilic necrosis, while MAC-PD displays multinucleated giant cells (Figure 4) (19). MAC-PD may also feature suppurative necrosis and vasculitis (non-necrotizing), mimicking granulomatosis with polyangiitis (20). In this study, the pathology test of the patient revealed local lymphocytic infiltration, granulomatous lesions, and scattered Langerhans giant cells, minimal fibrinoid exudates, and no caseous necrosis, and special staining resulted in acid-fast positive. MAC infection manifests as lung nodules in healthy individuals and are characterized by necrotizing granulomatous inflammation containing AFB. However, the pathological manifestations of TB and MAC infection are indistinguishable.

According to the Infectious Disease Society of America and the American Thoracic Society, patients with respiratory symptoms and imagological evidence of pulmonary disease, such as cavitary or nodular opacities on chest radiograph or multifocal bronchiectasis through high-resolution computed tomography, can be diagnosed with fungal infection if malignancy was excluded. Several findings also support the diagnosis of MAC infection: (1) positive culture

results from at least two separate expectorated sputum samples and/or NTM molecular positivity for the same pathogen; (2) positive culture results from at least one bronchial wash or lavage and/or NTM molecular positivity for at least one; (3) positive mycobacterial histologic features (granulomatous inflammation or AFB) of transbronchial or lung biopsies, and positive culture for MAC and/or molecular positivity; (4) transbronchial or lung biopsy exhibiting mycobacterial histologic features (granulomatous inflammation or AFB), and one or more sputum or bronchial washing samples that cultured positive for MAC and/or molecular positivity (6). In this study, we determined the diagnosis of MAC-PD based on multiple factors: (1) respiratory symptoms; (2) progression confirmed by high-resolution CT; (3) positive culture result of BALF; (4) histopathological test; (5) mNGS positive results; and (6) effective anti-MAC treatment.

Symptoms of MAC-PD are usually non-specific, and traditional methods for detecting pathogenic microorganism detection have limitations, making it challenging to accurately identify the strains in clinical practice. It is often misdiagnosed as TB or other AFB-positive bacilli. Furthermore, due to lipid-rich outer membranes, MAC are relatively resistant to chemical disinfection by chlorine, chloramines, and ozone, and MAC cultures are usually detected with particular assays. Therefore, positive MAC culture can be detected through direct examination of sputum staining or an acid-fast staining within 7–14 days, and by conventional bacterial culture methods within 21–28 days or even longer. Kodaka et al. (20) found that serum anti-GPL-core IgA testis is useful for diagnosing MAC-PD and determining patient prognosis. While MAC culture serves as the gold standard for diagnosis, it is not routinely tested due to the extended time required for pathogenic NTM to grow, typically taking 2 months. Laboratory tests of p-nitrobenzoic acid selective media culture, polymerase chain reaction (PCR), and MTP64 antigen detection are widely used for identifying TB and NTM (21). In recent years, laboratory testing methods have shifted from biochemical approaches to molecular techniques, and mass spectrometry (MS/MS) has shown promising results for providing rapid speciation of MAC (22, 23). However, the clinical application of MS/MS is limited due to the need for expensive instruments and high technical requirements. The rapid development of mNGS has enabled rapid and specific identification of NTM with high sensitivity (24, 25). In this case report, MAC diagnosis was achieved within 3 days using mNGS.

Conclusion

The incidence and prevalence of MAC-PD are increasing worldwide and can be a cause of AIDS, bronchiectasis, and immunosuppression. We emphasize the importance of identifying MAC in patients without predisposing conditions. Advancements in diagnostic technology make mNGS a promising diagnostic method for MAC infection and associated diseases in the clinic.

Ethics statement

The studies involving humans were approved by Ethics committee of Tianjin Beichen Hospital. The studies were conducted in accordance with the local legislation and institutional requirements. The participants provided their written informed consent to participate in this study. Written informed consent was obtained from the individual(s) for the publication of any potentially identifiable images or data included in this article.

Author contributions

HL, LW, and FL contributed to conception and design of the study and wrote sections of the manuscript. HL organized the database and wrote the first draft of the manuscript. All authors contributed to the article and approved the submitted version.

Acknowledgments

We would like to thank Xiaojing Zhang, Yafeng Zheng, and WillingMed Technology (Beijing) Co. for their technical support with mNGS.

Conflict of interest

The authors declare that the research was conducted in the absence of any commercial or financial relationships that could be construed as a potential conflict of interest.

Publisher's note

All claims expressed in this article are solely those of the authors and do not necessarily represent those of their affiliated organizations, or those of the publisher, the editors and the reviewers. Any product that may be evaluated in this article, or claim that may be made by its manufacturer, is not guaranteed or endorsed by the publisher.

References

1. Haworth CS, Banks J, Capstick T, Fisher AJ, Gorsuch T, Laurenson IF, et al. British thoracic society guidelines for the management of non-tuberculous mycobacterial pulmonary disease (Ntm-Pd). *Thorax*. (2017) 72:ii1–ii64. doi: 10.1136/thoraxjnl-2017-210927

2. Daley CL. *Mycobacterium avium* complex disease. *Microbiol Spectr*. (2017) 5. doi: 10.1128/microbiolspec.TNMI7-0045-2017

3. Koh WJ. Nontuberculous mycobacteria-overview. *Microbiol Spectr*. (2017) 5:1–7. doi: 10.1128/microbiolspec.TNMI7-0024-2016

4. Ryu YJ, Koh WJ, Daley CL. Diagnosis and treatment of nontuberculous mycobacterial lung disease: Clinicians' perspectives. *Tuberc Respir Dis (Seoul)*. (2016) 79:74–84. doi: 10.4046/trd.2016.79.2.74

5. Kwon YS, Koh WJ. Diagnosis and treatment of nontuberculous mycobacterial lung disease. *J Korean Med Sci*. (2016) 31:649–59. doi: 10.3346/jkms.2016.31.5.649

6. Chinese Society for Tuberculosis. Guidelines for the diagnosis and treatment of nontuberculous mycobacteriosis. *Chin J Tubere Respir Dis*. (2020) 43:918–46. doi: 10.3760/cma.j.cn112147-20200508-00570

7. Inderlied CB, Kemper CA, Bermudez LE. The *Mycobacterium avium* complex. *Clin Microbiol Rev*. (1993) 6:266–310. doi: 10.1128/CMR.6.3.266

8. Prince DS, Peterson DD, Steiner RM, Gottlieb JE, Scott R, Israel HL, et al. Infection with *Mycobacterium avium* complex in patients without predisposing conditions. *N Engl J Med*. (1989) 321:863–8. doi: 10.1056/NEJM198909283211304

9. Adelman MH, Addrizzo-Harris DJ. Management of nontuberculous mycobacterial pulmonary disease. *Curr Opin Pulm Med*. (2018) 24:212–9. doi: 10.1097/MCP.0000000000000473

10. American Journal of Respiratory and Critical Care Medicine. Diagnosis and treatment of disease caused by nontuberculous mycobacteria. This official statement of the American Thoracic Society was approved by the Board of Directors, March 1997. Medical Section of the American Lung Association. *Am J Respir Crit Care Med*. 156:S1–S25. doi: 10.1164/ajrccm.156.2.atsstatement

11. Fujita J, Kishimoto T, Ohtsuki Y, Shigeto E, Ohnishi T, Shiode M, et al. Clinical features of eleven cases of *Mycobacterium avium*-intracellulare complex pulmonary disease associated with pneumoconiosis. *Respir Med*. (2004) 98:721–5. doi: 10.1016/j.rmed.2004.02.011

12. Olivier KN, Weber DJ, Wallace RJ Jr, Faiz AR, Lee JH, Zhang Y, et al. Nontuberculous mycobacteria. I: multicenter prevalence study in cystic fibrosis. *Am J Respir Crit Care Med*. (2003) 167:828–34. doi: 10.1164/rccm.200207-678OC

13. Watanabe K, Fujimura M, Kasahara K, Yasui M, Myou S, Watanabe A, et al. Characteristics of pulmonary *Mycobacterium Avium*-Intracellulare complex (MAC) infection in comparison with those of tuberculosis. *Respir Med*. (2003) 97:654–9. doi: 10.1053/rmed.2003.1496

14. Martins AB, Matos ED, Lemos AC. Infection with the *Mycobacterium Avium* complex in patients without predisposing conditions: a case report and literature review. *Braz J Infect Dis*. (2005) 9:173–9. doi: 10.1590/S1413-86702005000200009

15. Zhu H, Zhu M, Lei J-H, Xiao Y-L, Zhao L-M. Metagenomic next-generation sequencing can clinch diagnosis of non-tuberculous mycobacterial infections: a case report. *Front Med*. (2021) 8:679755. doi: 10.3389/fmed.2021.679755

16. Liu Y, Ma X, Chen J, Wang H, Yu Z. Nontuberculous mycobacteria by metagenomic next-generation sequencing: three cases reports and literature review. *Front Public Health*. (2022) 10:972280. doi: 10.3389/fpubh.2022.972280

17. Jain D, Ghosh S, Teixeira L, Mukhopadhyay S. Pathology of pulmonary tuberculosis and non-tuberculous mycobacterial lung disease: facts, misconceptions, and practical tips for pathologists. *Semin Diagn Pathol*. (2017) 34:518–29. doi: 10.1053/j.semdp.2017.06.003

18. Tang S, Gao W. *Clinical Tuberculology (version two)*. Beijing: People's Health Publishing House (2019).

19. Kwon YS, Koh WJ. Diagnosis of pulmonary tuberculosis and nontuberculous mycobacterial lung disease in Korea. *Tuberc Respir Dis (Seoul)*. (2014) 77:1–5. doi: 10.4046/trd.2014.77.1.1

20. Kodaka N, Nakano C, Oshio T, Watanabe K, Niitsuma K, Imaizumi C, et al. Association between serum anti-Glycopeptidolipid-Core Iga antibody titers and clinical characteristics of *Mycobacterium Avium* complex pulmonary disease. *Int J Infect Dis*. (2021) 109:155–9. doi: 10.1016/j.ijid.2021.06.042

21. Huang H. Species identification technology of non-tuberculous mycobacteria. *Chinese Med J-Peking*. (2016) 51:155–9. doi: 10.3969/j.issn.1008-1070.2016.03.004

22. Fangous MS, Mougari F, Gouriou S, Calvez E, Raskine L, Cambau E, et al. Classification algorithm for subspecies identification within the *Mycobacterium Abscessus* species, based on matrix-assisted laser desorption ionization-time of flight mass spectrometry. *J Clin Microbiol*. (2014) 52:3362–9. doi: 10.1128/JCM.00788-14

23. Rodríguez-Sánchez B, Ruiz-Serrano MJ, Marín M, López Roa P, Rodríguez-Créixems M, Bouza E, et al. Evaluation of matrix-assisted laser desorption ionization-time of flight mass spectrometry for identification of nontuberculous mycobacteria from clinical isolates. *J Clin Microbiol*. (2016) 54:1929. doi: 10.1128/JCM.00815-16

24. Zhou X, Wu H, Ruan Q, Jiang N, Chen X, Shen Y, et al. Clinical evaluation of diagnosis efficacy of active *mycobacterium tuberculosis* complex infection via metagenomic next-generation sequencing of direct clinical samples. *Front Cell Infect Microbiol*. (2019) 9:351. doi: 10.3389/fcimb.2019.00351

25. Huang Z, Zhang C, Fang X, Li W, Zhang C, Zhang W, et al. Identification of musculoskeletal infection with non-tuberculous mycobacterium using metagenomic sequencing. *J Infect*. (2019) 78:158–69. doi: 10.1016/j.jinf.2018.10.002

frontiers | Frontiers in Medicine

TYPE Case Report
PUBLISHED 27 November 2023
DOI 10.3389/fmed.2023.1265373

OPEN ACCESS

EDITED BY
Santi Nolasco,
University of Catania, Italy

REVIEWED BY
Alessandro Libra,
Policlinico "G. Rodolico-San Marco" University Hospital, Italy
Mohamed Rahouma,
NewYork-Presbyterian, United States

*CORRESPONDENCE
Zhi-Ping Deng
✉ dengzp1016@163.com

†These authors have contributed equally to this work

RECEIVED 22 July 2023
ACCEPTED 07 November 2023
PUBLISHED 27 November 2023

CITATION
Wu H-M, Wen Y-L, He X-Y and Deng Z-P (2023) Selective bronchial occlusion for the prevention of pneumothorax after transbronchial lung cryobiopsy in a pulmonary alveolar proteinosis patient: a case report. *Front. Med.* 10:1265373.
doi: 10.3389/fmed.2023.1265373

Selective bronchial occlusion for the prevention of pneumothorax after transbronchial lung cryobiopsy in a pulmonary alveolar proteinosis patient: a case report

Hua-Man Wu†, You-Li Wen†, Xiao-Yu He and Zhi-Ping Deng*

Department of Respiratory and Critical Care Medicine, Zigong First People's Hospital, Zigong, Sichuan, China

The diagnosis of pulmonary alveolar proteinosis (PAP) is based on biopsies. Compared with other methods of taking biopsies, transbronchial lung cryobiopsy (TBLC) has a higher diagnostic rate and the likelihood of pneumothorax. Selective bronchial occlusion (SBO) is an effective technique for treating intractable pneumothorax. However, there are no data available about SBO for the prevention of pneumothorax after TBLC in a PAP patient. A 49-year-old man complained of recurrent cough and tachypnea, and his symptoms did not fully resolve until the diagnosis was confirmed, and he was treated with whole lung lavage. Our patient was ultimately diagnosed with PAP by TBLC but not multiple tests for the bronchoalveolar lavage fluid (BALF). The patient was discharged quickly after whole lung lavage due to the fact that he did not develop pneumothorax under SBO. This case illustrates that TBLC is a supplementary examination for PAP, especially for those in whom BALF results fail to confirm a diagnosis. Moreover, our report highlights that SBO is necessary to effectively prevent pneumothorax during and after multiple TBLCs in PAP patients.

KEYWORDS

pulmonary alveolar proteinosis, transbronchial lung cryobiopsy, selective bronchial occlusion, diagnosis, case report

1 Introduction

Pulmonary alveolar proteinosis (PAP) is a diffuse lung disorder, mainly characterized by surfactant lipids and proteins in alveolar macrophages and alveoli due to defective clearance by alveolar macrophages, resulting in impaired gas exchange (1). Pathological diagnosis which is based on bronchoalveolar lavage (BAL) or biopsies is often required for diagnosing PAP (2). Compared with other methods of taking biopsies, transbronchial lung cryobiopsy (TBLC) has a higher diagnostic rate and manageable complications (3, 4). However, pneumothorax, one of the complications, occurred in 6–9.4% of patients after TBLC (4–6). A number of studies have shown that the application of various materials for occlusion after lung biopsy can reduce the risk of pneumothorax (7–9). Therefore, we attempted to perform SBO immediately at the end of TBLC to prevent the occurrence of pneumothorax.

There are some studies on PAP; however, there are no data available about selective bronchial occlusion (SBO) for the prevention of pneumothorax after TBLC in PAP patients. Here, we report such a rare case with a literature review.

2 Case report

A 49-year-old man was admitted to the Department of Respiratory and Critical Care Medicine due to recurrent cough and tachypnea for more than 1 year, and the relapse worsened for 3 months. At first, the patient was treated with cefprozil, dextromethorphan hydrobromide, and montelukast in other hospitals, but his symptoms did not improve. Subsequently, the patient went to several hospitals and had symptomatic treatment, the symptoms were slightly relieved, but the symptoms repeated immediately after the drugs were discontinued. Before 3 months of admission, his symptoms were getting progressively worse.

He was afebrile but tachypneic (respiratory rate 24 breaths per minute), with room air oxygen saturation of 87% and blood pressure of 104/53 mmHg. Breath sounds in both lungs were rough, with scattered moist rales in both lower lungs. He is a farmer and has a smoking history of more than 20 years.

A year ago, pulmonary computed tomography (CT) found interstitial inflammation in both lungs, but the IgM antibodies of respiratory pathogens were negative (respiratory syncytial virus, adenovirus, influenza virus, *chlamydia pneumoniae*, *legionella pneumophila*, *mycoplasma pneumoniae*, coxsackie virus, and enteric cytopathic human orphan virus). The pulmonary function test revealed that the percentage of forced vital capacity to the predicted value (FVC%), the percentage of forced expiratory volume in 1 second to the predicted value (FEV_1%), FEV_1/FVC, and diffusion capacity of lung carbon monoxide (DLCO) were 75.1, 74.1, 80.10, and 44.8%, respectively. The bronchoalveolar lavage fluid (BALF) was not milky in appearance, and the BALF cell analysis revealed *mycobacterium tuberculosis* DNA and non-*mycobacterium tuberculosis* were negative. At the same time, BALF samples were sent to an external clinical laboratory for metagenomic next-generation sequencing and pathological diagnosis. However, all pathogens of the number of sequences were low and had no diagnostic significance, pathological examination showed a few columnar epithelial cells and histiocytes, and periodic acid–Schiff (PAS) was negative. Moreover, the results of the patient's two PAS by testing BALF samples at other hospitals prior to this admission were negative.

After this admission, initial investigations revealed normal renal and liver functions, D-dimer, coagulation function, and B-type natriuretic peptide and electrolyte. We further improved other examinations and found that anti-extracted nuclear antigens or antibodies, anti-cyclic citrullinated peptide, anti-neutrophil cytoplasmic antibodies, anti-O antibody, immunoglobulin E, and rheumatoid factor were negative. Preliminary consideration is interstitial pulmonary disease with infection. Therefore, he was given intravenous piperacillin–tazobactam (4.5 g each time, q8h) and methylprednisolone sodium succinate (40 mg, q12h). In addition, other treatments were used to improve symptoms.

Simultaneously, white cells, high sensitivity C-reactive protein, erythrocyte sedimentation rate, procalcitonin, and sputum examination were normal. The results of serum (1–3)-β-D-glucan and *Aspergillus* galactomannan were negative. However, arterial blood gas revealed a pH of 7.42 (7.35–7.45), $PaCO_2$ 36 mmHg (35–45 mmHg), and PaO_2 63 mmHg (80–100 mmHg). Lactate dehydrogenase (LDH) and alpha-hydroxybutyrate dehydrogenase (α-HBDH) were 334.0 U/L (120–250 U/L) and 231 U/L (72–182 U/L), respectively. Lipid profile revealed total cholesterol and low-density lipoprotein were 6.74 mmol/L (<5.17 mmol/L) and 4.53 mmol/L (0.00–3.37 mmol/L), respectively. Color Doppler echocardiography showed mild aortic regurgitation, minimal mitral regurgitation, normal left ventricular systolic function, and decreased diastolic function. In the detection of tumor markers, serum cancer antigen 15-3(CA15-3), carcinoembryonic antigen (CEA), cytokeratin 19 fragment (CYFRA21-1), neuron-specific enolase (NSE), and progastrin-releasing peptide (ProGRP) were slightly increased, with 54.9 U/mL (0-30 U/mL), 8.94 ng/mL (0–4.5 ng/mL), 26.1 ng/mL (0–3.3 ng/mL), 24.6 ng/mL (0-18 ng/mL) and 73.8 pg./mL (0–67.42 pg./mL), respectively. Pulmonary high-resolution CT (HRCT) detected ground glass opacity and patchy shadow on bilateral lung, showing a crazy-paving pattern, mainly in the lower lobes (Figures 1A,B).

Based on the clinical suspicion of PAP, we performed fiberoptic bronchoscopy again and collected BALF samples for examination, but the results were the same as a year ago. Considering a diagnosis of PAP, he received TBLC and SBO which consisted of tranexamic acid of 10 mL, thrombin of 500 IU, and cryoprecipitate of 2 U for the prevention of pneumothorax. He underwent mechanical ventilation under intravenous general anesthesia and electrocardiographic monitoring and a 50% fraction of inspired oxygen. Combined with the situation of chest CT, a balloon was placed in the outer basal segment of the right lower lobe, and a cryoprobe was placed in the anterior subsegment, posterior subsegment, outer basal segment, and posterior basal segment. After 5 s of freezing, four pieces of lung tissue with a size of approximately 3–8 mm were removed, and then the local area was squeezed by a balloon, and the plugging agent was injected in time. After squeezing for 2 min, the bronchoscope was pulled out after examination of the bronchus which showed there was no bleeding or other complications. Pathological examination showed pink particles and needle-like fissures in alveolar dilation, PAS was positive, and Congo red stain was negative (Figure 2).

We performed whole lung lavage immediately after the patient was clearly diagnosed. During the procedure, the cloudy milk liquid is irrigated until the collected liquid is clear. After that, the patient was given cefoxitin (2 g, q8h, ivgtt) to prevent infection and symptomatic treatment. Reexamination of pulmonary function showed that FVC%, FEV_1%, FEV_1/FVC, and DLCO were 95.2, 100.0, 85.38, and 42.3%, respectively. His symptoms improved significantly, and he was discharged from hospital 2 days later.

Abbreviations: PAP, pulmonary alveolar proteinosis; TBLC, transbronchial lung cryobiopsy; SBO, selective bronchial occlusion; FVC%, the percentage of forced vital capacity to the predicted value; FEV_1%, the percentage of forced expiratory volume in one second to the predicted value; DLCO, diffusion capacity of lung carbon monoxide; BALF, bronchoalveolar lavage fluid; CT, computed tomography; PAS, periodic acid–Schiff; LDH, lactate dehydrogenase; α-HBDH, alpha-hydroxybutyrate dehydrogenase; CA15-3, cancer antigen 15–3; CEA, carcinoembryonic antigen; CYFRA21-1, cytokeratin 19 fragment; NSE, neuron-specific enolase; ProGRP, progastrin-releasing peptide; HRCT, high-resolution computed tomography.

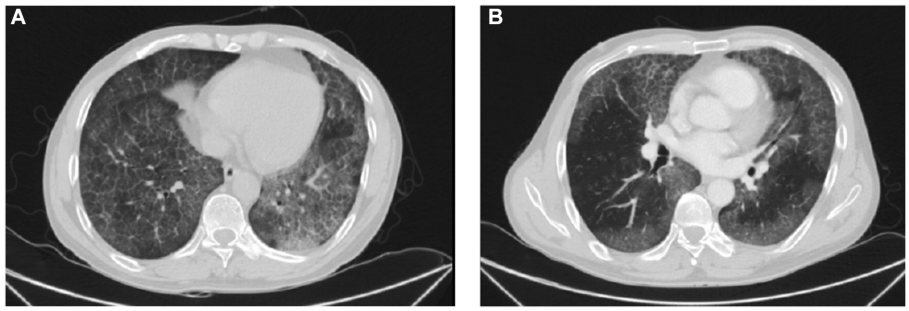

FIGURE 1
HRCT images. **(A,B)** Ground glass opacity and patchy shadow on bilateral lung, showing a crazy-paving pattern, mainly in the lower lobes.

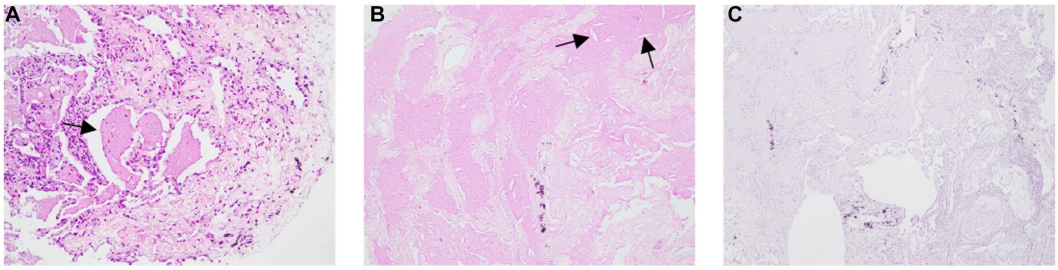

FIGURE 2
Pathological examination showing pink particles and needle-like fissures in alveolar dilation. **(B)** PAS was positive, **(C)** Congo red stain was negative.

3 Discussion

In our case, a diagnosis of PAP was confirmed after TBLC. The patient mainly presented with recurrent cough and tachypnea, which gradually got worse. His symptoms did not fully resolve until the diagnosis was confirmed, and he was treated with whole lung lavage. His lung function also improved although diffusing capacity was not ameliorated. Obviously, a clear diagnosis is particularly important, but our patient was not diagnosed after multiple tests for BALF.

It is well known that PAP involves bronchioles and terminal bronchioles, excessive deposition of protein-like substances in alveoli and pulmonary interstitial fibrosis, which can lead to compensatory emphysema and subpleural bulla. Therefore, TBLC is more likely to lead to pneumothorax or even intractable pneumothorax in PAP patients. TBLC inherits a higher risk for pneumothorax than other bronchoscopic biopsy techniques (10). The patient had high-risk factors for pneumothorax, such as multiple previous TBLC procedures, a history of severe cough (11), large radiological fibrotic lesion (12), and undergoing mechanical ventilation under intravenous general anesthesia (13). A previous study suggested that SBO is an effective technique for treating intractable pneumothorax (14–16). SBO includes a plugging agent and plugging device, and the former can be dissolved and absorbed, but the latter needs to be removed after the cure of pneumothorax. Therefore, in order to prevent patients from developing pneumothorax during or after the operation of TBLC, a plugging agent was selected to seal the sampling site, with a significant effect. However, there are no previous studies on SBO for the prevention of pneumothorax after TBLC in a PAP patient. Our case report represents a chance to help fill the gap of knowledge relative to it.

It was reported that LDH is a predictor of the severity (17). Meanwhile, our patient's α-HBDH level is high, which may be a potential indicator for the severity of PAP disease although no studies have reported it. Moreover, serum tumor markers such as CEA (18), CYFRA21-1 (19), and NSE (20) were also significantly associated with the severity of PAP. In our case, LDH, α-HBDH, CEA, CYFRA21-1, and NSE were only slightly increased, and all indicated a favorable prognosis. Although CA15-3 and ProGRP were also mildly elevated, there was no indication of gastrointestinal neoplasms, and the clinical significance of their rise in PAP patients is unclear.

There are several limitations to our study. We did not test for autoantibodies against granulocyte-macrophage colony-stimulating factor. Additionally, given conclusions were based on case reports, and multi-center and large-sample data are needed for verification in future.

In summary, TBLC is a supplementary examination for PAP, especially for those in whom BALF results fail to confirm a diagnosis. Furthermore, our report highlights that SBO is necessary to effectively prevent pneumothorax during and after TBLC in PAP patients.

Data availability statement

The original contributions presented in the study are included in the article/supplementary material, further inquiries can be directed to the corresponding author.

Ethics statement

The studies involving humans were approved by Zigong First People's Hospital Ethics Committee. The studies were conducted in accordance with the local legislation and institutional requirements. The participants provided their written informed consent to participate in this study. Written informed consent was obtained from the individual(s) for the publication of any potentially identifiable images or data included in this article.

Author contributions

H-MW: Data curation, Investigation, Methodology, Writing – original draft. Y-LW: Methodology, Resources, Supervision, Writing – review & editing. X-YH: Writing – original draft. Z-PD: Methodology, Resources, Supervision, Validation, Visualization, Writing – review & editing.

Funding

The author(s) declare that no financial support was received for the research, authorship, and/or publication of this article.

Conflict of interest

The authors declare that the research was conducted in the absence of any commercial or financial relationships that could be construed as a potential conflict of interest.

Publisher's note

References

1. Beeckmans H, Ambrocio GPL, Bos S, Vermaut A, Geudens V, Vanstapel A, et al. Allogeneic hematopoietic stem cell transplantation after prior lung transplantation for hereditary pulmonary alveolar proteinosis: a case report. *Front Immunol*. (2022) 13:931153. doi: 10.3389/fimmu.2022.931153

2. Iftikhar H, Nair GB, Kumar A. Update on diagnosis and treatment of adult pulmonary alveolar proteinosis. *Ther Clin Risk Manag*. (2021) 17:701–10. doi: 10.2147/TCRM.S193884

3. Pajares V, Nunez-Delgado M, Bonet G, Pérez-Pallarés J, Martínez R, Cubero N, et al. Transbronchial biopsy results according to diffuse interstitial lung disease classification. Cryobiopsy versus forceps: MULTICRIO study. *PLoS One*. (2020) 15:e0239114. doi: 10.1371/journal.pone.0239114

4. Kheir F, Uribe Becerra JP, Bissell B, Ghazipura M, Herman D, Hon SM, et al. Transbronchial lung Cryobiopsy in patients with interstitial lung disease: a systematic review. *Ann Am Thorac Soc*. (2022) 19:1193–202. doi: 10.1513/AnnalsATS.202102-198OC

5. Herth FJ, Mayer M, Thiboutot J, Kapp CM, Sun J, Zhang X, et al. Safety and performance of transbronchial Cryobiopsy for parenchymal lung lesions. *Chest*. (2021) 160:1512–9. doi: 10.1016/j.chest.2021.04.063

6. Sethi J, Ali MS, Mohananey D, Nanchal R, Maldonado F, Musani A. Are transbronchial Cryobiopsies ready for prime time?: a systematic review and meta-analysis. *J Bronchology Interv Pulmonol*. (2019) 26:22–32. doi: 10.1097/LBR.0000000000000519

7. Grange R, Sarkissian R, Bayle-Bleuez S, Tissot C, Tiffet O, Barral FG, et al. Preventive tract embolization with gelatin sponge slurry is safe and considerably reduces pneumothorax after CT-guided lung biopsy with use of large 16-18 coaxial needles. *Br J Radiol*. (2022) 95:20210869. doi: 10.1259/bjr.20210869

8. Malone LJ, Stanfill RM, Wang H, Fahey KM, Bertino RE. Effect of intraparenchymal blood patch on rates of pneumothorax and pneumothorax requiring chest tube placement after percutaneous lung biopsy. *AJR Am J Roentgenol*. (2013) 200:1238–43. doi: 10.2214/AJR.12.8980

9. Huo YR, Chan MV, Habib AR, Lui I, Ridley L. Post-biopsy manoeuvres to reduce pneumothorax incidence in CT-guided transthoracic lung biopsies: a systematic review and meta-analysis. *Cardiovasc Intervent Radiol*. (2019) 42:1062–72. doi: 10.1007/s00270-019-02196-8

10. Hetzel J, Eberhardt R, Petermann C, Gesierich W, Darwiche K, Hagmeyer L, et al. Bleeding risk of transbronchial cryobiopsy compared to transbronchial forceps biopsy in interstitial lung disease - a prospective, randomized, multicentre cross-over trial. *Respir Res*. (2019) 20:140. doi: 10.1186/s12931-019-1091-1

11. Mononen M, Saari E, Hasala H, Kettunen HP, Suoranta S, Nurmi H, et al. Risk factors of clinically significant complications in transbronchial lung cryobiopsy: a prospective multi-center study. *Respir Med*. (2022) 200:106922. doi: 10.1016/j.rmed.2022.106922

12. Ravaglia C, Wells AU, Tomassetti S, Gurioli C, Gurioli C, Dubini A, et al. Diagnostic yield and risk/benefit analysis of trans-bronchial lung cryobiopsy in diffuse parenchymal lung diseases: a large cohort of 699 patients. *BMC Pulm Med*. (2019) 19:16. doi: 10.1186/s12890-019-0780-3

13. Ravaglia C, Bonifazi M, Wells AU, Tomassetti S, Gurioli C, Piciucchi S, et al. Safety and diagnostic yield of transbronchial lung Cryobiopsy in diffuse parenchymal lung diseases: a comparative study versus video-assisted thoracoscopic lung biopsy and a systematic review of the literature. *Respiration*. (2016) 91:215–27. doi: 10.1159/000444089

14. Zeng Y, Hong M, Zhang H, et al. Transbronchoscopic selective bronchial occlusion for intractable pneumothorax. *Respirology*. (2010) 15:168–71. doi: 10.1111/j.1440-1843.2009.01650.x

15. Zeng YM, Hong ML, Zhang HP, Yang DY, Chen XY, Zhuang XB, et al. Transbronchoscopic balloon detection and selective bronchial occlusion for intractable pneumothorax. *Zhonghua Jie He He Hu Xi Za Zhi*. (2009) 32:274–7.

16. Himeji D, Tanaka GI, Fukuyama C, Shiiba R, Yamanaka A, Beppu K. Clinical evaluation of endoscopic bronchial occlusion with an endobronchial Watanabe spigot for the Management of Intractable Pneumothorax, pyothorax with bronchial fistula, and postoperative air leakage. *Intern Med*. (2020) 59:1835–9. doi: 10.2169/internalmedicine.3900-19

17. Zhang N, Jiang Z, Shao C. Pulmonary alveolar proteinosis: a single center retrospective analysis of 14 cases. *Med Clin (Barc)*. (2021) 156:555–7. doi: 10.1016/j.medcli.2020.05.066

18. Yang Y, Xu M, Huang H, Jiang X, Gong K, Liu Y, et al. Serum carcinoembryonic antigen elevation in benign lung diseases. *Sci Rep*. (2021) 11:19044. doi: 10.1038/s41598-021-98513-8

19. Bai JW, Gu SY, Sun XL, Lu HW, Liang S, Xu JF. CYFRA21-1 is a more sensitive biomarker to assess the severity of pulmonary alveolar proteinosis. *BMC Pulm Med*. (2022) 22:2. doi: 10.1186/s12890-021-01795-x

20. Shi S, Chen L, Qiu X, Zhao Q, Xiao Y, Yan X. Valuable serum markers in pulmonary alveolar proteinosis. *Dis Markers*. (2019) 2019:1–6. doi: 10.1155/2019/9709531

frontiers | Frontiers in Medicine

TYPE Case Report
PUBLISHED 11 January 2024
DOI 10.3389/fmed.2023.1323222

OPEN ACCESS

EDITED BY
Santi Nolasco,
University of Catania, Italy

REVIEWED BY
Apurva Patel,
Gujarat Cancer & Research Institute, India
Murat Yalçınsoy,
İnönü University, Türkiye
Hakki Ulutas,
İzmir University of Economics, Türkiye

*CORRESPONDENCE
Lifeng Wang
✉ lifengwang@nju.edu.cn

RECEIVED 17 October 2023
ACCEPTED 28 December 2023
PUBLISHED 11 January 2024

CITATION
Xu M, Sun Q, Lv X, Chen F, Su S and Wang L (2024) Sinus metastasis of lung adenocarcinoma: a case report. *Front. Med.* 10:1323222. doi: 10.3389/fmed.2023.1323222

Sinus metastasis of lung adenocarcinoma: a case report

Mingyuan Xu[1], Qi Sun[2], Xin Lv[1], Fangjun Chen[1], Shu Su[1] and Lifeng Wang[1]*

[1]Comprehensive Cancer Center, Nanjing Drum Tower Hospital, Nanjing, Jiangsu Province, China, [2]Department of Pathology, Nanjing Drum Tower Hospital, Nanjing, Jiangsu Province, China

Metastatic carcinoma of the paranasal sinuses in lung cancer is an extremely uncommon condition. We report here a 57-year-old female patient with epidermal growth factor receptor (EGFR)-positive stage IV non-small cell lung cancer (NSCLC) with multiple bone metastases. After resistance to second- and third-generation EGFR-tyrosine kinase inhibitors (TKIs), the patient presented with headache accompanied by progressively enlarging lesions of the nasal cavity on CT scan. Further endoscopic sinus neoplasmectomy confirmed sinus metastasis of lung adenocarcinoma. Although subsequent chemotherapy and immunotherapy were both administered, the disease continued to progress, and the patient passed away 21 months after diagnosis. Combined with real-time dynamic next-generation sequencing (NGS) during the different generations of EGFR-TKI treatments and dynamic tumour microenvironment analysis, we discussed the clinical manifestations of sinus metastasis and the molecular biology and tumour immune microenvironment changes after resistance to the second-and third- generation of EGFR-TKI therapy.

KEYWORDS

lung adenocarcinoma, sinus metastasis, next-generation sequencing, EGFR-TKI, immune microenvironment

Introduction

Lung cancer is a disease prone to multiple systemic metastases, common metastases including brain, bone, liver, lymph nodes, adrenal glands, thoracic cavity, and so on (1). Clinically, it is very rare for lung cancer to metastasize to unusual sites, such as the paranasal sinuses. Here, we report a patient with advanced lung cancer with EGFR-sensitive mutation who presented with recurring headaches during sequential second- and third-generation EGFR-TKI therapy, and it turned out to be sinus metastasis of lung adenocarcinoma by the following imaging and pathological examination. Unfortunately, the patient did not respond well to subsequent platinum-based doublet chemotherapy or immune therapy. Previous clinical data showed that EGFR-positive patients have a limited response to immunotherapy, and the underlying mechanism is uncertain (2, 3). Based on the patient's multiple prebiopsy tissue samples, dynamic NGS tests and the tumour microenvironment were further analyzed. We discuss this rare metastasis of lung cancer in terms of molecular biology, tumour immune microenvironment characteristics, and possible effects of sequential treatments on the evolution of tumour biological features.

Case presentation

A 57-year-old never-smoking female was admitted to our hospital with a paroxysmal headache complaint in January 2020. Magnetic resonance imaging (MRI) of the brain showed no obvious abnormality, and brain computed tomography (CT) showed no mass in the paranasal sinus. Enhanced CT scans of the chest revealed a left hilar mass with mediastinal and left hilar lymphadenopathy. Further transbronchial biopsy confirmed non-small cell lung cancer (NOS). Emission computed tomography (ECT) of the bone confirmed multiple bone metastases from the tumour. Due to the lack of enough tumour tissues for molecular analysis, next-generation sequencing (NGS) of blood samples showed EGFR exon 19 deletion. Hence, the patient was diagnosed with EGFR-positive stage IV non-small cell lung cancer (bone, NOS). Afatinib 40 mg daily was initiated as first-line treatment starting in February 2020, and 5 months later, it was further reduced to 30 mg due to the grade III mucocutaneous reaction. The headache was relieved after treatment, and the best response was partial response (PR) according to the Response Evaluation Criteria in Solid Tumour version 1.1 (RECIST 1.1). The disease progressed after 6 months, with repeat CT scans showing new multiple lesions in the liver. Further liver biopsy demonstrated metastatic adenocarcinoma, and PD-L1 expression on tumour cells (clone: 22C3) assessed on the basis of tumour proportion score (TPS) was <1%. NGS of liver tissues revealed the original EGFR exon 19 deletion and the exon 20 T790M mutation. Osimertinib (80 mg daily) was administered as a second-line treatment in August 2020. The patient had a PR and 7 months PFS to Osimertinib treatment. However, in April 2021, the patient complained of headache aggravation and lumbago. CT showed new liver metastasis and osteolytic lesions of the lumbar spine, and repeat ECT confirmed the progression of bone lesions. The patient then received doublet paclitaxel and platinum chemotherapy as the third-line treatment, as well as local radiotherapy of lumbar vertebra metastatic lesions (GTV 3 Gy/10 f) in April 2021. Since the lessening of headache pain, lumbar puncture was also performed with negative cerebrospinal fluid tests. In June 2021, a CT scan showed an enlarged lesion in the sinus. After ear, nose, and throat (ENT) consultation, local surgical treatment was suggested because of an unidentified sinus mass. In August 2021, nasal endoscopic sinus neoplasm resection was performed, and the postoperative pathological results demonstrated metastatic adenocarcinoma of lung origin with PD-L1 (22C3)-the negative expression of tumour cells (TPS<1%). Further NGS of sinus tissue revealed EGFR exon 20 cis-C797S missense and EGFR exon 19 deletion. In August 2021, enhanced CT showed extensive disease progression in the bilateral lungs, and anlotinib, a multitarget VEGFR TKI plus nivolumab, was administered as the fourth-line therapy. Unfortunately, the patient did not respond to the latter therapy and died in October 2021 with an overall survival (OS) of 21 months (Figure 1).

Discussion

Lung cancer is the leading cause of tumours worldwide, with the highest morbidity and mortality in China (4–7). Approximately 30–50% of lung cancer patients are diagnosed with stage IV disease, and the main sites of metastasis in non-small cell lung cancer (NSCLC) include the brain (47%), bone (36%), liver (22%), adrenal gland (15%), thoracic cavity (11%), and distant lymph nodes (10%) (8). Liver (35%) and brain (47%) metastases were common in patients with metastases from SCLC, whereas bone (39%) and respiratory (22%) metastases were common in adenocarcinoma (9). However, lung cancer metastasis to the paranasal sinuses is very rare. We searched PubMed[1] and CNKI[2] with the keyword lung cancer and paranasal sinus metastasis from 2001 to 2021, and only 10 cases of lung cancer metastasis to the paranasal sinuses were found (Table 1). All cases were non-small cell lung cancer with adenocarcinoma (8 cases) being the most common histological type and maxillary sinus (7 cases) being the most popular involved sites of these 10 patients, headache was the main symptom in 4 patients, nasal obstruction in 3 patients, epistaxis in 2 patients, nasal swelling in 2 patients and blurred vision in 2 patients. According to our search data, male is more likely to develop sinus metastases from lung cancer and 6 patients did not mention metastases from other sites, 3 had bone metastases, and 1 had brain metastases. In our case, the patient presented with headache at the time of initial diagnosis, when CT scans showed no definite sinus mass. During the patient's course of disease with recurrent symptoms of headache, brain or meningeal metastasis was once suspected clinically and closely observed, and finally, sinus metastasis of lung cancer was pathologically confirmed. When we retrospectively reviewed previous CT scans and found that the sinus mass progressed during sequential EGFR-TKI treatment, sinus metastasis should have been considered, especially in EGFR-positive patients with headache complaints and negative central nervous system tests. Intriguingly, the patient's duration of response to both afatinib (PFS 6 months) and (PFS 8 months) treatment was not as long, although she harboured the EGFR common sensitive mutation, exon 19 del. The persistence of EGFR high-copy number amplification combined with TP53 mutation during multiple dynamic tissue/peripheral blood genetic tests may be one of the main reasons for poor efficacy of EGFR-TKIs treatment (20) (Figure 2). Multiple studies have confirmed that TP53 mutation is a negative prognostic factor in NSCLC patients and a negative predictor of EGFR-TKI treatment in patients with EGFR mutation (20–23). Furthermore, TP53 mutations impact the natural history of EGFR-mutant NSCLC at least partially by allowing tolerance of a greater degree of genomic instability, which results in a higher somatic mutation burden and mutagenic potential (21, 23). EGFR amplification has been shown to be a poor prognostic factor in EGFR-mutated NSCLC patients treated with EGFR TKIs (24). In addition, during treatment with osimertinib, the EGFR exon 20 cis-C797S mutation was observed in plasma ctDNA before clinical imaging progression, suggesting the potential role of liquid monitoring in EGFR TKI resistance. Niederst identified a C797S resistance mutation and determined that the position of T790M affects the efficacy of therapeutic strategies (25). If the two mutations are in trans (on different alleles), a combination of first- and third-generation TKIs can inhibit EGFR. In contrast, if the two mutations are in cis (on the identical allele), the tumor cells are refractory to any of the EGFR TKIs that they tested as well as to the combination of first- and third-generation inhibitors. In contrast, if the two mutations are in cis (on the identical allele), the tumor cells are refractory to any of the EGFR TKIs that they tested as well as to the combination of first- and third-generation inhibitors. A study provides clinical evidence that combined targeted therapy of brigatinib and cetuximab could provide benefits and may potentially be an effective treatment strategy to improve

1 www.pubmed.ncbi.nlm.nih.gov
2 www.cnki.net

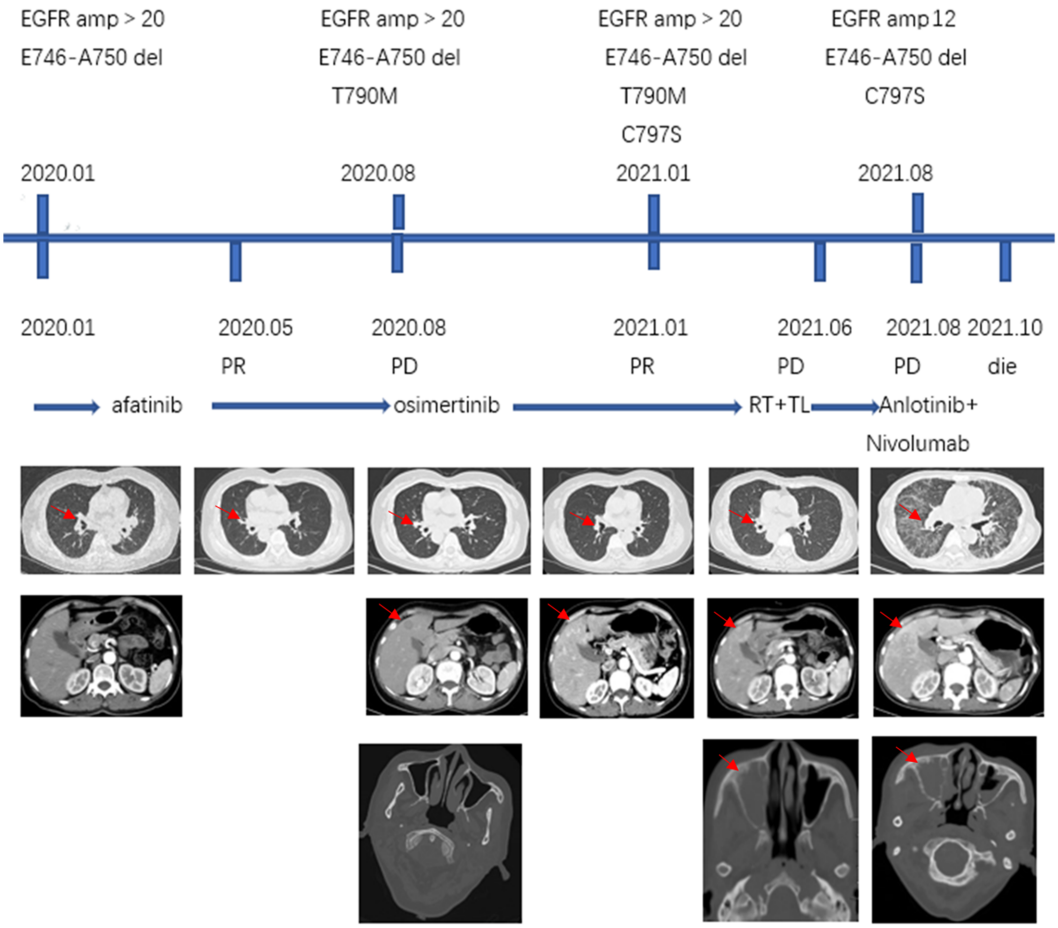

FIGURE 1
Treatment process: NGS results, treatment methods, CT (lung, abdomen, head; the red arrows on the first row of CT scans point to the lung lesions, the red arrow on the second row CT scans points to liver metastases and the red arrow on the third row CT scans points to sinus metastases). NGS, next-generation sequencing; amp, amplification; RT, radiation therapy; TL, paclitaxel liposome + lobaplatin.

survival outcomes of patients who acquired EGFR T790M-cis-C797S-mediated resistance to Osimertinib (26). However, there is no standard of care for NSCLC patients harbouring T790M-cis-C797S. Furthermore, loss of EGFR Exon 20 T790M was found after third-generation TKI resistance. Studies have shown that with the evolution of gene clones during EGFR-TKI treatment, there is loss of the T790M mutation, which may be accompanied by other gene mutations and is more conducive to the survival of drug-resistant clones during EGFR-TKI treatment. Patients without the T790M mutation or with EGFR C797S after osimertinib resistance usually have a worse clinical prognosis (27). In our case, loss of EGFR Exon 20 T790M and harbouring C797S are the main reasons for poor prognosis.

Although EGFR-mutant patients can benefit from EGFR TKIs to some extent, acquired resistance and efficient subsequent therapy are still unresolved. Recently, immunotherapy has opened a new avenue in many solid tumours, including lung cancer; however, current clinical studies have suggested that the efficacy of PD-1/PD-L1 immunotherapy is poor in NSCLC patients harbouring EGFR-sensitive mutations (2, 3). Further studies showed that the negative tumour microenvironment, including a lack of CD8+ T-cell infiltration (28), low levels of active cytokines (29), and high levels of immune-negative regulatory cells in EGFR-positive tumours, may be the underlying mechanism (30). Interestingly, the local tumour tissue microenvironment might be positively regulated by efficient EGFR TKI treatment, leading to infiltration of CD8+ T cells and an increased proportion of M1 macrophages. Thus, the exploration of the right timing of immunotherapy interventions may be the key to further improve the efficacy of immunotherapy in patients with EGFR mutations in the future (31). However, previous studies were mostly based on the use of first-generation EGFR TKIs, and the effect of third-generation EGFR TKIs on the tumour microenvironment is still unknown.

In our case, the patient did not respond to subsequent immunotherapy after resistance to osimertinib. To better understand the influence of third-generation EGFR TKIs on the TME and the possible reason for immune resistance, we found that CD8+ T-cell infiltration was consistently lacking in both the tumour parenchyma and stromal areas before and after osimertinib resistance, and the overall TME had characteristics of the immune desert type (Figure 3). Studies have shown that CD8+ T-cell density in tumour tissue has some correlation with the response and prognosis of patients to immunotherapy (32). In addition, we noticed that tumour-associated macrophages (TAMs) in the immune microenvironment of patients also changed in response to treatment with third-generation

TABLE 1 Reported cases of lung cancer with paranasal sinus metastasis, 2001–2022.

Year	Author	Histological type	Age/Sex	Involved sinus	Metastases symptoms	NGS	Outcome
2002	Zhang (10)	Squamous cell carcinoma	50/M	Paranasal	Nasal swelling epistaxis	NR	NR
2002	Clarkson (11)	Adenocarcinoma	79/F	frontal	Blurred vision Headache	NR	NR
2005	Rombaux (12)	Adenocarcinoma	71/M	frontal	Headache	NR	Survival (9mos)
2009	Chun-Ta Huang (13)	Adenocarcinoma	59/F	Paranasal	Nasal swelling	NR	Survival (2mos)
2010	Ma (14)	Adenocarcinoma	67/M	Maxillary	Epistaxis Hyposmia	NR	NR
2013	Luo (15)	Adenocarcinoma	61/M	Maxillary	Nasal obstruction Headache	NR	Survival (5 mos)
2015	Ates (16)	Adenocarcinoma	51/M	Maxillary	Blurred vision Eye pain	NR	NR
2016	Liang (17)	Adenocarcinoma	59/M	Maxillary	facial numbness Toothache	NR	NR
2016	Li (18)	Adenocarcinoma	46/F	Maxillary	Nasal obstruction	NR	NR
2021	Xu (19)	Adenocarcinoma	64/M	Sieve	Nasal obstruction Headache	EGFR mutations	Survival (13 mos)

Outcome: survival or follow-up period after presence of paranasal metastasis; F, female; M, male; NR, not reported; mos, months.

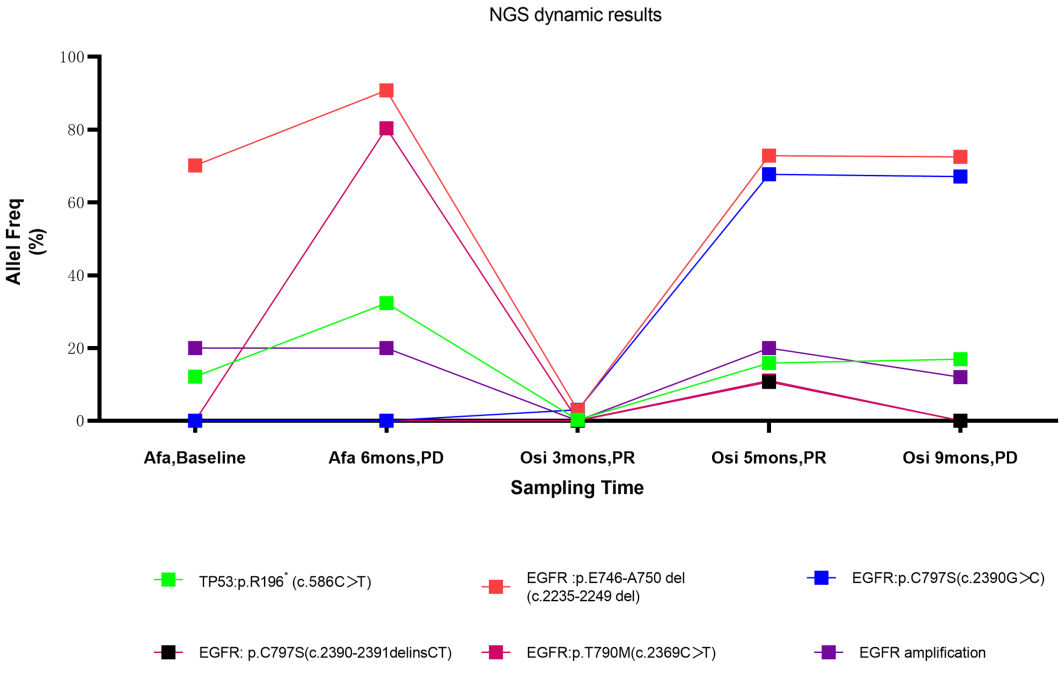

FIGURE 2
NGS changes in peripheral blood and tissue; Afa, Afatinib; Osi, Osimertinib; mons, months.

EGFR-TKIs. TAMs can be divided into the M1 type (antitumour) and M2 type (tumour-promoting) (33). The M1 type is activated by cytokines such as IFN-γ and produces proinflammatory and immunostimulatory cytokines such as IL-12 and IL-23, which are mainly involved in the inflammatory response and antitumour immune process and are related to good tumour prognosis. The M2 type, on the other hand, is activated by Th2-derived cytokines such as IL-4, IL-10, and IL-13 and mainly plays a tumour-promoting and immunosuppressive role. CD68 + HLA-DR+ cells are currently widely accepted as M1 markers and can be used to distinguish M1/2

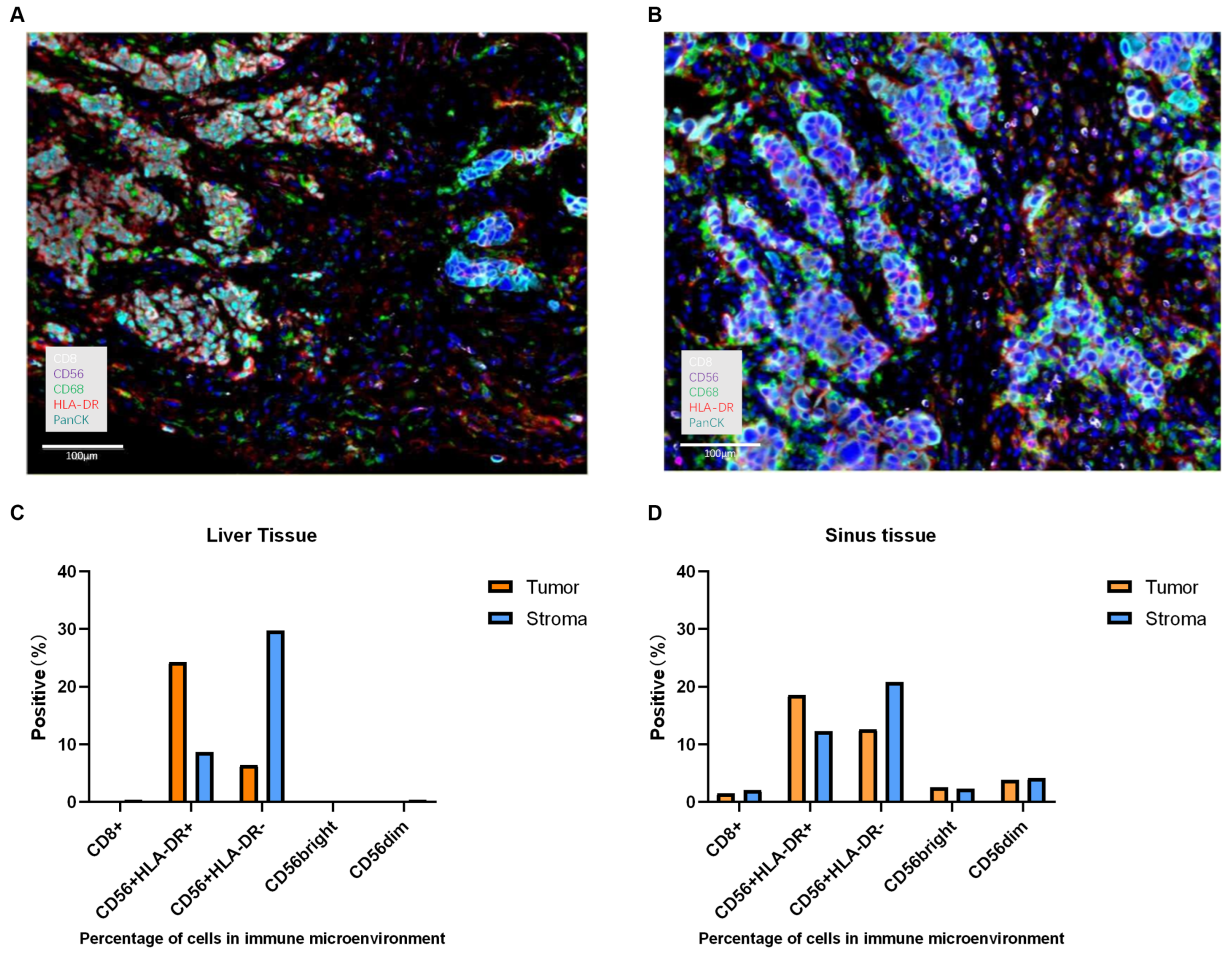

FIGURE 3
The histopathological characteristics of the tumour in the liver and sinus demonstrated by immunohistochemical staining. **(A)** expression level of the liver for CD8 (white), CD56 (purple), CD68 (green), HLA-DR (red), and Panck (cyan) was displayed in the immunohistochemical image (magnification, x100). **(B)** expression level of the sinuses for CD8 (white), CD56 (purple), CD68 (green), HLA-DR (red), and Panck (cyan) was displayed in the immunohistochemical image (magnification, x100). **(C)** Percentage of cells in the immune microenvironment of the liver. **(D)** Percentage of cells in the immune microenvironment of sinuses.

macrophages. In this patient, the proportion of positive M1 macrophages in the TME was significantly higher than that of negative M2 macrophages after second-generation EGFR TKI resistance. The proportion of negative M2 macrophages was significantly increased after third-generation EGFR TKI resistance. These results suggest that acquired resistance to osimertinib could lead to more immunoregulative features in the TME, combined with the immune desert phenotype of this patient, which also explains the lack of response of the patient to subsequent immunotherapy after the discovery of sinus metastases.

Conclusion

In summary, we report a rare case of sinus metastasis in NSCLC patients with EGFR-sensitive mutations. Clinically, the possibility of sinus metastasis should be considered in EGFR-positive patients with lung cancer, especially those with complaints of headache and negative central nervous system tests. We reviewed relevant literature and found that there are no characteristic clinical or radiologic features for metastatic sinus tumours; however, the diagnosis can be confirmed by histopathological examination of biopsied tumour sample. During the second-and third-generation EGFR TKIs, chemotherapy and immunotherapy treatment, we explained the reason why the second-and third-generation TKIs had difficulty maintaining long-term efficacy in this patient by real-time NGS detection based on both tumour tissues and peripheral blood and further verified the importance of peripheral blood ctDNA in prejudging early disease progression (34, 35). At the same time, we further analyzed the tumour microenvironment characteristics of patients after second-generation EGFR TKI and third-generation EGFR TKI resistance and found that the lack of CD8+ T-cell infiltration in tumour tissue and the increase in M2 macrophages after third-generation EGFR TKI resistance may be one of the main reasons for ineffective immunotherapy in patients.

Ethics statement

The studies involving humans were approved by Medical Ethics Committee of Drum Tower Hospital. The studies were conducted in

accordance with the local legislation and institutional requirements. The participants provided their written informed consent to participate in this study. Written informed consent was obtained from the individual(s) for the publication of any potentially identifiable images or data included in this article.

Author contributions

MX: Writing – original draft, Writing – review & editing. QS: Data curation, Writing – review & editing. XL: Data curation, Writing – review & editing. FC: Writing – review & editing. SS: Writing – review & editing. LW: Writing – original draft, Writing – review & editing.

Funding

The author (s) declare financial support was received for the research, authorship, and/or publication of this article. This work was fund by Nanjing health science and technology development key project (ZKX 23017).

Conflict of interest

The authors declare that the research was conducted in the absence of any commercial or financial relationships that could be construed as a potential conflict of interest.

Publisher's note

All claims expressed in this article are solely those of the authors and do not necessarily represent those of their affiliated organizations, or those of the publisher, the editors and the reviewers. Any product that may be evaluated in this article, or claim that may be made by its manufacturer, is not guaranteed or endorsed by the publisher.

References

1. Niu FY, Zhou Q, Yang JJ, Zhong WZ, Chen ZH, Deng W, et al. Distribution and prognosis of uncommon metastases from non-small cell lung Cancer. *BMC Cancer*. (2016) 16:16. doi: 10.1186/s12885-016-2169-5

2. Bruno D, Dowlati A. Immunotherapy in Egfr mutant non-small cell lung Cancer: when, who and how? *Transl Lung Cancer Res*. (2019) 8:710–4. doi: 10.21037/tlcr.2019.06.02

3. Lee CK, Man J, Lord S, Links M, Gebski V, Mok T, et al. Checkpoint inhibitors in metastatic Egfr-mutated non-small cell lung Cancer a Meta-analysis. *J Thorac Oncol*. (2017) 12:403–7. doi: 10.1016/j.jtho.2016.10.007

4. Siegel RL, Miller KD, Fuchs HE, Jemal A. Cancer statistics, 2021. *Ca-a Cancer J Clin*. (2021) 71:7–33. doi: 10.3322/caac.21654

5. Wu F, Wang L, Zhou C. Lung Cancer in China: current and Prospect. *Curr Opin Oncol*. (2021) 33:40–6. doi: 10.1097/cco.0000000000000703

6. Fan X, Zhang B, He Y, Zhou X, Zhang Y, Ma L, et al. Burden of disease due to Cancer-China, 2000-2019. *China Cdc Weekly*. (2022) 4:306–11. doi: 10.46234/ccdcw2022.036

7. Riihimaeki M, Hemminki A, Fallah M, Thomsen H, Sundquist K, Sundquist J, et al. Metastatic sites and survival in lung Cancer. *Lung Cancer*. (2014) 86:78–84. doi: 10.1016/j.lungcan.2014.07.020

8. Wang Z, Cheng Y, An T, Gao H, Wang K, Zhou Q, et al. Detection of Egfr mutations in plasma circulating tumour DNA as a selection criterion for first-line Gefitinib treatment in patients with advanced lung adenocarcinoma (benefit): a phase 2, single-arm, multicentre clinical trial. *Lancet Respir Med*. (2018) 6:681–90. doi: 10.1016/s2213-2600(18)30264-9

9. Canale M, Petracci E, Delmonte A, Bronte G, Chiadini E, Ludovini V, et al. Concomitant Tp53 mutation confers worse prognosis in Egfr-mutated non-small cell lung Cancer patients treated with Tkis. *J Clin Med*. (2020) 9:1047. doi: 10.3390/jcm9041047

10. Xu ZJ, Zhou M. Treatment of adenoid cystic carcinoma of sphenoid sinus with lung metastasis by Arotinib: a case report. *Zhonghua Zhong Liu Za Zhi*. (2020) 42:1054–5. doi: 10.3760/cma.j.cn112152-20191118-00746

11. Clarkson JHW, Kirkland PM, Mady S. Bronchogenic metastasis involving the frontal sinus and masquerading as a Pott's puffy tumour: a diagnostic pitfall. *Br J Oral Maxillofac Surg*. (2002) 40:440–1. doi: 10.1016/s0266-4356(02)00131-6

12. Rombaux P, Hamoir M, Liistro G, Bertrand B. Frontal sinus tumor as the first sign of adenocarcinoma of the lung. *Otolaryngol Head Neck Surg*. (2005) 132:816–7. doi: 10.1016/j.otohns.2004.09.070

13. Huang C-T, Hong R-L. Nasion swelling as the presenting symptom of lung adenocarcinoma. *J Thorac Oncol*. (2009) 4:555–8. doi: 10.1097/JTO.0b013e3181949f30

14. Ma HZ, Fang JG, Wang Q. Metastases to maxillary sinus of lung Cancer. *Chin Arch Otolaryngol Head Neck Surg*. (2010) 17:162. doi: 10.16066/j.1672-7002.2010.03.020

15. Luo XY, Xing SJ, Zeng WB, Deng WF, Xu JP, Chen YP, et al. A case report of nasal cavity and maxillary sinus metastasis of lung Cancer. *Cancer Res Prevent Treat*. (2013) 40:910–1.

16. Ates I, Yazici O, Ates H, Ozdemir N, Zengin N. Unusual metastases of lung Cancer: Bulbus oculi and maxillary sinus. *Exp Oncol*. (2015) 37:231–2. doi: 10.31768/2312-8852.2015.37(3):231-232

17. Liang W, Li Q, Zhang T. Distant metastases to maxillary sinus from an unknown lung Adenocarcin Oma: a cases report. *Lin Chung Er Bi Yan Hou Tou Jing Wai Ke Za Zhi*. (2016) 30:74–5.

18. Li WJ, Xue HX, You JQ, Chao CJ. Lung Adenocarcinoma Metastasis to Paranasal Sinus: A Case Report. *World J Clin Cases*. (2022) 10:5869–76. doi: 10.12998/wjcc.v10.i17.5869

19. Xu H, Cao YJ, Zhou NN, Qiao H, Zhong CS, Shan L. Misdiagnosis of lung Cancer with Sinonasal metastasis as the first symptom: a case report. *Chin J Clin Oncol*. (2021) 48:50–1.

20. Sun H, Liu SY, Zhou JY, Xu JT, Zhang HK, Yan HH, et al. Specific Tp53 subtype as biomarker for immune checkpoint inhibitors in lung adenocarcinoma. *EBioMedicine*. (2020) 60:60. doi: 10.1016/j.ebiom.2020.102990

21. Skoulidis F, Heymach JV. Co-occurring genomic alterations in non-small-cell lung Cancer biology and therapy. *Nat Rev Cancer*. (2019) 19:495–509. doi: 10.1038/s41568-019-0179-8

22. Aggarwal C, Davis CW, Mick R, Thompson JC, Ahmed S, Jeffries S, et al. Influence of Tp53 mutation on survival in patients with advanced Egfr-mutant non-small-cell lung Cancer. *JCO Precis Oncol*. (2018) 2018:1–29. doi: 10.1200/po.18.00107

23. Vokes NI, Chambers E, Nguyen T, Coolidge A, Lydon CA, Le X, et al. Concurrent Tp53 mutations facilitate resistance evolution in Egfr-mutant lung adenocarcinoma. *J Thorac Oncol*. (2022) 17:779–92. doi: 10.1016/j.jtho.2022.02.011

24. Gao X, Wei X-W, Zheng M-Y, Chen Z-H, Zhang X-C, Zhong W-Z, et al. Impact of Egfr amplification on survival of patients with Egfr exon 20 insertion-positive non-small cell lung Cancer. *J Thorac Dis*. (2020) 12:5822–32. doi: 10.21037/jtd-20-1630

25. Niederst MJ, Hu H, Mulvey HE, Lockerman EL, Garcia AR, Piotrowska Z, et al. The allelic context of the C797s mutation acquired upon treatment with third-generation Egfr inhibitors impacts sensitivity to subsequent treatment strategies. *Clin Cancer Res*. (2015) 21:3924–33. doi: 10.1158/1078-0432.Ccr-15-0560

26. Wang Y, Yang N, Zhang Y, Li L, Han R, Zhu M, et al. Effective treatment of lung adenocarcinoma harboring Egfr-activating mutation, T790m, and Cis-C797s triple mutations by Brigatinib and Cetuximab combination therapy. *J Thorac Oncol*. (2020) 15:1369–75. doi: 10.1016/j.jtho.2020.04.014

27. Oxnard GR, Hu Y, Mileham KF, Husain H, Costa DB, Tracy P, et al. Assessment of resistance mechanisms and clinical implications in patients with Egfr T790m-positive lung Cancer and acquired resistance to Osimertinib. *JAMA Oncol*. (2018) 4:1527–34. doi: 10.1001/jamaoncol.2018.2969

28. Miyauchi E, Matsuda T, Kiyotani K, Low S-K, Hsu Y-W, Tsukita Y, et al. Significant differences in T cell receptor repertoires in lung adenocarcinomas with and without epidermal growth factor receptor mutations. *Cancer Sci*. (2019) 110:867–74. doi: 10.1111/cas.13919

29. Watanabe S, Hayashi H, Haratani K, Shimizu S, Tanizaki J, Sakai K, et al. Mutational activation of the epidermal growth factor receptor Down-regulates major histocompatibility

complex class I expression via the extracellular signal-regulated kinase in non-small cell lung Cancer. *Cancer Sci*. (2019) 110:52–60. doi: 10.1111/cas.13860

30. Sugiyama E, Togashi Y, Takeuchi Y, Shinya S, Tada Y, Kataoka K, et al. Blockade of Egfr improves responsiveness to Pd-1 blockade in Egfr-mutated non-small cell lung Cancer. *Sci Immunol*. (2020) 5:eaav3937. doi: 10.1126/sciimmunol.aav3937

31. Li L, Lu G, Liu Y, Gong L, Zheng X, Zheng H, et al. Low infiltration of Cd8+Pd-L1+T cells and M2 macrophages predicts improved clinical outcomes after immune checkpoint inhibitor therapy in non-small cell lung carcinoma. *Front Oncol*. (2021) 11:658690. doi: 10.3389/fonc.2021.658690

32. Zhang L, Chen Y, Wang H, Xu Z, Wang Y, Li S, et al. Massive Pd-L1 and Cd8 double positive tils characterize an immunosuppressive microenvironment with high mutational burden in lung Cancer. *J Immunother Cancer*. (2021) 9:e002356. doi: 10.1136/jitc-2021-002356

33. Lin Y, Xu J, Lan H. Tumor-associated macrophages in tumor metastasis: biological roles and clinical therapeutic applications. *J Hematol Oncol*. (2019) 12:12. doi: 10.1186/s13045-019-0760-3

34. Mack PC, Banks KC, Espenschied CR, Burich RA, Zill OA, Lee CE, et al. Spectrum of driver mutations and clinical impact of circulating tumor DNA analysis in non-small cell lung Cancer: analysis of over 8000 cases. *Cancer*. (2020) 126:3219–28. doi: 10.1002/cncr.32876

35. Yuan C, Jiang H, Jiang W, Wang H, Su C, Zhou S. Comparison of different Egfr gene mutation status in patients with metastatic non-small lung Cancer after first-line Egfr-Tkis therapy and analyzing its relationship with efficacy and prognosis. *Cancer Manag Res*. (2021) 13:6901–10. doi: 10.2147/cmar.S329900

frontiers | Frontiers in Medicine

TYPE Case Report
PUBLISHED 26 January 2024
DOI 10.3389/fmed.2024.1340888

OPEN ACCESS

EDITED BY
Santi Nolasco,
University of Catania, Italy

REVIEWED BY
Abdurrahman Tufan,
Gazi University, Türkiye
Gonçalo Boleto,
Instituto Português de Reumatologia, Portugal

*CORRESPONDENCE
Ewa Więsik-Szewczyk
✉ ewa.w.szewczyk@gmail.com

RECEIVED 19 November 2023
ACCEPTED 08 January 2024
PUBLISHED 26 January 2024

CITATION
Więsik-Szewczyk E, Zegadło A, Sobczyńska-Tomaszewska A, Korzeniowska M and Jahnz-Rózyk K (2024) Case report: VEXAS as an example of autoinflammatory syndrome in pulmonology clinical practice.
Front. Med. 11:1340888.
doi: 10.3389/fmed.2024.1340888

Case report: VEXAS as an example of autoinflammatory syndrome in pulmonology clinical practice

Ewa Więsik-Szewczyk[1]*, Arkadiusz Zegadło[2], Agnieszka Sobczyńska-Tomaszewska[3], Marcelina Korzeniowska[1] and Karina Jahnz-Rózyk[1]

[1]Department of Internal Medicine, Pneumonology, Allergology and Clinical Immunology, Central Clinical Hospital of the Ministry of National Defense, Military Institute of Medicine, National Health Institute, Warsaw, Poland, [2]Department of Radiology, Central Clinical Hospital of the Ministry of National Defense, Military Institute of Medicine, National Health Institute, Warsaw, Poland, [3]MedGen Medical Centre, Warsaw, Poland

Lung involvement is not widely recognized as a complication of autoinflammatory diseases. We present a broad approach to diagnose a severe form of autoinflammatory syndrome in an adult male patient. A 63-year-old Caucasian male presented with recurrent episodes of high fever, interstitial lung infiltration, and pleural effusion. Laboratory tests performed during the flares revealed lymphopenia and increased levels of C-reactive protein and ferritin. Broad diagnostic research on infections, connective tissue diseases, and malignancies yielded negative results. The patient's symptoms promptly resolved upon the administration of glucocorticoids; however, they reappeared when the prednisone dose was reduced. All attempts to administer immunomodulatory and immunosuppressive medications were ineffective. During follow-up, autoinflammatory syndrome was suspected; however, no pathological variants of monogenic autoinflammatory diseases were identified by genome-exome sequencing. The patient did not respond to interleukin 1 blockade with anakinra. He died due to multi-organ failure, and his condition remained unresolved until the first reported description of vacuole, E1 enzyme, X-linked, autoinflammatory, and somatic syndrome (VEXAS). We describe the diagnostic traps and reasoning process involved in establishing that the patient's symptoms were autoinflammatory in nature based on clinical symptoms, in addition to the proof of concept gained from genetic reevaluation and identification of pathogenic variants in the *UBA1* gene. The aim of this review is to increase the awareness of VEXAS among pulmonologists. Genetic screening for *UBA1* should be considered in patients with recurrent pneumonitis of unknown origin with elevated inflammatory markers and signs of cytopenia, especially if they require chronic steroids to control the disease. Respiratory manifestations are part of VEXAS; these may be dominant in the course of the disease and severe at presentation.

KEYWORDS

autoinflammation, mosaicism, *UBA1*, somatic mutations, respiratory manifestations

1 Introduction

Lung involvement is a well-recognized complication of autoimmune systemic diseases; there is an increasing awareness of its importance and significance in patient prognosis and survival (1). In contrast, autoinflammatory diseases, which are rare, are not widely recognized to be associated with lung involvement. Here, we present long path to the diagnosis and treatment of a severe form of autoinflammatory syndrome in an adult male patient. We describe the diagnostic traps and reasoning processes involved in the phases: first, the patient's symptoms were autoinflammatory in nature based on clinical reasoning; and second, the proof of the concept gained from repeated genetic evaluation, which led to the diagnosis of vacuoles, E1 enzyme, X-linked, autoinflammatory, and somatic syndrome (VEXAS), as described by Beck and colleagues (2) after patient death.

2 Case description and diagnostic assessment

The patient was a 63-year-old Caucasian man with a history of episodes of a fever reaching up to 39.8°C, with chills and weakness. Fever appeared without any prodromal symptoms, recurred regularly every 3 weeks, and lasted for 5–7 days from January 2014 to March 2014. The episode in April 2014 was accompanied by cough, dyspnea, and pneumonia, which resulted in admission to a local hospital. Upon admission, the patient had elevated C-reactive protein (CRP) levels, low-grade anemia, transient leukopenia, and mild thrombocytopenia. None of his symptoms improved after antibiotic treatment; however, they were promptly resolved when the patient was administered glucocorticoids (40 mg prednisone/day). Six months before these episodes, the patient had an episode of orchitis and was treated with ciprofloxacin. His family history of chronic diseases was unremarkable. He denied the use of tobacco, alcohol, or illicit drugs.

In May 2014, he was referred to our department for further evaluation. On admission, the patient was stable without fever and continued to receive 30 mg prednisone/day. Bronchoscopy revealed a normal bronchial tree. In the immunophenotyping of cells obtained from the bronchoalveolar lavage, the low percentage of lymphocytes was noteworthy; CD45+ lymphoid cells constituted only 0.3% of the white blood cells and 0.2% of CD3 + T lymphocytes, including CD4+ (30%) and CD8+ (5%). A blind lung biopsy revealed no specific changes. Plethysmography findings were within the reference range (June 2014). A detailed evaluation for chronic infections, systemic connective tissue diseases, and solid malignancies, including positron emission tomography scanning, were unremarkable. Bone marrow aspirate biopsy and histopathology revealed normal cellularity, which was age-appropriate. The presence of vacuoles has not been described. Owing to the stabilization of the patient's condition, normalization of laboratory inflammatory markers, normal pulmonary function test results, and resolution of radiological abnormalities, we recommended the complete discontinuation of glucocorticoids.

However, in August 2014, when the prednisone dose was reduced to 15 mg/day, a high-grade fever with subsequent dyspnea reappeared, without any prodromal symptoms. On physical examination, the patient was febrile with signs and symptoms of pneumonia. Chest computed tomography (CT) revealed bilateral ground-glass opacities, inflammatory consolidation with bronchial wall thickening, reticulation, thickened septal lines in the parenchyma, subpleural micronodules, and effusion in the right pleural cavity (Figure 1A). The patient denied any additional symptoms, such as joint pain or swelling, muscle pain, skin rash, chondritis, polymyalgia rheumatic-like symptoms or lymphadenopathy. To control the disease, 40 mg of prednisolone was administered daily. Normalization of inflammatory markers and regression of radiological abnormalities (Figure 1B) were accompanied by a clinical improvement.

Despite chronic steroid therapy (15–20 mg/prednisolone per day), fever and dyspnea reappeared regularly every 3–4 weeks. The patient's condition improved only after an increase in the steroid dose. Episodes of fever documented in the patient's diary from 2015 to 2019 lasted, on average, 5 days, the shortest being 2 days and the longest 7 days, with a temperature range from 37.2 to 39.2°C. The patient was evaluated by multiple specialists. Repeat bronchoscopy and CT were inconclusive. Pulmonary function tests (PFTs) performed during the flare up revealed severe abnormalities (Table 1), and laboratory tests revealed lymphopenia and elevated levels of CRP and ferritin (Table 2). The lymphocyte subpopulation analysis showed a significantly lower proportion and number of B cells, with a high proportion of switched memory B cells and plasmablasts (Table 3). Among the T lymphocytes, a high proportion of Th17 was observed (Table 3).

In August 2015, immunomodulatory and immunosuppressive treatments were initiated as steroid-sparing agents. The patient initially received azathioprine (150 mg/day), mycophenolate mofetil (2 × 1000 mg/day), and hydroxychloroquine (200 mg/day). All therapeutic attempts, except for steroids, were ineffective.

In 2019, autoinflammatory syndrome was suspected. During the flare up, the interleukin 1 (IL-1) inhibitor anakinra was administered, initially one dose of 100 mg subcutaneously (sc), followed by one 200 mg sc dose, as a new therapeutic trial. However, no significant clinical effects were observed. In November 2019, whole exome sequencing (without copy number variation analysis) was performed to identify known pathogenic and likely pathogenic variants described in the ClinVar database with the detailed analysis of variants (pathogenic/likely pathogenic/variation of uncertain significance (VUS)) in 578 genes associated with autoinflammatory diseases and inborn errors of immunity. The analysis did not reveal any pathogenic variants; only a few VUS-type variants were identified and described for clinical analysis. However, they did not support the diagnosis of autoinflammatory syndrome. Ultimately, the patient received cyclophosphamide (CYC) infusion, which was complicated by severe infection. The patient died of multi-organ failure as an unresolved case in May 2020. In October 2020, following the first description of VEXAS, genetic reevaluation was performed.

Pathogenic variants of the *UBA1* gene: NM_003334.3:c.121A > G, NP_003325.2:p. Met41Val was detected in about 65% of the cells (Supplementary Figure S1). This variant is classified as pathogenic in ClinVar database and is associated with VEXAS syndrome. The identification of pathogenic somatic mutations in *UBA1* led to the correct diagnosis on November 4, 2020.

3 Discussion

We report a case of recurrent fever with pneumonia that was steroid-dependent and resistant to immunosuppressive treatment.

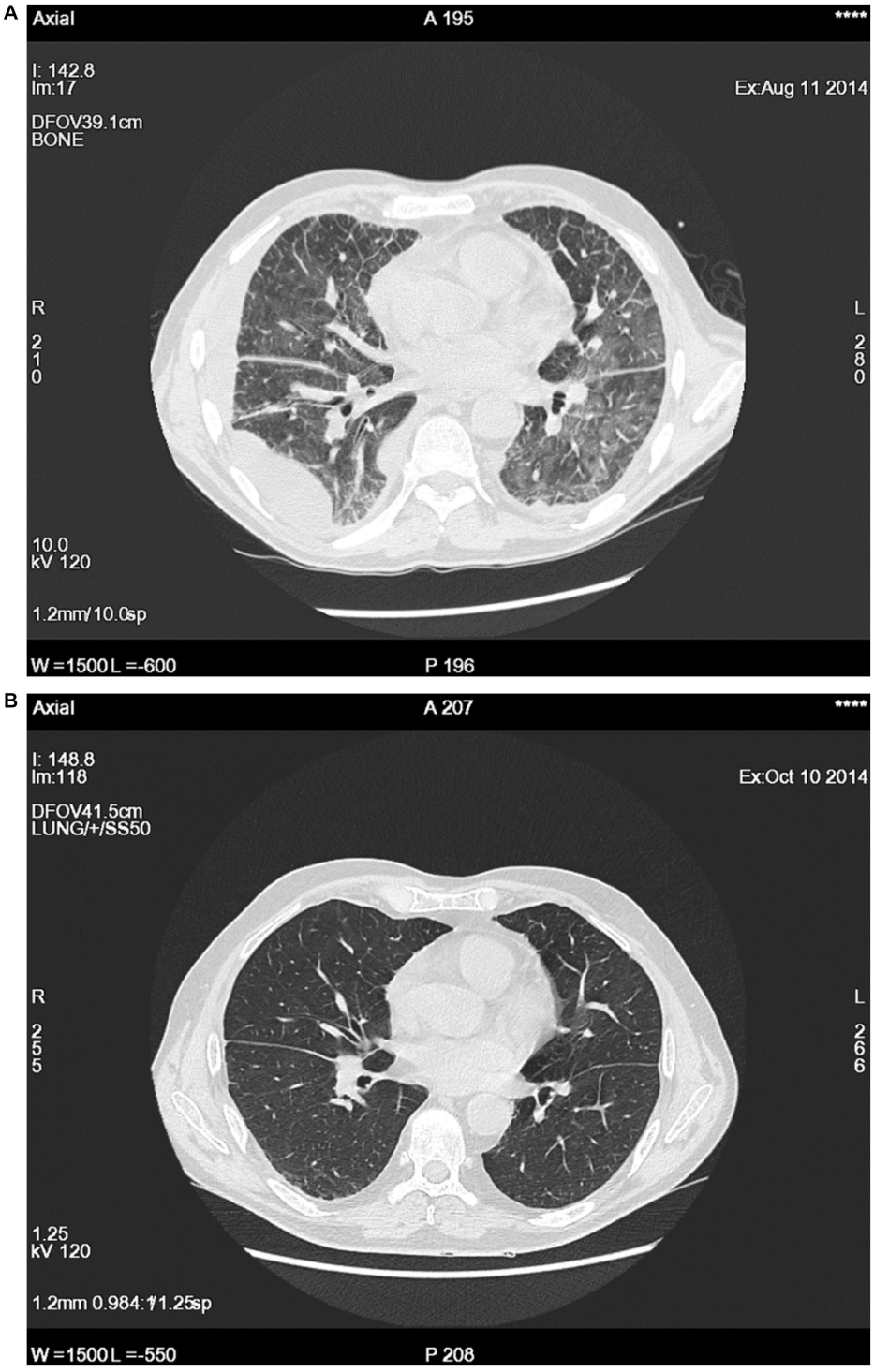

FIGURE 1
Examples of imagining studies during a flare up **(A)** and after 2 months of steroids treatment **(B)**.

The differential diagnosis of autoinflammatory syndromes in adults is challenging. At the first instance, infections, malignancies, and systemic autoimmune diseases were excluded. We performed serological, imaging, and pathological evaluations that did not explain the patient's condition; therefore, we suspected autoinflammatory syndrome, which was mainly based on the clinical pattern of recurrent inflammatory syndromes accompanied by high levels of inflammatory markers. The treatment trial with IL-1 inhibition, which, if effective, would have supported the suspicion autoinflammatory syndrome, was negative. The same result was observed during the initial genetic evaluation. However, the results were misleading. Despite

TABLE 1 Results of body plethysmography and diffusion examination during the flare up.

	Pred	Pre	%(Pre/Pred)	*p*	Z-score
VC MAX	3.63	1.43	39	0.12	−4.00
FRCpleth	3.37	1.99	59	1.95	−2.30
RV	2.41	1.40	58	1.51	−2.46
TLC	6.10	2.83	46	0.04	−4.68
RV % TLC %	40.09	49.45	123	94.86	1.71
DLCO_SB mmol/(mln*kPa)	7.51	2.17	29	0.05	−5.71

TABLE 2 Examples of laboratory results obtained during different time points and clinical states.

	19 May 2015 4 days after flare up	08 Dec 2016 3 days after flare up	11 Jun 2019 day 4 of flare up, temp. 38.2°C	24 Sep 2019 2 weeks asymptomatic	22 Oct 2019 day 1 of fever
Inflammatory markers					
ESR (0–20 mm/h)	NR	109	NR	16	NA
CRP (0–0.8 mg/dL)	12	12.3	23.2	0.2	44.6
Ferritin (30–400 ng/mL)	NR	NR	NR	1710	2,770
Complete blood count					
WBCx10^9/l (4.0–10.0)	4.40	7.53	5.57	2.82	6.77
RBCx10^{12}/l (3.5–5.5)	2.84	3.49	3.44	3.68	4.02
Hgb g/dl (11.0–18.0)	9.0	11.5	11.4	12.4	14.3
HCT % (35–55)	29	36	34	37	43
MCV fL (80–100)	102	103	90	101	107
MCHC g/dl (31–37)	31	31.9	33.5	33.3	33.3
PLT x 10^9/l (150–400)	223	158	90	128	97
Lymph x10^3/uL (0.9–4.5)	0.84	0.84	0.26	0.69	0.34
NEUT x10^3/uL (1.9–8.0)	3.43	6.30	5.06	2.02	6.16
Mono x10^3/uL (0.16–1.0)	0.12	0.35	0.24	0.10	0.15

WBC, white blood cell count; Hgb, hemoglobin; HCT, hematocrit; PLT, platelet; CRP, C-reactive protein; ESR, erythrocyte sedimentation rate; NR, not reported.

comprehensive investigations, the diagnosis was unknown until the first reported description of VEXAS syndrome. VEXAS is an adult-onset autoinflammatory syndrome due to somatic mutations affecting *UBA1* reported by Beck and colleagues (2). The first patient, as in our report, was identified among unresolved cases with unexplained inflammation. Thus, there is an argument to re-evaluate similar cases in pneumonology practice. Although the frequency of this condition is unknown, it appears to be the most common autoinflammatory syndrome in adults. The prevalence estimates are approximately 1 in 4269 males aged 50 years and 1 in 26,238 females aged 50 years (3). Currently, in males aged >50 years with an inflammation of unknown origin, VEXAS should be included early in the differential diagnosis. However, there are no available recommendations regarding when and for

10.3389/fmed.2024.1340888

TABLE 3 Lymphocyte subset analysis performed during the flare up.

Cells	% Total	Lymphocytic field (reference values)			
T cells (CD3+)	20.1	85.4	(60–82%)	569	(900–2,100 c/ul)
Th cells (CD3 + CD4+)	11.5	48.8	(33–55%)	323	(500–1,300 c/ul)
Ts cells (CD3 + CD8+)	8.4	35.6	(18–40%)	238	(280–900 c/ul)
CD4:CD8		1.4	1.1–2.8		
NK cells (CD3 + CD16 + CD56+)	2.8	11.8	(7–23%)	79	(90–630 c/ul)
B cells (CD19+)	0.7	2.8	(5–16%)	20	(120–400 c/ul)
B cells				% CD19 + (reference %)	
Transitional B cells IgM++IgD++CD38++CD27-CD21+				1.4	(0.9–6.3)
Naïve B cells IgM + IgD++CD38 + CD27-CD21+				18.0	(53.3–86.0)
Non-switched memory B cells (MZ-like B cells) IgM++IgD + CD38 + CD27 + CD21+				4.3	(3.3–12.8)
Class-switched memory B cells IgM-IgD-CD38 + CD27 + CD21+				4.3	(4.0–22.1)
$CD21^{low}$ B cells IgM + IgD + $CD38^{low}$CD27-$CD21^{low}$				54.7	(0.6–7.6)
Plasmablasts IgM−/+IgD-CD38+++CD27++CD21+				19.8	(0.1–1.5)

T cells	%CD4+ (reference %)		%CD8+ (reference %)	
Naïve T cells CD45RA + CD197+	22.5	18.2–53.2	2.2	18.6–70.6
Effector T cells CD45RA+ CD197-	1.4	1.1–9.0	65.0	4.0–24.0
Central memory T cells CD45RO + CD197+	48.2	8.3–27.1	7.1	0.5–5.4
Effector memory T cells CD45RO + CD197-	27.9	17.2–51.4	25.7	16.7–42.6
Th17 CD45RO + CD196+	55.2	10.8–39.0	–	–
Recent thymic emigrants T cells CD45RA + CD62L + CD31+	3.5	14.4–38.3	3.1	16.7–64.7

whom genetic evaluation should be performed. Recently, Maeda et al. (4) proposed a scoring system that can efficiently identify patients with *UBA1* variants. Their clinical scoring system included age > 50 years, cutaneous lesions, lung involvement, chondritis, and macrocytic anemia; it predicts *UBA1*-positive patients as those with a maximum score of 6 and *UBA1*-negative patients as those with low scores of 0–2, while recommending that patients with intermediate scores of 3–5 definitely undergo *UBA1* testing (4). The retrospectively presented patient had positive scores regarding age and pulmonary involvement. In the present analysis of this case, the hematologist excluded central anemiaand diagnosed anemia related to chronic disease, which in the retrospective analysis, seemed to be questionable and should be re-evaluated, resulting in a score of 4 points. In another study, a higher initial mean corpuscular volume predicted the diagnosis of VEXAS in a rheumatology cohort (5). It is important to closely monitor hematologic abnormalities in cases of suspected VEXAS, as they can be absent at the initial phase or can fluctuate, as in the present patient.

VEXAS is multidisciplinary and involves numerous branches of internal medicine, including pulmonology. Currently, VEXAS is recognized in patients diagnosed with myelodysplastic syndrome and various rheumatological and dermatological conditions (5–13). The present case is unique, as fever and lung involvement dominated the clinical picture, without dermatosis, arthritis, recurrent chondritis, polymyalgia rheumatica-like symptoms or bone marrow abnormalities, which are often present in VEXAS. Reduced awareness of the disease among pulmonologists may result in omission of the diagnosis of VEXAS in patients with predominant pulmonary involvement. The pulmonological aspects of VEXAS are less precisely characterized, although they are reported as constant clinical features during

follow-up and seldom as the main clinical complaint (14). In 2022, the first systematic review aimed to summarize the respiratory manifestations of VEXAS as described in the literature (15). The most commonly described manifestation was pulmonary infiltrates, present in 43% of patients, often coexisting with other lung pathologies, such as nonspecific interstitial pneumonia, pulmonary vasculitis, and pleural effusion. In our patient, several abnormalities were present on CT, including an abnormal PFT during the flare up. In a cohort study conducted on all patients with VEXAS syndrome evaluated at the Mayo Clinic (16) the authors reported respiratory symptoms in 93% of the patients, accompanied by skin lesions and fever in 91 and 82% of the patients, respectively. Chest CT showed abnormalities in 91% of patients; however, these were nonspecific. PFTs were available for a minority of patients (40%) who presented with mild restrictive impairment or normal results. In general, the authors concluded that the pulmonary manifestations were relatively nonspecific. In a French cohort, lung pathology was one of the most common clinical features of VEXAS and was associated with mortality (12). When assessing phenotype–genotype correlations, lung infiltrates were more common in those with *UBA1* p.Met41Thr or p.Met41Val mutations than in those with p.Met41Leu (15), which also occurred in the present case. The currently available data on lung involvement may be biased because the reported cohorts were recruited mainly by rheumatologists or hematologists. Therefore, further studies including pulmonology cohorts are required.

The therapeutic approach to VEXAS is challenging, and data are limited and inhomogeneous (7, 15). Steroids are often the first choice and administered in doses ≥20 mg once daily; this is the only therapeutic approach to improve the inflammatory manifestations (7). Among anti-inflammatory drugs administered to decrease the corticosteroid dose, partial or negative responses are often observed (7). From the onset of the disease, the patient required >20 mg/day of prednisolone to control inflammation, and none of the immunosuppressive or immunomodulatory steroid-sparing agents provided additional benefits. Based on the assumption of an autoinflammatory condition in which excessive production of inflammatory cytokines occurs, anakinra was used, although without any effect. According to a recent systematic review, anti-IL-1-directed therapy was used in 6.0% of reported patients (17). Five patients received anakinra and two received canakinumab. Interestingly, two patients treated with anakinra and one patient treated with canakinumab received combination therapy with cyclosporin A. (17). Blockade of IL-6 with tocilizumab is another anti-inflammatory approach (18). In one patient with VEXAS and a previous diagnosis of spondyloarthropathy, treatment with intravenous immunoglobulin and an IL-17 inhibitor was effective (19). Furthermore, Th17 lymphocytes were present at a very high proportion in our patient, which supports this idea. Currently, data are accumulating regarding the efficacy of Janus kinase inhibitors, azacitidine, or allogeneic stem cell transplantation; however, treatment should be individualized based on the endotype of the disease, comorbidities, and the overall patient condition (16, 20–22). Therefore, there is an urgent need to collect clinical data over longer follow-up periods (23).

The present case report provides insights into the 7-year follow-up of an adult patient with autoinflammatory syndrome and predominant lung involvement. Clinical management and decision-making were more difficult when the patient's condition was not recognized in the medical literature prior to death. A limitation of our description is that data from the patient's first hospitalization in a local hospital were not available. Follow-up from the first admission to our institution is presented as precisely as possible. Our aim was to increase awareness of VEXAS among pulmonologists. As the primary take-away from this case report, we would like to propose that genetic screening for *UBA1* should be considered in patients with recurrent pneumonitis of unknown origin with elevated inflammatory markers and signs of cytopenia, especially if they require chronic steroids to control the disease. Based on the present case, respiratory manifestations are part of the primary disease and may be severe.

Data availability statement

The original contributions presented in the study are included in the article/Supplementary material, further inquiries can be directed to the corresponding author.

Ethics statement

Ethical approval was not required for the studies involving humans because the studies were conducted in accordance with the local legislation and institutional requirement. The participant provided his written informed consent to diagnostic and therapeutic procedures. Written informed consent was obtained from the individual(s) for the publication of any potentially identifiable images or data included in this article.

Author contributions

EW-S: Conceptualization, Data curation, Formal analysis, Investigation, Methodology, Supervision, Writing – original draft, Writing – review & editing. AZ: Data curation, Visualization, Writing – review & editing. AS-T: Data curation, Visualization, Writing – review & editing. MK: Investigation, Writing – review & editing. KJ-R: Supervision, Writing – review & editing.

Funding

The author(s) declare financial support was received for the research, authorship, and/or publication of this article. This publication was funded by Military Institute of Medicine—National Research Institute, grant number 0000000592.

Conflict of interest

The authors declare that the research was conducted in the absence of any commercial or financial relationships that could be construed as a potential conflict of interest.

Publisher's note

All claims expressed in this article are solely those of the authors and do not necessarily represent those of their affiliated organizations, or those of the publisher, the editors and the reviewers. Any product that may be evaluated in this article, or claim that may be made by its manufacturer, is not guaranteed or endorsed by the publisher.

Supplementary material

The Supplementary material for this article can be found online at: https://www.frontiersin.org/articles/10.3389/fmed.2024.1340888/full#supplementary-material

References

1. Xanthouli P, Echampati I, Lorenz HM, Heussel CP, Benjamin N. Respiratory involvement in connective tissue diseases. *Eur J Intern Med*. (2023):S0953620523003370. doi: 10.1016/j.ejim.2023.09.016

2. Beck DB, Ferrada MA, Sikora KA, Ombrello AK, Collins JC, Pei W, et al. Somatic mutations in UBA1 and severe adult-onset autoinflammatory disease. *N Engl J Med*. (2020) 383:2628–38. doi: 10.1056/NEJMoa2026834

3. Beck DB, Bodian DL, Shah V, Mirshahi UL, Kim J, Ding Y, et al. Estimated prevalence and clinical manifestations of UBA1 variants associated with VEXAS syndrome in a clinical population. *JAMA*. (2023) 329:318–24. doi: 10.1001/jama.2022.24836

4. Maeda A, Tsuchida N, Uchiyama Y, Horita N, Kobayashi S, Kishimoto M, et al. Efficient detection of somatic *UBA1* variants and clinical scoring system predicting patients with variants in VEXAS syndrome. *Rheumatology*. (2023):kead425. doi: 10.1093/rheumatology/kead425

5. Ferrada MA, Sikora KA, Luo Y, Wells KV, Patel B, Groarke EM, et al. Somatic mutations in UBA1 define a distinct subset of relapsing Polychondritis patients with VEXAS syndrome. *Arthritis Rheumatol Hoboken NJ*. (2021) 73:1886–95. doi: 10.1002/art.41743

6. Muratore F, Marvisi C, Castrignanò P, Nicoli D, Farnetti E, Bonanno O, et al. VEXAS syndrome: a case series from a Single-Center cohort of Italian patients with Vasculitis. *Arthritis Rheumatol*. (2022) 74:665–70. doi: 10.1002/art.41992

7. Mascaro JM, Rodriguez-Pinto I, Poza G, Mensa-Vilaro A, Fernandez-Martin J, Caminal-Montero L, et al. Spanish cohort of VEXAS syndrome: clinical manifestations, outcome of treatments and novel evidences about *UBA1* mosaicism. *Ann Rheum Dis*. (2023) 82:1594–605. doi: 10.1136/ard-2023-224460

8. Lee SMS, Fan BE, Lim JHL, Goh LL, Lee JSS, Koh LW. A case of VEXAS syndrome manifesting as Kikuchi-Fujimoto disease, relapsing Polychondritis, venous thromboembolism and macrocytic Anaemia. *Rheumatol Oxf Engl*. (2021) 60:e304–6. doi: 10.1093/rheumatology/keab200

9. Lacombe V, Kosmider O, Prévost M, Lavigne C, Urbanski G. Severe joint involvement in VEXAS syndrome: a case report. *Ann Intern Med*. (2021) 174:1025–7. doi: 10.7326/L21-0023

10. Huang H, Zhang W, Cai W, Liu J, Wang H, Qin T, et al. VEXAS syndrome in myelodysplastic syndrome with autoimmune disorder. *Exp Hematol Oncol*. (2021) 10:23. doi: 10.1186/s40164-021-00217-2

11. Bruno A, Gurnari C, Alexander T, Snowden JA, Greco R. Autoimmune manifestations in VEXAS: opportunities for integration and pitfalls to interpretation. *J Allergy Clin Immunol*. (2023) 151:1204–14. doi: 10.1016/j.jaci.2023.02.017

12. Georgin-Lavialle S, Terrier B, Guedon AF, Heiblig M, Comont T, Lazaro E, et al. Further characterization of clinical and laboratory features in VEXAS syndrome: large-scale analysis of a multicentre case series of 116 French patients*. *Br J Dermatol*. (2022) 186:564–74. doi: 10.1111/bjd.20805

13. Zakine È, Papageorgiou L, Bourguiba R, Mekinian A, Terrier B, Kosmider O, et al. Clinical and pathological features of cutaneous manifestations in VEXAS syndrome: a multicenter retrospective study of 59 cases. *J Am Acad Dermatol [Internet]*. (2023) 88:917–20. doi: 10.1016/j.jaad.2022.10.052

14. Borie R, Debray MP, Guedon AF, Mekinian A, Terriou L, Lacombe V, et al. Pleuropulmonary manifestations of vacuoles, E1 enzyme, X-linked, autoinflammatory, somatic (VEXAS) syndrome. *Chest*. (2023) 163:575–85. doi: 10.1016/j.chest.2022.10.011

15. Kouranloo K, Ashley A, Zhao SS, Dey M. Pulmonary manifestations in VEXAS (vacuoles, E1 enzyme, X-linked, autoinflammatory, somatic) syndrome: a systematic review. *Rheumatol Int*. (2023) 43:1023–32. doi: 10.1007/s00296-022-05266-2

16. Casal Moura M, Baqir M, Tandon YK, Samec MJ, Hines AS, Reichard KK, et al. Pulmonary manifestations in VEXAS syndrome. *Respir Med*. (2023) 213:107245. doi: 10.1016/j.rmed.2023.107245

17. Boyadzhieva Z, Ruffer N, Kötter I, Krusche M. How to treat VEXAS-syndrome: a systematic review on effectiveness and safety of current treatment strategies. *Rheumatol Oxf Engl*. (2023) 62:3518–25. doi: 10.1093/rheumatology/kead240

18. Oganesyan A, Jachiet V, Chasset F, Hirsch P, Hage-Sleiman M, Fabiani B, et al. VEXAS syndrome: still expanding the clinical phenotype. *Rheumatol Oxf Engl*. (2021) 60:e321–3. doi: 10.1093/rheumatology/keab225

19. Magnol M, Couvaras L, Degboé Y, Delabesse E, Bulai-Livideanu C, Ruyssen-Witrand A, et al. VEXAS syndrome in a patient with previous spondyloarthritis with favorable response to intravenous immunoglobulin anti-IL17 therapy. *Rheumatol Oxf Engl*. (2021) 60:e314–5. doi: 10.1093/rheumatology/keab211

20. Bourbon E, Heiblig M, Gerfaud-Valentin M, Barba T, Durel CA, Lega JC, et al. Therapeutic options in Vexas syndrome: insights from a retrospective series. *Blood*. (2021) 137:3682–4. doi: 10.1182/blood.2020010177

21. Mekinian A, Zhao LP, Chevret S, Desseaux K, Pascal L, Comont T, et al. A phase II prospective trial of azacitidine in steroid-dependent or refractory systemic autoimmune/inflammatory disorders and VEXAS syndrome associated with MDS and CMML. *Leukemia*. (2022) 36:2739–42. doi: 10.1038/s41375-022-01698-8

22. Bindoli S, Baggio C, Doria A, Bertoldo E, Sfriso P. JAK inhibitors for the treatment of VEXAS syndrome. *Exp Biol Med Maywood NJ*. (2023) 248:394–8. doi: 10.1177/15353702231165030

23. Vitale A, Caggiano V, Della Casa F, Hernández-Rodríguez J, Frassi M, Monti S, et al. Development and implementation of the AIDA international registry for patients with VEXAS syndrome. *Front Med*. (2022) 9:926500. doi: 10.3389/fmed.2022.926500

frontiers | Frontiers in Medicine

TYPE Case Report
PUBLISHED 01 February 2024
DOI 10.3389/fmed.2024.1301941

OPEN ACCESS

EDITED BY
Santi Nolasco,
University of Catania, Italy

REVIEWED BY
Vera Svobodova Donnenberg,
University of Pittsburgh, United States
Albino Eccher,
Integrated University Hospital Verona, Italy

*CORRESPONDENCE
Wang Deng
✉ dengwang@hospital.cqmu.edu.cn

RECEIVED 25 September 2023
ACCEPTED 17 January 2024
PUBLISHED 01 February 2024

CITATION
Xiao L-X, Liu L and Deng W (2024) Case report: The first account of undifferentiated sarcoma with epithelioid features originating in the pleura.
Front. Med. 11:1301941.
doi: 10.3389/fmed.2024.1301941

Case report: The first account of undifferentiated sarcoma with epithelioid features originating in the pleura

Ling-Xi Xiao[1], Li Liu[2] and Wang Deng[1]*

[1]Department of Respiratory and Critical Care Medicine, Second Affiliated Hospital of Chongqing Medical University, Chongqing, China, [2]Department of Pathology, Second Affiliated Hospital of Chongqing Medical University, Chongqing, China

Undifferentiated epithelioid sarcoma (USEF) is a rare subtype of undifferentiated soft tissue sarcoma that presents unique challenges in clinical diagnosis and treatment. Here, we report a case of USEF occurring in the pleura of a 51-year-old man for the first time. Thoracoscopic examination revealed widespread nodular changes, and pathological analysis confirmed the presence of numerous epithelioid atypical cells. Immunohistochemical (IHC) analysis demonstrated an undifferentiated phenotype with distinct characteristics: epithelial membrane antigen (foci +), vimentin (+), Ki-67 (+70% +), TTF-1 (+), P53 (mutant type +90%), INI-1 (+), and CK5/6 (small foci +). Immunohistochemical examination of the tumor showed that the tumor was an undifferentiated epithelioid sarcoma. High-throughput DNA sequencing revealed pivotal mutations, including a nonsense mutation in the *NF1* gene (c.641A > G(p.H214R)). and critical *TP53* missense mutation (c.641A > G(p.H214R)). This *TP53* mutation, with a tumor mutation burden of 16.5 Muts/Mb, signifies a high level of genomic instability, likely contributing to the rapid progression and aggressiveness of the disease. Detection of the *TP53* mutation provides essential insights, indicating the disease's rapid progression and highlighting the potential for targeted therapies. Although the patient's disease progressed extremely rapidly and he tragically died within a week, we discussed the results of IHC and DNA sequencing in detail and discussed his possible treatment options. Insights gained from this case will be critical in shaping future diagnostic and therapeutic paradigms for USEF, particularly in the context of TP53 mutations.

KEYWORDS

undifferentiated sarcoma, epithelioid features, pleural tumors, immunohistochemistry, TP53 genes

1 Introduction

Undifferentiated soft tissue sarcoma (USTS) constitutes a rare and heterogeneous group of soft tissue cancers that pose challenges for their effective differentiation using current diagnostic tools. Undifferentiated pleomorphic sarcoma, undifferentiated spindle cell sarcoma, undifferentiated round cell sarcoma, and undifferentiated epithelioid sarcoma (USEF) are among the subtypes of USTS (1). However, the existing literature on USEF is notably sparse.

USEF is commonly identified in older age groups, displaying no gender bias and often presenting with a larger size at diagnosis. It frequently occurs centrally, such as in the proximal

thigh and torso (1). Traditional treatment methods for USEF, including surgical resection, chemotherapy, and radiotherapy, present significant challenges due to the biological complexity and varied treatment responses of USEF, resulting in a generally poor prognosis (2).

Due to limited research, the understanding of USTS and their anticipated outcomes remains insufficient. Among adults, undifferentiated pleomorphic sarcoma (UPS) originating from the limbs or trunk has been reported to have a 5-year metastasis-free survival rate of 83% (3). However, USEF appears to exhibit higher aggressiveness (2). highlighting the importance of discussing potential therapeutic approaches.

In this report, we aim to provide a comprehensive and detailed description of a unique case involving a pleural tumor presenting as USEF, contributing to an enhanced understanding of this extremely rare condition.

2 Case description

A 51-year-old man was admitted to the Department of Respiratory and Critical Care Medicine on March 31, 2023, with a 5-month history of cough and sputum and recent exacerbation of shortness of breath, wheezing, and fatigue lasting for 3 days. He had a 20-year history of smoking (approximately 20 cigarettes per day) and alcohol consumption (approximately 200 mL per day) and no known family history of cancer, genetic diseases, psychiatric disorders, nor a history of long-term medication use. Additionally, there was no evidence of current or previous soft tissue tumors or history of radiation exposure. Physical examination revealed diminished breath sounds in the right lung with solid percussion.

Upon admission, the patient's complete blood work showed abnormal values. Specifically, the CRP was significantly high at 69.84 mg/L (<10 mg/L), and the leukocyte count was elevated at 16.88 × 10^9/L (3.50–9.50 × 10^9/L). Chest computed tomography (CT) demonstrated substantial right pleural effusion, causing significant compression of the right lung, and irregular thickening of the right pleura, measuring approximately 14.7 mm at its thickest point (Figures 1A,B), with no evidence of lymph node or visceral dissemination at presentation. Subsequent thoracentesis was performed, and the pleural fluid, appearing hemorrhagic, was identified as an exudate. Biochemical analysis indicated high lactate dehydrogenase levels.

Immunohistochemical (IHC) analysis of the pleural effusion sample further revealed cytokeratin (CK) (foci +), vimentin (+), calretinin (−), MC (−), D2–40 (−), CK5/6 (−), TTF − 1 (+), NapsinA (−), P63 (−), CK7 (foci +), Ki-67 (+30%+), and WT-1 (−). This comprehensive analysis played a crucial role in elucidating the underlying pathology and guiding subsequent steps in patient management. Images of immunohistochemical staining are shown in Supplementary Figure S1.

Abbreviations: USEF, undifferentiated sarcoma with epithelioid features; UPS, undifferentiated pleomorphic sarcoma; MPM, malignant pleural mesothelioma; IHC, immunohistochemical; EMA, epithelial membrane antigen; USTS, undifferentiated soft tissue sarcoma; NGS, next-generation sequencing.

The patient underwent a thoracoscopic biopsy, which revealed a significant amount of hemorrhagic pleural effusion within the pleural cavity. The pleural wall exhibited diffuse nodular lesions of varying sizes (Figure 1C). The pathological biopsy revealed a grayish-white color on the cut surface. Microscopic examination of sections prepared from the surgical specimen displayed extensive areas filled with epithelioid atypical cells. These cells were large and had abundant cytoplasm, and some areas showed eosinophilic staining. The nuclei were large, with a high nucleo-cytoplasmic ratio. In some tumor cells, nucleoli were visible, and pathological nuclear division was apparent (Figure 2A).

IHC analysis of the pleural nodules revealed the following results: epithelial membrane antigen (EMA) (foci +), Vim (+), Ki-67 (+70% +), TTF-1 (+), P53 (mutant type +90%), P40(−), calretinin (−), INI-1 (+), CK5/6 (small foci +), WT-1 (−), NapsinA (−), and CK7 (−). The immunohistochemical phenotype was undifferentiated, complicating the determination of the origin of tumor cells (Figures 2B–H).

Next,-Generation Sequencing covered exons, fusion-related introns, variable splicing regions, and specific microsatellite (MS) site areas of 506 genes associated with soft tissue sarcoma typing and mutations, totaling approximately 1.73-Mb base positions. Next-Generation Sequencing (NGS) revealed two significant mutations: a nonsense mutation in the NF1 gene, c.3721C > T(p.R1241*), depicted in Figure 3A, and a missense mutation in the TP53 gene, c.641A > G(p.H214R), illustrated in Figure 3B. The abundance and specific details of these mutations are summarized in Table 1. For comprehensive data on additional gene mutations identified in this study, please refer to Supplementary Table S1. Additionally, a high tumor mutation burden (TMB) of 16.5 Muts/Mb was noted. These findings related to *NF1* and *TP53* are significant as they could influence the tumor's characteristics and potential treatment strategies. Additionally, MS instability–high (MSI-H) status was not detected, and HLA-I typing was assessed as partially pure. However, these findings did not clarify the origin of the tumor cells.

Considering the unfavorable prognosis and high treatment costs, the patient chose against aggressive therapies, such as radiotherapy, chemotherapy, and surgery. Instead, the patient received targeted supportive care. However, the patient's condition rapidly deteriorated. Within a week, he developed respiratory failure with persistent hypotension, unresponsive to vasopressors. This was accompanied by significantly elevated infection markers: leukocyte count leukocyte count was 24.61 × 10^9/L (3.50–9.50 × 10^9/L), Procalcitonin (PCT) level was 1.2798 ng/mL(0.0000–0.0500 ng/mL), and CRP was >200 mg/L (<10 mg/L). Due to these circumstances, the family decided to cease all treatments, and the patient unfortunately died on April 7, 2023 (Figure 4).

3 Immunohistochemistry and next-generation sequencing techniques

IHC was performed in the Department of Pathology of the Second Affiliated Hospital of Chongqing Medical University. Initially, the slides undergo dewaxing and hydration. Subsequently, they are incubated in a 3% hydrogen peroxide solution for 10 min to block endogenous peroxidase activity. This step is followed by washing the slides three times with phosphate-buffered saline (PBS)

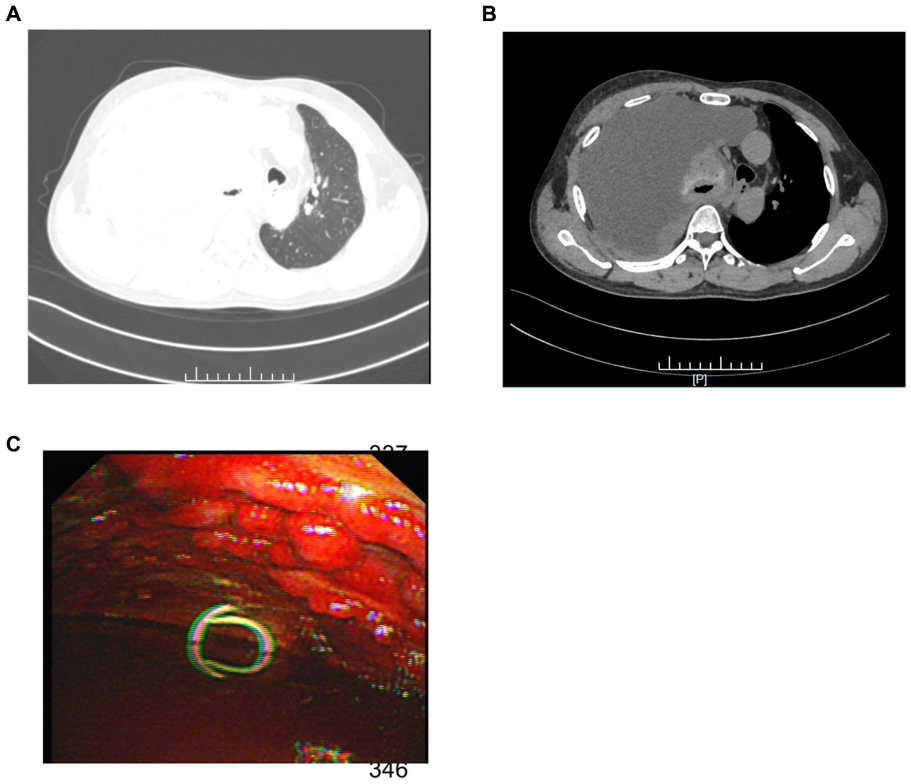

FIGURE 1
(A) The patient's chest CT (lung window) exhibited extensive right pleural effusion. **(B)** The mediastinal window of the chest CT revealed significant right lung compression and irregular pleural thickening. **(C)** Thoracoscopy exposed diffuse nodular changes of diverse sizes in the parietal pleura along with substantial hemorrhagic effusion in the pleural cavity.

at pH 7, each time for 3 min. The slides are then placed in a citrate buffer solution (pH 6.0) and subjected to microwave heating for antigen retrieval, twice, each time for 10 min. After heating, the slides are allowed to cool at room temperature. Subsequently, they are again washed three times with PBS at pH 7.4, each for 3 min. Depending on the tissue size, an appropriate amount of primary antibody is applied and incubated overnight at 4°C. After incubation, the slides are washed three times with PBS, each for 3 min. This is followed by the addition of an appropriate amount of enzyme-labeled polymer goat anti-mouse/rabbit IgG; thereafter, the slides undergo incubation at room temperature for 20 min. After incubation, the slides are washed three times with PBS, each for 3 min. Finally, the slides are visualized using a freshly prepared diaminobenzidine chromogen solution. Post-visualization, the slides are rinsed with PBS and counterstained with hematoxylin. We added positive and negative controls during the experiment to demonstrate the validity and reliability of the staining process, as seen in Supplementary Figure S2. IHC results are evaluated and interpreted by independent pathologists.

Next,-Generation Sequencing (NGS) was performed employing the GENESEEQ PRIME™ platform (Geneseeq Technology Inc., Nanjing, China). The process encompassed the following steps: Nucleic Acid Extraction: Formalin-Fixed Paraffin-Embedded (FFPE) nucleic acids were extracted using the FFPE Nucleic Acid Extraction Kit (Geneseeq Medical Device and Diagnostic Inc., Nanjing, China). Library Preparation: the library was constructed using the EGFR/ALK/ROS1/BRAF/KRAS/HER2 Gene Mutation Detection Kit (Geneseeq Medical Device and Diagnostic Inc., Nanjing, China). The method utilized for sequencing was the reversible terminator-based method, which offers high accuracy and read lengths. DNA Quantification and Purity Assessment: DNA concentration in the prepared samples was quantified using the highly sensitive Qubit® 3.0 Fluorometer along with the Qubit® DNA Assay Kit (Thermo Fisher Scientific Inc., Waltham, MA, United States). The purity of the DNA was assessed using the NanoDrop™ spectrophotometer (Thermo Fisher Scientific Inc., Waltham, MA, United States).

4 Discussion

Due to the limited ongoing research on USEF, both identification and treatment pose significant challenges. Treating USEF is notably difficult due to the scarcity of prospective studies and reliance on case reports within the academic community. In the present case, the patient initially exhibited symptoms of cough, sputum production, wheezing, and fatigue, leading to hospitalization. Throughout the diagnostic process, we utilized various methods, including chest CT, thoracoscopic pleural biopsy, immunocytochemical analysis (ICC), IHC, and genetic testing. Among these methods, ICC analysis is a rapid, minimally invasive, and cost-effective diagnostic tool, offering lower invasiveness, reduced complication risks, lower costs, and faster results than tissue biopsy. This approach proves particularly effective for differential diagnosis in patients with pleural effusion. Additionally, the utilization of positron emission tomography–CT scans holds

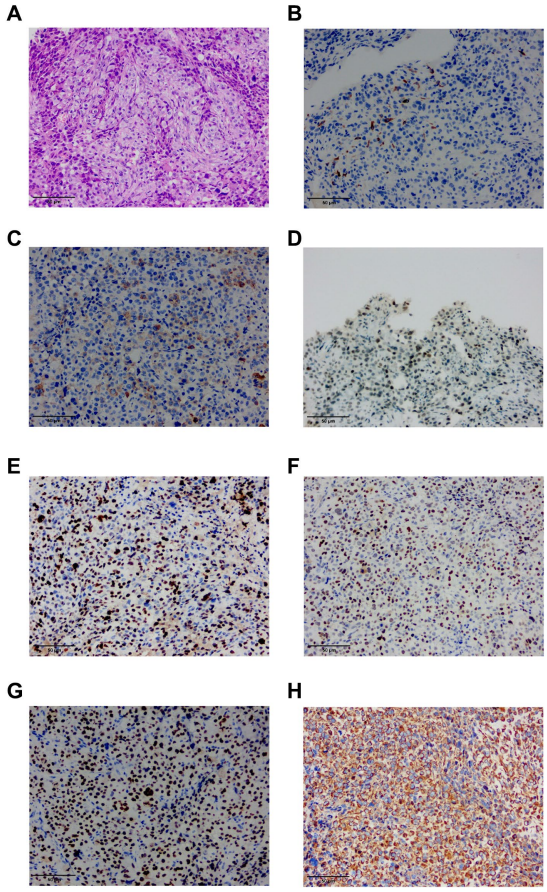

FIGURE 2
(A) HE staining finding at 20x magnification of the ultrasound-guided endoscopic fine-needle aspiration (USEF) sample from the right parietal pleura is shown. **(B)** Immunohistochemical staining for CK5/6 shows positive staining in small foci.
(C) Immunohistochemical staining for EMA demonstrates positive staining in the lesion. **(D)** Immunohistochemical staining for INI-1 shows positive results. **(E)** Immunohistochemical staining for Ki-67 shows a high proliferation index with >70% positivity.
(F) Immunohistochemical staining for P53 shows a mutant type with approximately 90% positive staining. **(G)** Immunohistochemical staining for TTF-1 indicates positive results.
(H) Immunohistochemical staining for vimentin (Vim) shows positive staining.

significant value in such cases, allowing for the assessment of tumor response to treatment before and after therapy.

According to the 2020 WHO Classification of Soft Tissue and Bone Tumours, USTS can broadly be categorized into pleomorphic, spindle cell, round cell, and epithelioid subgroups (4). However, they lack specific defining features other than the absence of recognizable differentiation. Among these, UPS represents the largest group, with USEF being less extensively studied. The diagnostic criteria for USEF include epithelioid cell morphology and the absence of any immunohistochemical feature of specific differentials, demonstrating the absence of distinctive molecular aberration.

USEF represents a heterogeneous group of tumors that share certain pathological and immunohistochemical characteristics with epithelioid sarcoma (ES). However, these tumors do not meet the criteria for a definitive ES diagnosis (2). Studies have indicated that CK and EMA are more frequently present in ES, with a majority of ES cases exhibiting a loss of INI-1, as demonstrated using IHC (5). In contrast, every USEF sample expresses at least one epithelial marker (pan-CK and/or EMA). Unlike ES, USEF usually does not express CD34, and the absence of INI-1 and expression of CA-125 are less common (2). In this particular case, locally positive EMA and positive INI-1 were observed.

USEF is typically diagnosed by exclusion. MPM serves as a significant differential diagnosis based on radiological features. The presence of CK5/6 might suggest an MPM phenotype, but the absence of WT-1, calretinin, and D2-40, which are typically positive in MPM, reduces the likelihood of this condition (6). Additionally, although this case included an examination of pleural effusion cytology, it failed to identify MPM-associated markers, such as MTAP, 5-hmC, GLUT1, IMP3, and EZH2 (7).

From a clinical incidence perspective, differentiating pleural tumors from pleural metastasis caused by primary lung cancer is crucial (8). The presence of TTF-1 and Vim, which can also be seen in some cases of lung adenocarcinoma, suggests this possibility (9). However, the absence of CK7 and NapsinA further rules out the likelihood of lung adenocarcinoma (10).

After eliminating common tumors, it is crucial to consider and exclude rare conditions such as SMARCA4-deficient thoracic sarcoma. This recently discovered and uncommon condition is suggested by the presence of TTF-1, EMA, CK, INI-1, and Vim. However, the final next-generation sequencing test ruled out the possibility by not detecting the SMARCA4 inactivating mutation (11, 12).

In this study, the expression rate of Ki-67 in patient lesions exceeded 70%, signifying a significant predictor of poor prognosis. Ki-67, a nuclear protein associated with cellular proliferation, has elevated expression levels closely correlated with worsened clinical outcomes, especially in patients with high-risk soft tissue sarcomas (STS) (13). A high Ki-67 proliferation index has been established as a critical factor affecting the prognosis of patients with STS. A prospective study has indicated that using a Ki-67 grading system for assessing STS malignancy is more effective and reproducible than the traditional system adopted by the French Federation of Cancer Centers Sarcoma Group (FNCLCC) (14).

Finally, the diagnosis of USEF is made based on the absence of lineage-specific markers or corresponding fusion and mutation genes, as well as considering its histological appearance as epithelioid. Understanding this rare, the diagnosis of highly invasive soft tissue tumor requires careful examination of available literature. Reported cases of USEF, excluding occasional cases reported in non-English literature, have been summarized in Table 2.

Due to their high malignancy, tendency for early metastasis, rapid progression, and poor prognosis, surgery has become the primary treatment method for undifferentiated sarcomas. According to the 8th edition of the AJCC classification for soft tissue sarcomas, this case was classified as stage T1N0M0 II, thus making surgery the preferred treatment (15). Preoperative radiotherapy is an option, with benefits including a lower total dose and reduced irradiation of normal tissue volumes. However, its major drawback is the increased risk of acute wound healing complications. Regardless of the type of resection, excellent local control rates are achieved when preoperative radiotherapy is incorporated into patient care (16, 17).

Treatment options for sarcomas also include chemotherapy. Standard chemotherapy agents for undifferentiated sarcomas include

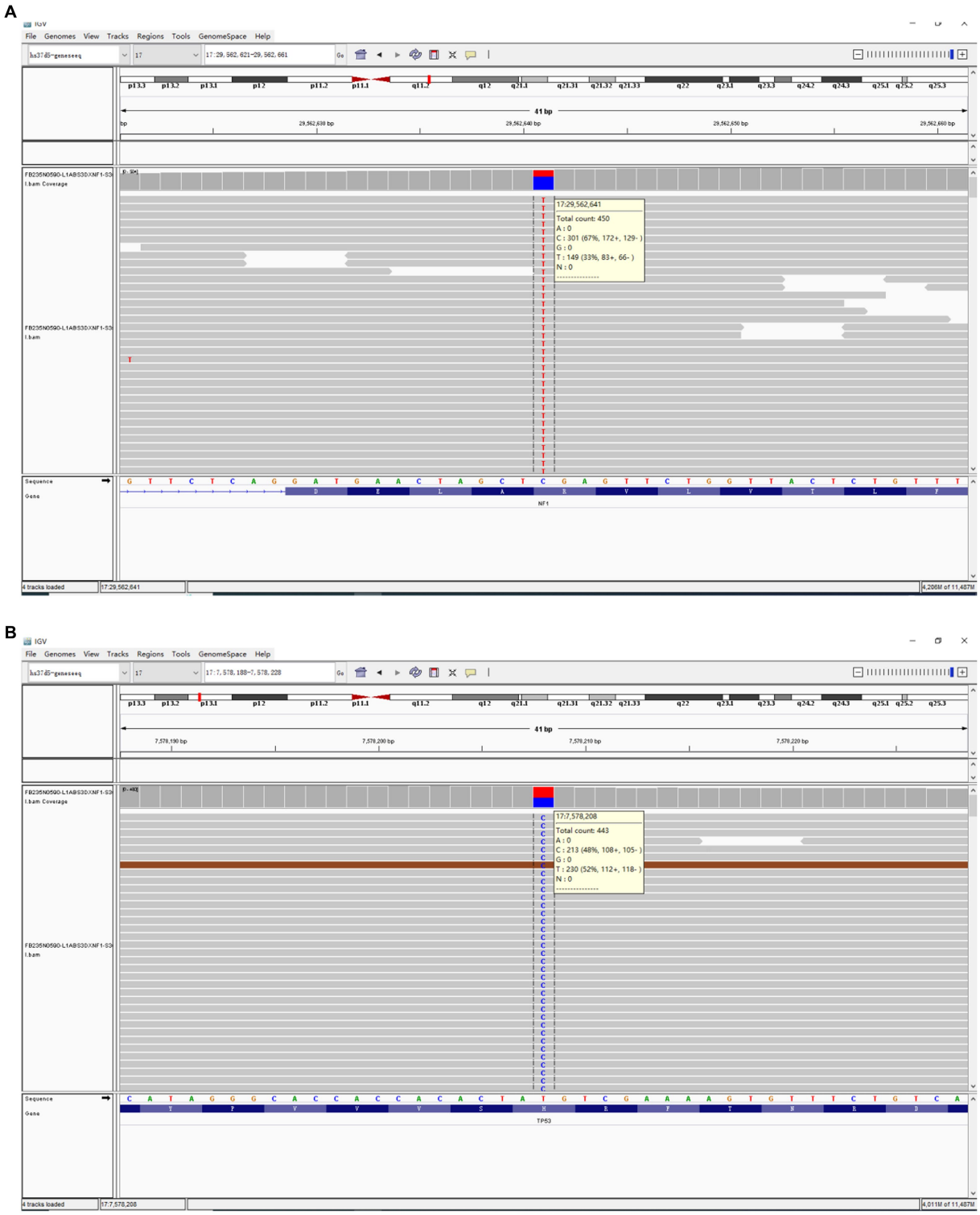

FIGURE 3
The comprehensive genomic profiling based on Next-Generation Sequencing has revealed a nonsense mutation in the NF1 gene (c.3721C > T(p.R1241*)) **(A)** within the USEF component and a missense mutation in the TP53 gene (c.641A > G(p.H214R)) **(B)**.

doxorubicin, ifosfamide, gemcitabine, and paclitaxel (18, 19). However, there is currently no standard treatment protocol specifically for USEF, and not all patients with advanced or metastatic soft tissue sarcomas benefit from conventional chemotherapy.

Targeted therapy is pivotal in treating patients resistant to or who have failed conventional chemotherapy. Anlotinib has demonstrated efficacy in refractory metastatic UPS, with a 12-week progression-free rate of 58% and median progression-free survival of 4.1 months (20).

TABLE 1 Main mutation frequencies of unclassified sarcoma with epithelioid features.

Gene	Mutation	Alteration	Variant allele fraction
NF1	p.R1241* exon 28 nonsense mutation	c.3721C > T(p.R1241*)	32.99%
TP53	p.H214R exon 6 missense mutation	c.641A > G(p.H214R)	48.14%

TABLE 2 Previously reported cases of unclassified sarcoma with epithelioid features.

Case number	Author	Sex/ age, y	Anatomical site	Initial therapy	Immunohistochemical findings	Genetic analysis	Outcome (duration of follow up)
1 (33)	Lang Y	F/66	Left lower leg	Surgical resection	Positive for vimentin, TFE3, CD68 and CD34	TFE3 gene amplification	No evidence of disease (8 months)
2 (34)	Li ZX	F/10	Right forearm	None	Weakly positive for vimentin; approximately 5% were positive for Ki-67	No genetic testing	Alive with disease (6 months)
3 (35)	El Ochi MR	M/61	Right lung	Surgical resection	diffusely positive staining for vimentin and smooth muscle actin, with focal positivity for CD99.	No genetic testing	Alive with disease (1 months)
4 (36)	Sajko N	M/73	Left thigh	Left thigh	Not described	No genetic testing	Alive with disease (9 months)

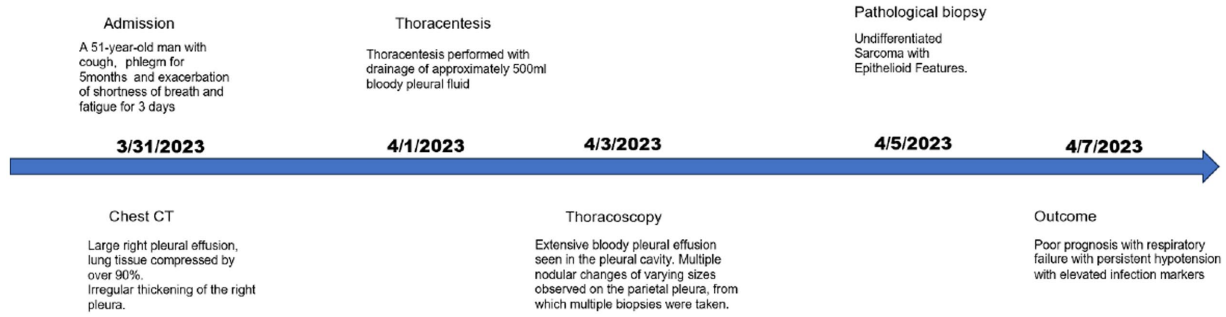

FIGURE 4
Timeline scheme of the major clinical event of the patient.

Additionally, in this case, we detected a nonsense mutation p.R1241* in the *NF1* gene, which may lead to NF1 protein inactivation, increasing Ras-GTP levels and activating downstream RAS pathways, thereby promoting excessive cell proliferation. NF1 inactivating mutations might reduce sensitivity to EGFR-targeted drugs, although clinical evidence remains insufficient (21). This mutation could also increase sensitivity to MEK inhibitors such as selumetinib (22).

In this case, the detected p.H214R missense mutation in the *TP53* gene could diminish the tumor-suppressing function of TP53 and is associated with tumor progression and chemotherapy resistance (23). Adavosertib, a WEE1 kinase inhibitor targeting G2 checkpoint control, has shown potential efficacy in preclinical studies against TP53-mutated tumor cells, especially in combination with chemotherapy (24). Further phase II clinical trials have found that Adavosertib significantly enhances chemotherapy sensitivity in patients with TP53 mutations (25). Phase Ib clinical trials have indicated that the combination of Adavosertib and Olaparib is safe and effective in some patients with TP53 mutations (26). These findings underscore the importance of TP53 mutations in guiding drug choices for this case, with Adavosertib being a potential treatment option.

The NCCN Clinical Practice Guidelines recommend pembrolizumab, an immune checkpoint inhibitor, for the treatment of undifferentiated sarcomas (27). The high TMB detected in this case further enhances the potential for immunotherapy. Exome sequencing revealed a TMB of 16.5 Muts/Mb, suggesting that the patient may respond well to pembrolizumab immunotherapy. FDA has approved pembrolizumab for the treatment of patients with solid tumors with high TMB (TMB-H) (28). In the KEYNOTE-158 trial, patients with high TMB showed significant overall response rates (29). TP53 mutations might be positive predictors for immunotherapy, as such genetic alterations can lead to increased PD-L1 expression (30). Patients with TP53 mutations, especially those with concurrent TP53/KRAS mutations, could significantly benefit from PD-1 inhibitors (31, 32). Therefore, considering the high TMB and presence of TP53 mutation, pembrolizumab immunotherapy emerges as a promising treatment option for this case. We summarize the treatment strategies for unclassified sarcomas with epithelioid features outlining treatment in Table 3.

TABLE 3 Overview of treatment strategies for unclassified sarcoma with epithelioid features therapy.

Treatment strategies		Descriptions
Surgery		Surgery is the primary treatment method for undifferentiated sarcomas (15).
Preoperative radiotherapy		Preoperative radiotherapy, offering benefits such as lower dosage and minimal irradiation of normal tissues, is an effective option. Excellent local control rates are consistently achieved with this approach, regardless of the resection type (16, 17).
Chemotherapy		Standard chemotherapy agents for undifferentiated sarcomas include doxorubicin, ifosfamide, gemcitabine, and paclitaxel (18, 19).
Targeted therapy	Erlotinib and gefitinib	NF1 inactivating mutations might reduce sensitivity to EGFR-targeted drugs, although clinical evidence is not yet sufficient (21)
	Selumetinib	NF1 inactivating mutations increase sensitivity to MEK inhibitors like Selumetinib (22)
	Adavosertib	Adavosertib, a WEE1 kinase inhibitor, has demonstrated effectiveness in enhancing chemotherapy sensitivity in TP53-mutated tumor cells, suggesting its potential as a treatment option for tumors with TP53 mutations (24).
Immunotherapy	Pembrolizumab	Pembrolizumab has been approved by the FDA for treating patients with high Tumor Mutation Burden (TMB-H) solid tumors, as these patients have shown significant overall response rates in the KEYNOTE-158 trial (28, 29).
		TP53 mutations, which can lead to increased PD-L1 expression, may serve as positive predictors for the effectiveness of pembrolizumab immunotherapy, especially in patients with concurrent TP53/KRAS mutations (30–32).

TABLE 4 TP53 mutation types and their impact on survival and prognosis across three different types of cancers.

Cancer type	TP53 mutation type	Survival impact	Prognostic impact	Notes
Diffuse large B-cell lymphoma (DLBCL)	74% missense mutations, predominantly in exons 5–8 DNA-binding domain. High-frequency mutations at codons 175, 273, 248	No significant impact on overall survival (OS), poorer prognosis in GCB subtype	TP53WT&CD58MUT with worst OS (median 92.3 months); TP53MUT&CD58WT with best OS (median 110.8 months)	TP53 mutation rate: 30% (37)
Hepatocellular carcinoma (HCC)	63.3% missense, 20.2% nonsense, 16.5% frameshift mutations. Hotspots at R249S, R175H, R273H, R248Q, R282W	High-risk group with median survival 2.46 years, low-risk group 6.81 years	TP53MLncSig prognostic model differentiates high and low-risk patients, correlates with response to immune checkpoint blockade (ICB) therapy	TP53 mutation rate: 29% (38)
Breast cancer	Inactive (64.7%), Structural (23.5%, e.g., R175H, G245S, R249S, Y220C), Contact (11.8%, e.g., R273H/C, R248W)	Inactive: OS median 12.5 months, PFS 5.5 months; Structural: OS median 22.5 months, PFS 10.5 months; Contact: OS median 24.5 months, PFS 11.5 months	Inactive type associated with significantly worse prognosis compared to Contact and Structural types	(39)

Tumor DNA sequencing serves a dual purpose: guiding drug selection and providing prognostic insights into the disease course. In this case, we detected a *TP53* mutation in the patient. This mutation, identified as pathogenic in multiple databases, including UMD, is anticipated to reduce the tumor-suppressive function of the *TP53* gene. It is likely involved in tumor development, progression, and poor prognosis. To discuss the impact of *TP53* mutations on tumor progression, especially given the rapid progression of the tumor in this case, in Table 4, we incorporate *TP53* mutations that show a positive correlation with outcomes or overall survival.

This case represents the first instance of USEF originating from the pleura encountered by our team, marked by its rapid development and challenges in detection. Despite the patient's decision to forego antineoplastic treatment, the severity and invasiveness of USEF were underscored by the disease's swift advancement, culminating in the patient's death due to respiratory failure. Given that the patient did not receive any form of treatment, this report primarily focuses on the diagnosis of USEF and the discussions surrounding potential therapeutic implications based on the patient's NGS results. In this context, we thoroughly analyze the clinical and pathological characteristics of this specific case, contemplate the patient's potential treatment options, and provide insights for future care strategies in similar scenarios.

Data availability statement

The datasets presented in this study can be found in online repositories. The names of the repository/repositories and accession number(s) can be found at: https://www.ncbi.nlm.nih.gov/genbank/, PRJNA1063166.

Ethics statement

The studies involving humans were approved by Institutional Review Board (IRB) of the Second Affiliated Hospital of Chongqing Medical University. The studies were conducted in accordance with the local legislation and institutional requirements. The participants provided their written informed consent to participate in this study.

Written informed consent was obtained from the individual(s) for the publication of any potentially identifiable images or data included in this article.

Author contributions

L-XX: Conceptualization, Data curation, Visualization, Writing – original draft. LL: Formal analysis, Supervision, Writing – review & editing. WD: Funding acquisition, Investigation, Project administration, Supervision, Writing – review & editing.

Funding

The author(s) declare financial support was received for the research, authorship, and/or publication of this article. This work is supported by the Chongqing Science and Health Joint Medical Research Project (no. 2023MSXM091), the Chongqing Natural Science Foundation (no. cstc2020jcyj-msxmX0008), and the Senior Medical Talents Program of Chongqing for Young and Middle-Aged (no. 2020219).

Conflict of interest

The authors declare that the research was conducted in the absence of any commercial or financial relationships that could be construed as a potential conflict of interest.

Publisher's note

Supplementary material

The Supplementary material for this article can be found online at: https://www.frontiersin.org/articles/10.3389/fmed.2024.1301941/full#supplementary-material

References

1. Choi JH, Ro JY. The 2020 WHO classification of tumors of soft tissue: selected changes and new entities. *Adv Anat Pathol*. (2021) 28:44–58. doi: 10.1097/PAP.0000000000000284

2. Sakharpe A, Lahat G, Gulamhusein T, Liu P, Bolshakov S, Nguyen T, et al. Epithelioid sarcoma and unclassified sarcoma with epithelioid features: Clinicopathological variables, molecular markers, and a new experimental model. *Oncologist*. (2011) 16:512–22. doi: 10.1634/theoncologist.2010-0174

3. Fletcher CD, Gustafson P, Rydholm A, Willén H, Akerman M. Clinicopathologic re-evaluation of 100 malignant fibrous histiocytomas: prognostic relevance of subclassification. *J Clin Oncol*. (2001) 19:3045–50. doi: 10.1200/JCO.2001.19.12.3045

4. Sbaraglia M, Bellan E, Dei Tos AP. The 2020 WHO classification of soft tissue Tumours: news and perspectives. *Pathologica*. (2020) 113:70–84. doi: 10.32074/1591-951X-213

5. Thway K, Jones RL, Noujaim J, Fisher C. Epithelioid sarcoma: diagnostic features and genetics. *Adv Anat Pathol*. (2016) 23:41–9. doi: 10.1097/PAP.0000000000000102

6. Chapel DB, Schulte JJ, Husain AN, Krausz T. Application of immunohistochemistry in diagnosis and management of malignant mesothelioma. *Transl Lung Cancer Res*. (2020) 9:S3–S27. doi: 10.21037/tlcr.2019.11.29

7. Girolami I, Lucenteforte E, Eccher A, Marletta S, Brunelli M, Graziano P, et al. Evidence-based diagnostic performance of novel biomarkers for the diagnosis of malignant mesothelioma in effusion cytology. *Cancer Cytopathol*. (2022) 130:96–109. doi: 10.1002/cncy.22509

8. Attanoos RL, Gibbs AR. "Pseudomesotheliomatous" carcinomas of the pleura: a 10-year analysis of cases from the environmental lung disease research group, Cardiff. *Histopathology*. (2003) 43:444–52. doi: 10.1046/j.1365-2559.2003.01674.x

9. Matsukuma S, Takeo H, Kato K, Sato K. Numerous osteoclast-like giant cells in metastases from lung adenocarcinoma, but absent from primary tumor. *Thoracic Cancer*. (2014) 5:354–7. doi: 10.1111/1759-7714.12090

10. Halimi M, BeheshtiRouy S, Salehi D, Rasihashemi SZ. The role of immunohistochemistry studies in distinguishing malignant mesothelioma from metastatic lung carcinoma in malignant pleural effusion. *Iran J Pathol*. (2019) 14:122–6. doi: 10.30699/ijp.14.2.122

11. Mehta A, Bansal D, Tripathi R, Jajodia A. SMARCA4/BRG1 protein-deficient thoracic tumors dictate re-examination of small biopsy reporting in non–small cell lung cancer. *J Pathol Transl Med*. (2021) 55:307–16. doi: 10.4132/jptm.2021.05.11

12. Anžič N, Krasniqi F, Eberhardt AL, Tzankov A, Haslbauer JD. Ipilimumab and Pembrolizumab mixed response in a 41-year-old patient with SMARCA4-deficient thoracic sarcoma: an interdisciplinary case study. *Case Reports in Oncology*. (2021) 14:706–15. doi: 10.1159/000515416

13. Hasegawa T, Yamamoto S, Yokoyama R, Umeda T, Matsuno Y, Hirohashi S. Prognostic significance of grading and staging systems using MIB-1 score in adult patients with soft tissue sarcoma of the extremities and trunk. *Cancer*. (2002) 95:843–51. doi: 10.1002/cncr.10728

14. Tanaka K, Hasegawa T, Nojima T, Oda Y, Mizusawa J, Fukuda H, et al. Prospective evaluation of Ki-67 system in histological grading of soft tissue sarcomas in the Japan clinical oncology group study JCOG 0304. *World J Surg Oncol*. (2016) 14:110. doi: 10.1186/s12957-016-0869-6

15. Nystrom LM, Reimer NB, Reith JD, Dang L, Zlotecki RA, Scarborough MT, et al. Multidisciplinary Management of Soft Tissue Sarcoma. *ScientificWorldJournal*. (2013) 2013:852462:1–11. doi: 10.1155/2013/852462

16. Sampath S, Schultheiss TE, Hitchcock YJ, Randall RL, Shrieve DC, Wong JYC. Preoperative versus postoperative radiotherapy in soft-tissue sarcoma: multi-institutional analysis of 821 patients. *Int J Radiat Oncol Biol Phys*. (2011) 81:498–505. doi: 10.1016/j.ijrobp.2010.06.034

17. O'Sullivan B, Davis AM, Turcotte R, Bell R, Catton C, Chabot P, et al. Preoperative versus postoperative radiotherapy in soft-tissue sarcoma of the limbs: a randomised trial. *Lancet*. (2002) 359:2235–41. doi: 10.1016/S0140-6736(02)09292-9

18. Goy BW, Syed S, Padmanabhan A, Burchette RJ, Helmstedter CS. The role of Ifosfamide–doxorubicin chemotherapy in histology-specific, high grade, locally advanced soft tissue sarcoma, a 14-year experience. *Radiother Oncol*. (2021) 165:174–8. doi: 10.1016/j.radonc.2021.10.019

19. Novetsky AP, Powell MA. Management of sarcomas of the uterus. *Curr Opin Oncol*. (2013) 25:546–52. doi: 10.1097/CCO.0b013e328363e0ef

20. Chi Y, Fang Z, Hong X, Yao Y, Sun P, Wang G, et al. Safety and efficacy of Anlotinib, a multikinase angiogenesis inhibitor, in patients with refractory metastatic soft-tissue sarcoma. *Clin Cancer Res*. (2018) 24:5233–8. doi: 10.1158/1078-0432.CCR-17-3766

21. de Bruin EC, Cowell C, Warne PH, Jiang M, Saunders RE, Melnick MA, et al. Reduced NF1 expression confers resistance to EGFR inhibition in lung cancer. *Cancer Discov*. (2014) 4:606–19. doi: 10.1158/2159-8290.CD-13-0741

22. Nissan MH, Pratilas CA, Jones AM, Ramirez R, Won H, Liu C, et al. Loss of NF1 in cutaneous melanoma is associated with RAS activation and MEK dependence. *Cancer Res*. (2014) 74:2340–50. doi: 10.1158/0008-5472.CAN-13-2625

23. Giacomelli AO, Yang X, Lintner RE, McFarland JM, Duby M, Kim J, et al. Mutational processes shape the landscape of TP53 mutations in human cancer. *Nat Genet*. (2018) 50:1381–7. doi: 10.1038/s41588-018-0204-y

24. Leijen S, van Geel RMJM, Pavlick AC, Tibes R, Rosen L, Razak ARA, et al. Phase I study evaluating WEE1 inhibitor AZD1775 as monotherapy and in combination with gemcitabine, cisplatin, or carboplatin in patients with advanced solid tumors. *J Clin Oncol*. (2016) 34:4371–80. doi: 10.1200/JCO.2016.67.5991

25. Leijen S, van Geel R, Sonke GS, de Jong D, Rosenberg EH, Marchetti S, et al. Phase II study with Wee1 inhibitor AZD1775 plus carboplatin in patients with p53 mutated ovarian cancer refractory or resistant (<3 months) to standard first line therapy. *JCO*. (2015) 33:2507–7. doi: 10.1200/jco.2015.33.15_suppl.2507

26. AstraZeneca. A Phase Ib Study of AZD1775 and Olaparib in Patients With Refractory Solid Tumours [Internet]. clinicaltrials.gov; (2019) [cited 2023 Jan 1]. Report No.: NCT02511795. Available at: https://clinicaltrials.gov/study/NCT02511795

27. von Mehren M, Kane JM, Bui MM, Choy E, Connelly M, Dry S, et al. NCCN guidelines insights: soft tissue sarcoma, version 1.2021. *J Natl Compr Cancer Netw*. (2020) 18:1604–12. doi: 10.6004/jnccn.2020.0058

28. Marcus L, Fashoyin-Aje LA, Donoghue M, Yuan M, Rodriguez L, Gallagher PS, et al. FDA approval summary: Pembrolizumab for the treatment of tumor mutational burden-high solid tumors. *Clin Cancer Res*. (2021) 27:4685–9. doi: 10.1158/1078-0432.CCR-21-0327

29. Marabelle A, Le DT, Ascierto PA, Di Giacomo AM, De Jesus-Acosta A, Delord JP, et al. Efficacy of Pembrolizumab in patients with noncolorectal high microsatellite instability/mismatch repair-deficient Cancer: results from the phase II KEYNOTE-158 study. *J Clin Oncol*. (2020) 38:1–10. doi: 10.1200/JCO.19.02105

30. Yu J, Ling S, Hong J, Zhang L, Zhou W, Yin L, et al. TP53/mTORC1-mediated bidirectional regulation of PD-L1 modulates immune evasion in hepatocellular carcinoma. *J Immunother Cancer*. (2023) 11:e007479. doi: 10.1136/jitc-2023-007479

31. Dong ZY, Zhong WZ, Zhang XC, Su J, Xie Z, Liu SY, et al. Potential predictive value of TP53 and KRAS mutation status for response to PD-1 blockade immunotherapy in lung adenocarcinoma. *Clin Cancer Res*. (2017) 23:3012–24. doi: 10.1158/1078-0432.CCR-16-2554

32. Frost N, Kollmeier J, Vollbrecht C, Grah C, Matthes B, Pultermann D, et al. KRASG12C/TP53 co-mutations identify long-term responders to first line palliative treatment with pembrolizumab monotherapy in PD-L1 high (≥50%) lung adenocarcinoma. *Transl Lung Cancer Res*. (2021) 10:737–52. doi: 10.21037/tlcr-20-958

33. Lang, Y, Li, X, Chen, S, Xiang, P, Han, A. The clinicopathological features of epithelioid undifferentiated sarcoma with TFE3 amplification with one case report. *Arch Clin Med Case Rep*. (2021) 5:129–36.

34. Li, ZX, Zheng, S, Jiang, HH, Sun, YZ, Qi, RQ, Hong, YX, et al. A 10-year-old girl with metastatic unclassified sarcoma with epithelioid features. *Chin Med J (Engl)*. (2017) 130:1385–6. doi: 10.4103/0366-6999.206351

35. El Ochi, MR, el Hammoumi, M, Biyi, A, Allaoui, M, Kabiri, EH, Albouzidi, A, et al. Pulmonary tumor diagnosed as an undifferentiated sarcoma with epithelioid features: a case report. *J. Med. Case Rep.* (2016) 10.

36. Sajko, N, Murphy, S, Tran, A. Undifferentiated epithelioid sarcoma presenting as a fever of unknown origin: a case report. *J. Med. Case Rep.* (2019) 13:24. doi: 10.1186/s13256-019-1927-7

37. Zhang, T, Lu, Y, Liu, X, Zhao, M, He, J, Liu, X, et al. Comprehensive analysis of TP53 mutation characteristics and identification of patients with inferior prognosis and enhanced immune escape in diffuse large B-cell lymphoma. *Am. J. Hematol.* (2022) 97:E14–7. doi: 10.1002/ajh.26323

38. Chu, C, Liu, D, Wang, D, Hu, S, Zhang, Y. Identification and development of TP53 mutation-associated long non-coding RNAs signature for optimized prognosis assessment and treatment selection in hepatocellular carcinoma. *Int J Immunopathol Pharmacol.* (2023) 37:03946320231211795. doi: 10.1177/03946320231211795

39. Lu, Q, Wei, L, Cai, S, Zhang, Z, Zhang, L. Detection of TP53 gene mutation in blood of breast cancer patients based on circulating tumor DNA and its application in prognosis. *Cellular and Molecular Biology.* (2023) 69:200–6. doi: 10.14715/cmb/2023.69.11.34

frontiers | Frontiers in Medicine

TYPE Case Report
PUBLISHED 07 February 2024
DOI 10.3389/fmed.2024.1268008

OPEN ACCESS

EDITED BY
Santi Nolasco,
University of Catania, Italy

REVIEWED BY
Mila Stajevic,
University of Belgrade, Serbia
Cosimo Bleve,
San Bortolo Hospital, Italy

*CORRESPONDENCE
Jun Wang
jnwj660606@163.com

RECEIVED 27 July 2023
ACCEPTED 08 January 2024
PUBLISHED 07 February 2024

CITATION
Cai C-S, Li B, Yuan Y-c, Fu L-n, Zhang X-y and Wang J (2024) Bronchopulmonary foregut malformation with severe hemoptysis in advanced age: a case report and literature review.
Front. Med. 11:1268008.
doi: 10.3389/fmed.2024.1268008

Bronchopulmonary foregut malformation with severe hemoptysis in advanced age: a case report and literature review

Cheng-Sen Cai[1], Bin Li[2], Yu-chun Yuan[2], Li-na Fu[1], Xiao-ye Zhang[3] and Jun Wang[1]*

[1]Department of Respiratory and Critical Care Medicine, Second Affiliated Hospital of Shandong University of Traditional Chinese Medicine, Jinan, Shandong, China, [2]Department of Radiology, Second Affiliated Hospital of Shandong University of Traditional Chinese Medicine, Jinan, Shandong, China, [3]Department of Pathology, Second Affiliated Hospital of Shandong University of Traditional Chinese Medicine, Jinan, Shandong, China

Bronchopulmonary foregut malformation (BPFM) is a rare developmental malformation disease due to embryonic defects, with an even rarer occurrence in adults. We report a diagnosed case in an adult patient, and notably, this is the first reported case of such advanced age. Additionally, she experienced coughing up approximately 1 liter of blood and partial lung tissue, accompanied by respiratory failure and shock. Following treatment with transcatheter arterial embolization, her condition improved, and she has remained stable during follow-up. We present a case report and conducted a systematic review on this particular case.

KEYWORDS

BPFM, hemoptysis, advanced age, case report, literature review

Introduction

Bronchopulmonary foregut malformation (BPFM) is a developmental malformation of the respiratory and digestive systems (1). It is caused by budding defects, differentiation, and abnormal separation of the embryonic foregut, ultimately manifesting in isolation of the lung and bronchial–esophageal fistula formation. As a rare disease, it is primarily diagnosed in childhood. We report the case of one elderly patient with BPFM. She presented with significant hemoptysis and expectorated a clot that was confirmed to contain lung tissue. She later developed respiratory failure and hypovolemic shock. A chest CT showed anomalous masses in the lower lobe of the right lung, aortography detected an abnormal feeding artery, and esophageal angiography revealed an esophageal–bronchial fistula. The patient's condition was stabilized after artery embolism and comprehensive treatment.

Case report

The patient, a 67-year-old woman, was admitted to the hospital for 5 days with hemoptysis and a history of repeated cough over many years. She had a history of drinking approximately 100 g per day for 15 years, with no other remarkable personal or family history. Moist rales were found in the lower lobe of the right lung.

After admission, multiple laboratory tests were arranged. The patient's white blood cell and neutrophil counts were $11.1*10^9$/L and $7.1*10^9$/L, respectively; her D-dimer level was 1.97 mg/L; her procalcitonin level was normal; and her tuberculin test and tumor-related indicators were negative. A chest CT showed a nodular shadow with a relatively regular morphology and uneven enhancement in the right lung (Figure 1).

Fiberoptic bronchoscopy showed obvious local congestion of the mucosa in the right lower lobe, and the lumen of the posterior segment of the right lower lobe was suspected to be blocked by a neoplasm. A brush biopsy was taken for pathological examination which later indicated inflammation; approximately 100 mL of bleeding occurred during the process, which was treated with local hemostasis.

Upon differential diagnosis, hemoptysis-causing diseases such as lung malignancy, tuberculosis, and pulmonary embolism were ruled out. A normal cranial CT excluded cough caused by swallowing reflex dysfunction. Thus, evaluation of the patient only revealed mild pulmonary inflammation.

During treatment, the patient had two episodes of massive hemoptysis. During the first episode, the patient expectorated approximately 300 mL of material, including clots, which was later sent for pathological examination. Hematoxylin and eosin (H&E) staining showed degenerated alveolar tissue structure (Figure 2).

Although the bleeding stopped temporarily after hemostasis treatment, the patient had another episode of massive hemoptysis around 8 h later, expectorating a volume of approximately 700 mL. She subsequently developed confusion, respiratory failure, and hemorrhagic shock. We immediately arranged for a blood transfusion and mechanical ventilation and performed an emergency vascular intervention. Body arterial angiography revealed a twisted and deformed artery originating from the thoracic aorta that was supplying blood to the lesion in the right lower lobe of the lung (Figures 3A,B).

Therefore, arterial embolization of this blood vessel was performed. After polyvinyl alcohol particle embolization (particle size: 350–560 μm), the hemoptysis stopped abruptly. The patient recovered

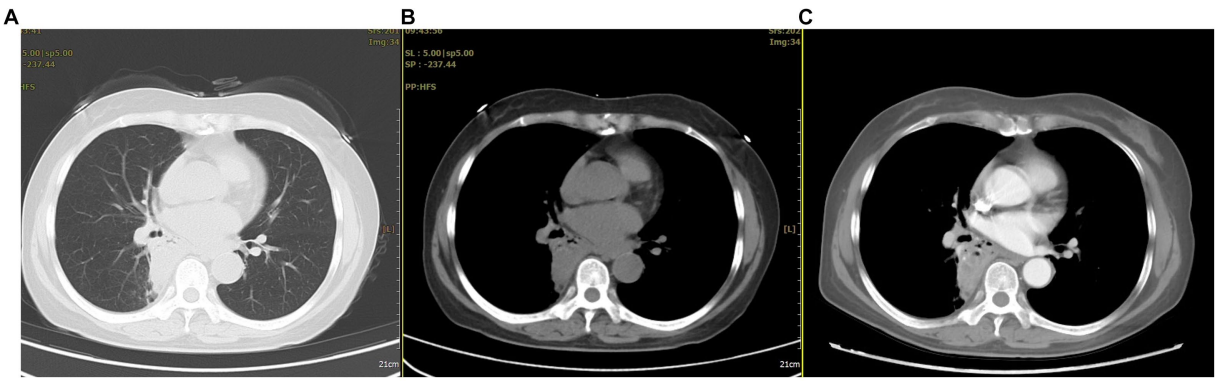

FIGURE 1
The chest CT revealed abnormal lesions in the lower lobe of the right lung. **(A)** In the lung window, a consolidation shadow was observed in the posterior segment of the right lower lobe. **(B)** In the mediastinal window, the lesion appeared to have regular margins. **(C)** After contrast enhancement, heterogeneous enhancement was noted within the lesion.

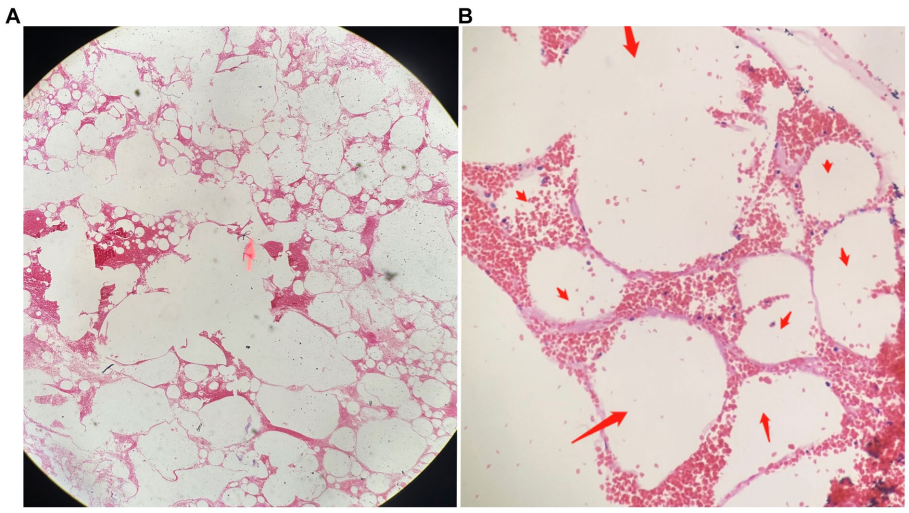

FIGURE 2
The pathological findings of the expectorated mass on HE staining. **(A)** Dilated and degenerated alveolar contours are visible in the field of view (HE, ×40). **(B)** Interstitial congestion and loss of alveolar epithelial cells can be observed (indicated by red arrows; HE, ×100).

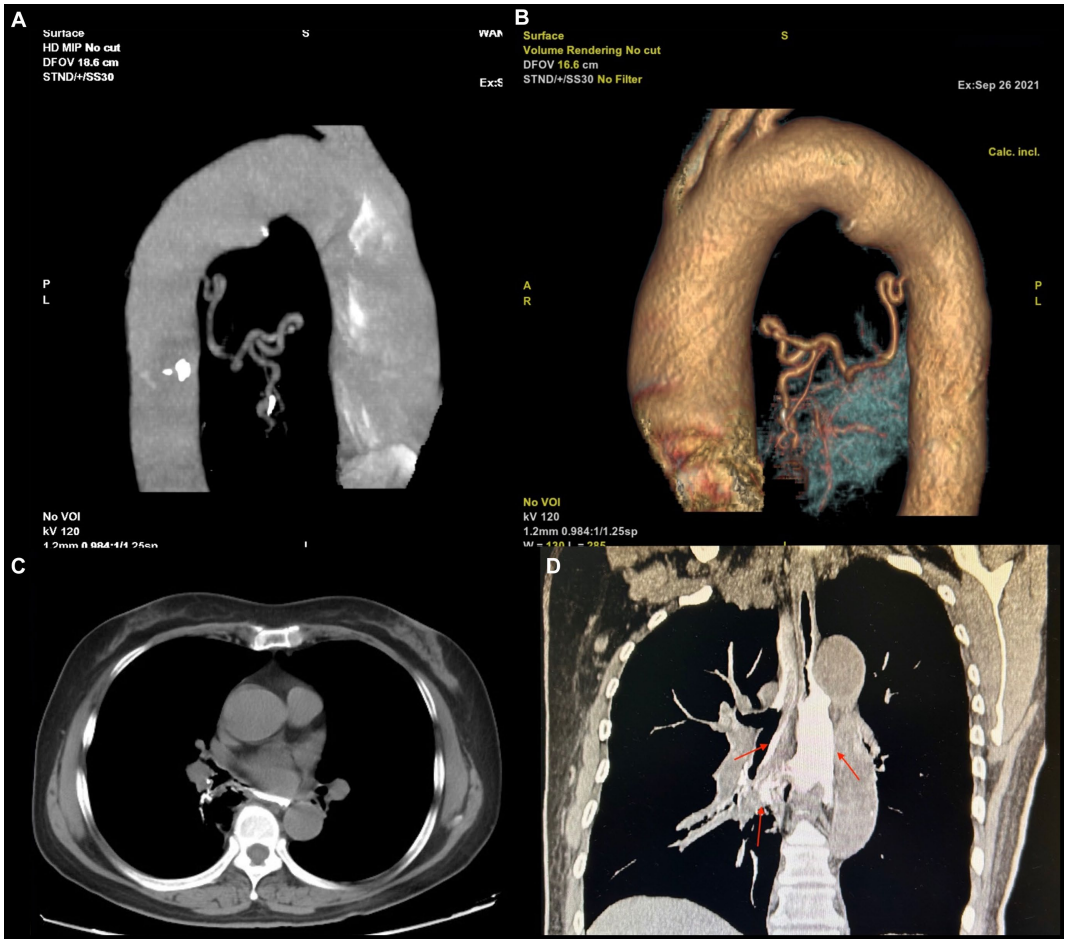

FIGURE 3
(A,B) The blood supply vascular reconstruction of the lesion reveals a large, tortuous, and malformed artery originating from the descending aorta, extending toward the site of the lesion. **(C,D)** The upper gastrointestinal (UGI) contrast study. **(A)** In the axial view, an abnormal communication between the trachea and esophagus is observed. **(B)** In the coronal view, the contrast agent is seen entering the bronchus through the fistula and remaining within the airway (indicated by a red arrow).

soon after basic treatment and the ventilator was removed. In addition, upper gastrointestinal (UGI) radiography revealed an abnormal connection between the bronchus and esophagus (Figures 3C,D), so we diagnosed the patient with BPFM.

However, she refused surgical treatment due to fear of the risks associated with her advanced age and chose to be discharged. Therefore, we advised her to avoid a stimulating diet, especially alcohol. Assessed through telephone follow-up, the patient's condition remained stable after discharge, but occasional coughing still occurred. Eighteen months later, a chest CT showed that the lesion had significantly decreased in size and showed local cystic changes (Figure 4). Therefore, we remain concerned that the patient's condition may worsen in the future.

Discussion

BPFM is a subcategory of pulmonary isolation that was first described in 1968 (2). It occurs due to developmental abnormalities present during the fourth week of embryonic development. Srikanth et al. divide BPFM into four different groups. In group I (16%), the anomaly is associated with esophageal atresia and tracheoesophageal fistula. In group II (33%), one lung originates from the lower esophagus. In group III (46%), an isolated anatomic lung lobe or segment communicates with the esophagus or stomach. In group IV (5%), a portion of the normal bronchial system communicates with the esophagus (3).

Epidemiologically, patients often present with respiratory symptoms because of the abnormal entrance between the esophagus and bronchi. Therefore, most cases are diagnosed in childhood. However, a small proportion of patients have no obvious symptoms early in life and the condition is not detected until adulthood. We found fewer than 20 cases of adult BPFM in the literature. Two hypotheses may explain the absence of obvious symptoms in adults. The first is that the membranous tissue covering the fistula is perforated in adulthood, and the second is that the esophageal wall fold that overlaps the fistula loses mobility with aging (4). In the present case, the patient was 67 years old at the time of diagnosis, 3 years older than the oldest patient reported in the literature, thus providing new insight into the oldest possible age of presentation (5).

The symptoms of BPFM are atypical and vary according to age and disease subgroup (1). Generally, recurrent pneumonia or bucking when intaking fluid or food are common in childhood, whereas chest

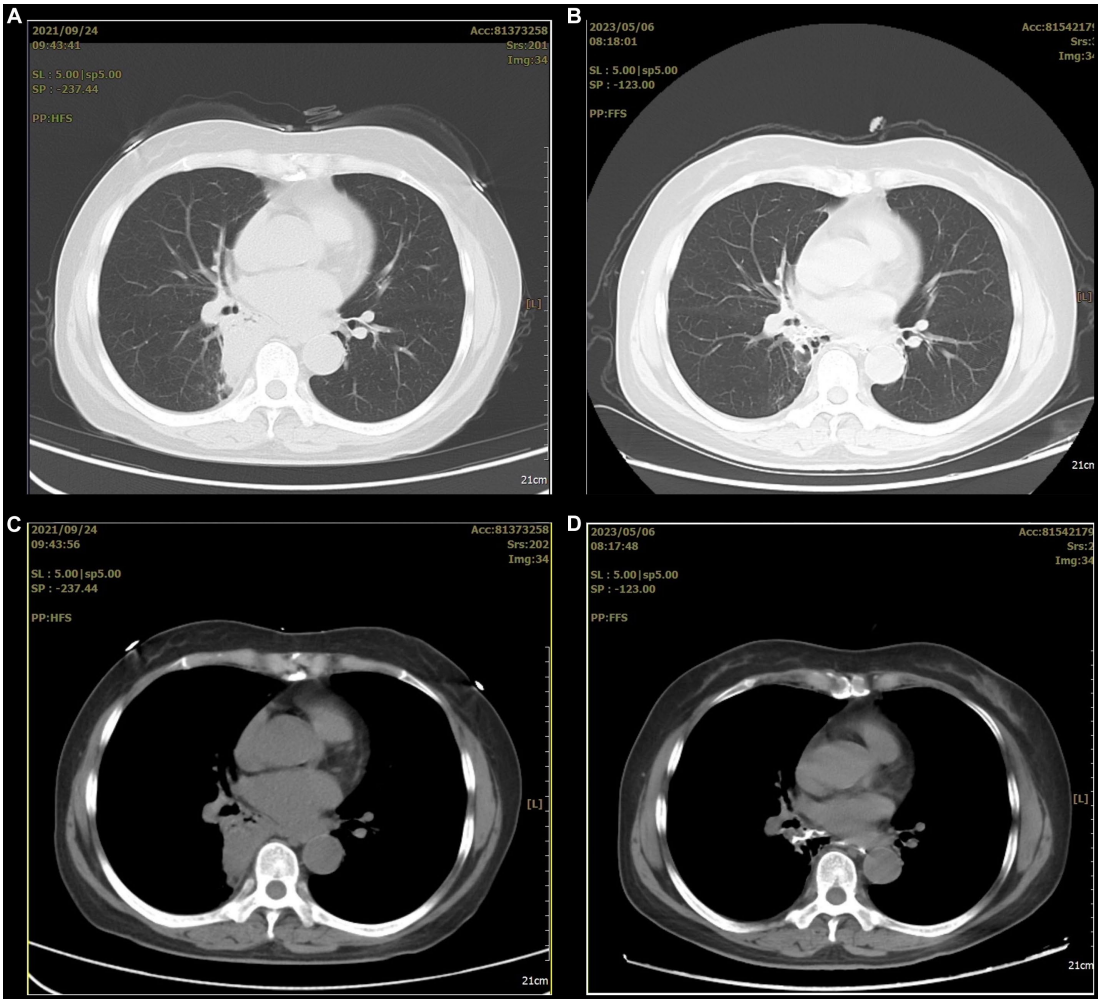

FIGURE 4
The before and after comparison of the arterial embolization treatment for the lesion. **(A,C)** A consolidation shadow can be seen in the right lung before the treatment. **(B,D)** After the treatment, the consolidation shadow appears significantly reduced.

pain, dyspnea, and hemoptysis are common in adults (5–8). The pathological factors underlying the development of hemoptysis are not clear. We speculate that the abnormal entrance allows food particles to enter the bronchi, causing chronic infection and inflammation. Thus, some deformed blood vessels might be injured by physical and chemical stimulation of the lung, ultimately resulting in bleeding. In the present case, hemoptysis was the patient's primary symptom; approximately 1 liter of blood had accumulated, causing respiratory failure and hypovolemic shock, which is rare. In particular, this patient expectorated a mass during one of her hemoptysis episodes. Necrotic alveolar structures revealed by H&E staining confirmed another diagnosis: necrotizing pneumonia. We considered that this chronic infection caused local lung tissue necrosis, as well as rupture and bleeding of the deformed, fragile blood vessel, all of which was ultimately expectorated like the old Chinese saying, "fruits fall off when ripe."

As a congenital anomaly, BPFM can involve cystic lesions in the bronchial–esophageal junction, covered with squamous and columnar epithelium. This phenomenon demonstrates a close correlation between BPFM and abnormal embryonic development (9). Through operative pathology, Xie et al. found underdeveloped, structurally disordered lung tissue containing dilated cysts of varying sizes, necrosis, and abundant foam cells in the lumen (10). In the present case, we could only detect structurally disordered and degraded alveolar structures through pathological staining of the expectorated clots. Unfortunately, we did not obtain surgical pathology results because the patient refused surgery. However, this refusal did not affect the diagnosis of the disease.

The diagnosis of BPFM primarily relies upon imaging. Yang et al. reviewed 61 cases of BPFM and found that the diagnostic methods used were mainly UGI radiography (62.3%) and CT (11.5%) (7). Caro-Domínguez et al. reported that BPFM can also be diagnosed by ultrasound and MRI (11). A UGI series can detect abnormal bronchial–esophageal channels. According to Yutaka et al., CT scans reveal that approximately 75% of BPFM patients have lesions in the right lung, particularly in the posterior basal segment of the right lower lobe, and the typical manifestations are consolidation and cystic shadows (4). Additionally, systemic circulation arteriography can reveal abnormal artery blood supply at the focus, some of which is returned by the pulmonary vein (5, 8). In the present case, CT revealed a solid lesion in the lower lobe of the right lung, with a visible gas–liquid appearance. After

absorption, the lesion formed a cystic shadow. UGI radiography revealed an esophageal–bronchial fistula and contrast agent could be seen flowing out of the bronchus. This patient presented with almost all of these symptoms.

With respect to treatment, because BPFM is primarily discovered in childhood, early surgery is the first-line treatment, after which the prognosis is good. However, given the possibility of significant surgical damage, some authors recommend artery embolization in later stages; however, this method cannot achieve a radical cure (12). Indeed, the outcomes of conservative management are poor and may result in repeated lung infection or even hemoptysis. If not properly managed, the patient's life may be in danger. The patient in the present case was older at the time of onset and presented with massive hemoptysis, hypovolemic shock, and respiratory failure; approximately 800 mL of red blood cells were transfused accumulatively. The patient feared the risks of surgery, so she was treated by embolization. Although the treatment was effective and the lesion was relatively stable after reexamination, the patient's cough persisted, indicating she may be at risk for a secondary infection.

To conclude, BPFM is a rare disease that primarily occurs in children. Bronchial–esophageal fistulae can be found through UGI radiography, chest CT shows lesions often located at the periphery of the right lung, and abnormal blood supply in the systemic circulatory arteries can be found by systemic circulation arteriography. This case and literature review provide us with indications that symptoms of BPFM become more severe in older patients, even to the point of life-threatening conditions. Early detection of BPFM can be achieved through chest CT or UGI radiography. Additionally, surgical intervention is the preferred treatment method for BPFM. In cases where surgery is not feasible, transcatheter arterial embolization can be considered as an alternative. However, it is important to note that this method does not provide a definitive cure for BPFM.

Data availability statement

The original contributions presented in the study are included in the article/supplementary material, further inquiries can be directed to the corresponding author.

Ethics statement

Written informed consent was obtained from the individual(s), and minor(s) legal guardian/next of kin, for the publication of any potentially identifiable images or data included in this article.

Author contributions

C-SC: Writing – original draft, Writing – review & editing. BL: Data curation, Resources, Visualization, Writing – review & editing. Y-cY: Data curation, Visualization, Writing – review & editing. L-nF: Writing – original draft, Writing – review & editing. X-yZ: Data curation, Visualization, Writing – review & editing. JW: Funding acquisition, Writing – original draft, Writing – review & editing.

Funding

The author(s) declare financial support was received for the research, authorship, and/or publication of this article. This work was supported by the Shandong Provincial Education Commission Foundation (SDYAL21057 and SDYAL20052).

Conflict of interest

The authors declare that the research was conducted in the absence of any commercial or financial relationships that could be construed as a potential conflict of interest.

Publisher's note

References

1. Barnes NA, Pilling DW. Bronchopulmonary foregut malformations: embryology, radiology and quandary. *Eur Radiol*. (2003) 13:2659–73. doi: 10.1007/s00330-002-1812-5

2. Gerle RD, Jaretzki A, Ashley CA, Berne AS. Congenital bronchopulmonary-foregut malformation. Pulmonary sequestration communicating with the gastrointestinal tract. *N Engl J Med*. (1968) 278:1413–9. doi: 10.1056/NEJM196806272782602

3. Srikanth MS, Ford EG, Stanley P, Mahour GH. Communicating bronchopulmonary foregut malformations: classification and embryogenesis. *J Pediatr Surg*. (1992) 27:732–6. doi: 10.1016/s0022-3468(05)80103-4

4. Yutaka Y, Omasa M, Shikuma K, Taki T. Bronchopulmonary foregut malformation in an adult. *Gen Thorac Cardiovasc Surg*. (2007) 55:476–8. doi: 10.1007/s11748-007-0170-2

5. Tunsupon P, Arshad A, Patel S, Mador MJ. Incidental finding of bronchopulmonary sequestration in a 64-year-old female. *Ochsner J*. (2017) 17:288–91. doi: 10.1043/1524-5012-17.3.288

6. Liu J, Yin J, Liu XY, Yin J, Liu XY, Hu YH, et al. Clinical characteristics of bronchopulmonary foregut malformation. *Zhonghua Er Ke Za Zhi*. (2017) 55:628–31. doi: 10.3760/cma.j.issn.0578-1310.2017.08.016

7. Yang G, Chen L, Xu C, Yuan M, Li Y. Congenital bronchopulmonary foregut malformation: systematic review of the literature. *BMC Pediatr*. (2019) 19:305. doi: 10.1186/s12887-019-1686-1

8. Verma A, Mohan S, Kathuria M, Baijal SS. Esophageal bronchus: case report and review of the literature. *Acta Radiol*. (2008) 49:138–41. doi: 10.1080/02841850701673391

9. Katayama Y, Kusagawa H, Komada T, Shomura S, Tenpaku H. Bronchopulmonary foregut malformation. *Gen Thorac Cardiovasc Surg*. (2011) 59:767–70. doi: 10.1007/s11748-010-0763-z

10. Xie GX, Li HL, Li YC. Bronchopulmonary foregut malformation: report of a case. *Zhonghua Bing Li Xue Za Zhi*. (2017) 46:433–4. doi: 10.3760/cma.j.issn.0529-5807.2017.06.020

11. Caro-Domínguez P, Victoria T, Ciet P, de la Torre E, Toscano ÁC, Diaz LG, et al. Prenatal ultrasound, magnetic resonance imaging and therapeutic options for fetal thoracic anomalies: a pictorial essay. *Pediatr Radiol*. (2023) 53:2106–19. doi: 10.1007/s00247-023-05681-y

12. Corbett HJ, Humphrey GME. Pulmonary sequestration. *Paediatr Respir Rev*. (2004) 5:59–68. doi: 10.1016/j.prrv.2003.09.009

frontiers | Frontiers in Medicine

TYPE Case Report
PUBLISHED 12 February 2024
DOI 10.3389/fmed.2024.1328471

OPEN ACCESS

EDITED BY
Santi Nolasco,
University of Catania, Italy

REVIEWED BY
Helen Parfrey,
Royal Papworth Hospital NHS Foundation Trust, United Kingdom
Stephen C. Land,
University of Dundee, United Kingdom

*CORRESPONDENCE
Malene Helligsø Kirkeby
✉ mhk92@hotmail.com

RECEIVED 26 October 2023
ACCEPTED 29 January 2024
PUBLISHED 12 February 2024

CITATION
Kirkeby MH, Bendstrup E and Rose HK (2024) Case report: If it is not asthma—think of lymphangioleiomyomatosis in younger female patients.
Front. Med. 11:1328471.
doi: 10.3389/fmed.2024.1328471

Case report: If it is not asthma—think of lymphangioleiomyomatosis in younger female patients

Malene Helligsø Kirkeby[1]*, Elisabeth Bendstrup[2,3] and Hanne Krogh Rose[1]

[1]Department of Oncology, Aarhus University Hospital, Aarhus, Denmark, [2]Department of Respiratory Diseases and Allergy, Center for Rare Lung Diseases, Aarhus University Hospital, Aarhus, Denmark, [3]Department of Clinical Medicine, Aarhus University, Aarhus, Denmark

Lymphangioleiomyomatosis (LAM) is a rare lung disease predominantly affecting women, and it is characterized by the proliferation of smooth muscle cells and cystic lung destruction. LAM diagnosis is challenging due to varied clinical presentations and resemblance to common conditions such as asthma. We present two female cases where LAM was initially misdiagnosed. Case 1 describes a woman treated for asthma–chronic obstruction pulmonary disease overlap syndrome, while also undergoing treatment with vascular endothelial growth factor (VEGF) inhibitor pazopanib for a retroperitoneal leiomyoma, the latter responding well to treatment. Due to progressive dyspnea, pazopanib-induced pneumonitis was suspected. High-resolution computed tomography (HRCT) showed changes compatible with LAM. A revision of biopsies showed that the leiomyoma was in fact a lymphangioleiomyoma, and VEGF-D was increased. Both supported the LAM diagnosis. Treatment with mTORC1 inhibitor sirolimus was initiated. Case 2 describes a woman, who in resemblance with the woman from case 2 was also suspected of asthma and did not respond clinically to treatment. After several years, HRCT was performed and suspicion of LAM was raised. Transbronchial biopsy and later, an increased VEGF-D supported the LAM diagnosis. As in case 1, treatment with sirolimus was initiated. These cases underscore the importance of reevaluating diagnoses when treatments fail to yield expected results. Improved awareness and early detection of LAM can enhance patient outcomes and life quality. Early LAM diagnosis is vital as mTORC1 inhibitors such as sirolimus can prevent further decline in lung function. Notably, the response of case 2 to pazopanib treatment supports suggestions of its potential as a second-line therapy for perivascular epithelioid cell tumors (PEComas), including LAM.

KEYWORDS

lymphangioleiomyomatosis, perivascular epithelial cell tumor, high-resolution computed tomography (HRCT), angiomyolipoma (AML), case report, asthma, mTOR inhibition (mTORi)

Introduction

Lymphangioleiomyomatosis (LAM) is a low-malignant rare disease of the lungs characterized by the proliferation of smooth muscle cells surrounding the lymphatics, blood vessels, and alveoli, and it leads to progressive cystic lung destruction and abdominal lymphangioleiomyomas (1). Half of LAM patients have angiomyolipomas (AML), which are

often located in the kidneys (2). The classic clinical presentation of LAM includes progressive dyspnea, cough, and recurrent spontaneous pneumothorax, whereas chylothorax, chylous ascites, and hemoptysis are less common initial symptoms of LAM (2, 3). The extra-pulmonary symptoms of LAM may be abdominal distension and nausea due to lymphangioleiomyomas in the abdomen, pelvis, and retroperitoneum (4). LAM patients with renal AML may present with bleeding, which in some cases can be life-threatening (2).

LAM almost exclusively affects women, and the mean age of initial presentation is approximately 34 years. The prevalence is approximately 1/1.000.000, and up to 40% of all cases are associated with tuberous sclerosis complex (TSC) (2). The female sex hormones are important factors in LAM due to estrogen and progesterone receptors in LAM cells. This is of clinical importance because an accelerated decline in lung function can be seen during pregnancy or with exogenous estrogen use, and it also explains why the decline in lung function is more rapid in premenopausal women (3).

According to the American Thoracic Society/Japanese Respiratory Society LAM guidelines, a definite diagnosis of LAM requires one or more of the following factors in a patient who presents with clinical findings of LAM and characteristic findings in high-resolution computed tomography (HRCT): (1) tuberous sclerosis complex, (2) renal angiomyolipoma, (3) elevated serum VEGF-D $\geq$ 800 pg/mL, (4) chylous effusion, (5) lymphangioleiomyomas, (6) demonstrations of LAM cells or LAM cell clusters on cytological examination of effusions or lymph nodes, or (7) histopathological confirmation of LAM by lung biopsy or biopsy of retroperitoneal or pelvic masses (5).

Lymphangioleiomyomatosis can be medically treated with mTORC1 inhibitors such as sirolimus and everolimus. The end-stage disease may require lung transplantation (3).

In the following, two cases of LAM in young women are presented. In the first case, the medical presentation initially led to the diagnosis of a leiomyoma and asthma–chronic obstructive pulmonary disease (COPD) overlap syndrome. In the second case, the condition was initially interpreted as asthma. The aim of this case report is to emphasize the importance of recognizing features of rare conditions such as LAM, especially in cases where the initial symptoms can be quite common. Moreover, reevaluation of the initial diagnosis should be considered when therapeutic interventions are without the expected clinical effect.

Case report

Case 1

The course of the disease is outlined in Figure 1. In 2019, a 46-year-old woman was brought to the Emergency Department due to coughing and dyspnea and was diagnosed with pneumonia. She was a smoker, and pulmonary function tests (PFTs) were obstructive (Figure 1). Therefore, underlying asthma–COPD overlap syndrome was suspected. Treatment with combined inhaled corticoid steroid (ICS) and long-acting beta-antagonist (LABA) was initiated, and she was referred for follow-up at the Asthma and Allergy Center at the Department of Respiratory Diseases and Allergy, where treatment was supplemented with a leukotriene antagonist. PFTs were still obstructive. At the time, she was perimenopausal with no history of hormone therapy. She had a 10-year-old child, and there was no record of respiratory symptoms during pregnancy and no additional pregnancies.

In 2020, she was brought to the Emergency Department once again, this time presenting with abdominal pain, nausea, and vomiting. Computed tomography (CT) was performed, showing a retroperitoneal process and bullous emphysema. Several years before, in 2008, she had had a CT performed due to increased chromogranin A and suspicion of a neuroendocrine tumor. Back then, the same cystic process was seen and interpreted as a lymphocele. In 2020, CT was supplemented with magnetic resonance imaging (MRI), which raised suspicion of a benign leiomyoma infiltrating both the aorta and the inferior vena cava (Figure 2). A biopsy confirmed the diagnosis, and she was referred to the Oncology Department. Due to estrogen receptor positivity in the tumor, she was initially treated with an anti-estrogen. However, after 3 months, the tumor had not responded to treatment and the patient was experiencing progressive dyspnea. Due to the infiltrative nature of the tumor, the leiomyoma was inoperable and considered to be malignant by the treating oncologists. Treatment with anti-estrogen was discontinued, and treatment with the vascular endothelial growth factor receptor (VEGFR) inhibitor pazopanib was initiated. Concurrently, her asthma treatment was supplemented with long-acting anticholinergics.

The patient was regularly followed with an MRI, showing regression of the tumor (Figure 2). Each time, the scans were evaluated at a highly specialized gastrointestinal multidisciplinary conference, attended by oncologists, pathologists, gastrointestinal surgeons, and radiologists. Due to the infiltration of the large blood vessels, curative surgery was not an option. Clinically, she was experiencing increased abdominal pain despite tumor regression. For a period of 3 months in 2021, the treatment with pazopanib was put on pause, which resulted in tumor progression. Therefore, the treatment was resumed.

In 2022, follow-up related to her asthma–COPD overlap syndrome was concluded, and her health care was continued at her general practitioner. At the time, PFTs were still obstructive, but with an increase in forced expiratory volume in 1 s (FEV1) and forced vital capacity (FVC) (Figure 1).

In February 2023, the patient experienced increasing breathlessness and was referred to an HRCT by the Oncology Department based on suspicion of treatment-induced pneumonitis due to ongoing treatment with pazopanib. The HRCT showed similar findings as before but this time interpreted as cysts and not emphysematous bullae (Figure 3A). In a multidisciplinary team discussion with thoracic radiologists and pulmonologists, the findings were found to be compatible with LAM. She was referred to the Center for Rare Lung Diseases at the Department of Respiratory Diseases and Allergy, where pathology re-evaluation of the retroperitoneal tumor was performed. It was initially evaluated as a leiomyoma with a predominance of smooth muscle cells. Upon second opinion, immunohistochemistry was highly positive for microphthalmia-associated transcription factor (MITF), muscle-specific actin, and human melanoma black 45 (HMB45) and negative for Melan-A, thus supporting a diagnosis of LAM. Later, the LAM diagnosis was supported by an elevated VEGF-D (Figure 1). She showed no other intra-abdominal features of LAM. Treatment with pazopanib was discontinued and treatment with sirolimus was initiated, supplemented by leukotriene antagonist and combined ICS/LABA/long-acting anticholinergics. Pulmonary

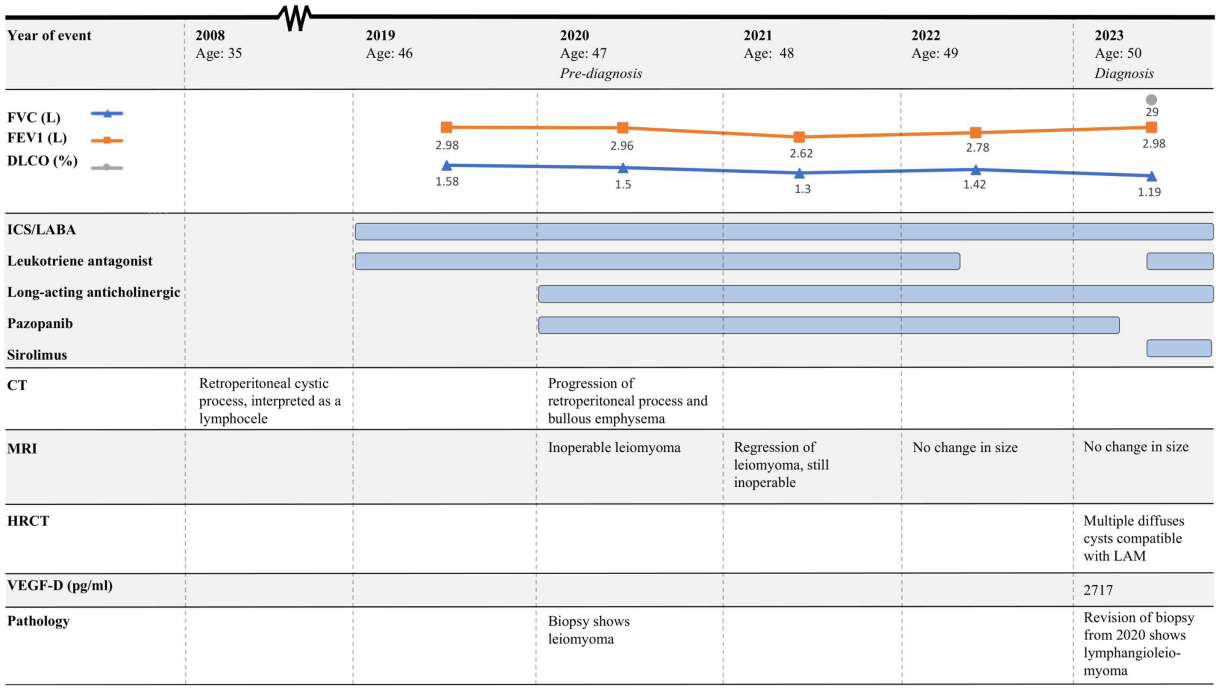

FIGURE 1
Timeline of case 1. CT, Computed tomography; MRI, Magnetic resonance imaging, HRCT, High-resolution computed tomography; FEV1, Forced expiratory volume in 1 s; FVC, Forced vital capacity; DLCO, Diffusion capacity for the lungs for carbon monoxide; LAM, Lymphangioleiomyomatosis; ICS, Inhaled corticosteroids; LABA, Long-acting beta-agonist; VEGFR, Vascular endothelial growth factor receptor.

function tests showed severe obstructive reduction and a low diffusion capacity for carbon monoxide (DLCO) (Figure 1). After 6 months of treatment with sirolimus, MRI showed no change in the size of the lymphangioleiomyoma.

In conclusion, the asthma–COPD overlap syndrome and the leiomyoma/lymphangioleiomyoma were both features of underlying LAM.

Case 2

The course of the disease is outlined in Figure 4. The second case describes a woman, who at the age of 16 was suspected of exercise-induced asthma, but the symptoms subsided without treatment. At age 29, she was diagnosed and treated for asthma at a private clinic. She was a non-smoker with no history of pregnancies or hormone therapy. Because she had had no clinical benefit from her asthma therapy, at age 32, she was referred to the Center for Rare Lung Diseases at the Department of Respiratory Diseases and Allergy in 2015. There, PFTs showed severe obstruction and DLCO reduction (Figure 4). An HRCT was performed showing multiple cysts compatible with LAM (Figure 3B). Cell differential count by bronchoalveolar lavage was normal, but a transbronchial biopsy showed a slight thickening of the alveolar septae with spindle-formed cells. By immunohistochemistry, these cells were positive for smooth muscle α-actin, muscle-specific actin, and estrogen receptors, and negative for Melan-A, thus compatible both morphologically and by immunohistochemistry with LAM. Later, a VEGF-D of 3,505 pg/mL supported the LAM diagnosis. Treatment with sirolimus was initiated. As indicated in Figure 4, her lung function has been stable since the initiation of the treatment. Due to skin changes, she was investigated for TSC at the Clinical Genetics Department, but this was disconfirmed.

In similarity to the first case, her asthma showed to be a feature of LAM.

Discussion

While there is no universally agreed-upon global definition of a rare disease, a suggested threshold is approximately 50/100.000 (6). This indeed categorizes LAM as a rare disease, hence making the diagnosis of LAM, whether is it sporadic or related to TSC, challenging. The diagnosis is further complicated due to clinical variability and the presence of obstructive lung function, which often leads to initial misdiagnosis as asthma or COPD (3). In addition to mimicking obstructive lung diseases, LAM also belongs to a broader category of cystic lung diseases, which encompass various conditions characterized by the development of cystic spaces within the lung parenchyma. These diseases may have overlapping clinical presentations with LAM and include pulmonary Langerhans' cell histiocytosis, Birt–Hogg–Dubé syndrome, lymphoid interstitial pneumonia, and amyloidosis (7). Due to the many differential diagnoses, comprehensive clinical, radiological, and histopathological assessments are essential to diagnose LAM. In addition, a family history of cystic lung disease and hamartomatous lesions in different organs including the skin is suggestive of TSC, and genetic testing should be performed in such patients (5).

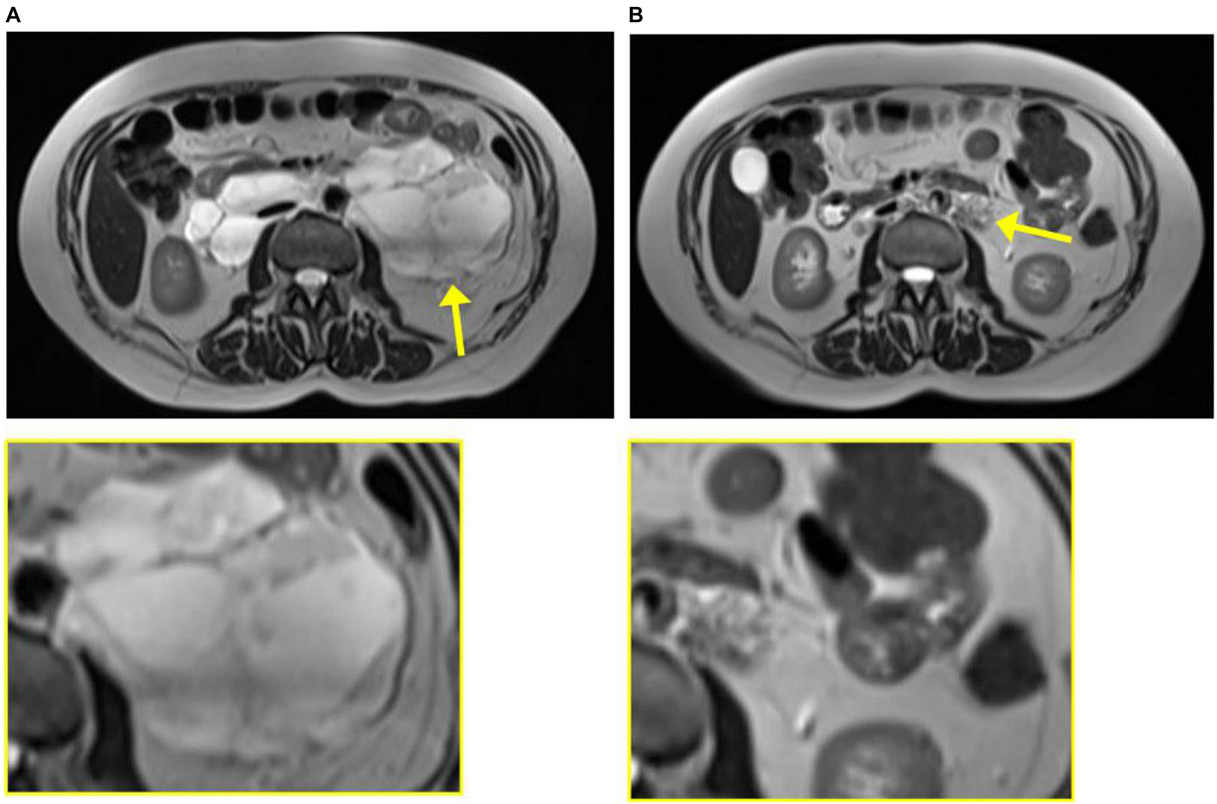

FIGURE 2
Magnetic resonance imaging from case 1 from 2020 at diagnosis of leiomyoma **(A)** and 2023 at diagnosis of lymphangioleiomyomatosis **(B)**. The tumor is indicated by the yellow arrow and enlarged in the yellow box.

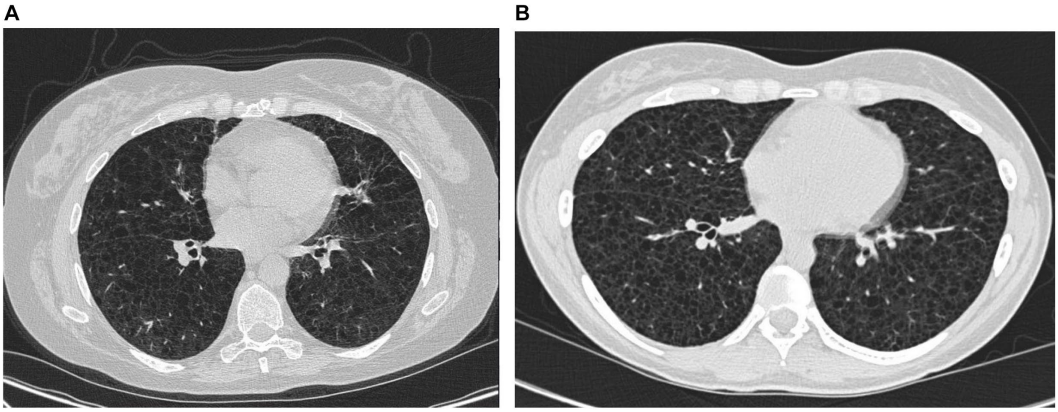

FIGURE 3
High-resolution computed tomography from case 1 **(A)** and case 2 **(B)**.

In the two cases described above, respiratory symptoms were initially misinterpreted as asthma–COPD overlap syndrome and asthma, respectively. This led to a delayed diagnosis of LAM. The challenges associated with diagnosing LAM are particularly evident in case 1, where both CT and MRI were evaluated at highly specialized gastrointestinal multidisciplinary conferences. Despite this, LAM was not suspected. This oversight might be attributed to the rarity and limited awareness of the condition. Hence, the involvement of specialists in pulmonary medicine is essential for accurate LAM diagnosis. While it is understood that not all clinicians can be familiar with every medical condition, both cases underscore the importance of reevaluating initial diagnoses when therapeutic interventions fail to produce the expected clinical effect.

Moreover, case 2 emphasizes the importance of an early diagnosis and treatment initiation; the woman had a decline in lung function from the onset of respiratory symptoms until LAM diagnosis and

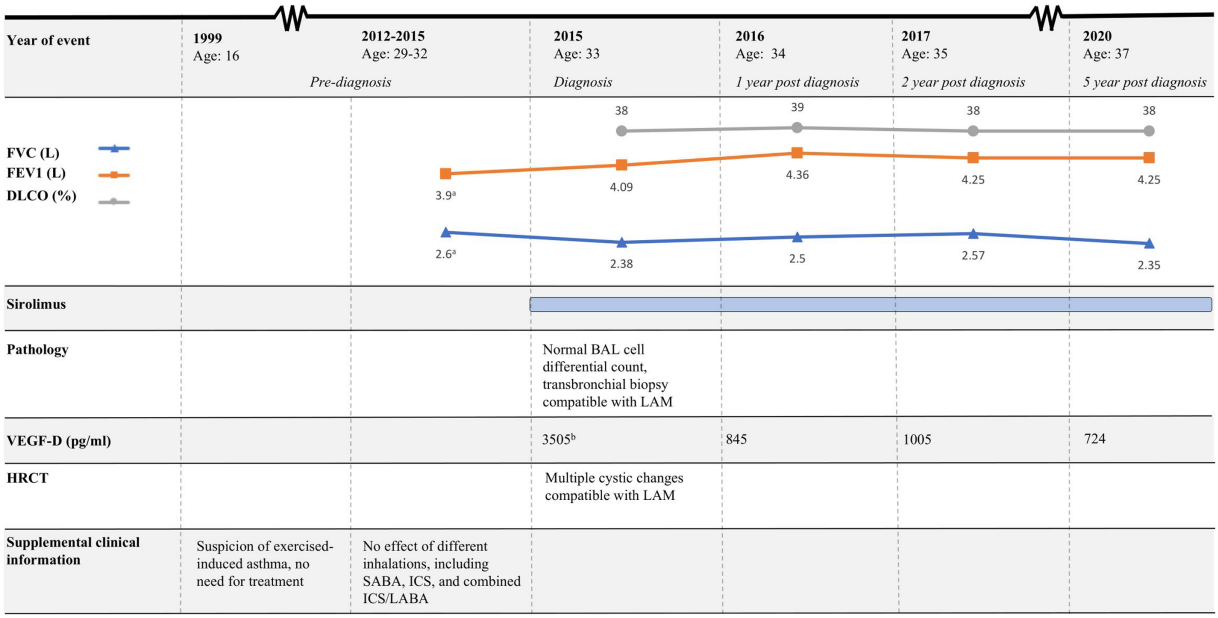

FIGURE 4
Timeline of case 2. HRCT, High-resolution computed tomography; FEV1, Forced expiratory volume in 1 s; FVC, Forced vital capacity; DLCO, Diffusion capacity for the lungs for carbon monoxide; LAM, Lymphangioleiomyomatosis; BAL, Bronchoalveolar lavage; SABA, Short-acting beta agonist; ICS, Inhaled corticosteroids; LABA, Long-acting beta-agonist. [a]Pulmonary function tests performed in 2014. [b]Result from VEGF-D analysis was available 4 months after BAL was performed.

treatment with sirolimus was initiated. It is important to note that mTORC1 inhibitors such as sirolimus only prevent further decline in lung function and do not restore lost lung function (3). Therefore, early detection of LAM is crucial for improving LAM patients' quality of life and life expectancy. Due to the recent LAM diagnosis in case 1, it is premature to make similar conclusions.

Perivascular epithelioid cell tumors (PEComas) are a group of rare mesenchymal tumors originating from the perivascular epithelioid cell line. LAM is considered to be part of the PEComa family. There are no specific treatment guidelines for PEComas, but mTORC1 inhibitors such as sirolimus have proven effective. When it comes to second-line treatment, evidence is even weaker, but among others, VEGFR inhibitors such as pazopanib, sorafenib, and sunitinib are suggested as possible treatment options (8, 9). In the light of this, case 2 becomes rather interesting. There was significant regression of the lymphangioleiomyoma when treated with pazopanib, and the tumor further progressed in the 3-month-long treatment pause. This contributes to the list of case reports in which VEGFR inhibitors were effective in the treatment of PEComas such as LAM.

In conclusion, these case reports highlight the critical importance of identifying LAM in patients with respiratory symptoms, even when initial assessments suggest more common conditions such as asthma or COPD. The rarity and clinical variability of LAM can complicate diagnosis, leading to delays and adverse patient outcomes. The primary key learning point from the two cases is the necessity of reevaluating initial diagnoses when treatments prove ineffective. Furthermore, the response to pazopanib treatment in case 2 sheds light on potential second-line therapies for PEComas such as LAM, emphasizing the suggested effectiveness of VEGFR inhibitors.

Patient perspective

In the first case, the patient naturally desired that a timely and accurate diagnosis be established in order to preserve pulmonary function. Nonetheless, she stated, "I understand and respect that it was very challenging for you to diagnose me, and I am just very pleased that you did so in the end."

In the second case, the patient understandably experienced frustration due to the substantial duration between the onset of symptoms and the LAM diagnosis. Being diagnosed with a rare lung disease, previously unfamiliar to her, came as a surprise. However, she said that "finally having knowledge about my condition gives me great relief, and makes it possible for me to look ahead."

Data availability statement

The original contributions presented in the study are included in the article/supplementary material, further inquiries can be directed to the corresponding author.

Ethics statement

Ethical approval was not required for the studies involving humans because formal ethical permission is not required for case stories. The studies were conducted in accordance with the local legislation and institutional requirements. The participants provided their written informed consent to participate in this study. Written informed consent was obtained from the individual(s) for the

publication of any potentially identifiable images or data included in this article.

Author contributions

MK: Writing – original draft. EB: Writing – review & editing. HR: Writing – review & editing.

Funding

The author(s) declare that no financial support was received for the research, authorship, and/or publication of this article.

Conflict of interest

The authors declare that the research was conducted in the absence of any commercial or financial relationships that could be construed as a potential conflict of interest.

Publisher's note

References

1. Johnson S. Rare diseases. 1. Lymphangioleiomyomatosis: clinical features, management and basic mechanisms. *Thorax*. (1999) 54:254–64. doi: 10.1136/thx.54.3.254

2. Johnson SR. Lymphangioleiomyomatosis. *Eur Respir J*. (2006) 27:1056–65. doi: 10.1183/09031936.06.00113303

3. McCarthy C, Gupta N, Johnson SR, Yu JJ, McCormack FX. Lymphangioleiomyomatosis: pathogenesis, clinical features, diagnosis, and management. *Lancet Respir Med*. (2021) 9:1313–27. doi: 10.1016/S2213-2600(21)00228-9

4. Mavroudi M, Zarogoulidis P, Katsikogiannis N, Tsakiridis K, Huang H, Sakkas A, et al. Lymphangioleiomyomatosis: current and future. *J Thorac Dis*. (2013) 5:74–9. doi: 10.3978/j.issn.2072-1439.2013.01.03

5. Gupta N, Finlay GA, Kotloff RM, Strange C, Wilson KC, Young LR, et al. Lymphangioleiomyomatosis diagnosis and management: high-resolution chest computed tomography, transbronchial lung biopsy, and pleural disease management. An official American Thoracic Society/Japanese respiratory society clinical practice guideline. *Am J Respir Crit Care Med*. (2017) 196:1337–48. doi: 10.1164/rccm.201709-1965ST

6. Richter T, Nestler-Parr S, Babela R, Khan ZM, Tesoro T, Molsen E, et al. Rare disease terminology and definitions-a systematic global review: report of the ISPOR rare disease special interest group. *Value Health*. (2015) 18:906–14. doi: 10.1016/j.jval.2015.05.008

7. Xu KF, Lo BH. Lymphangioleiomyomatosis: differential diagnosis and optimal management. *Ther Clin Risk Manag*. (2014) 10:691–700. doi: 10.2147/TCRM.S50784

8. Czarnecka AM, Skoczylas J, Bartnik E, Świtaj T, Rutkowski P. Management strategies for adults with locally advanced, Unresectable or metastatic malignant perivascular epithelioid cell tumor (PEComa): challenges and solutions. *Cancer Manag Res*. (2023) 15:615–23. doi: 10.2147/CMAR.S351284

9. Liapi A, Mathevet P, Herrera FG, Hastir D, Sarivalasis A. VEGFR inhibitors for uterine metastatic perivascular epithelioid tumors (PEComa) resistant to mTOR inhibitors. A case report and review of literature. *Front Oncol*. (2021) 11:641376. doi: 10.3389/fonc.2021.641376

frontiers | Frontiers in Medicine

TYPE Case Report
PUBLISHED 27 February 2024
DOI 10.3389/fmed.2024.1329381

OPEN ACCESS

EDITED BY
Talat Kilic,
İnönü University, Türkiye

REVIEWED BY
Ronald Balczon,
University of South Alabama, United States
Hilal Ermis,
İnönü University, Türkiye

*CORRESPONDENCE
Degan Lu
✉ deganlu@126.com

RECEIVED 28 October 2023
ACCEPTED 16 February 2024
PUBLISHED 27 February 2024

CITATION
Guo Z, Zuo A, Liu X, Jiang Y, Yang S and Lu D (2024) Multiple pulmonary cavities in an immunocompetent patient: a case report and literature review.
Front. Med. 11:1329381.
doi: 10.3389/fmed.2024.1329381

Multiple pulmonary cavities in an immunocompetent patient: a case report and literature review

Zihan Guo, Anli Zuo, Xinyi Liu, Yunxiu Jiang, Shuran Yang and Degan Lu*

Department of Respiratory, The First Affiliated Hospital of Shandong First Medical University and Shandong Provincial Qianfoshan Hospital, Shandong Institute of Respiratory Diseases, Shandong Institute of Anesthesia and Respiratory Critical Medicine, Jinan, China

Legionella pneumonia (LP) is a relatively uncommon yet well-known type of atypical community-acquired pneumonia (CAP). It is characterized by a rapid progression to severe pneumonia and can be easily misdiagnosed. In most patients, chest computed tomography (CT) showed patchy infiltration, which may progress to lobar infiltration or even lobar consolidation. While pulmonary cavities are commonly observed in immunocompromised patients with LP, they are considered rare in immunocompetent individuals. Herein, we present a case of LP in an immunocompetent patient with multiple cavities in both lungs. Pathogen detection was performed using metagenomic next-generation sequencing (mNGS). This case highlights the unusual radiographic presentation of LP in an immunocompetent patient and emphasizes the importance of considering LP as a possible diagnosis in patients with pulmonary cavities, regardless of their immune status. Furthermore, the timely utilization of mNGS is crucial for early pathogen identification, as it provides multiple benefits in enhancing the diagnosis and prognosis of LP patients.

KEYWORDS

Legionella, *Legionella pneumophila*, immunocompetent patient, Legionella pneumonia, pulmonary cavity, metagenomic next-generation sequencing

1 Introduction

Legionella pneumonia (LP) is a severe form of bacterial pneumonia caused by Legionella species. Without appropriate and timely treatment, LP can be life-threatening (1). The mortality rate for LP varies globally, ranging from 5% to 33% among the general population. However, in immunocompromised patients, the mortality rate can exceed 50% (2).

Although the imaging findings of LP are nonspecific, they are closely related to the clinical presentations and outcomes of the disease. Computed tomography (CT) is essential in detecting lung abnormalities, monitoring disease progression, and assessing therapy response. The most common CT pattern observed in LP patients is the presence of well-circumscribed infiltrates with ground-glass opacities, which can involve multiple lobes or segments (3, 4). In immunocompromised patients, it is occasionally observed that abscesses and cavitation may develop during the course of the disease. However, these findings are relatively uncommon in individuals with a healthy immune system (3, 4).

Herein, we present a case of community-acquired LP in an immunocompetent patient who exhibited multiple cavities in the lungs. This case highlights the importance of

considering LP as a potential diagnosis in patients with pulmonary cavities, even among those who do not have compromised immune systems.

2 Case description

A 67 years-old Chinese female patient was admitted to our hospital presenting with a 5 days history of fever, cough, and exertional dyspnea. She had a productive cough with scant mucus-like sputum. She had no history of smoking and no evidence of *Mycobacterium tuberculosis* infection. On admission, her vital signs were recorded as follows: a body temperature of 39.6°C, a pulse rate of 79 beats per minute, a respiratory rate of 21 breaths per minute, and a blood pressure of 150/84 mmHg. Pulmonary auscultation revealed coarse breath sounds and bilateral rales.

Laboratory results upon admission showed a white blood cell count of 14.29×10^9 cells/L (reference range: $3.5–9.5 \times 10^9$ cells/L) with an elevated neutrophil ratio of 88%. C-reactive protein and procalcitonin concentrations were markedly elevated at 81.40 mg/L (0–3.48 mg/L) and 1.20 ng/mL (0–0.05 ng/mL), respectively. Serum 1-3-beta-D-glucan and galactomannan tests yielded negative results. CT scans of the patient's lungs on admission revealed multiple lung nodules and patchy infiltrations (Figure 1). The sequence of relevant events after the patient was admitted has been shown in the timeline (Figure 2).

The patient received empiric treatment with cefoperazone/sulbactam for suspected community-acquired pneumonia (CAP) after blood and sputum samples were obtained. Clinical response assessment after 3 days showed inadequate improvement in the patient's clinical condition. Microbiological cultures from samples were negative for general bacteria, acid-fast bacilli and fungal elements.

Subsequently, a bronchoscopy with bronchoalveolar lavage was performed on the fourth day after admission. Bronchoalveolar lavage fluid (BALF) was sent to Jiangsu Simcere Medical Diagnostics Co., Ltd., and then metagenomic next-generation sequencing (mNGS) was performed on the Illumina next-generation high-throughput sequencing platform. For detailed methodological description, please refer to State Key Laboratory of Translational Medicine and Innovative Drug Development & Jiangsu Simcere Diagnostics Co., Ltd. previously published paper (5). The mNGS results on the 5th day after admission showed that 17,667 original sequences of *Legionella pneumophila* were identified, with a relative abundance of 98.3% and a coverage of 7.22% (Figure 3). Meanwhile, a number of other pathogens have been identified, including certain fungi and bacteria (Table 1). After our analysis, we are more inclined to classify them as respiratory custom flora or background flora derived from the environment or samples, regardless of considering them as pathogenic bacteria. On the same day, a repeated CT scan revealed the presence of bilateral lung cavities (Figure 4). These findings were consistent with LP. Immediate treatment with moxifloxacin injection at a dosage of 0.4 g daily was initiated. After 3 days, the patient's fever resolved, and there was improvement in cough symptoms. A follow-up CT scan 2 weeks later showed that the cavity in the right lung was smaller. Although the cavity in the left lung was slightly enlarged, the walls of the cavity were thinner, and the infiltration from both lungs had been resolved (Figure 5).

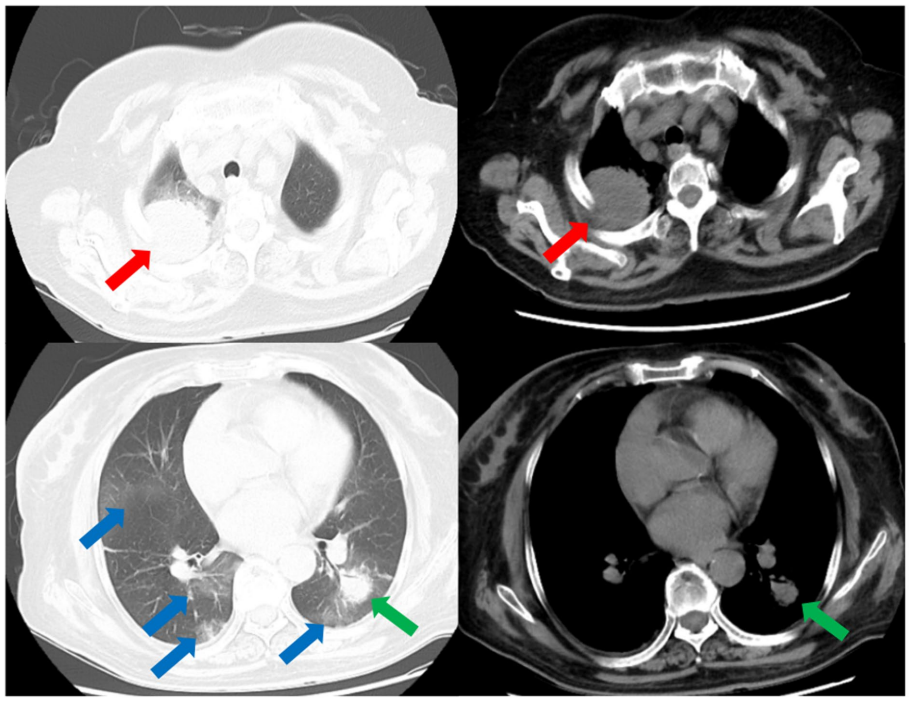

FIGURE 1
CT scans of the thorax on the day of admission demonstrates multiple nodular and patchy infiltrates in the lungs. Nodular infiltrate in the right lung (red arrows). Nodular infiltrate in the left lung (green arrows). Patchy infiltrates in both lungs (blue arrows).

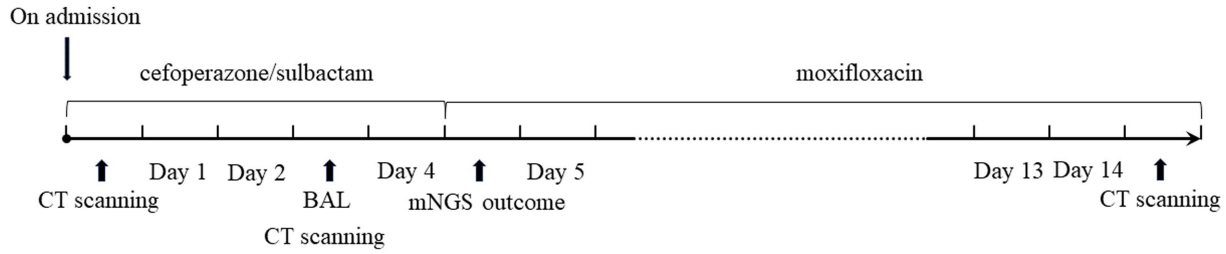

FIGURE 2
Timeline of treatment process.

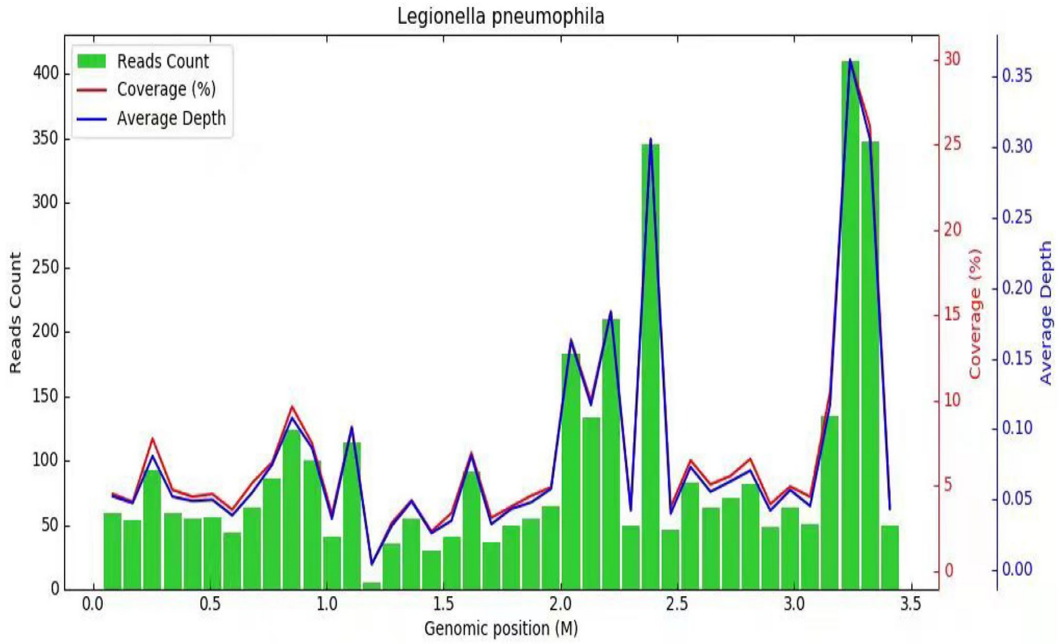

FIGURE 3
Diagnosis of *Legionella pneumophila* infection using mNGS. The horizontal axis (abscissa) represents the genome of the Legionella bacterium and the vertical axis (ordinate) represents the number of reads detected. The red line indicates the coverage, which represents the ratio of the detected nucleic acid sequence of Legionella to the entire gene sequence of Legionella. The blue line represents the sequencing depth, which is a measure of how many times a specific segment of the Legionella genome has been detected during the sequencing process.

TABLE 1 Reported cases of Legionella pneumonia.

Genus	Number of original sequences	Relative abundance	Species	Number of original sequences
Legionella	17,667	98.30%	*Legionella pneumophila*	17,667
Candida	4	26.67%	*Candida albicans*	4
Pneumocystis	2	13.33%	*Pneumocystis jirovecii*	2
Neisseria	97	0.54%	*Neisseria subflava*	55
Streptococcus	71	0.40%	*Streptococcus australis*	25
Tannerella	29	0.16%	*Tannerella forsythia*	27
Rothia	21	0.12%	*Rothia mucilaginosa*	21
Fusobacterium	19	0.11%	*Fusobacterium nucleatum*	18
Parvimonas	15	0.08%	*Parvimonas micra*	15

Number of original sequences: refers to the number of sequences matching the microbial pathogen at the genus/species level. Relative abundance: the proportion of microorganisms of the same type detected in the entire specimen.

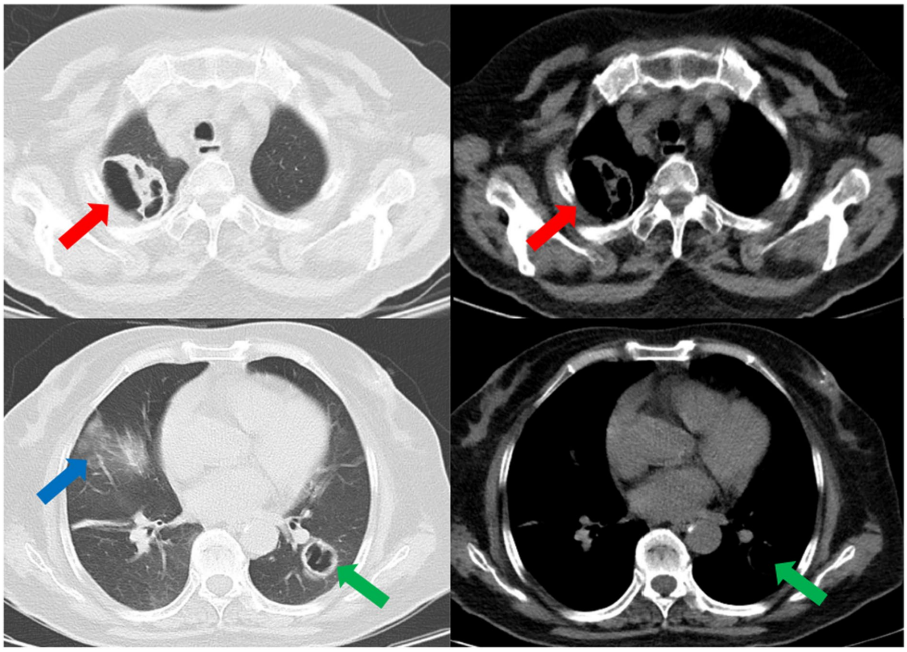

FIGURE 4
The repeated CT scan conducted on the fourth day after admission showed cavitary lesions in both lungs (red arrows and green arrows). Remaining patchy infiltrate in the right lung (blue arrow).

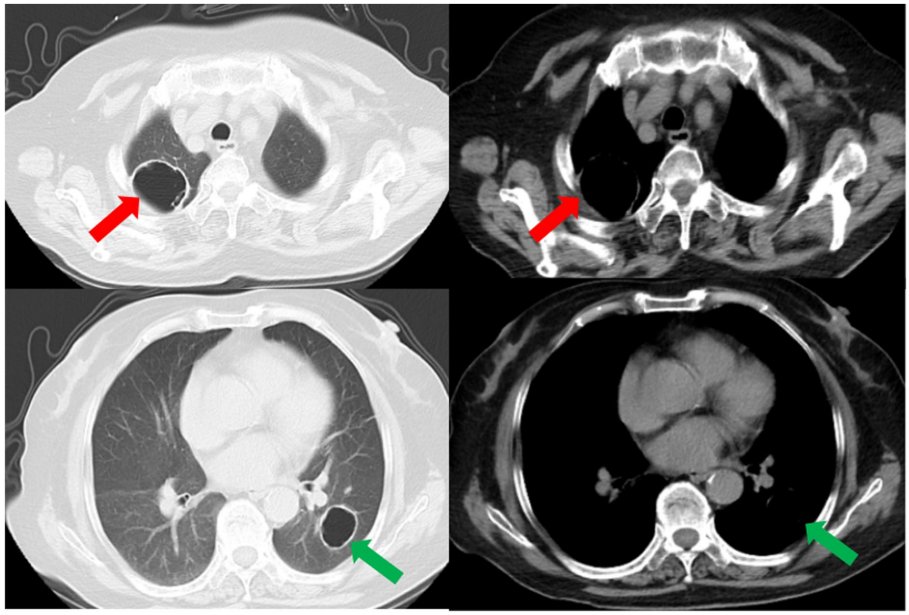

FIGURE 5
A subsequent CT scan 2 weeks later showed that the cavity in the right lung had decreased in size (red arrow), while the cavity in the left lung had slightly enlarged (green arrow). However, the thickness of the walls of both cavities had diminished, and the bilateral pulmonary infiltration indicated by the blue arrows had been resolved.

3 Discussion and literature review

To begin, a literature search was conducted using relevant databases such as Embase and Medline, spanning up to October 2023. The process carried out during this literature search is further detailed in Supplementary Table S3. After identifying the target papers through this search, the titles and abstracts of the database records were reviewed. Based on this initial screening, the full text of studies that were considered suitable for the evaluation were retrieved. Following the retrieval of the full text, the relevant case data was extracted from these studies.

Among the 14 previously reported cases of LP that were reviewed, 8 patients developed cavitation or abscesses, accounting for 57.1% of the cases (Table 2). Among these 8 patients, 7 were accompanied by immunosuppressive factors, accounting for 87.5%. This suggests that

TABLE 2 Reported cases of Legionella pneumonia.

Case No.	Gender	Age	Underlying condition/ immunosuppression factors	Imaging findings	Diagnosis mode	Therapeutic drugs	Serogroup	Treatment effect
1 (6)	M	52	Good's syndrome; methylprednisolone 60 mg daily for 2 weeks	Bilateral pleural effusion with patchy shadows and consolidation; pulmonary abscess and cavity formation	Blood mNGS; BALF and soft tissue specimens PCR	FQ, MA	N/D	Good response
2 (7)	F	34	N/D	Interstitial inflammation with multiple lymphadenopathies	tNGS on thoracic lymph nodes specimen	FQ	N/D	Good response
3 (8)	M	31	Smoking history	Consolidation of the right middle and lower lobe	Blood mNGS; culture with BALF	GA, CP, FQ, AG	N/D	Good response
4 (9)	F	34	Liver transplantation	Infiltration progressive cavitation	Urine serotype 1 antigen assay, tissue specimens culture	FQ	I	Good response
5 (10)	F	65	Breast cancer	Patchy consolidation	Blood, sputum, and pleural effusion NGS	FQ	N/D	Good response
6 (11)	F	39	SLE	Cavity, diffuse infiltration & abscess	Serotype 1 antigen assay	MA, LS	I	Good response
7 (12)	M	44	N/D	Alveolar infiltrates, cavitation	Postmortem Pus antigen analysis	BA, MA, AG	I	Bad response
8 (12)	M	31	N/D	Infiltrates	Postmortem tissue antigen analysis	BA, MA, AG, LS	N/D	Bad response
9 (13)	F	39	Breast cancer	Infiltration, cavitation	Culture with BALF, urine serotype 1 antigen assay	MA	I	Good response
10 (14)	M	10	Idiopathic thrombocytopaenia	Round-shaped infiltrates, segmental both-sided pneumonia, a central abcedation inside the infiltrate	BALF PCR& urine by a serotype 1 antigen assay	FQ	I	Good response
11 (15)	F	20	SLE	Patchy infiltrate	Lung tissue autopsy	AG, LS, BA	N/D	Bad response
12 (16)	M	63	N/D	Extensive consolidation	BALF mNGS	FQ	N/D	Good response
13 (17)	F	30	Idiopathic thrombocytopaenia, SLE	Cavitation appeared in consolidation	tracheal aspirates DFA	MA, AG, BA	VI	Bad response
14 (18)	M	45	Chronic myelogenous leukemia	Consolidation, with a abscess formation	Pus biopsy, urine serotype 1 antigen assay	CP, MA, LS	I	Good response

N/D, not determined; MA, macrolides antibiotics; FQ, fluoroquinolone; GA, glycopeptide antibiotic; CP, carbapenem; AG, aminoglycoside; LS, lincosamides; BA, β-lactam antibiotics; F, female; M, male.

TABLE 3 Keywords for searching case reports on abscesses or cavities caused by Legionella and its diagnostic methods.

Medline	(Legionnaires pneumonia) AND (abscess); (legionnaires pneumonia) AND (cavity); (legionnaires pneumonia) AND (Next-Generation Sequencing)
Embase	("Legionnaires pneumonia" OR (legionnaires AND ("pneumonia"/exp OR pneumonia))) AND ("abscess"/exp OR abscess); ("legionnaires pneumonia" OR (legionnaires AND ("pneumonia"/exp OR pneumonia))) AND cavity; ("legionnaires pneumonia" OR (legionnaires AND ("pneumonia"/exp OR pneumonia))) AND ("high throughput sequencing"/exp OR "high throughput sequencing")

LP patients with immunodeficiency factors are more likely to develop cavities or abscesses, phenomena that are less likely to occur in LP patients with normal immune function. Within the reviewed LP cases, there were 4 deaths (Table 2). In 75% of the fatal cases, the correct pathogen was not identified before the patients' deaths. Among the 11 surviving cases, 36.4% had Next-Generation Sequencing (NGS) used in diagnosis, and only 27.3% had metagenomic Next-Generation Sequencing (mNGS) used (Table 2). While the application of NGS or mNGS is not yet widespread, all patients who used NGS for LP diagnosis survived and achieved satisfactory results. As evident from the cases reviewed in Table 2, the vast majority of patients received appropriate anti-infective treatment following a correct diagnosis (see Table 3).

Based on the reviewed literature and the presented case, there are several noteworthy points that deserve attention and discussion. Firstly, the presence of cavities in the lungs, which is more commonly seen in immunosuppressed patients with LP, was found in an immunocompetent individual. Generally, immunocompetent individuals are more efficient in clearing Legionella bacteria, leading to fewer abscesses and cavities compared to immunocompromised patients (19, 20). In cases where immune function is compromised due to factors such as immune deficiency, organ transplantation, chemotherapy, or prolonged use of immunosuppressants, the immune response may become inadequate, potentially allowing bacterial growth and resulting in abscesses and cavities in the lungs (6, 9, 10, 15, 17, 18). In our patient, investigations for underlying causes of immunosuppression did not reveal any significant findings. When the immune system recognizes the presence of Legionella bacteria, it mounts a strong inflammatory response to eliminate the infection (20). However, this intense immune response can also cause collateral damage to the surrounding lung tissue, leading to the formation of abscesses or cavities (21).

Secondly, mNGS plays an important role in detecting *Legionella pneumophila* based on the analysis of BALF. Since LP lacks specific radiographic features, pathogen evidence seems to be more convincing in diagnosis compared with radiographic findings. In our case, the routine microbiological tests yield negative results and it is difficult to diagnose the causative agent *Legionella pneumophila* using traditional methods. Legionella culture and urine antigen testing are commonly used clinical methods for Legionella detection. However, they have limitations such as time-consuming culture results, sensitivity issues, and potential false positives (3, 22–24). In contrast, mNGS has proven to be effective in identifying challenging-to-culture pathogens like Legionella (25). It utilizes nucleic acid detection and molecular techniques, which offer enhanced sensitivity, specificity, and rapid pathogen detection throughput (26). This technology can be particularly useful in clinical settings for precise diagnosis and timely treatment (27).

Finally, this patient responded well to treatment for LP, indicating the effectiveness of the selected antibiotics in combating the infection. According to the etiological characteristics of Legionella, most macrolides, tetracyclines, ketolides, and quinolones are effective, with good efficacy and relatively few side effects, while Beta-lactams and aminoglycosides are ineffective (3). For severe or life-threatening LP, the British Thoracic Society recommends the use of fluoroquinolones (28). Studies have shown that moxifloxacin, in comparison to levofloxacin, exhibits at least an equivalent anti-Legionella effect and superior pharmacological parameters *in vitro* (29–31), as well as in clinical treatment (32). Notably, moxifloxacin does not require dosage adjustment in patients with liver and kidney dysfunction, making it a preferred choice due to its convenient dosing frequency and feasible administration method. The optimal duration of LP treatment varies based on clinical presentation and individual factors, however, a 2 weeks course of highly active anti-Legionella antibiotics is typically deemed sufficient (24). In severe cases of LP, particularly in patients who are immunocompromised or have failed initial treatment, the treatment duration should be extended to 4–6 weeks (24, 33). While there is still uncertainty about the ideal treatment for cavitary LP, studies have suggested that both macrolides and quinolones have shown efficacy against cavitary disease (34). In general, anti-infective treatment for cavitary LP is recommended for at least 4 weeks or until the lung cavity disappears (35).

4 Conclusion

In summary, this case illustrates an unusual form of multiple cavities in both lungs in an immunocompetent patient with LP. mNGS is an advanced diagnostic tool that can be valuable in confirming the diagnosis of Legionella infection and guiding treatment decisions. Either a fluoroquinolone or a macrolide is recommended as a first-line antibiotic treatment for LP, including cavitary LP. Although rare, LP should be considered in the differential diagnosis of cavitary lung diseases, even in immunocompetent patients.

Data availability statement

The original contributions presented in the study are included in the article/Supplementary material, further inquiries can be directed to the corresponding author.

Ethics statement

The studies involving humans were approved by Ethics Committee of the First Affiliated Hospital of Shandong First Medical University. The studies were conducted in accordance with the local legislation and institutional requirements. The participants provided their written informed consent to participate in this study. Written informed consent was obtained from the individual(s) for the publication of any potentially identifiable images or data included in this article.

Author contributions

ZG: Conceptualization, Data curation, Investigation, Writing – original draft, Writing – review & editing, Software, Visualization. AZ: Conceptualization, Investigation, Writing – original draft. XL: Investigation, Writing – original draft. YJ: Software, Writing – original draft. SY: Investigation, Writing – original draft. DL: Funding acquisition, Project administration, Resources, Supervision, Writing – review & editing.

Funding

The author(s) declare financial support was received for the research, authorship, and/or publication of this article. The present study was supported by the Collaborative Innovation Center for Intelligent Molecules with Multi-effects and Nanomedicine (Grant No. 2019-01), Shandong Province, China.

Conflict of interest

The authors declare that the research was conducted in the absence of any commercial or financial relationships that could be construed as a potential conflict of interest.

Publisher's note

Supplementary material

The Supplementary material for this article can be found online at: https://www.frontiersin.org/articles/10.3389/fmed.2024.1329381/full#supplementary-material

References

1. Barimani MJ. Legionella: an uncommon cause of community-acquired pneumonia. *JAAPA*. (2022) 35:38–42. doi: 10.1097/01.Jaa.0000873792.00538.78

2. El-Ebiary M, Sarmiento X, Torres A, Nogué S, Mesalles E, Bodí M, et al. Prognostic factors of severe Legionella pneumonia requiring admission to ICU. *Am J Respir Crit Care Med*. (1997) 156:1467–72. doi: 10.1164/ajrccm.156.5.97-04039

3. Cunha BA, Burillo A, Bouza E. Legionnaires' disease. *Lancet*. (2016) 387:376–85. doi: 10.1016/s0140-6736(15)60078-2

4. Mittal S, Singh AP, Gold M, Leung AN, Haramati LB, Katz DS. Thoracic imaging features of Legionnaire's disease. *Infect Dis Clin N Am*. (2017) 31:43–54. doi: 10.1016/j.idc.2016.10.004

5. Zhang J, Gao L, Zhu C, Jin J, Song C, Dong H, et al. Clinical value of metagenomic next-generation sequencing by Illumina and Nanopore for the detection of pathogens in bronchoalveolar lavage fluid in suspected community-acquired pneumonia patients. *Front Cell Infect Microbiol*. (2022) 12:1021320. doi: 10.3389/fcimb.2022.1021320

6. Li S, Jiang W, Wang CY, Weng L, Du B, Peng JM. A case of disseminated Legionnaires' disease: the value of metagenome next-generation sequencing in the diagnosis of legionnaires. *Front Med*. (2022) 9:955955. doi: 10.3389/fmed.2022.955955

7. Li S, Tong J, Li H, Mao C, Shen W, Lei Y, et al. L. pneumophila infection diagnosed by tNGS in a lady with lymphadenopathy. *Infect Drug Resist*. (2023) 16:4435–42. doi: 10.2147/idr.S417495

8. McBee DB, Mizu R, Hamdi AM. A case of severe, difficult-to-diagnose Legionnaires' disease in a young welder. *Cureus*. (2023) 15:e42250. doi: 10.7759/cureus.42250

9. Fraser TG, Zembower TR, Lynch P, Fryer J, Salvalaggio PR, Yeldandi AV, et al. Cavitary Legionella pneumonia in a liver transplant recipient. *Transpl Infect Dis*. (2004) 6:77–80. doi: 10.1111/j.1399-3062.2004.00053.x

10. Yi H, Fang J, Huang J, Liu B, Qu J, Zhou M. *Legionella pneumophila* as cause of severe community-acquired pneumonia, China. *Emerg Infect Dis*. (2020) 26:160–2. doi: 10.3201/eid2601.190655

11. Senécal JL, St-Antoine P, Béliveau C. *Legionella pneumophila* lung abscess in a patient with systemic lupus erythematosus. *Am J Med Sci*. (1987) 293:309–14. doi: 10.1097/00000441-198705000-00005

12. Lewin S, Brettman LR, Goldstein EJ, Holzman RS, Devila H, Taubman F, et al. Legionnaires' disease. A cause of severe abscess-forming pneumonia. *Am J Med*. (1979) 67:339–42. doi: 10.1016/0002-9343(79)90411-x

13. Guy SD, Worth LJ, Thursky KA, Francis PA, Slavin MA. *Legionella pneumophila* lung abscess associated with immune suppression. *Intern Med J*. (2011) 41:715–21. doi: 10.1111/j.1445-5994.2011.02508.x

14. Heine S, Fuchs A, von Müller L, Krenn T, Nemat S, Graf N, et al. Legionellosis must be kept in mind in case of pneumonia with lung abscesses in children receiving therapeutic steroids. *Infection*. (2011) 39:481–4. doi: 10.1007/s15010-011-0131-7

15. Jacox RF, Stuard ID. Legionnaires' disease in a patient with systemic lupus erythematosus. *Arthritis Rheum*. (1978) 21:975–7. doi: 10.1002/art.1780210816

16. Du R, Feng Y, Wang Y, Huang J, Tao Y, Mao H. Metagenomic next-generation sequencing confirms the diagnosis of Legionella pneumonia with rhabdomyolysis and acute kidney injury in a limited resource area: a case report and review. *Front Public Health*. (2023) 11:1145733. doi: 10.3389/fpubh.2023.1145733

17. Dowling JN, Kroboth FJ, Karpf M, Yee RB, Pasculle AW. Pneumonia and multiple lung abscesses caused by dual infection with *Legionella micdadei* and *Legionella pneumophila*. *Am Rev Respir Dis*. (1983) 127:121–5. doi: 10.1164/arrd.1983.127.1.121

18. Schindel C, Siepmann U, Han S, Ullmann AJ, Mayer E, Fischer T, et al. Persistent Legionella infection in a patient after bone marrow transplantation. *J Clin Microbiol*. (2000) 38:4294–5. doi: 10.1128/jcm.38.11.4294-4295.2000

19. Palusinska-Szysz M, Janczarek M. Innate immunity to Legionella and toll-like receptors—review. *Folia Microbiol*. (2010) 55:508–14. doi: 10.1007/s12223-010-0084-8

20. Friedman H, Yamamoto Y, Newton C, Klein T. Immunologic response and pathophysiology of Legionella infection. *Semin Respir Infect*. (1998) 13:100–8.

21. Cunha LD, Zamboni DS. Recognition of *Legionella pneumophila* nucleic acids by innate immune receptors. *Microbes Infect*. (2014) 16:985–90. doi: 10.1016/j.micinf.2014.08.008

22. Pierre DM, Baron J, Yu VL, Stout JE. Diagnostic testing for Legionnaires' disease. *Ann Clin Microbiol Antimicrob*. (2017) 16:59. doi: 10.1186/s12941-017-0229-6

23. Mercante JW, Winchell JM. Current and emerging Legionella diagnostics for laboratory and outbreak investigations. *Clin Microbiol Rev*. (2015) 28:95–133. doi: 10.1128/cmr.00029-14

24. Cunha BA. The atypical pneumonias: clinical diagnosis and importance. *Clin Microbiol Infect*. (2006) 12:12–24. doi: 10.1111/j.1469-0691.2006.01393.x

25. Zhu N, Zhou D, Yuan R, Ruzetuoheti Y, Li J, Zhang X, et al. Identification and comparison of *Chlamydia psittaci*, Legionella and Mycoplasma pneumonia infection. *Clin Respir J*. (2023) 17:384–93. doi: 10.1111/crj.13603

26. Maurer FP, Christner M, Hentschke M, Rohde H. Advances in rapid identification and susceptibility testing of bacteria in the clinical microbiology laboratory: implications for patient care and antimicrobial stewardship programs. *Infect Dis Rep*. (2017) 9:6839. doi: 10.4081/idr.2017.6839

27. Gu W, Miller S, Chiu CY. Clinical metagenomic next-generation sequencing for pathogen detection. *Annu Rev Pathol*. (2019) 14:319–38. doi: 10.1146/annurev-pathmechdis-012418-012751

28. Levy ML, Le Jeune I, Woodhead MA, Macfarlaned JT, Lim WS. Primary care summary of the British Thoracic Society guidelines for the management of community acquired pneumonia in adults: 2009 update. Endorsed by the Royal College of General Practitioners and the Primary Care espiratory Society UK. *Prim Care Respir J*. (2010) 19:21–7. doi: 10.4104/pcrj.2010.00014

29. Schubert S, Dalhoff A, Stass H, Ullmann U. Pharmacodynamics of moxifloxacin and levofloxacin simulating human serum and lung concentrations. *Infection*. (2005) 33:15–21. doi: 10.1007/s15010-005-8203-1

30. Gómez-Lus R, Adrián F, del Campo R, Gómez-Lus P, Sánchez S, García C, et al. Comparative *in vitro* bacteriostatic and bactericidal activity of trovafloxacin, levofloxacin and moxifloxacin against clinical and environmental isolates of *Legionella* spp. *Int J Antimicrob Agents*. (2001) 18:49–54. doi: 10.1016/s0924-8579(01)00339-9

31. Jonas D, Engels I, Friedhoff C, Spitzmüller B, Daschner FD, Frank U. Efficacy of moxifloxacin, trovafloxacin, clinafloxacin and levofloxacin against intracellular *Legionella pneumophila*. *J Antimicrob Chemother*. (2001) 47:147–52. doi: 10.1093/jac/47.2.147

32. Garau J, Fritsch A, Arvis P, Read RC. Clinical efficacy of moxifloxacin versus comparator therapies for community-acquired pneumonia caused by *Legionella* spp. *J Chemother*. (2010) 22:264–6. doi: 10.1179/joc.2010.22.4.264

33. Fields BS, Benson RF, Besser RE. Legionella and Legionnaires' disease: 25 years of investigation. *Clin Microbiol Rev*. (2002) 15:506–26. doi: 10.1128/cmr.15.3.506-526.2002

34. Domingo C, Roig J, Planas F, Bechini J, Tenesa M, Morera J. Radiographic appearance of nosocomial Legionnaires' disease after erythromycin treatment. *Thorax*. (1991) 46:663–6. doi: 10.1136/thx.46.9.663

35. O'Reilly KM, Urban MA, Barriero T, Betts RF, Trawick DR. Persistent culture-positive Legionella infection in an immunocompromised host. *Clin Infect Dis*. (2005) 40:e87–9. doi: 10.1086/429826

frontiers | Frontiers in Medicine

TYPE Case Report
PUBLISHED 04 March 2024
DOI 10.3389/fmed.2024.1365096

OPEN ACCESS

EDITED BY
Talat Kilic,
İnönü University, Türkiye

REVIEWED BY
Supat Chamnanchanunt,
Mahidol University, Thailand
Sibel Altunışık Toplu,
İnönü University, Türkiye

*CORRESPONDENCE
Qiong-Fang Yang
✉ qfy195581@163.com

RECEIVED 03 January 2024
ACCEPTED 22 February 2024
PUBLISHED 04 March 2024

CITATION
Yang Q-F, Shu C-M and Ji Q-Y (2024) Diagnosis of pulmonary hemorrhagic leptospirosis complicated by invasive pulmonary aspergillosis complemented by metagenomic next-generation sequencing: a case report.
Front. Med. 11:1365096.
doi: 10.3389/fmed.2024.1365096

Diagnosis of pulmonary hemorrhagic leptospirosis complicated by invasive pulmonary aspergillosis complemented by metagenomic next-generation sequencing: a case report

Qiong-Fang Yang*, Cai-Min Shu and Qiao-Ying Ji

Department of Respiratory Medicine, Affiliated Dongyang Hospital of Wenzhou Medical University, Dongyang, Zhejiang, China

Background: Leptospirosis is a bacterial zoonosis with variable clinical manifestations. Pulmonary diffuse hemorrhagic leptospirosis often occurs rapidly and, when not promptly diagnosed and treated, it can be life-threatening. *Aspergillus flavus* is an opportunistic fungus that is commonly seen in immunosuppressed patients. Invasive pulmonary aspergillosis also progresses rapidly. This case study describes a patient with severe pneumonia caused by pulmonary hemorrhagic leptospirosis combined with invasive pulmonary aspergillosis. We have found almost no clinical reports to date on these two diseases occurring in the same patient.

Case presentation: A 73-year-old male arrived at our hospital complaining of fever, general malaise, and hemoptysis that had lasted 4 days. The patient was initially diagnosed with severe pneumonia in the emergency department, but he did not respond well to empiric antibiotics. Subsequently, the patient's condition worsened and was transferred to the ICU ward after emergency tracheal intubation and invasive ventilator. In the ICU, antibacterial drugs were adjusted to treat bacteria and fungi extensively. Although the inflammatory indices decreased, the patient still had recurrent fever, and a series of etiological tests were negative. Finally, metagenomic next-generation sequencing (mNGS) of bronchial alveolar lavage fluid detected *Leptospira interrogans* and *Aspergillus flavus*. After targeted treatment with penicillin G and voriconazole, the patient's condition improved rapidly, and he was eventually transferred out of the ICU and recovered.

Conclusion: Early recognition and diagnosis of leptospirosis is difficult, especially when a patient is co-infected with other pathogens. The use of mNGS to detect pathogens in bronchial alveolar lavage fluid is conducive to early diagnosis and treatment of the disease, and may significantly improve the prognosis in severe cases.

KEYWORDS

pulmonary hemorrhagic leptospirosis, pulmonary aspergillosis, co-infection, metagenomic next-generation sequencing, case report

Introduction

Leptospira interrogans is a zoonotic pathogen that is mainly transmitted by rats and domestic animals (1). Planting, slaughtering, and swimming are the risk factors for leptospirosis infection (2). Its clinical manifestations in humans are diverse and can lead to multiple organ involvement (1). *Aspergillus flavus* is a fungus that is widely distributed in the world. It is common in soil, plants, and basements, and often colonizes in the respiratory tract. It is commonly found in patients with low immune function, and can cause invasive lung disease, ear, nose and throat infection, meningitis, and other diseases (3). To the best of our knowledge, there are almost no reports of both pathogens causing the same patient to become ill at the same time. Our case report attempts to improve clinical awareness of such diseases.

Case presentation

A 73-year-old male patient was admitted to the emergency department with the chief complaints of fever, general malaise, and hemoptysis that had lasted for 4 days. He had a history of coronary and valvular heart disease, and underwent coronary artery bypass grafting and mitral valve replacement 7 years ago in our hospital. He had recovered well after the heart surgery and had been taking aspirin enteric-coated tablets and atorvastatin calcium regularly since the surgery. Four days prior to his current visit, the patient developed fever without obvious inducement, accompanied by a small amount of hemoptysis, general fatigue, and chest tightness. The fever reached a peak of 38.3°C. The patient was diagnosed on arrival with severe pneumonia and received empirical antibiotic treatment with piperacillin/tazobactam. The patient's condition worsened the same day to impaired consciousness and shock. Arterial blood gas analysis showed an oxygenation index of 80.98, which is significantly lower than the normal range. Therefore, emergency tracheal intubation and invasive ventilator were used to assist oxygenation. The patient was admitted to the ICU ward on the same day after stabilization.

Physical examination in the ICU showed a temperature of 36.3°C (after the use of antipyretic drugs), pulse rate 74 times/min, respiration rate 16 times/min, and blood pressure 165/115 mmHg (with norepinephrine maintained at 0.27 μg/kg. min). The patient was in a sedated state with tracheal intubation and ventilator assisted respiration, bilateral pupil diameter was 2.0 mm with no light response, bilateral lung exam showed thick breathing with audible moist rales, heart was in atrial fibrillation, abdomen was flat and soft, and both lower limbs had slight edema, with negative Babinski's sign on both sides.

Laboratory tests showed a significant increase in neutrophils, C-reactive protein, and procalcitonin levels. Arterial blood gas analysis suggested type I respiratory failure with a PaO_2/FiO_2 ratio of 80.89. Blood work resulted in a white blood cell count, hemoglobin, and platelet count of 14.03 * 10^9/L, 100 g/L, and 48 * 10^9/L, respectively. Blood biochemistry indicated creatinine was 285 μmol/L, liver enzymes and direct bilirubin were slightly elevated, and pro-brain natriuretic peptide (Pro-BNP) was significantly higher than normal, suggesting heart failure (Table 1).

Chest computed tomography (CT) on admission to our hospital showed diffuse exudative lesions in both lungs (Figures 1: 1A–C), and CT pulmonary angiography revealed multiple pulmonary artery branch embolisms in both lungs (Figure 2). Color Doppler ultrasound of the heart showed decreased left ventricular systolic function, enlarged right heart, and a cardiac ejection fraction of 45%. Lower limb vascular Doppler ultrasound did not indicate deep vein thrombosis. Bedside electrocardiogram revealed atrial fibrillation with a rapid ventricular rate of 114 times/min.

To detect the etiology of the pneumonia, we performed a series of microbiologic diagnostics including staining and culture and serologic testing for viruses, bacteria, and fungi, all of which were negative (Table 2).

After the patient was transferred to the ICU, due to the consideration of severe community-acquired pneumonia, the condition progressed rapidly, and the initial anti infection treatment failed. Moreover, the pathogen of the infection was not clear, so he was given imipenem and cilastatin sodium (1.0 g, I.V. infusion, q12h), vancomycin (0.5 g, I.V. infusion, qd), and voriconazole (0.2 g, I.V. infusion, qd). The dosage of antibiotics was based on the creatinine clearance rate. The patient was also given methylprednisone (40 mg, I.V., q12h) as an anti-inflammatory, lyophilized recombinant human brain natriuretic peptide (0.0075 μg/kg. min, I.V. infusion) to treat heart failure, and nadroparin calcium (4,100 IU, I.H., q12h) for anticoagulation after platelet count recovery.

After 3 days, the blood inflammation indices decreased, but the patient still had current fever. Chest CT reexamination showed the progression of bilateral lung lesions, as illustrated in Figures 1: 2A–C, and so bedside bronchoscopy was given. Bronchoscopy displayed diffuse blood infiltration and mucosal swelling in the left and right bronchial lumens. The bronchial alveolar lavage fluid was sent for mNGS examination. Three days later, mNGS showed seven sequence numbers of *Leptospira interrogans* and 1,289,906 sequences of *Aspergillus flavus*. A culture of the bronchial alveolar lavage fluid revealed *Aspergillus flavus*: 1+. Therefore, in consideration of pulmonary hemorrhagic leptospirosis complicated with pulmonary aspergillosis, administration of vancomycin, imipenem cilastatin, and voriconazole injection was stopped, and the patient was given penicillin G (400,000 U I.V. infusion, q4h) combined with voriconazole tablets (0.2 g, p.o., q12h). After using penicillin G for a week, the patient's condition improved and he was returned to the general ward. The chest CT reexamination on day 17 showed that the exudative lesions in bilateral lungs were obviously absorbed, and some nodules were enlarged, as shown in Figures 1: 3A–C. Inflammation indices in the blood were normal, so penicillin sodium was stopped. The enlarged pulmonary nodules were considered to be associated with *Aspergillus flavus* infection, so the blood concentration of voriconazole was detected. The detection result was 1.0 mg/L (the reference value range was 0.5–5 mg/L), which was at the normal lower limit level. Therefore, voriconazole was increased to 250 mg once every 12 h for antifungal treatment. Methylprednisolone was gradually reduced to stop, and the patient was discharged with voriconazole tablets. Figure 3 illustrates the timeline of hospitalization and clinical

Abbreviations: mNGS, Metagenomic next-generation sequencing; CRP, C-Reactive protein; Pro-BNP, Pro-brain natriuretic peptide; CT, Computed tomography; CTPA, Computed tomography pulmonary angiography; PCR, Polymerase chain reaction; MAT, Modified agglutination test; ELISA, Enzyme linked immunosorbent assay.

TABLE 1 Changes in laboratory indicators.

Test	On admission	Day 3	Day 6	Day 11	Day 16	Day21	Reference range
WBC	14.03	12.45	15.62	11.54	10.30	9.86	3.5–9.5 (10^9/L)
CRP	229.46	114.96	14.94	5.50	1.30	4.80	<8 (mg/L)
PCT	100.00	78.40	1.51	0.34	0.13	0.08	<0.1 (ng/mL)
D-dimer	2.17	1.74	13.21	1.68	0.60	0.75	<0.5 (ug/mL)
Cr	285	370	96	79	55	56	57-111 (μmol/L)
Pro-BNP	19,604	4,683	3,235	6,044	2,948	3,442	5-125 (pg/mL)
PaO_2/FiO_2	81	325	217	342	370	358	400-500 mmHg
AST	48	21	14	29	34	39	9-50 (U/L)
ALT	56	17	18	25	33	36	15-40 (U/L)
CK	204	55	32	46	----	----	50-310 (U/L)
CK-MB	16	8	8	6	----	----	≤25 (U/L)
Alb	26.9	28.7	34.3	34.3	31.2	30.1	40-55 (g/L)
FIB	7.07	4.91	3.17	2.83	2.31	2.74	2-4 (g/L)
TBIL	16.5	14.4	19.2	23.0	20.2	14.2	≤26 (μmol/L)
DBIL	12.2	8.0	8.4	8.4	6.6	5.8	≤7 (μmol/L)

WBC, White blood cell count; CRP, C-reactive protein; PCT, Procalcitonin; Cr, creatinine; Pro-BNP, Pro-Brain Natriuretic Peptide; ALT, alanine aminotransferase; AST, aspartate aminotransferase; CK, Creatine kinase; CK-MB, Creatine kinase isoenzyme; Alb, Albumin; FIB, Fibrinogen; TBIL, total bilirubin; DBIL, Direct bilirubin.

treatments, and Table 1 shows the changes in relevant laboratory indicators during the course of the disease. Chest CT reexamination 3 weeks after discharge showed that the bilateral lung lesions were obviously absorbed, and there were new cavities, as shown in Figures 1: 4A–C. The images showed an air crescent sign typical of aspergillosis. Therefore, the patient continued to receive oral antifungal treatment with voriconazole tablets for 3 to 6 months.

Discussion and conclusions

Leptospirosis is a zoonosis caused by the *Leptospira interrogans* bacteria. Its incidence is on the rise globally, and is 10 times higher in tropical areas than in temperate regions (4). Transmission of the organism to humans occurs via portals of entry such as cuts or abraded skin, mucous membranes, or conjunctivae (5). Human exposures that lead to infection include contact with urine-contaminated soil or water (e.g., floodwater, ponds, rivers, streams, and sewage), ingestion of food or water contaminated by urine, or direct contact with the urine or reproductive fluids from infected animals (6). The patient of our case study was a farmer who had a history of drinking stream water and bathing in the wild. It was considered that he might have been infected with *Leptospira* by contacting and drinking contaminated water before he became ill. The onset of the patient's illness was at the end of August, which is consistent with the seasonal occurrence of leptospirosis in Asia. Most cases occur from July to October, with the peak in August and September each year (7). In addition, this farmer had been exposed to mold in foods such as cereals and beans. We theorized that *Aspergillus flavus* had colonized in his respiratory tract for a long time, and that the continuous use of hormones during the treatment of leptospirosis led to the final growth of the fungus.

Leptospirosis can be categorized as non-icteric or icteric, and its clinical symptoms are variable. Most non-icteric cases are mild and self-limited or asymptomatic, while the icteric type is severe and potentially fatal (8). In the acute stage of leptospirosis, there are many nonspecific symptoms such as fever, muscle soreness, headache. The icteric phase is distinguished by significantly raised serum bilirubin levels. Also, very few patients have rapidly progressive pulmonary hemorrhage and respiratory distress, but this manifestation is often seen in icteric leptospirosis (9).

Invasive pulmonary aspergillosis is mainly characterized by fever, cough, hemoptysis, and progressive dyspnea (10) and is impossible to distinguish from leptospirosis based only on clinical manifestations. Although the patient in our case study had non-icteric leptospirosis, because of the co-infection with *Aspergillus flavus*, he had severe pulmonary hemorrhage, and rapidly progressed to acute respiratory distress syndrome, ultimately needing emergency tracheal intubation. Therefore, when it is difficult to identify the pathogen based on clinical symptoms, more attention should be paid to detailed medical history collection.

Imaging of pulmonary diffuse hemorrhagic leptospirosis typically reveals bilateral patchy peripheral infiltrates, often with a "snowflake" appearance, that can progress to confluent consolidation or a ground-glass appearance (11). The lesions are obvious in the middle and lower lobes of bilateral lungs, and the imaging manifestations are consistent with the clinical symptoms. After timely treatment, the lung lesions mostly disappear within a week.

Early imaging of invasive pulmonary aspergillosis is characterized by a halo sign, which represents hemorrhagic nodules (10). Our patient was initially diagnosed with leptospirosis and the possibility of aspergillus infection was considered. After standard treatment with penicillin G, the exudative lesions in the lung were obviously absorbed, but some nodules were still enlarged. The enlarged nodules further supported a diagnosis of aspergillus infection. Finally, after 4 weeks, the lung imaging showed an air crescent sign typical of aspergillus infection. It is difficult to distinguish overlapping infections of leptospirosis and aspergillosis from imaging alone. Misdiagnosis of

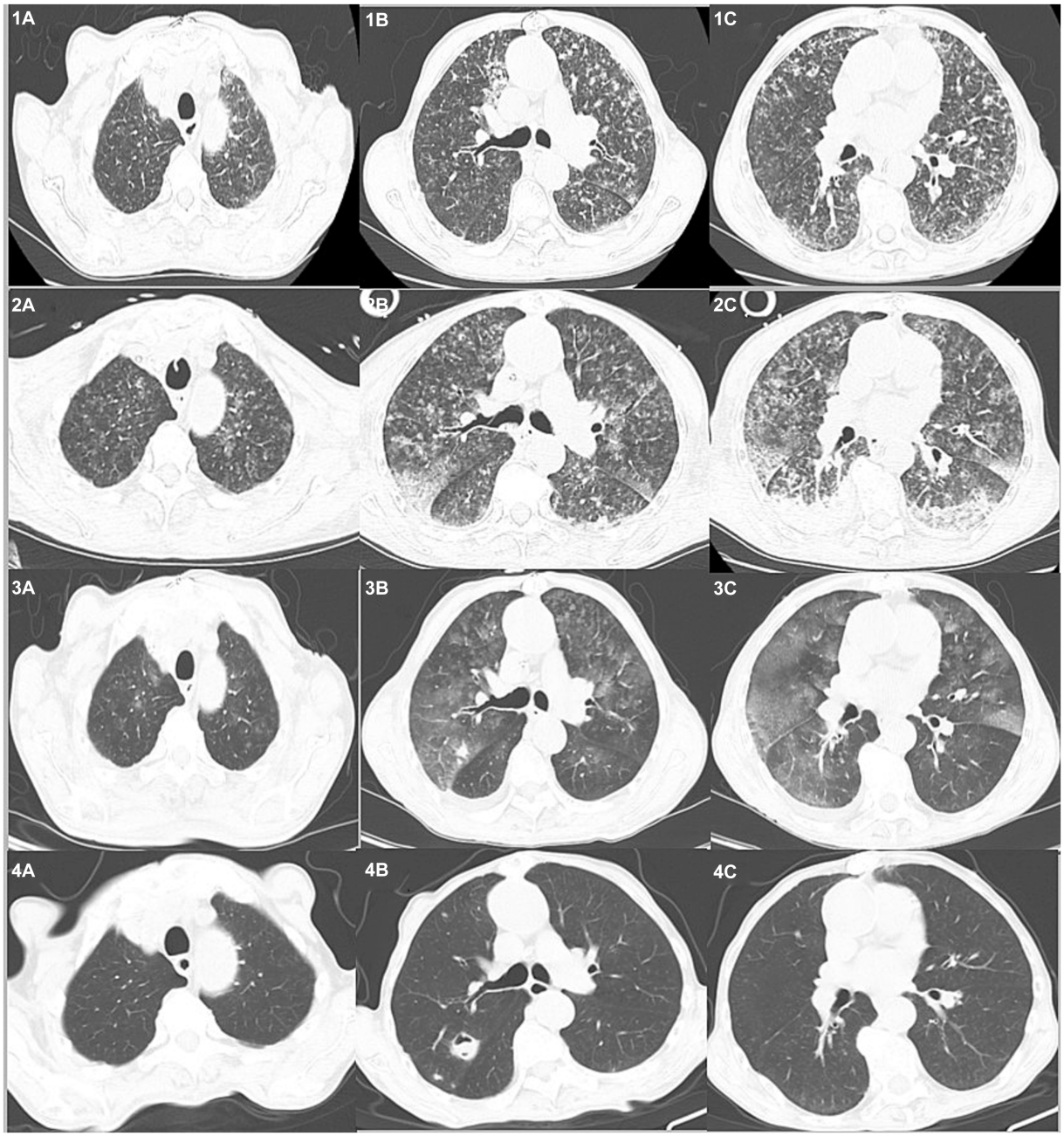

FIGURE 1
Chest CTs of the patient over time. On admission **(1A–C)** diffuse exudative lesions are evident in both lungs. Day 3 **(2A–C)** shows the progression of bilateral lung lesions. On day 17 **(3A–C)**, the bilateral exudative lesions are obviously absorbed and some nodules are enlarged. Day 40^{+} **(4A–C)** reveals the lesions are absorbed and new cavities have formed.

overlapping syndromes can lead to delayed diagnosis and treatment, which further emphasizes the importance of detailed inquiry of the patient's epidemiological history.

Leptospira is typically identified by molecular, serological, or culturing methods. Polymerase chain reaction (PCR), modified agglutination test, enzyme linked immunosorbent assay, and mNGS can all be used for early diagnosis of leptospirosis (12), but traditional detection methods have their shortcomings. For example, although PCR provides rapid results, its overall sensitivity is relatively low (13). Moreover, traditional methods of detecting leptospirosis can only help confirm an existing diagnosis. Use of mNGS can not only help confirm the diagnosis, but also provide important diagnostic clues for patients with atypical symptoms or with multiple overlapping infections (14). At the initial disease stage in our case study, the empirical effect of anti-infection measures was not good, and the routine pathogenic test results were negative. Finally, mNGS confirmed the presence of both *Leptospira* and *Aspergillus flavus*. From this it can be concluded that if the clinical symptoms are serious and the pathogen is not clear, the early use of mNGS to detect pathogens can buy valuable time for saving lives.

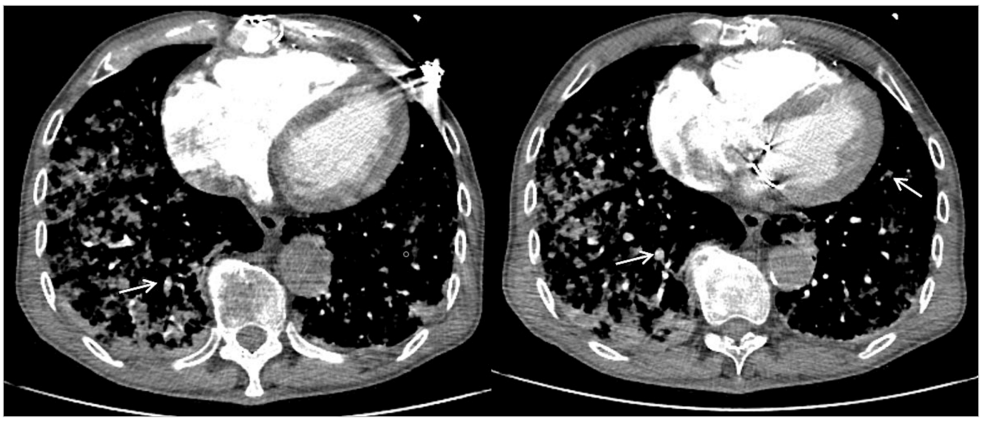

FIGURE 2
Computed tomography pulmonary angiography showing multiple pulmonary artery branch embolisms in both lungs. White arrows indicate pulmonary artery branch thrombosis.

TABLE 2 Pathogenic test results.

Test	Results	Reference range
Blood culture	Negative	Negative
Sputum culture	Negative	Negative
Cryptococcus antigen	Negative	Negative
Fungus-D glucan determination	<37.50 pg./mL	≤70
Galactomannan determination	0.26	≤0.5
Sputum smear for acid-fast bacilli	Negative	Negative
Sputum tuberculosis culture	Negative	Negative
Anti-HIV	Negative	Negative
COVID-19 antigen	Negative	Negative

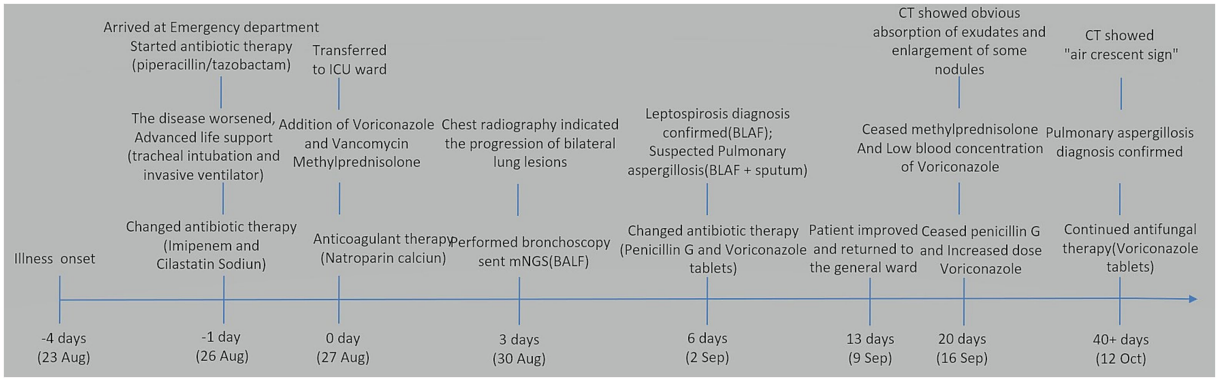

FIGURE 3
Hospitalization timeline and clinical treatments.

Current recommendations in domestic and foreign literature suggest that patients with leptospirosis lung involvement have good clinical reactions to penicillin, third-generation cephalosporins, meropenem, and fluoroquinolone antibiotics. For patients with a clear diagnosis of severe leptospirosis, penicillin and hormones are recommended for symptomatic treatment (15). However, when our patient was given anti-infective treatment with piperacillin/tazobactam on admission, his clinical symptoms worsened, resulting in the need for tracheal intubation. After comprehensive analysis, we concluded that the patient had a Herxheimer reaction. This reaction is an aggravation of clinical symptoms such as high fever, chills, myalgia, increased heart rate and respiration, and decreased

blood pressure, and it is caused by the release of toxins during the treatment with penicillin or other antibacterial drugs (16). Following a Herxheimer reaction, symptomatic supportive treatment is the main approach (16). Penicillin can be gradually increased in small doses, supplemented by glucocorticoids, and the symptoms are usually relieved quickly. For our patient, we changed to penicillin G supplemented by glucocorticoid and respiratory support, and the condition gradually stabilized. Voriconazole is the first choice of medication for pulmonary aspergillus infection (3). The patient was given voriconazole for antifungal treatment at the beginning of the disease. The conventional dose did not reach the expected clinical efficacy, but the final focus absorption was good after an appropriate dosage increase.

In conclusion, the causes of respiratory tract infections are complex and diverse, with nonspecific clinical symptoms. Therefore, clinicians cannot ignore the importance of epidemiological history during medical intake. In addition, the new diagnostic technology mNGS is helpful for the early diagnosis of patients with severe overlapping infection. When the clinical efficacy of treatment for a single pathogen is inconsistent with the changes in lung imaging, the possibility of co-infection should be considered to reduce missed diagnosis and misdiagnosis.

Data availability statement

The original contributions presented in the study are included in the article/supplementary material, further inquiries can be directed to the corresponding author.

Ethics statement

Written informed consent was obtained from the individual(s) for the publication of any potentially identifiable images or data included in this article.

Author contributions

Q-FY: Data curation, Formal analysis, Investigation, Methodology, Writing – original draft, Writing – review & editing. C-MS: Supervision, Writing – review & editing. Q-YJ: Writing – review & editing.

Funding

The author(s) declare that no financial support was received for the research, authorship, and/or publication of this article.

Acknowledgments

The authors would like to thank the nurses, and residents from the department of respiratory (Affiliated Dongyang Hospital of Wenzhou Medical University, Dongyang, China), who were involved in the management of the patient.

Conflict of interest

The authors declare that the research was conducted in the absence of any commercial or financial relationships that could be construed as a potential conflict of interest.

Publisher's note

References

1. Bonhomme D, Werts C. Host and species-specificities of pattern recognition receptors upon infection with *Leptospira interrogans*. *Front Cell Infect Microbiol*. (2022) 12:932137. doi: 10.3389/fcimb.2022.932137

2. Quintero-Velez JC, Rodas JD, Rojas CA, Ko AI, Wunder EA. Leptospira infection in rural areas of Uraba region, Colombia: a prospective study. *Am J Trop Med Hyg*. (2022) 107:1267–77. doi: 10.4269/ajtmh.21-1103

3. Cadena J, Thompson GR 3rd, Patterson TF. Aspergillosis: epidemiology, diagnosis, and treatment. *Infect Dis Clin N Am*. (2021) 35:415–34. doi: 10.1016/j.idc.2021.03.008

4. Costa F, Hagan JE, Calcagno J, Kane M, Torgerson P, Martinez-Silveira MS, et al. Global morbidity and mortality of leptospirosis: a systematic review. *PLoS Negl Trop Dis*. (2015) 9:e0003898. doi: 10.1371/journal.pntd.0003898

5. Le Turnier P, Epelboin L. Update on leptospirosis. *Rev Med Interne*. (2019) 40:306–12. doi: 10.1016/j.revmed.2018.12.003

6. Karpagam KB, Ganesh B. Leptospirosis: a neglected tropical zoonotic infection of public health importance-an updated review. *Eur J Clin Microbiol Infect Dis*. (2020) 39:835–46. doi: 10.1007/s10096-019-03797-4

7. Xu GY, Zhu HS, Liu WJ, Zeng ZW, Wang JX, Han TW, et al. Incidence of leptospirosis in Fujian province, 2015-2020. *Zhonghua Liu Xing Bing Xue Za Zhi*. (2022) 43:548–53. doi: 10.3760/cma.j.cn112338-20210819-00664

8. Pavli A, Maltezou HC. Travel-acquired leptospirosis. *J Travel Med*. (2008) 15:447–53. doi: 10.1111/j.1708-8305.2008.00257.x

9. Phillips JA. Leptospirosis. *Workplace Health Saf*. (2019) 67:148. doi: 10.1177/2165079918818582

10. Tudesq JJ, Peyrony O, Lemiale V, Azoulay E. Invasive pulmonary aspergillosis in nonimmunocompromised hosts. *Semin Respir Crit Care Med*. (2019) 40:540–7. doi: 10.1055/s-0039-1696968

11. Li D, Liang H, Yi R, Xiao Q, Zhu Y, Chang Q, et al. Clinical characteristics and prognosis of patient with leptospirosis: a multicenter retrospective analysis in south of China. *Front Cell Infect Microbiol*. (2022) 12:1014530. doi: 10.3389/fcimb.2022.1014530

12. Koizumi N. Laboratory diagnosis of leptospirosis. *Methods Mol Biol*. (2020) 2134:277–87. doi: 10.1007/978-1-0716-0459-5_25

13. Perez LJ, Lanka S, DeShambo VJ, Fredrickson RL, Maddox CW. A validated multiplex real-time PCR assay for the diagnosis of infectious Leptospira spp.: a novel assay for the detection and differentiation of strains from both pathogenic groups I and II. *Front Microbiol*. (2020) 11:457. doi: 10.3389/fmicb.2020.00457

14. Chen M, Lu W, Wu S, Wang S, Lu T, Peng C. Metagenomic next-generation sequencing in the diagnosis of leptospirosis presenting as severe diffuse alveolar hemorrhage: a case report and literature review. *BMC Infect Dis*. (2021) 21:1230. doi: 10.1186/s12879-021-06923-w

15. Guidugli F, Castro AA, Atallah AN. Antibiotics for treating leptospirosis. *Cochrane Database Syst Rev*. (2000) 2:CD001306.

16. Dhakal A, Sbar E. *Jarisch Herxheimer Reaction*. Treasure Island, FL: StatPearls (2022).

frontiers | Frontiers in Medicine

TYPE Case Report
PUBLISHED 05 March 2024
DOI 10.3389/fmed.2024.1357362

OPEN ACCESS

EDITED BY
Talat Kilic,
İnönü University, Türkiye

REVIEWED BY
Giovanni Paoletti,
Humanitas Research Hospital, Italy
Premanand Balraj,
North Dakota State University, United States
Sangeeta Bhallamudi,
New York University, United States

*CORRESPONDENCE
Corrado Pelaia
✉ pelaia.corrado@gmail.com

RECEIVED 18 December 2023
ACCEPTED 16 February 2024
PUBLISHED 05 March 2024

CITATION
Maiorano A, Lupia C, Montenegro N, Neri G, Bruni A, Garofalo E, Longhini F, Crimi C, Maglio A, Vatrella A, Pelaia G and Pelaia C (2024) Effects of inhaled beclomethasone dipropionate/formoterol fumarate/glycopyrronium on diaphragmatic workload and lung function in uncontrolled asthma: a case report.
Front. Med. 11:1357362.
doi: 10.3389/fmed.2024.1357362

Effects of inhaled beclomethasone dipropionate/formoterol fumarate/glycopyrronium on diaphragmatic workload and lung function in uncontrolled asthma: a case report

Antonio Maiorano[1], Chiara Lupia[1], Nicola Montenegro[1], Giuseppe Neri[2], Andrea Bruni[2], Eugenio Garofalo[2], Federico Longhini[2], Claudia Crimi[3], Angelantonio Maglio[4], Alessandro Vatrella[4], Girolamo Pelaia[1] and Corrado Pelaia[2]*

[1]Department of Health Sciences, University "Magna Graecia" of Catanzaro, Catanzaro, Italy, [2]Department of Medical and Surgical Sciences, University "Magna Graecia" of Catanzaro, Catanzaro, Italy, [3]Department of Clinical and Experimental Medicine, University of Catania, Catania, Italy, [4]Department of Medicine, Surgery and Dentistry, University of Salerno, Salerno, Italy

Beclomethasone dipropionate/formoterol fumarate/glycopyrronium (BDP/FF/G) single inhaler extrafine triple therapy is effective for the treatment of uncontrolled asthma. Nevertheless, there is a lack of data about the use of diaphragmatic ultrasonography to monitor adult asthmatics while they are receiving inhaled treatment. We took into consideration a 78-year-old woman complaining of asthma, treated with inhaled corticosteroid/long-acting β_2-adrenergic agonist (ICS/LABA), characterized by an asthma control questionnaire-5 (ACQ-5) score and a lung function test suggestive of uncontrolled asthma. Moreover, a diaphragmatic ultrasound showed signs of high diaphragm workload. Because of these findings, we proposed to our patient a shift toward triple inhaled therapy with BDP/FF/G, and she underwent a second evaluation after 7 days of treatment. Improvements in the diaphragmatic ultrasound parameters, lung function test, and ACQ-5 score were found. In particular, we detected a reduction of thickening fraction (TF), and a normalization of the other diaphragmatic measures, indicative of a decrease in diaphragmatic workload. To our knowledge, this is the first literature report showing concomitant improvements of both lung function tests and diaphragmatic ultrasonography parameters, observed in an adult patient with uncontrolled asthma after short-term treatment with the single inhaler triple therapy BDP/FF/G.

KEYWORDS

asthma, triple inhaled therapy, diaphragmatic ultrasound, thickening fraction, ACQ-5

Background

Single inhaler extrafine triple therapy with beclomethasone dipropionate/formoterol fumarate/glycopyrronium (BDP/FF/G) is efficacious in the treatment of uncontrolled asthma (1). However, current evidence is quite scarce about the application of ultrasound to follow-up adult asthmatic patients during inhaled therapy. Scioscia et al. evaluated 72 patients complaining of severe uncontrolled asthma using a transthoracic ultrasound (TUS) examination, thus finding thickened and/or irregular pleural lines, associated with either a lack or reduction of the gliding sign (2). Del Colle et al. carried out TUS in three patients using the M-mode pattern, and they did not detect gliding and barcode signs (3). Nevertheless, these observations were based only on TUS, not associated with diaphragmatic ultrasound. Therefore, we herein describe the first reported case of a patient with uncontrolled asthma, treated with the single inhaler extrafine triple therapy BDP/FF/G, who experienced relevant improvements of diaphragmatic function detected by an ultrasound, paralleled by marked amelioration of symptom control and lung function.

Case presentation

Due to a severe asthma exacerbation, a 78-year-old atopic and never-smoker Caucasian woman was referred to the Pulmonology Unit of "Magna Graecia" University Hospital located in Catanzaro, Italy. The patient was taking high dosages of beclomethasone/formoterol (BDP/FF) inhaled therapy; she correctly performed the therapeutic inhalations and displayed a high degree of adherence to the inhaled treatment. The asthma control questionnaire-5 (ACQ-5) score was 3.8. Vital signs at admission included a body temperature of 36.6°C, arterial blood pressure of 140/90 mmHg, heart rate of 82 beats/min, respiratory rate of 20 breaths/min, and hemoglobin oxygen saturation of 91% in room air. Physiologic chest breathing sounds were diffusely reduced, and relevant wheezing was present. Blood analysis revealed the following values: hemoglobin, 12.3 g/dL; white blood cell count, 10.83×10^3 cells/μL; neutrophils, 57.1% (6,184 cells/μL); eosinophils, 2.8% (303 cells/μL); C-reactive protein level, 17.3 mg/L; erythrocyte sedimentation rate (ESR), 40 mm/h; and total immunoglobulin E (IgE) levels, 852.6 IU/mL. Blood gas analysis at admission (room air/FiO_2 21%) yielded the following results: pH, 7.44; PaO_2, 63 mmHg; $PaCO_2$, 35 mmHg; HCO_3^-, 24 mmol/L. Echocardiography revealed an estimated pulmonary arterial systolic pressure of 40 mmHg, left ventricular ejection fraction of 61%, reduced right ventricular systolic function, and normal inferior vena cava diameter. Lung function tests performed during ICS/LABA therapy evidenced the following values (Figure 1A): forced expiratory volume in 1 s (FEV_1), 0.88 L (41% of predicted); forced vital capacity (FVC), 1.34 L (48% of predicted); FEV_1/FVC ratio, 65.67%; peak expiratory flow (PEF), 2.54 L/s (44% of predicted); residual volume (RV), 2.59 L (113% of predicted); total lung capacity (TLC), 3.93 L (74% of predicted); Motley index (RV/TLC ratio), 65.85%; forced expiratory flow at 75% of FVC (FEF_{75}), 2.07 L/s (41% of predicted); forced expiratory flow at 50% of FVC (FEF_{50}), 0.66 L/s (39% of predicted); forced expiratory flow at 25% of FVC (FEF_{25}), 0.22 L/s (56% of predicted); forced expiratory flow at 25–75% of forced vital capacity (FEF_{25-75}), 0.54 L/s (32% of predicted); and total airway resistance (R_{tot}), 0.42 kPa x s/L (140% of predicted).

Moreover, baseline diaphragmatic ultrasound evaluation was carried out by a pulmonologist with many years of certified experience. All measurements were made under conditions of spontaneous and resting tidal breathing, during seated and lying down positions, in an abdominal setting, using a 3.5–5-MHz convex ultrasound probe in brightness mode (B-mode) for thickness, and a 7–15-MHz linear probe in B-mode and motion mode (M-mode) for right diaphragmatic shift, respectively (Esaote MyLab XPro30, Esaote S.p.A., Genoa, Italy). The liver was considered as a marker to find an echographic window for the right hemidiaphragm. During the lying down position, the probe was placed between the midclavicular and anterior axillary lines, using the B-mode pattern to select the right hemidiaphragm exploration line. The normal diaphragm contracts and moves to the transducer during inspiration. This is recorded as an upward motion during M-mode, regarded as the diaphragmatic excursion during inspiration, measured on the vertical axis from baseline to the point of maximum height of inspiration. Diaphragmatic excursion was recorded in a frozen image made up of at least three consecutive respiratory cycles, to reduce the measurement error. In the seated position, the diaphragmatic thickness was assessed by B-mode ultrasonography, fixing the linear probe below the phrenicocostal sinus, near the mid-axillary line at the eighth intercostal space, thus identifying the diaphragm as a structure with two parallel echogenic lines, among which there was the hypoechoic diaphragmatic muscle. Its thickness was considered as the distance between the pleural and peritoneal membranes. The measurements were performed at the end of inspiration and expiration during quiet breathing at tidal volume and the end of inspiration after deep breathing. We took into consideration three different breathing cycles. Normal ranges were considered according to those previously described by Boussuges et al. (4, 5) and Zambon et al. (6). We detected the following ultrasound baseline parameters (Figures 2A, 3A): tidal volume excursion, 3.1 cm (normal range: 0.9–2.5 cm); tidal volume inspiratory time, 0.98 s (normal range: 0.5–1.7 s); tidal volume inspiratory velocity, 3.5 cm/s (normal range: 0.7–2.6 cm/s); tidal volume expiratory time, 2.7 s (normal range: 0.4–1.6 s); tidal volume expiratory velocity, 1.2 cm/s (normal range: 0.2–2.8 cm/s); tidal volume duration of motion, 3.8 s (normal range: 1.1–3.4 s); deep breathing excursion, 8.26 mm (normal range: 3.3–7.5 mm); deep breathing inspiratory time, 1.7 s (normal range: 0.4–2.4 s); deep breathing inspiratory velocity, 4.2 cm/s (normal range: 1.5–7.3 cm/s); thickness at end-expiration (FRC), 1.1 mm (normal range: 1.1–2.7 mm); thickness at end-inspiration, 2.0 mm (normal range: 1.3–3.7 mm); tidal volume thickening fraction (TF), 81% (normal range: 30–36%); and thickness at deep breathing, 3.6 mm (normal range: 2.4–5.4 mm).

Because of these findings and clinical worsening, inhaled therapy was changed from BDP/FF to triple fixed-combination BDP/FF/G. After a week of therapy, the ACQ-5 score decreased to 1.2, and follow-up functional lung tests yielded the following results (Figure 1B): FEV_1, 1.20 L (56% of predicted; +0.32 L/+36.4%); FVC, 1.78 L (63% of predicted; +0.44 L/+32.8%); FEV_1/FVC ratio, 67.43% (+2.7%); PEF, 3.77 L/s (65% of predicted; +48.4%); RV, 1.48 L (65% of predicted; −1.11 L/−42.9%); TLC, 3.26 L (61% of predicted; −0.67 L/−17.0%); RV/TLC ratio, 45.49 (−30.9%); FEF_{75}, 3.30 L/s (65% of predicted; +59.4%); FEF_{50}, 1.35 L/s (80% of predicted; +104.5%); FEF_{25}, 0.32 L/s (83% of predicted; +45.5%); FEF_{75-25}, 0.75 L/s (45% of predicted; +38.9%); and R_{tot}, 0.39 kPa x s/L (130% of predicted; −7.1%). Diaphragmatic

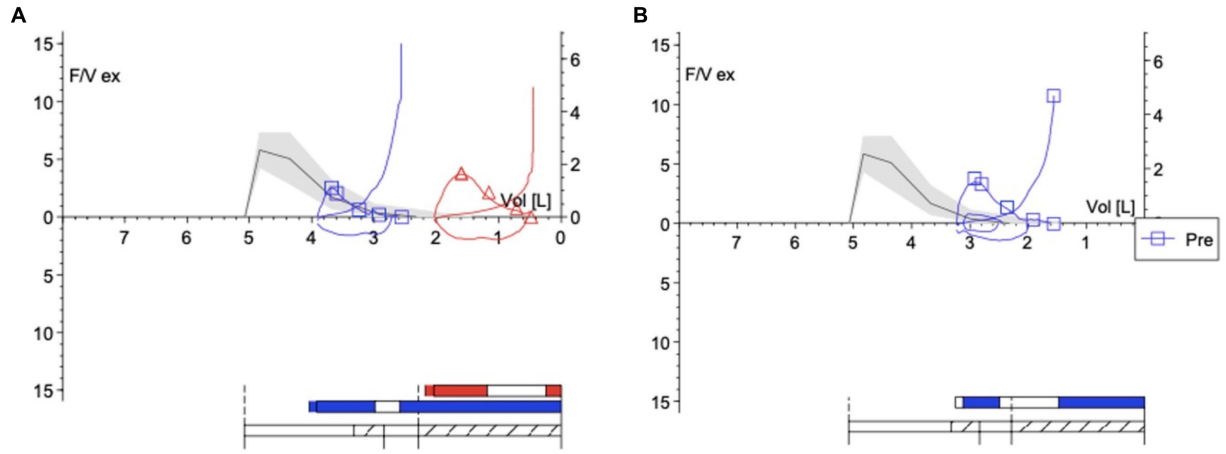

FIGURE 1
(A) Flow–volume curves before BDP/FF/G (blue line for baseline curve and red line for post-bronchodilator test curve), showing the reversibility of airflow limitation. **(B)** Flow–volume curve after BDP/FF/G.

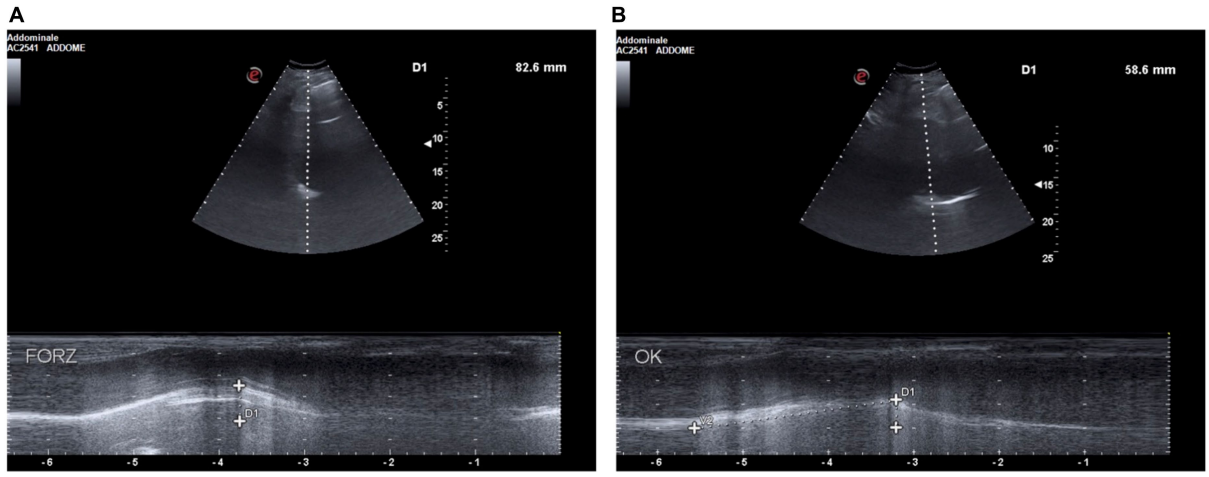

FIGURE 2
(A) D1: deep breathing motion before BDP/FF/G. **(B)** D1: deep breathing motion after BDP/FF/G.

ultrasound was also performed, thereby evidencing the following measures (Figures 2B, 3B): tidal volume excursion, 1.6 cm (normal range: 0.9–2.5 cm); tidal volume inspiratory time, 1.12 s (normal range: 0.5–1.7 s); tidal volume inspiratory velocity, 1.6 cm/s (normal range: 0.7–2.6 cm/s); tidal volume expiratory time, 1.2 s (normal range 0.4–1.6 s); tidal volume expiratory velocity, 1.6 cm/s (normal range: 0.2–2.8 cm/s); tidal volume duration of motion, 2.3 s (normal range: 1.1–3.4 s); deep breathing excursion, 5.86 mm (normal range: 3.3–7.5 mm); deep breathing inspiratory time, 2.3 s (normal range: 0.4–2.4 s); deep breathing inspiratory velocity, 2.5 cm/s (normal range: 1.5–7.3 cm/s); thickness at end-expiration (FRC), 1.1 mm (normal range: 1.1–2.7 mm); thickness at end-inspiration, 1.6 mm (normal range: 1.3–3.7 mm); tidal volume thickening fraction (TF), 45% (normal range: 30–36%), and thickness at deep breathing, 2.8 mm (normal range: 2.4–5.4 mm). The patient did not experience any adverse effects during treatment with BDP/FF/G.

Discussion

This case report highlights the improvements in diaphragmatic thickness and motion, detected by ultrasound after 7 days of single inhaler triple therapy with BDP/FF/G (Table 1). Asthma is a chronic obstructive respiratory disease, characterized by bronchial hyperresponsiveness and reversible airflow limitation, caused by airway inflammation and remodeling. In asthma, airway structural changes include subepithelial fibrosis, neo-angiogenesis, smooth muscle thickening, and goblet cell metaplasia/hyperplasia (7). Asthma heterogeneity is expressed by many phenotypes sustained by different endotypes (8). The most common endotypes are included under the umbrella term "type 2 asthma," referring to either allergic or non-allergic traits, very often associated with airway eosinophilic inflammation (9).

Over time, small airway inflammation can promote expiratory airflow limitation and dynamic hyperinflation, causing daily exercise

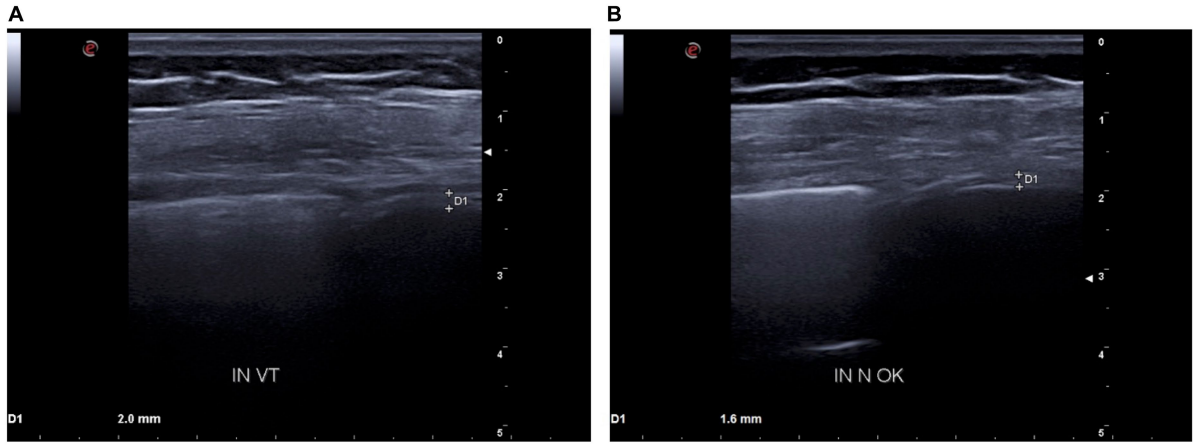

FIGURE 3
(A) D1: tidal volume inspiratory thickness before BDP/FF/G. **(B)** D1: tidal volume inspiratory thickness after BDP/FF/G.

TABLE 1 Diaphragmatic parameters before and after BDP/FF/G treatment.

	Before BDP/FF/G	After BDP/FF/G	Normal values
Excursion (cm)	3.1	1.6	0.9–2.5
Inspiratory velocity (cm/s)	3.5	1.6	0.7–2.6
Expiratory time (s)	2.7	1.2	0.4–1.6
Duration of motion (s)	3.8	2.3	1.1–3.4
Thickening fraction (TF) (%)	81	45	30–36

intolerance, especially in obese asthmatic patients because of reduced chest wall compliance (10). This finding is well-known in chronic obstructive pulmonary disease (COPD), resulting from expiratory airflow limitation and ventilatory demand, thus contributing to dyspnea and activity impairment (11). These functional limitations can be improved in COPD patients by BDP/FF/G treatment, which decreases air trapping and lung hyperinflation, and also improves lung diffusing capacity (12). Moreover, COPD patients may develop both respiratory and locomotor muscle dysfunctions (13). In hyperinflated patients, the diaphragm works against increased mechanical loads, caused by airflow limitation and geometrical chest changes driven by RV increase (14). Hence, ultrasound may be helpful to evaluate diaphragmatic function in COPD patients, with regard to thickening (15) and motion parameters (16). Moreover, in COPD patients, BDP/FF/G could positively impact the structural changes of the diaphragm (e.g., fiber type transformation, sarcomere injury, and diaphragm atrophy), which contributes to its dysfunction. Thus far, no report has been published about the potential utility of diaphragmatic ultrasound in adult patients with uncontrolled asthma. However, considering the increasing application of ultrasounds in clinical practice, e.g., to evaluate right heart dysfunction (17), presence or absence of pleural effusion (18), COPD abnormalities (19), and liver diseases (20), we decided to study diaphragmatic function using ultrasound in a patient with uncontrolled asthma, before and after therapy with BDP/FF/G. Diaphragmatic ultrasound is not routinely used to follow-up adult patients with severe asthma, before and after inhaled treatments. However, we hypothesized that the occurrence in asthmatic patients of small airway impairment, eventually associated with dynamic hyperinflation (10), could cause diaphragmatic dysfunction (14). The patient evaluated in the present case report was characterized by severe reversible airway obstruction and small airway impairment. This dysfunctional condition was associated with an increased work of the diaphragm, documented by ultrasound and reasonably explained by increased tidal volume motion, expiratory time, motion time, and thickening fraction. The single inhaler double therapy BDP/FF was shifted to single inhaler triple therapy BDP/FF/G, and after a week, the tidal volume TF value was 45%. Other parameters changed and were found to be included within normal ranges. Such data were also reflected by functional respiratory improvements. Therefore, it is reasonable to speculate that the relevant improvement of the diaphragmatic function, which we detected in our patients after BDP/FF/G treatment, was mainly due to a marked decrease in airway resistance, consequently associated with a reduced work of the diaphragm muscle fibers. Furthermore, the patient reported a marked reduction in cough and dyspnea, associated with good control of asthma symptoms, as shown by a decrease in the ACQ-5 score. To the best of our knowledge, this case report represents the first evidence of concomitant improvements involving lung function tests and diaphragmatic ultrasound evaluation, experienced after treatment with single inhaler triple therapy BDP/FF/G by an adult asthmatic patient with uncontrolled asthma.

Conclusion

This case report highlights for the first time the utility of diaphragmatic ultrasound as a follow-up examination of severe asthmatic patients. In particular, after short-term treatment with the single inhaler triple therapy BDP/FF/G, we detected relevant improvements in functional diaphragmatic performance, paralleled by an important amelioration of lung function. Such a preliminary

observation suggests that it could be useful to carry out further studies with the aim of better elucidating the role of diaphragmatic ultrasound evaluation in the management and monitoring of patients with severe uncontrolled asthma. Indeed, although our present considerations are restricted to only one patient, we think that the innovative methodological approach proposed in this case report deserves extensive application in asthmatic patients treated with triple inhaled therapy. The well-known beneficial effect exerted by BDP/FF/G might also depend on the positive role played by this inhaled treatment on the diaphragmatic function of patients with uncontrolled asthma.

Data availability statement

The raw data supporting the conclusions of this article will be made available by the authors, without undue reservation.

Ethics statement

The studies involving humans were approved by the Local Ethical Committee of Calabria Region (Catanzaro, Italy; document no. 263 – 23 July 2020). The studies were conducted in accordance with the local legislation and institutional requirements. The participants provided their written informed consent to participate in this study. Written informed consent was obtained from the individual(s) for the publication of any potentially identifiable images or data included in this article.

Author contributions

AMai: Data curation, Investigation, Methodology, Resources, Visualization, Writing – original draft, Writing – review & editing. CL: Formal analysis, Investigation, Methodology, Visualization, Writing – original draft, Writing – review & editing. NM: Investigation, Methodology, Visualization, Writing – original draft, Writing – review & editing. GN: Supervision, Validation, Visualization, Writing – original draft, Writing – review & editing. AB: Supervision, Validation, Visualization, Writing – original draft, Writing – review & editing. EG: Supervision, Validation, Visualization, Writing – original draft, Writing – review & editing. FL: Supervision, Validation, Visualization, Writing – original draft, Writing – review & editing. CC: Supervision, Validation, Visualization, Writing – original draft, Writing – review & editing. AMag: Supervision, Validation, Visualization, Writing – original draft, Writing – review & editing. AV: Supervision, Validation, Visualization, Writing – original draft, Writing – review & editing. GP: Formal analysis, Investigation, Methodology, Project administration, Supervision, Validation, Visualization, Writing – original draft, Writing – review & editing. CP: Conceptualization, Data curation, Formal analysis, Funding acquisition, Investigation, Methodology, Project administration, Resources, Software, Supervision, Validation, Visualization, Writing – original draft, Writing – review & editing.

Funding

The author(s) declare that no financial support was received for the research, authorship, and/or publication of this article.

Conflict of interest

The authors declare that the research was conducted in the absence of any commercial or financial relationships that could be construed as a potential conflict of interest.

The author(s) declared that they were an editorial board member of Frontiers, at the time of submission. This had no impact on the peer review process and the final decision.

Publisher's note

References

1. Virchow JC, Kuna P, Paggiaro P, Papi A, Singh D, Corre S, et al. Single inhaler extrafine triple therapy in uncontrolled asthma (TRIMARAN and TRIGGER): two double-blind, parallel group, randomised, controlled phase 3 trials. *Lancet*. (2019) 394:1737–49. doi: 10.1016/S0140-6736(19)32215-9

2. Scioscia G, Lacedonia D, Quarato CMI, Tondo P, Del Colle A, Sperandeo M, et al. Could transthoracic ultrasound be useful to suggest a small airways disease in severe uncontrolled asthma? *Ann Allergy Asthma Immunol*. (2022) 129:461–6. doi: 10.1016/j.anai.2022.05.024

3. Del Colle A, Carpagnano GE, Feragalli B, Foschino Barbaro MP, Lacedonia D, Scioscia G, et al. Transthoracic ultrasound sign in severe asthmatic patients: a lack of "gliding sign" mimic pneumothorax. *BJR Case Rep*. (2019) 5:20190030. doi: 10.1259/bjrcr.20190030

4. Boussuges A, Rives S, Finance J, Chaumet G, Vallée N, Risso JJ, et al. Ultrasound assessment of diaphragm thickness and thickening: reference values and limits of normality when in a seated position. *Front Med (Lausanne)*. (2021) 8:742703. doi: 10.3389/fmed.2021.742703

5. Boussuges A, Finance J, Chaumet G, Brégeon F. Diaphragmatic motion recorded by M-mode ultrasonography: limits of normality. *ERJ Open Res*. (2021) 7:00714–2020. doi: 10.1183/23120541.00714-2020

6. Zambon M, Greco M, Bocchino S, Cabrini L, Beccaria PF, Zangrillo A. Assessment of diaphragmatic dysfunction in the critically ill patient with ultrasound: a systematic review. *Intensive Care Med*. (2017) 43:29–38. doi: 10.1007/s00134-016-4524-z

7. Liu G, Philp AM, Corte T, Travis MA, Schilter H, Hansbro NG, et al. Therapeutic targets in lung tissue remodelling and fibrosis. *Pharmacol Ther*. (2021) 225:107839. doi: 10.1016/j.pharmthera.2021.107839

8. Pelaia C, Pelaia G, Crimi C, Maglio A, Stanziola AA, Calabrese C, et al. Novel biological therapies for severe asthma Endotypes. *Biomedicines*. (2022) 10:1064. doi: 10.3390/biomedicines10051064

9. Pelaia C, Pelaia G, Crimi C, Maglio A, Gallelli L, Terracciano R, et al. Tezepelumab: a potential new biological therapy for severe refractory asthma. *Int J Mol Sci*. (2021) 22:4369. doi: 10.3390/ijms22094369

10. Ferreira PG, Freitas PD, Silva AG, Porras DC, Stelmach R, Cukier A, et al. Dynamic hyperinflation and exercise limitations in obese asthmatic women. *J Appl Physiol*. (1985) 123:585–93. doi: 10.1152/japplphysiol.00655.2016

11. O'Donnell DE, Laveneziana P. The clinical importance of dynamic lung hyperinflation in COPD. *COPD*. (2006) 3:219–32. doi: 10.1080/15412550600977478

12. Pelaia C, Procopio G, Rotundo FL, Deodato MR, Ferrante Bannera A, Tropea FG, et al. Real-life therapeutic effects of beclomethasone dipropionate/formoterol fumarate/

glycopyrronium combined triple therapy in patients with chronic obstructive pulmonary disease. *Ther Adv Respir Dis*. (2023) 17:17534666231155778. doi: 10.1177/17534666231155778

13. Gea J, Agustí A, Roca J. Pathophysiology of muscle dysfunction in COPD. *J Appl Physiol*. (2013) 114:1222–34. doi: 10.1152/japplphysiol.00981.2012

14. Orozco-Levi M. Structure and function of the respiratory muscles in patients with COPD: impairment or adaptation? *Eur Respir J Suppl*. (2003) 22:41s–51s. doi: 10.1183/09031936.03.00004607

15. Rittayamai N, Chuaychoo B, Tscheikuna J, Dres M, Goligher EC, Brochard L. Ultrasound evaluation of diaphragm force Reserve in Patients with chronic obstructive pulmonary disease. *Ann Am Thorac Soc*. (2020) 17:1222–30. doi: 10.1513/AnnalsATS.202002-129OC

16. Dos Santos Yamaguti WP, Paulin E, Shibao S, Chammas MC, Salge JM, Ribeiro M, et al. Air trapping: the major factor limiting diaphragm mobility in chronic obstructive pulmonary disease patients. *Respirology*. (2008) 13:138–44. doi: 10.1111/j.1440-1843.2007.01194.x

17. Pelaia C, Armentaro G, Lupia C, Maiorano A, Montenegro N, Miceli S, et al. Effects of high-flow nasal cannula on right heart dysfunction in patients with acute-on-chronic respiratory failure and pulmonary hypertension. *J Clin Med*. (2023) 12:5472. doi: 10.3390/jcm12175472

18. Sorino C, Mondoni M, Lococo F, Marchetti G, Feller-Kopman D. Optimizing the management of complicated pleural effusion: from intrapleural agents to surgery. *Respir Med*. (2022) 191:106706. doi: 10.1016/j.rmed.2021.106706

19. Zanforlin A, Smargiassi A, Inchingolo R, di Marco BA, Valente S, Ramazzina E. Ultrasound analysis of diaphragm kinetics and the diagnosis of airway obstruction: the role of the M-mode index of obstruction. *Ultrasound Med Biol*. (2014) 40:1065–71. doi: 10.1016/j.ultrasmedbio.2013.12.009

20. Abenavoli L, Spagnuolo R, Scarlata GGM, Scarpellini E, Boccuto L, Luzza F. Ultrasound prevalence and clinical features of nonalcoholic fatty liver disease in patients with inflammatory bowel diseases: a real-life cross-sectional study. *Medicina (Kaunas)*. (2023) 59:1935. doi: 10.3390/medicina59111935

frontiers | Frontiers in Medicine

TYPE Case Report
PUBLISHED 17 April 2024
DOI 10.3389/fmed.2024.1357714

OPEN ACCESS

EDITED BY
Santi Nolasco,
University of Catania, Italy

REVIEWED BY
Claudio Farina,
ASST Papa Giovanni XXIII, Italy
Po Lin Chen,
National Cheng Kung University, Taiwan

*CORRESPONDENCE
Xiaoju Zhang
✉ zhangxiaoju@zzu.edu.cn

RECEIVED 18 December 2023
ACCEPTED 05 April 2024
PUBLISHED 17 April 2024

CITATION
Wang C, Wei N, Zhang M and Zhang X (2024) Pulmonary infection with *Aeromonas dhakensis* in a patient with acute T lymphoblastic leukemia: a case report and review of the literature.
Front. Med. 11:1357714.
doi: 10.3389/fmed.2024.1357714

Pulmonary infection with *Aeromonas dhakensis* in a patient with acute T lymphoblastic leukemia: a case report and review of the literature

Chaoyang Wang[1], Nan Wei[1], Moyuan Zhang[2,3] and Xiaoju Zhang[1]*

[1]Department of Respiratory and Critical Care Medicine, Zhengzhou University People's Hospital, Henan Provincial People's Hospital, Zhengzhou, China, [2]Xinxiang Medical University, Xinxiang, China, [3]Department of Respiratory and Critical Care Medicine, Henan Provincial People's Hospital, Zhengzhou, China

Background: *Aeromonas dhakensis* is a gram-negative bacterium. In recent years, *Aeromonas dhakensis* has gradually attracted increasing attention due to its strong virulence and poor prognosis. Clinical reports of pulmonary infection caused by *Aeromonas dhakensis* are rare.

Case presentation: A patient with acute T lymphoblastic leukemia experienced myelosuppression after chemotherapy, developed a secondary pulmonary infection with *Aeromonas dhakensis* and was hospitalized due to fever. The patient underwent testing for inflammatory markers, chest imaging, blood culture, bronchoalveolar lavage, pleural drainage, and metagenomic next-generation sequencing of alveolar lavage fluid and pleural fluid to obtain evidence of *Aeromonas dhakensis* infection, and was treated with four generations of cephalosporin combined with fluoroquinolone antibiotics. The patient's condition significantly improved.

Discussion: Among pulmonary infectious pathogens, *Aeromonas dhakensis* is relatively rare. Once an *Aeromonas* strain is cultured in the clinical work, pathogenic sequencing should be performed on the detected samples for early accurate diagnosis and effective anti-infection treatment.

KEYWORDS

***Aeromonas dhakensis*, *Aeromonas*, pulmonary infection, mNGS, antibiotic**

1 Introduction

Aeromonas dhakensis is an emerging opportunistic pathogen. It was first found in the feces of children with diarrhea in Dhaka, Bangladesh, and described in 2002 (1). It is present in polluted water, fish and food. It often occurs in people with poor immune function, malignant tumors or biliary tract infections and can also be seen in healthy people who are in contact with polluted water. *Aeromonas dhakensis* can cause severe infection in the gastrointestinal tract, skin and soft tissues, even throughout the global body. Due to the complex classification of *Aeromonas*, routine laboratory tests cannot accurately identify *Aeromonas* species, and the

epidemiology of *Aeromonas dhakensis* is underestimated in the clinic (2). Currently, *Aeromonas dhakensis* is considered the second most common pathogen of *Aeromonas* species and the most virulent (3–5). We report a case of pulmonary infection with *Aeromonas dhakensis* secondary to chemotherapy in a patient with acute T lymphoblastic leukemia. This infection was cured with standard antibiotics. This paper also reviews the treatment and prognosis of pulmonary infection with *Aeromonas dhakensis* and provides experience for clinicians in diagnosing and treating this disease.

2 Case report

An 18-year-old female patient was diagnosed with acute T-lymphoblastic leukemia more than 8 months earlier. She was started on vincristine, daunorubicin, cyclophosphamide, prednisone, and asparaginase (VDCLP) chemotherapy and leucocyte elevation therapy. Two days later, the patient developed fever, with a fluctuating body temperature and a highest temperature of 39°C. She was referred to our hospital the next day.

The admission test results were as follows: hemoglobin, 93 g/L (reference range: 115–150 g/L); platelet count, 74×10^9/L (reference range: 125–350 $\times 10^9$/L); white blood cell count, 0.06×10^9/L (reference range: 3.5–9.5 $\times 10^9$/L); neutrophils, not detected (reference range: 1.8–6.3 $\times 10^9$/L); lymphocytes, not detected (reference range: 1.1–3.2 $\times 10^9$/L); C-reactive protein (CRP), 25.32 mg/L (reference range: 0–10 mg/L); procalcitonin (PCT), 15 ng/L (reference range: < 0.05 ng/L); serum galactomannan (GM) test, negative; fungal detection (G) test, 86.2 pg/mL (reference range: < 60 pg/mL: negative, > 100 pg/mL: positive); cytokines: interleukin-6: 29.73 pg/mL (reference range: ≤5.4 pg/mL); interleukin-4: 9.03 pg/mL (reference range: ≤8.56 pg/mL); interferon-α: 49.3 pg/mL (reference range: ≤23.1 pg/mL); Lymphocyte immunoassay: CD19 + B lymphocytes: 0.27% (reference range: 6.58–24.52%); CD3 + T lymphocytes: 90.47% (reference range: 55.62–84.84%); CD3+/CD8+ toxic T lymphocytes: 49.69% (reference range: 13.27–40.63%); (CD3-CD16+/56+) NK cells: 4.31% (reference range: 5.15–27.08%); absolute number of lymphocytes: 37.6/μL (reference range: 1530–3,700/μL); absolute number of total T lymphocytes: 33.6/μL (reference range: 955–2,860/μL); absolute number of CD4+ helper T lymphocytes: 11.9/μL (reference range: 550–1,440/μL); absolute number of CD8+ toxic T lymphocytes: 17.3/μL (reference range: 320–1,250/μL); absolute number of B lymphocytes: 0.101/μL (reference range: 90–560/μL); and absolute number of NK cells: 1.72/μL (reference range: 150–1,100/μL). Acid-fast staining of the sputum smear was negative; fungal examination of the sputum smear was negative. Gram staining and microscopic examination of the sputum smear showed gram-positive cocci and gram-negative bacilli. Combined with the fever symptoms and laboratory results, the patient's immune status was low at the time. Considering the diagnosis of "bone marrow suppression period after chemotherapy and coinfection," anti-infection treatment made up of Biapenem 300 mg q8h as an intravenous infusion, vancomycin 0.5 g q8h as an intravenous infusion combined with posaconazole oral suspension 200 mg tid po was given for 6 days.

However, she still had fever and developed right chest pain on the 7th day after admission. Auscultation of the right lung indicated reduced breathing sounds. Complete chest computed tomography (CT) showed streaks and clumps of high-density shadows in the middle and lower lobes of the right lung with cavity formation and a small amount of fluid in the right chest cavity and interlobar fissure (Figure 1A). Blood in the sputum appeared on the 8th day. Blood examination showed that the white blood cell count was 6.24×10^9/L, the neutrophil count was 5.98×10^9/L, the lymphocyte count was 0.07×10^9/L, CRP was 152.89 mg/L, and PCT was 1.96 ng/mL. The BD PhoenixTM Automated Microbiology System (BD Diagnostic Systems, Sparks, United States) was used for bacterial identification and drug sensitivity tests. Blood culture showed the growth of *Aeromonas hydrophila*. The drug sensitivity test results were as follows

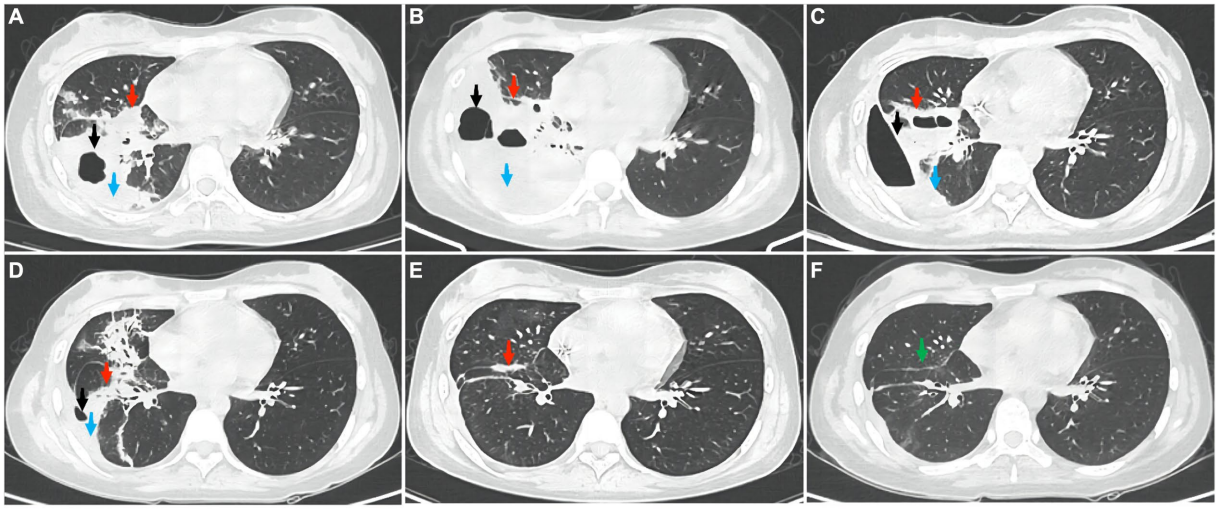

FIGURE 1
The picture shows the changes in the chest CT images during treatment. **(A)** the first CT scan in the hospital taken on 29 June 2023. The patient underwent a CT scan of the chest to observe the therapeutic effect on **(B)** 12 July 2023 and **(C)** 31 July 2023. Outpatient re-examinations using a repeat CT scan on **(D)** 25 August 2023, **(E)** 3 October 2023, and **(F)** 14 November 2023. The red arrow represents the inflammatory lesion, the black arrow shows the cavity, the blue arrow indicates fluid accumulation, and the green arrow represents residual striped shadows.

TABLE 1 Antibiotic susceptibility test for *Aeromonas dhakensis*.

Antibiotic	MIC (ug/mL)	Sensitivity
Amikacin	≤8	Sensitive
Aztreonam	≤2	Sensitive
Cefepime	≤2	Sensitive
Cefotaxime	≤1	Sensitive
Ceftazidime	≤1	Sensitive
Chloramphenicol	≤4	Sensitive
Ciprofloxacin	≤0.5	Sensitive
Gentamicin	4	Sensitive
Imipenem	≤1	Sensitive
Levofloxacin	≤1	Sensitive
Meropenem	≤1	Sensitive
Piperacillin/tazobactam	≤4/4	Sensitive
Tetracycline	>8	Resistant
Compound sulfamide	≤0.5/9.5	Sensitive

(Table 1): *Aeromonas hydrophila* was sensitive to amikacin, aztreonam, cefepime, cefotaxime, ceftazidime, chloramphenicol, ciprofloxacin, gentamicin, imipenem, levofloxacin, meropenem, piperacillin/tazobactam, and the compound sulfamide but resistant to tetracycline. Therefore, the antibiotic regimen was adjusted to Ceftazidime 2 g q8h as an intravenous infusion combined with moxifloxacin 0.4 g qd as an intravenous infusion for 13 days.

On the 20th day after admission, chest CT showed increased density in the middle and lower lobes of the right lung with stripy and clump shapes, a larger cavity area than before, and increased pleural effusion on the right side (Figure 1B). Considering the worsening of the patient's hemoptysis symptoms, chest CT indicated progressive inflammation and pleural effusion. Therefore, bronchoalveolar lavage and pleural drainage were performed to help find unknown pathogens. Conventional testing of the pleural effusion revealed the following results: color, orange yellow; transparency, turbidity, visible solidification; Rivalta test, positive; and white blood cell count, $10{,}154 \times 10^6$/L. The biochemistry of the pleural effusion showed the following: total protein 37.3 g/L, albumin 21.3 g/L, lactate dehydrogenase 6,537 U/L, and glucose 0.48 mmol/L. Ordinary bacterial culture of the pleural effusion detected no bacteria. Cytological staining of alveolar lavage fluid and pleural fluid via hematoxylin–eosin staining showed inflammatory cells (Figure 2). To identify potential pathogenic microorganisms, we performed metagenomic next-generation sequencing (mNGS) on the pleural effusion and bronchoalveolar lavage fluid. Pleural effusion mNGS indicated *Aeromonas dhakensis* (number of sequences: 43, identification confidence: 99%) (reference range: not found). Bronchoalveolar lavage fluid mNGS showed *Aeromonas dhakensis* (number of sequences: 101, identification confidence: 99%) (reference range: not found). According to the ABX POC-IT guidelines and published literature (6–12), *Aeromonas* is sensitive to fluoroquinolones and fourth-generation cephalosporins. Therefore, the antibiotic was adjusted to cefepime 2 g q8h as an intravenous infusion combined with levofloxacin 0.5 g qd as an intravenous infusion.

On the 38th day after admission, her body temperature returned to normal, and her symptoms of hemoptysis disappeared. Blood examination revealed a white blood cell count of 6.15×10^9/L, a neutrophil count of 3.55×10^9/L, a lymphocyte count of 1.81×10^9/L, CRP of 28.85 mg/L, and PCT of <0.05 ng/mL. Chest CT showed that the cord-like and flaky-like high-density shadows in the middle and lower lobes of the right lung were reduced in scope, and the pleural effusion on the right side was less than that of the previous lesions (Figure 1C). Therefore, the patient was discharged home, and the original antibiotic regimen was continued. On the 63rd day of follow-up, her white blood cell count was 3.74×10^9/L, her neutrophil count was 2.13×10^9/L, her lymphocyte count was 1.05×10^9/L, and her CRP level was 2.51 mg/L. Chest CT showed that the extent of inflammation and pleural effusion both significantly improved (Figure 1D). On the 101st day of follow-up, chest CT indicated that most of the inflammatory lesions had been absorbed (Figure 1E), so antibiotics were discontinued. On the 144th day of follow-up, chest CT showed that the inflammatory lesions had basically resolved, though a few traces remained (Figure 1F).

3 Discussion

Aeromonas infection often occurs in people who come into contact with contaminated water or food, people with liver and biliary diseases, people with blood diseases and people with weakened immunity. More than 30 phenotypes of *Aeromonas* have been reported (13), among which *Aeromonas dhakensis* can cause purulent lesions. According to the previously reported cases (Table 2), most were out-of-hospital infections, the disease progressed rapidly, the 14-day mortality rate was high, and the cause of death was mostly bacteremia or systemic infection. These reported cases were all misjudged in the early diagnostic process based on routine biochemical tests and were eventually confirmed by etiological sequencing (6, 14, 16, 18). Pulmonary infection caused by *Aeromonas dhakensis* has rarely been reported.

The common pathogens of community-acquired pneumonia in patients with hematological malignancies were *fungi*,

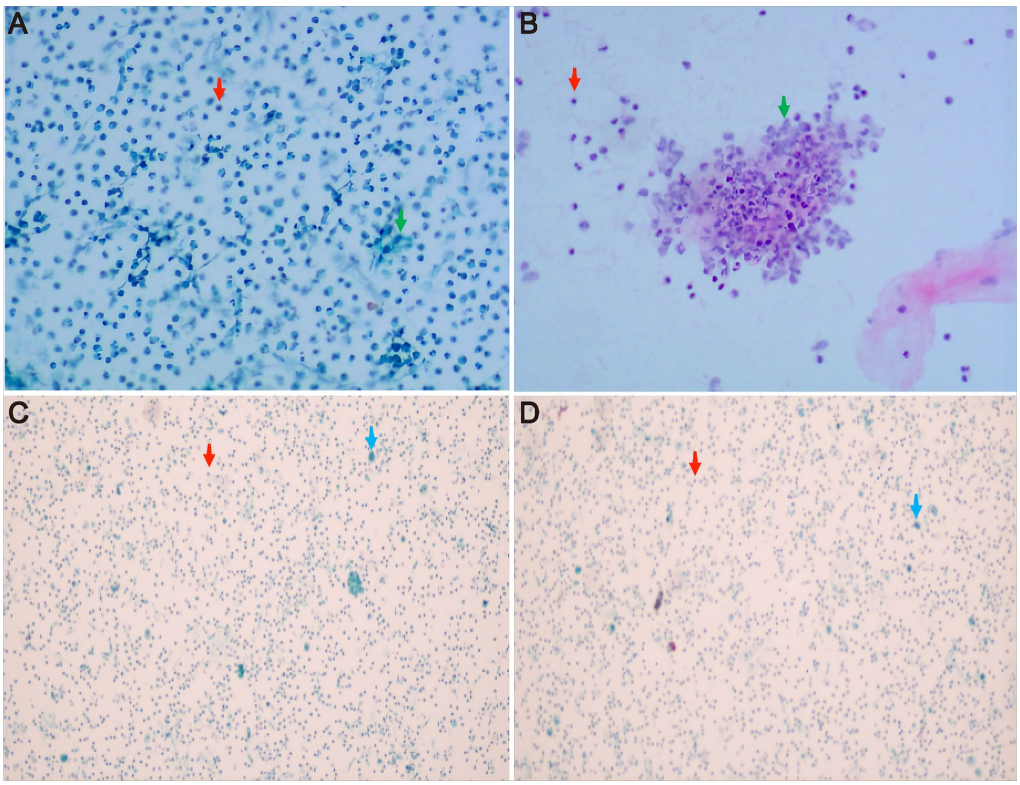

FIGURE 2
Cytological results of pleural fluid and alveolar lavage fluid by hematoxylin–eosin staining. **(A,B)** the pleural fluid Thinprep cytologic test showed inflammatory cells, with a small number of mesothelial cells and tissue cells, but no clear atypical tumor cells were observed. **(C,D)** alveolar lavage fluid under the microscope indicated ciliated columnar epithelial cells and inflammatory cells in the right middle lobe bronchial lavage fluid, but no clear atypical tumor cells were observed. The red arrow represents inflammatory cells, the green arrow shows mesothelial cells, and the blue arrow indicates ciliated columnar epithelial cells.

Mycobacterium tuberculosis, *Pseudomonas aeruginosa* and *Staphylococcus aureus*. Identification of pathogenic microorganisms occurs at least 24–48 h after admission, and empirical antibiotic treatment is one of the factors that leads to prolonged disease and then worsening infection (19, 20). *Aeromonas* is not a common opportunistic pathogen in patients with hematological malignancies. The patient in this case had no history of contact with fish or sewage, any history of travel, or any skin injuries before the onset of the disease. No significant therapeutic effect was achieved by the early empirical anti-infection treatment. After blood culture indicated the presence of *Aeromonas hydrophila*, we adjusted the antibiotic regimen to ceftazidime combined with moxifloxacin according to the drug sensitivity test results. Unfortunately, re-examination via chest CT indicated that the pulmonary infection had progressed. We wondered whether there was an undetected pathogen in the lungs or whether the pathogens were not fully covered by the original antibiotic regimen. To better identify the pathogen, the patient underwent bronchoalveolar lavage and pleural drainage, and the respiratory tract samples were subjected to mNGS by Vision Medicals (Guangzhou, China). Only *Aeromonas dhakensis* was detected in both bronchoalveolar lavage fluid and pleural effusion by mNGS, which was not consistent with the blood culture results. Traditional mNGS requires clinical presets to select DNA and/or RNA assay procedures, which may cause pathogen omission. We did mNGS with IDseq™ Ultra, which is a bidirectional enrichment technique (forward enrichment: multiple primers were designed to amplify the target pathogen; reverse enrichment: reducing the proportion of human cells or nucleic acids to the host) based on the combination of pathogen metagenomics and probe capture. It has the advantages of being comprehensive, sensitive and in depth. Some studies have shown that *Aeromonas dhakensis* can be misidentified as *Aeromonas hydrophila* by blood culture and subsequent phenotypic identification. According to the above data, the possibility of *Aeromonas hydrophila* and *Aeromonas dhakensis* coinfection cannot be ruled out. In addition, *Aeromonas* was not cultured from the pleural effusion, which may be due to differences in the *in vitro* and *in vivo* bacterial culture environments of the pleural effusion. Therefore, in clinical practice, when the anti-infective treatment regimen based on blood culture and corresponding drug sensitivity tests has not effectively improved the patient's condition, it is particularly important to combine mNGS to further discover evidence of etiological infection to guide diagnosis and treatment. Both *Aeromonas dhakensis* and *Aeromonas hydrophila* are *Aeromonas* strains, but the former is more virulent. It is important to use antibiotics that can cover *Aeromonas dhakensis* and *Aeromonas hydrophila*. We consulted the ABX guidelines and found that *Aeromonas* was sensitive to aminoglycosides, fluoroquinolones, cabapenem, aztreonam, and

TABLE 2 Previous reports of *Aeromonas dhakensis* infection.

First author	Year	Location	Number	Age	Gender	Risk factor/ comorbidity	Etiology	Position	Treatment	Mic	Prognosis
Chen et al. (3)	2013	China	7			Exposure to environmental water	rpoD and gyrB genes sequencing: *Aeromonas dhakensis*			/	
				33	Male	Flame burn		Multiple	Cefazolin, Gentamicin	/	Survival
				45	Male	Necrotizing fasciitis		Foot	Cefotaxime, Doxycycline	/	Survival
				47	Female	Trauma		Multiple	Nil	/	Survival
				62	Male	Necrotizing fasciitis		Foot	Cefazolin, Gentamicin	/	Survival
				67	Female	Surgical wound infection		Upper limb	Cephalexin	/	Survival
				74	Male	Necrotizing fasciitis		Lower limb	Ceftriaxone, Doxycycline	/	Survival
				75	Male	Cellulitis		Lower limb	Amoxicillin-clavulanic acid	/	Survival
Chang et al. (14)	2018	China	2				Blood or/and pus culture: *Aeromonas Hydrophila*. rpoD gene sequencing: *Aeromonas dhakensis*			/	
				65	Female	Dengue, Necrotizing Fasciitis		Bloodstream, left leg	Ceftazidime	/	Death
				75	Male	Dengue, Necrotizing Fasciitis		Bloodstream, lower limb	/	/	Death
Melo-Bolivar et al. (15)	2019	Australia	1	/	/	/	rpoB and gyrB genes sequencing: *Aeromonas dhakensis*	Necrotizing Fasciitis	/	/	Death
Huang et al. (16)	2019	China	1	29	Male	Snake headed fish, HBV	Blood culture and biochemical tests: *Aeromonas hydrophila*. The whole-genome sequencing: *Aeromonas dhakensis*	Bloodstream	Ceftriaxone Meropenem	≤1 ≤0.25	Death
Kitagawa et al. (6)	2019	Japan	4	57 to 90	2 males and 2 females	Solid cancer/ Obstructive Biliary disease/Surgical History	Blood culture and biochemical tests: *Aeromonas hydrophila, Aeromonas caviae,* and *Aeromonas jandaei*. rpoD and gyrB genes sequencing: *Aeromonas dhakensis*	Bloodstream	/	/	3 survived and 1 died
Sun et al. (17)	2021	China	26	/	/	/	Blood culture and biochemical tests: *Aeromonas hydrophila*. gyrB gene sequencing: *Aeromonas dhakensis*	Bloodstream	/	/	12 died or treatment failed

10.3389/fmed.2024.1357714

third-and fourth-generation cephalosporins (11). Related studies have shown that second-and third-generation cephalosporins (cefuroxime, ceftriaxone, and ceftazidime) and carbapenem antibiotics (imipenem) have higher minimum inhibitory concentrations and drug resistance rates against *Aeromonas dhakensis* than against *Aeromonas hydrophila*, while both bacteria are sensitive to fourth-generation cephalosporins (cefepime) and fluoroquinolone antibiotics (levofloxacin) (3, 8, 9). With the overuse of antibiotics in agriculture, fish culture and clinical environments, the resistance of *Aeromonas* to drugs has increased in recent years, and the prevalence of multidrug-resistant *Aeromonas* has been on the rise (7, 17). Furthermore, pathogenic *Aeromonas* species are reported to be resistant to carbapenems due to the presence of the *CphA* gene, which encodes a metallo-β-lactamases that hydrolyzes carbapenems but not fourth-generation cephalosporins (9, 12, 21). Chromosomal AmpC β-lactamases which species-specifically distributes in *Aeromonas* strains and included AsbA1 (*Aeromonas jandaei*), CepH and CepS (*Aeromonas hydrophila*), CAV1 and MOX (*Aeromonas caviae*), TRU-1 (*Aeromonas enteropelogenes*), and AQU-1 (*Aeromonas dhakensis*) (9, 19, 22–26), can hydrolyze cephamycins and third-generation cephalosporins (27, 28). Based on the above data, we selected a fourth-generation cephalosporin (cefepime) combined with a fluoroquinolone drug (levofloxacin), and the patient's symptoms and signs improved significantly. Compared with the deaths reported by Chang et al. and Huang et al. (14, 16), in which all patients received third-generation cephalosporin treatment immediately after admission but still died quickly, timely adjustment of the antibiotic to a fourth-generation cephalosporin in this case may have been critical to reduce the risk of death and improve the condition of the patient.

4 Conclusion

Aeromonas dhakensis is virulent and has potential drug resistance, which causes rapid progression of pulmonary infection. Because it is not common in the clinic, the diagnostic specificity is poor when the evidence is based only on the characteristics of symptoms and blood culture. Once the *Aeromonas* strain is cultured in the clinical work, the detected sample can be further subjected to mNGS for accurate diagnosis and improvement of the antibiotic regimen. Therefore, when specific antibiotics are selected for anti-infection treatment based on biological sample culture and the corresponding drug sensitivity tests, but the patient's condition still does not improve much, adding mNGS may identify the etiology and guide the choice of anti-infection therapy.

Data availability statement

The original contributions presented in the study are included in the article/supplementary material, further inquiries can be directed to the corresponding author.

Ethics statement

The studies involving humans were approved by the Ethics Committee of Zhengzhou University People's Hospital. The studies were conducted in accordance with the local legislation and institutional requirements. The participants provided their written informed consent to participate in this study. Written informed consent was obtained from the individual(s) for the publication of any potentially identifiable images or data included in this article.

Author contributions

CW: Conceptualization, Data curation, Formal analysis, Writing – original draft. NW: Data curation, Investigation, Writing – review & editing. MZ: Data curation, Methodology, Writing – original draft. XZ: Conceptualization, Writing – review & editing.

Funding

The authors declare that no financial support was received for the research, authorship, and/or publication of this article.

Conflict of interest

The authors declare that the research was conducted in the absence of any commercial or financial relationships that could be construed as potential conflict of interest.

Publisher's note

All claims expressed in this article are solely those of the authors and do not necessarily represent those of their affiliated organizations, or those of the publisher, the editors and the reviewers. Any product that may be evaluated in this article, or claim that may be made by its manufacturer, is not guaranteed or endorsed by the publisher.

References

1. Huys G, Kämpfer P, Albert MJ, Kühn I, Denys R, Swings J. *Aeromonas hydrophila* subsp. dhakensis subsp. nov., isolated from children with diarrhoea in Bangladesh, and extended description of *Aeromonas hydrophila* subsp. hydrophila (Chester 1901) Stanier 1943 (approved lists 1980). hydrophila (Chester 1901) Stanier 1943 (approved lists 1980). *Int J Syst Evol Microbiol*. (2002) 52:705–12. doi: 10.1099/00207713-52-3-705

2. Reclassification of Aeromonas hydrophila subsp. dhakensis Huys et al. 2002 and Aeromonas aquariorum Martínez-Murcia et al. 2008 as Aeromonas dhakensis sp. nov. comb nov. and emendation of the species Aeromonas hydrophila

3. Chen PL, Wu CJ, Chen CS, Tsai PJ, Tang HJ, Ko WC. A comparative study of clinical Aeromonas dhakensis and *Aeromonas hydrophila* isolates in southern Taiwan: *A.dhakensis* is more predominant and virulent. *Clin Microbiol Infect*. (2014) 20:O428–34. doi: 10.1111/1469-0691.12456

4. Fernández-Bravo A, Fort-Gallifa I, Ballester F, Pujol I, Gomez-Bertomeu F, et al. A case of *Aeromonas trota* in an immunocompromised patient with Diarrhea. *Microorganisms*. (2020) 8:399. doi: 10.3390/microorganisms8030399

5. Pérez L, Abarca ML, Latif-Eugenín F, Beaz-Hidalgo R, Figueras MJ, Domingo M. Aeromonas dhakensis pneumonia and sepsis in a neonate Risso's dolphin *Grampus griseus* from the Mediterranean Sea. *Dis Aquat Org*. (2015) 116:69–74. doi: 10.3354/dao02899

6. Kitagawa H, Ohge H, Yu L, Kayama S, Hara T, Kashiyama S, et al. Aeromonas dhakensis is not a rare cause of Aeromonas bacteremia in Hiroshima, Japan. *J Infect Chemother*. (2020) 26:316–20. doi: 10.1016/j.jiac.2019.08.020

7. Moreno-Sanchez F, Gomez-Gomez B. Antibiotic Management of Patients with hematologic malignancies: from prophylaxis to unusual infections. *Curr Oncol Rep*. (2022) 24:835–42. doi: 10.1007/s11912-022-01226-y

8. Xu C, Lin Q, Zhao Y, Zhu G, Jiang E, Li S, et al. Clinical characteristics and risk factors of Aeromonas bloodstream infections in patients with hematological diseases. *BMC Infect Dis*. (2022) 22:303. doi: 10.1186/s12879-022-07277-7

9. Chen PL, Lamy B, Ko WC. Aeromonas dhakensis, an increasingly recognized human pathogen. *Front Microbiol*. (2016) 7:793. doi: 10.3389/fmicb.2016.00793

10. Puah SM, Khor WC, Aung KT, Lau TTV, Puthucheary SD, Chua KH. Aeromonas dhakensis: clinical isolates with high carbapenem resistance. *Pathogens*. (2022) 11:833. doi: 10.3390/pathogens11080833

11. Johns Hopkins Division of Infectious Diseases Antibiotic Guide. Available at: http://www.hopkins-abxguide.org (Accessed 16 September 2002) (2002).

12. Xu C, Zhang T, Cai J, Yu Z, Qiu J, Yin J. Progress in regulatory mechanism for inducing β-lactamase in gram-negative bacteria. *Sheng Wu Gong Cheng Xue Bao*. (2018) 34:1288–96. doi: 10.13345/j.cjb.180187

13. Puah SM, Khor WC, Kee BP, Tan JAMA, Puthucheary SD, Chua KH. Development of a species-specific PCR-RFLP targeting rpo D gene fragment for discrimination of Aeromonas species. *J Med Microbiol*. (2018) 67:1271–8. doi: 10.1099/jmm.0.000796

14. Chang HL, Chen PL, Lin SY, Chen TC, Chang K, Ko WC, et al. Two fatal cases of Aeromonas dhakensis bacteremia and necrotizing fasciitis in severe dengue patients. *J Microbiol Immunol Infect*. (2018) 51:692–4. doi: 10.1016/j.jmii.2018.03.003

15. Melo-Bolivar JF, Sinclair HA, Sidjabat HE. Draft genome sequence of Aeromonas dhakensis, isolated from a patient with fatal necrotizing fasciitis. *Microbiol Resour Announc*. (2019) 8:e00009–19. doi: 10.1128/MRA.00009-19

16. Huang M, Chen H, Li C, Liu Y, Gan C, el-Sayed Ahmed MAEG, et al. Rapid fulminant progression and mortality secondary to Aeromonas dhakensis Septicemia with hepatitis B virus infection following the ingestion of snakehead fish in mainland China: a case report. *Foodborne Pathog Dis*. (2020) 17:743–9. doi: 10.1089/fpd.2019.2780

17. Sun Y, Zhao Y, Xu W, Fang R, Wu Q, He H, et al. Taxonomy, virulence determinants and antimicrobial susceptibility of Aeromonas spp. isolated from bacteremia in southeastern China. *Antimicrob Resist Infect Control*. (2021) 10:43. doi: 10.1186/s13756-021-00911-0

18. Murata M, Morinaga Y, Akamatsu N, Matsuda J, Uno N, Kosai K, et al. The rapid induction of carbapenem-resistance in an Aeromonas dhakensis blood isolate. *Jpn J Infect Dis*. (2016) 69:439–41. doi: 10.7883/yoken.JJID.2015.098

19. Wu CJ, Chen PL, Hsueh PR, Chang MC, Tsai PJ, Shih HI, et al. Clinical implications of species identification in monomicrobial Aeromonas bacteremia. *PLoS One*. (2015) 10:e0117821. doi: 10.1371/journal.pone.0117821

20. di Pasquale MF, Sotgiu G, Gramegna A, Radovanovic D, Terraneo S, Reyes LF, et al. Prevalence and Etiology of community-acquired pneumonia in immunocompromised patients. *Clin Infect Dis*. (2019) 68:1482–93. doi: 10.1093/cid/ciy723

21. Wu CJ, Ko WC, Lee NY, Su SL, Li CW, Li MC, et al. AeromonasIsolates from fish and patients in Tainan City, Taiwan: genotypic and phenotypic characteristics. *Appl Environ Microbiol*. (2019) 85:e01360–19. Published 2019 Oct 16. doi: 10.1128/AEM.01360-19

22. Alksne LE, Rasmussen BA. Expression of the AsbA1, OXA-12, and AsbM1 beta-lactamases in *Aeromonas jandaei* AER 14 is coordinated by a two-component regulon. *J Bacteriol*. (1997) 179:2006–13. doi: 10.1128/jb.179.6.2006-2013.1997

23. Avison MB, Niumsup P, Walsh TR, Bennett PM. *Aeromonas hydrophila* AmpH and CepH beta-lactamases: derepressed expression in mutants of *Escherichia coli* lacking creB. *J Antimicrob Chemother*. (2000) 46:695–02. doi: 10.1093/jac/46.5.695

24. de Luca F, Giraud-Morin C, Rossolini GM, Docquier JD, Fosse T. Genetic and biochemical characterization of TRU-1, the endogenous class C beta-lactamase from *Aeromonas enteropelogenes*. *Antimicrob Agents Chemother*. (2010) 54:1547–54. doi: 10.1128/AAC.01252-09

25. Fosse T, Giraud-Morin C, Madinier I, Labia R. Sequence analysis and biochemical characterisation of chromosomal CAV-1 (*Aeromonas caviae*), the parental cephalosporinase of plasmid-mediated AmpC 'FOX' cluster. *FEMS Microbiol Lett*. (2003) 222:93–8. doi: 10.1016/S0378-1097(03)00253-2

26. Wu CJ, Wang HC, Chen PL, Chang MC, Sunny Sun H, Chou PH, et al. AQU-1, a chromosomal class C β-lactamase, among clinical Aeromonas dhakensis isolates: distribution and clinical significance. *Int J Antimicrob Agents*. (2013) 42:456–61. doi: 10.1016/j.ijantimicag.2013.08.002

27. Bush K, Jacoby GA, Medeiros AA. A functional classification scheme for beta-lactamases and its correlation with molecular structure. *Antimicrob Agents Chemother*. (1995) 39:1211–33. doi: 10.1128/AAC.39.6.1211

28. Spiliopoulou I, Kazmierczak K, Stone GG. *In vitro* activity of ceftazidime/avibactam against isolates of carbapenem-non-susceptible Enterobacteriaceae collected during the INFORM global surveillance programme (2015-17). *J Antimicrob Chemother*. (2020) 75:384–91. doi: 10.1093/jac/dkz456

frontiers | Frontiers in Medicine

TYPE Case Report
PUBLISHED 09 May 2024
DOI 10.3389/fmed.2024.1357260

OPEN ACCESS

EDITED BY
Santi Nolasco,
University of Catania, Italy

REVIEWED BY
Yutaka Yoshii,
The Jikei University School of Medicine, Japan
Masoud Sadeghi,
Islamic Azad University, Iran

*CORRESPONDENCE
Jing Xia
✉ xiajing@kmmu.edu.cn

RECEIVED 17 December 2023
ACCEPTED 15 April 2024
PUBLISHED 09 May 2024

CITATION
Li WZ, Liu S, Luo JL and Xia J (2024) Pulmonary alveolar microlithiasis combined with gastric mucosal calcification: a case report. *Front. Med.* 11:1357260. doi: 10.3389/fmed.2024.1357260

Pulmonary alveolar microlithiasis combined with gastric mucosal calcification: a case report

Wen-Zhuo Li[1], Shuo Liu[2], Ji-Li Luo[2] and Jing Xia[2]*

[1]Yunnan Cancer Hospital, Kunming, China, [2]The First Affiliated Hospital of Kunming Medical University, Kunming, Yunnan, China

Background: Pulmonary alveolar microlithiasis (PAM) is a rare disease whose clinical and imaging manifestations are non-specific, characterized by the deposition of microliths, which primarily consist of calcium and phosphorus, within the alveoli. In the cases of PAM, patients combined with calcification of other organs such as gastric mucosal calcification are less common.

Case presentation: A 59-year-old woman was admitted to our hospital due to cough producing white, foamy sputum, accompanied by dyspnea and fever for 20 days. The CT scan showed diffuse ground-glass opacities and calcification of the gastric mucosa. Lung tissue biopsy revealed the presence of calcification and granulomatous foreign bodies in the interstitium and alveolar cavity. In the later stages, she developed painful skin petechiae. For this patient, the diagnosis of PAM, gastric mucosal calcification, and purpura fulminans was made. However, the genetic test results hinted that the patient and her son had a heterozygous mutation in the *FBN1* gene, but her daughter's genetic test results were normal. Although the patient received anti-infection treatment, steroids, and oxygen therapy, her condition did not improve.

Conclusion: We reported a rare case of PAM combined with calcification of other organs and purpura fulminans. Treatment of steroids did not show any benefit. The causative mechanism and effective treatment of this disease remain unclear. More treatments need to be explored.

KEYWORDS

pulmonary alveolar microlithiasis, PAM, gastric mucosal calcinosis, case report, *FBN1*

Background

Pulmonary alveolar microlithiasis (PAM) is an unusual disease that leads to the accumulation of calcium phosphate microliths throughout the interstitium and alveolar cavity (1, 2). The prevalence of PAM is likely <1 per million. PAM may have no obvious symptoms in its early stages and is detected incidentally by lung imaging. As the lung condition progresses, non-specific manifestations such as cough, dyspnea, and hemoptysis may develop. In a few cases, extrapulmonary organs are involved, with the genitalia being more common, along with other organs such as the kidneys, heart valves, and gallbladder (3, 4). The differentiation of PAM from other calcifying diseases is rather complex. Currently, no definite and effective treatment plan for PAM exists, and most treatment approaches are supportive.

Here, we report the case of a 59-year-old woman diagnosed with PAM using lung tissue biopsy and presented with calcification of gastric mucosa and painful purpura fulminans.

Case presentation

A 59-year-old woman was admitted to our hospital on June 2021 because of cough producing white, foamy sputum, accompanied by dyspnea and fever for 20 days. The local hospital considered interstitial pneumonia, and the symptoms did not resolve even after an antiinfective treatment with cefoperazone sodium sulbactam and meropenem for 2 weeks, so she was transferred to our hospital. Lung auscultation showed rales in both lungs. The patient's body temperature rose to 38.5°C. Computed tomography (CT) scan revealed severe diffuse ground-glass opacities (Figure 1), calcification of heart valves (Figure 2), and gastric mucosa (Figure 2). The patient's procalcitonin (PCT) and C-reactive protein (CRP) levels were within the normal range. Based on the patient's symptoms, serological indicators, and imaging presentation, a viral or atypical pathogenic infection was considered. Therefore, she received empirical antiinfective treatment with ganciclovir, moxifloxacin, sulfamethoxazole, and caspofungin. Other treatments included oxygen therapy combined with the prone position and steroids. Her body temperature fluctuated between 37°C- and 37.5°C after 7 days of treatment. However, she still complained of dyspnea and skin pain, followed by the appearance of herpes and petechiae (Figure 3). The CT scan of her lungs did not improve and showed a high-density shadow resembling calcification. To make a definitive diagnosis, we improved relevant inspections. Lung tissue biopsy showed the presence of crystalline materials with calcification and granulomatous foreign bodies in the interstitium and alveolar cavity (Figure 4). Skin biopsy showed purpura fulminans.

Considering that organ calcification may be related to tumors, organ transplantation, renal failure, hyperparathyroidism, abnormal calcium and phosphorus metabolism, and so on, we conducted an etiological search. She did not have a history of organ transplantation, gastric tumor, hypervitaminosis A, or the use of sucralfate. Her creatinine was 75.5 umol/L and her urine output was normal, so renal failure was ruled out. The patient's blood calcium ion level was 2.3 mmoml/L, and blood phosphorus ion level was 1.2 mmol/L, which were within the normal range, so parathyroid disease was not considered. Magnetic resonance imaging (MRI) did not show osteoporosis. Her parents were not consanguineously married, and her siblings had no similar symptoms. However, she said that she had a history of transient elevated calcium levels, the details of which were not clear, which might be a clue.

Based on her symptoms and test results, she showed strong indications for PAM, gastric mucosal calcinosis (GMC), and purpura fulminans. Since the disease was associated with a genetic mutation for which there was no effective treatment, we recommended her to undergo genetic testing. However, the genetic test results showed that the patient and her son had a heterozygous mutation in the *FBN1* gene, and sequence 4,163 of the cDNA in the coding region of exon 34 on chromosome 15 was changed from C base to T, thus changing the amino acid GCG (arginine R) to GTG (histidine H) (Figure 5), while her daughter's results were normal. Her 29-year-old son did not show clinical symptoms such as cough or dyspnea, and a CT scan of the lungs did not reveal any abnormalities. The patient did not receive specific medicine interventions (i.e., etidronate, sodium thiosulfate) and then chose to be discharged. During follow-up, the patient showed no improvement in lung imaging and developed hypocalcemia. A partial debridement of the patient's necrotic skin was performed, followed by a skin grafting procedure (Figure 3C).

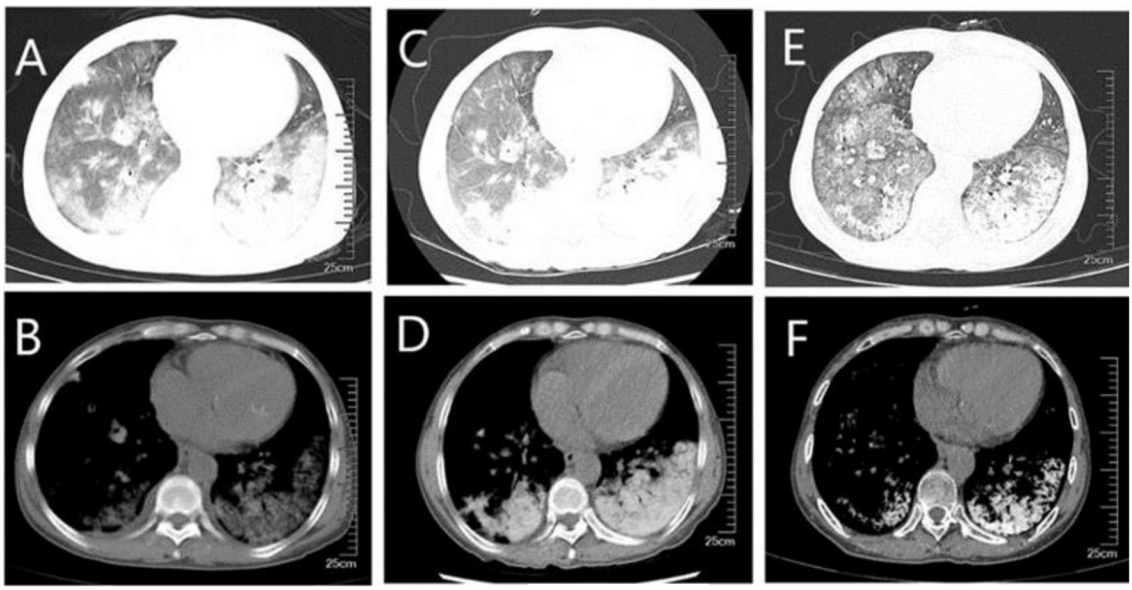

FIGURE 1
CT of the lungs **(A, B)** diffuse ground-glass shadow and high-density shadow in both lungs were seen in the lung window and mediastinal window when the patient was first admitted to the hospital; **(C, D)** higher density was seen on repeat CT after a period of treatment; **(E, F)** higher density shadow was still seen on repeat CT before discharge, although the ground-glass shadow was absorbed.

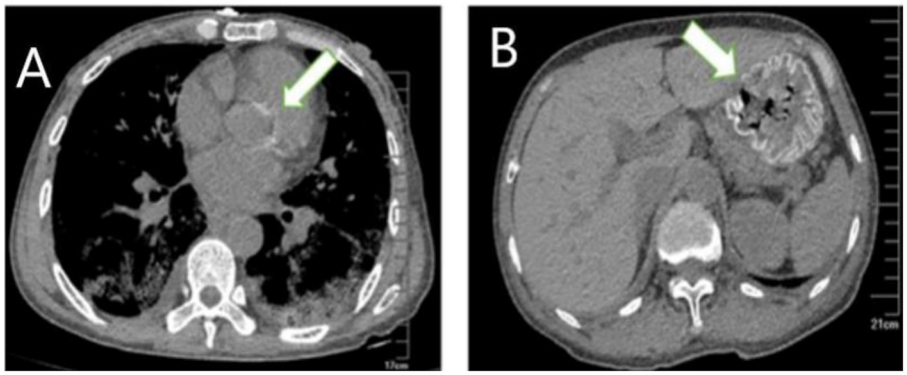

FIGURE 2
Extrapulmonary organ calcification **(A)** cardiac valve calcification; **(B)** Gastric mucosal calcification.

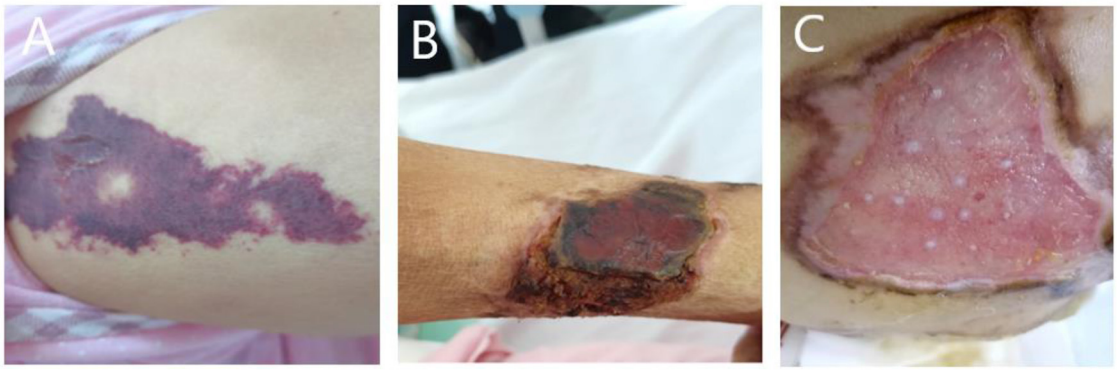

FIGURE 3
(A) Painful skin followed by herpes and purpura; **(B)** follow-up skin condition. **(C)** Patient's buttocks after skin grafting.

Discussion

Calcium deposition of organs and tissue may be metastatic, dystrophic, iatrogenic, and idiopathic in etiology (3, 5). Metastatic calcification is the most frequent subtype in which calcification in normal tissues is caused by hypercalcemia or hyperphosphatemia. Dystrophic calcification occurs as calcium deposition in fibrotic or inflamed tissue without abnormal metabolism of calcium and phosphorus. Iatrogenic calcification is a direct result of pharmacological or therapeutic interventions. Idiopathic calcification occurs in normal tissue without serum biochemical abnormalities. The kidneys and lungs are the preferred sites of calcification, mainly due to the relative intracellular alkalinity (6). Calcinosis rarely occurs in the stomach (GMC) (5). However, our patient did not have a clear history of the abovementioned diseases that could have caused organ calcification.

PAM is a rare lung disease usually caused by a mutation in the *SLC*34A2 gene encoding type IIb sodium phosphate cotransporter called NPT2b (2). There is no literature suggesting that the disease is caused by mutations in other genes (4). However, in this case, the patient had a mutation in the *FBN1* gene. The primary function of the *FBN1* gene is to encode fibrillin-1, which causes it to polymerize into microfibrils in connective tissue, forming the tissue-specific structural framework (7). The mutation was reported more frequently in patients with Marfan syndrome (MFS) (8), which is

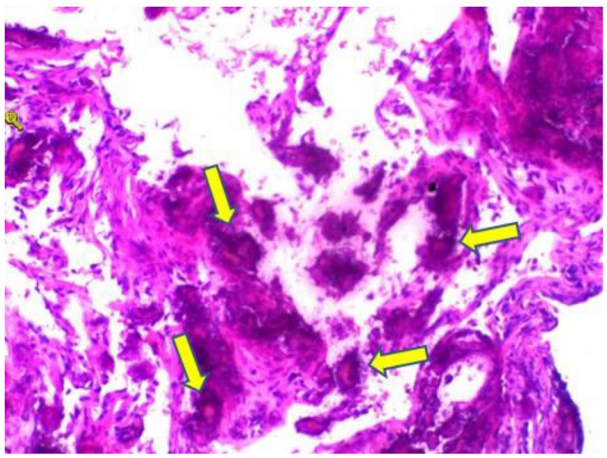

FIGURE 4
Hematoxylin and eosin stain sections of lung tissue biopsy showing crystalline materials with calcification and foreign body (arrows) granulomas in the interstitium and alveolar cavity (×100).

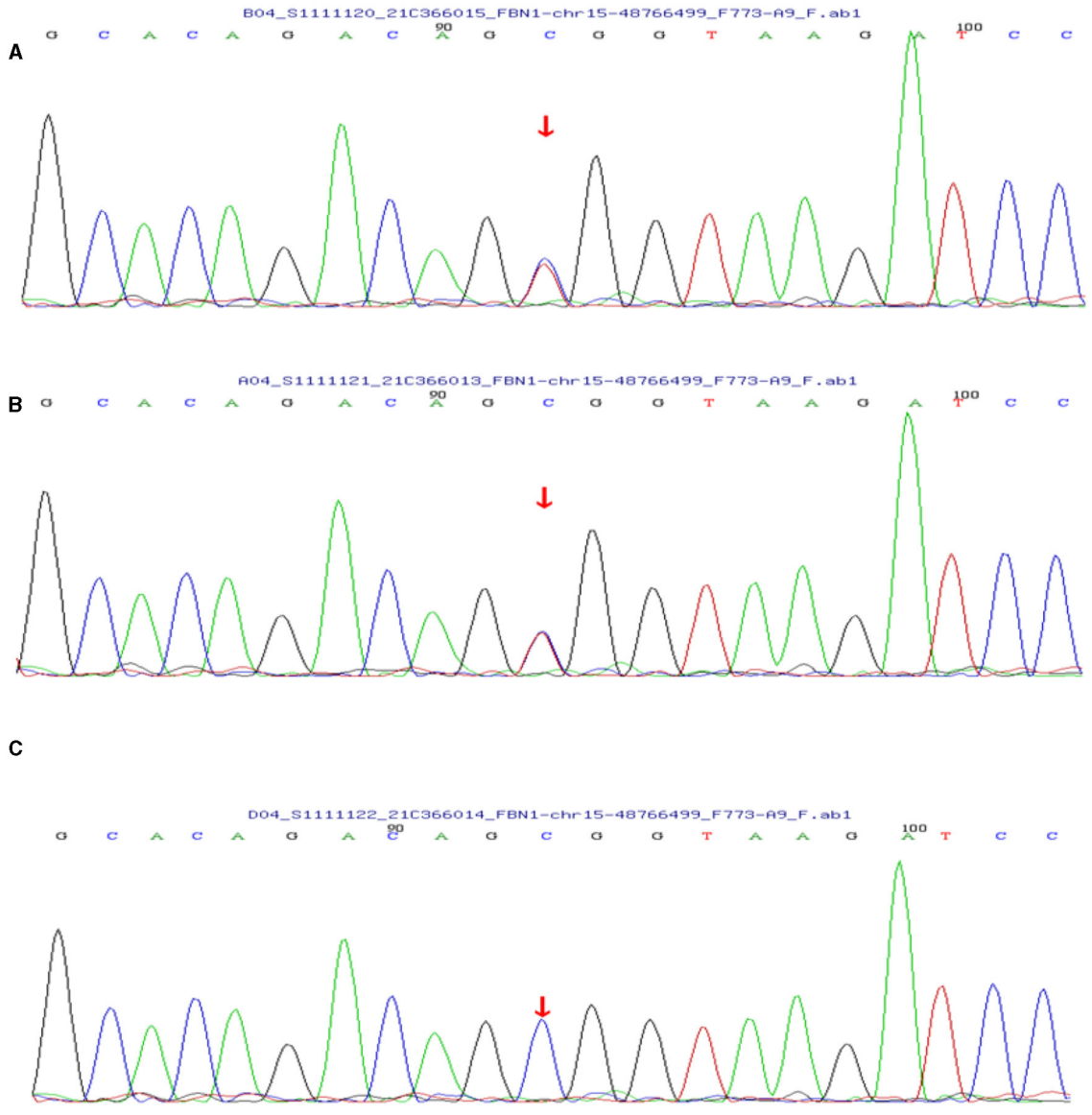

FIGURE 5
(A) The patient's genetic test results suggested a mutation in the *FBN1* gene. **(B)** Her son's test results also showed a mutation in the *FBN1* gene. **(C)** Her daughter's results were normal.

a relatively common genetic disorder of connective tissue (1 in 3,000–5,000) with different clinical features in the musculoskeletal, cardiovascular, and ocular systems (7). Calcification in patients with MFS usually occurs in connective tissues such as the aorta and heart valves, but alveolar calcification has not been reported (9). The patient and her family did not have symptoms associated with MFS but rather presented with multiorgan calcification as well as skin lesions, which were rarely reported. The two major building blocks of fibrillin-1 are the calcium-binding epidermal growth factor-like domain (cbEGF) and the transforming growth factor-binding protein-like domain (TB or 8-Cys) (10). Most mutations reported to date affect residues of the calcium-binding common sequence, resulting in an incomplete calcium-binding protein structural domain and reduced calcium-binding capacity of cbEGF (11). Although organ calcium deposition caused by mutations in the *FBN1* gene has been rarely reported, this mutation may be a potential mechanism for the development of multiorgan calcification in this patient.

Most patients with PAM are asymptomatic at diagnosis. As the disease progresses, dyspnea often develops along with cough, chest pain, hemoptysis, and pneumothorax, which are non-specific. Over time, adult patients often experience deterioration in lung function, and respiratory failure due to chronic cor pulmonale is the leading cause of death (12). In this case, the patient's main symptoms were cough and dyspnea with nasal cannula oxygenation, and oxygen saturation was maintained at 92%. No changes in cardiac structure or function were noted, so she was still in the early stages of the disease. The diagnosis of PAM is usually confirmed by radiological and histopathological features. High-resolution computed tomography typically shows diffuse

hyperdense micronodules, which are most widely located in the middle and lower lung lobes just like this patient (10). In some cases, the calcified areas of the lungs are more extensive, which is called a sandstorm-like pattern, and even a black pleural line will appear between the lung parenchyma and the ribs (12, 13). In addition, calcification of extrapulmonary tissues, such as gastric mucosal and cardiac valve, was observed in this case, which was not reported in other cases. Microliths visible in alveolar lavage fluid or lung biopsy are necessary for a definitive diagnosis, while detection of genetic mutations is not necessary for the diagnosis. Treatments reported in the past included bisphosphonates, corticosteroids, sodium thiosulfate, and low-phosphorus diets, but none have been reported to be effective. Lung transplantation in advanced stages of PAM may be a potential treatment.

In this case, we suggest that PAM belongs in metastatic calcification or idiopathic calcification. Although calcium and phosphorus levels were normal upon admission, the patient had a history of transiently elevated calcium levels during follow-ups, which was not taken seriously and left untreated. Iatrogenic calcification and dystrophic calcification were excluded because she did not use pharmacological or therapeutic interventions of calcium, and antibacterial drugs did not reduce symptoms or improve imaging performance. Corticosteroid therapy did not affect this case. It is also not known how the patient's electrolyte levels will change as the disease progresses.

Conclusion

PAM is already a rare disease, and there is even less literature on the combination of GMC and skin lesions. The causative mechanism of PAM remains unclear, and it may be a common manifestation of multiple diseases. At present, no effective medical therapy for PAM exists; nevertheless, lung transplantation can be an effective treatment option for end-stage patients with grave respiratory deficiency. More studies are needed to help understand the risk factors, pathogenic mechanism, treatment methods, and outcome of PAM.

Data availability statement

The original contributions presented in the study are included in the article/supplementary material, further inquiries can be directed to the corresponding author.

Ethics statement

Ethical approval was not required for the studies involving humans because this study is a case report, a single case observational study, and the informed consent of the patient was obtained. The studies were conducted in accordance with the local legislation and institutional requirements. The human samples used in this study were acquired from a by-product of routine care or industry. Written informed consent to participate in this study was not required from the participants or the participants' legal guardians/next of kin in accordance with the national legislation and the institutional requirements. Written informed consent was obtained from the individual(s) for the publication of any potentially identifiable images or data included in this article.

Author contributions

W-ZL: Writing – original draft, Writing – review & editing. SL: Methodology, Writing – review & editing. J-LL: Investigation, Writing – review & editing. JX: Investigation, Writing – review & editing.

Funding

The author(s) declare that no financial support was received for the research, authorship, and/or publication of this article.

Conflict of interest

The authors declare that the research was conducted in the absence of any commercial or financial relationships that could be construed as a potential conflict of interest.

Publisher's note

All claims expressed in this article are solely those of the authors and do not necessarily represent those of their affiliated organizations, or those of the publisher, the editors and the reviewers. Any product that may be evaluated in this article, or claim that may be made by its manufacturer, is not guaranteed or endorsed by the publisher.

References

1. Shaw BM, Shaw SD, Mccormack FX. Pulmonary alveolar microlithiasis. *Semin Respir Crit Care Med.* (2020) 41:280–7. doi: 10.1055/s-0040-1702211

2. Kosciuk P, Meyer C, Wikenheiser-Brokamp KA, McCormack FX. Pulmonary alveolar microlithiasis. *Eur Respir Rev.* (2020) 29:200024. doi: 10.1183/16000617.0024-2020

3. Proesmans M, Boon M, Verbeken E, Ozcelik U, Kiper N, Van de Casseye W, et al. Pulmonary alveolar microlithiasis: a case report and review of the literature. *Eur J Pediatr.* (2012) 171:1069–72. doi: 10.1007/s00431-012-1678-8

4. Castellana G, Castellana G, Gentile M, Castellana R, Resta O. Pulmonary alveolar microlithiasis: review of the 1022 cases reported worldwide. *Eur Respir Rev.* (2015) 24:607–20. doi: 10.1183/16000617.0036-2015

5. Garber A, Arora Z, Welch N, Lapinski J, Burke CA. Extraosseous calcification of the esophagus: clinicopathologic correlates of esophageal mucosal calcinosis. *ACG Case Rep J.* (2017) 4:e108. doi: 10.14309/crj.2017.108

6. Kosuru V, Mohammed A, Kapoor R, Jhaveri K, Medepalli V, Mulloy L, et al. Metastatic Calcinosis of Gastric Mucosa. *J Investig Med High Impact Case Rep.* (2020) 8:2324709620940482. doi: 10.1177/2324709620940482

7. Sakai LY, Keene DR, Renard M, De Backer J. FBN1: The disease-causing gene for Marfan syndrome and other genetic disorders. *Gene.* (2016) 591:279–91. doi: 10.1016/j.gene.2016.07.033

8. Dietz HC, Pyeritz RE. Mutations in the human gene for fibrillin-1 (FBN1) in the Marfan syndrome and related disorders. *Hum Mol Genet.* (1995) 4:1799–1809. doi: 10.1093/hmg/4.suppl_1.1799

9. Wanga S, Hibender S, Ridwan Y, van Roomen C, Vos M, Van Der Made I, et al. Aortic microcalcification is associated with elastin fragmentation in Marfan syndrome. *J Pathol.* (2017) 243:294–306. doi: 10.1002/path.4949

10. Robinson PN, Arteaga-Solis E, Baldock C, Collod-Béroud G, Booms P, De Paepe A, et al. The molecular genetics of Marfan syndrome and related disorders. *J Med Genet.* (2006) 43:769–87. doi: 10.1136/jmg.2005.039669

11. Dietz HC, McIntosh I, Sakai LY, Corson GM, Chalberg SC, Pyeritz RE, et al. Four novel *FBN1* mutations: significance for mutant transcript level and EGF-like domain calcium binding in the pathogenesis of Marfan syndrome. *Genomics.* (1993) 17:468–75. doi: 10.1006/geno.1993.1349

12. Nawawi YS, Soewondo W. A case report of pulmonary alveolar microlithiasis: focus on radiologic findings. *Am J Case Rep.* (2023) 24:e938456–1. doi: 10.12659/AJCR.938456

13. Ufuk F. Pulmonary alveolar microlithiasis. *Radiology.* (2021) 298:567. doi: 10.1148/radiol.2021203272

frontiers | Frontiers in Medicine

TYPE Case Report
PUBLISHED 12 June 2024
DOI 10.3389/fmed.2024.1380236

OPEN ACCESS

EDITED BY
Daniel Prantner,
University of Maryland, United States

REVIEWED BY
Jeffrey Don McBride,
University of Oklahoma Health Sciences Center, United States
Tomoyuki Mukai,
Kawasaki Medical School, Japan

*CORRESPONDENCE
Yasuo Shimizu
✉ yasuo-s@dokkyomed.ac.jp

RECEIVED 01 February 2024
ACCEPTED 20 May 2024
PUBLISHED 12 June 2024

CITATION
Shimizu Y, Kushima Y, Tanaka A, Takemasa A, Ishida K and Niho S (2024) Pulmonary granulomas confirmed in Blau syndrome using TBLC specimens: Case report.
Front. Med. 11:1380236.
doi: 10.3389/fmed.2024.1380236

Pulmonary granulomas confirmed in Blau syndrome using TBLC specimens: Case report

Yasuo Shimizu[1,2,3]*, Yoshitomo Kushima[1], Ayae Tanaka[4], Akihiro Takemasa[1,2], Kazuyuki Ishida[5] and Seiji Niho[1]

[1]Department of Pulmonary Medicine and Clinical Immunology, Dokkyo Medical University, Mibu, Tochigi, Japan, [2]Respiratory Endoscopy Center, Dokkyo Medical University Hospital, Mibu, Japan, [3]Center of Regenerative Medicine, Dokkyo Medical University Hospital, Mibu, Japan, [4]Department of Rheumatology, Dokkyo Medical University, Mibu, Japan, [5]Department of Diagnostic Pathology, Dokkyo Medical University, Tochigi, Japan

Blau syndrome (BS), is an autoinflammatory granulomatosis disease characterized by a distinct triad of skin, joint, and eye disorders similar to those of sarcoidosis, but the lung involvement frequently observed in sarcoidosis are rare. Granulomas from patients with BS displayed a distinct morphology indicating an exuberant chronic inflammatory response. Patients with BS may have granulomatous lung lesions, which require early diagnosis. To determine whether therapeutic intervention is needed for lung lesions, examining transbronchial lung cryobiopsy specimens and accumulating cases of BS with lung involvement could be contributed to improving BS management in the future.

KEYWORDS

***NOD2*, cryobiopsy, lung, sarcoidosis, granulomas, Blau syndrome, bronchoscopy, interstitial lung disease**

Introduction

Juvenile sarcoidosis, known as Blau syndrome (BS), is an autoinflammatory granulomatosis disease characterized by a distinct triad of skin, joint, and eye disorders (1). Nucleotide-binding oligomerization domain 2 (*NOD2)* has been identified as the gene responsible for this disease, and the autosomal dominant or sporadic gene mutations induce autoactivation of nuclear factor kappa B (2).

The symptoms of BS are similar to those of sarcoidosis, but the lymphadenopathy and lung involvement frequently observed in sarcoidosis are rare, and the first case of interstitial lung disease in BS was reported in 2007 (3). In the present case, the patient had early-onset BS at the age of 2 years, and the M513T mutation in the *NOD2* was identified and previously reported (2). Transbronchial lung cryobiopsy (TBLC) was performed on the tiny but diffuse granular shadows in the lungs, and pathological examination of the specimens confirmed the granulomas. There have been very few reports of lung lesions in BS, and to date, no report has pathologically proven granulomas in the lung and adult-onset lung granulomas in BS.

Case presentation

Herein, a 22-years-old man was referred to our department for the examination of extensive bilateral lung granular shadows. On admission to receive TBLC, the vital signs of the patient were body temperature of 36.3°C, regular pulse of 75 bpm, SpO_2 of 99% in room air, and auscultation for the heart and lungs was normal. He had been having dry cough for 3 months before bronchoscopic examination (the day X-3M) (Figure 1), and painful swelling of the right knee and right wrist, and diffuse tiny scaly erythematous in abdomen, back and extremities of cutaneous with mild pigmentation, were accompanied with emergence of cough.

Laboratory examination revealed a normal range of leukocytes (4800 cells/μL) and fraction of neutrophils (56%), eosinophils (2.9%), basophils (1.0%), monocytes (16.9%), and lymphocytes (23.2%), but elevated angiotensin-converting enzyme (33.4 U/L), soluble interleukin 2 receptor (3440 U/ml), and matrix metalloproteinase-3 (233 ng/ml). The electrocardiogram showed incomplete right bundle branch block, spirometry showed a normal range of forced vital capacity (83.7%), forced expiratory volume in 1 second (83.1%), and DLCO (84.6%). Chest X-rays and CT scans showed diffuse fine granular shadows extending into the bilateral lungs (Figures 2A–C) and minor swelling of the mediastinal lymph nodes (Figure 2D).

The patient was treated with prednisolone (5–10 mg/day) and human IgG1 monoclonal antibody specific for tumor necrosis factor-α (TNF-α, adalimumab) at a dose of 40 mg once every two weeks, which was introduced 2 years ago to treat arthritis and reduce the adverse effects of steroids. Differential diagnosis for granular shadows in the bilateral lungs suggested fungal and acid-fast bacillus infections, drug-induced granulomatosis, lymphoma, vasculitis, and granulomas due to BS.

Bronchoscopy was performed on the lesions of the lung field and mediastinal lymph nodes on day X (Figure 1). The lumen of the main bronchus showed reticulated dilation of the capillaries, appearing like sarcoidosis. Bronchoalveolar lavage fluid (BALF) was collected from the left B^5a, and 101/150 mL of lavage was recovered. The cell fraction of BALF was predominantly lymphocytes (87%), and the CD4/8 ratio was not elevated (0.97). Transbronchial needle biopsy (TBNA) was performed on longitudinal lymph nodes #7 and #2R, where access was feasible. TBLC was performed on right B^8a, right B^4a, and right B^3a. In a previous report, granulomas from patients with BS displayed a distinct morphology characterized by large polycyclic granulomas with dense lymphocytic coronas, forming a large granulomatous complex without inter granulomatous sclerosis, indicating an exuberant chronic inflammatory response (4). In the present case, specimens obtained by TBLC were sufficiently large to observe complex of granulomas and inter granulomas, and those specimens showed non-caseating epithelioid granulomas scattered around the alveolar septum, bronchi, and vessels forming a large granulomatous complex without inter granulomatous sclerosis at low magnification (Figure 3A). At high magnification, prominent epithelioid cells and multinucleated giant cells around bronchioles were observed, similar to previous reports on polycyclic granuloma observed in lymph nodes or skin biopsy specimens from BS patients (4), but in the present case, they were not seen in granulomas with dense lymphocytic coronas (Figure 3B). TBNA specimens contained epithelioid cells. The cultures of cells obtained from saline for washing needle of TBNA and for probe of TBLC, BALF and an aspirated sputum sample through bronchoscopy did not reveal bacterial or fungus infections and mycobacterial infection by Ziehl-Neelsen stain and culture using mycobacterium growth indicator tube (MGIT) system. Based on clinical, hematological, and pathological findings, the lung lesions were diagnosed as pulmonary granulomas caused by BS. While an additional dose of prednisolone was considered for the therapy of cough and lung lesions, taking into account the lack of SpO2 decrease, the patient's young age, the increased risk of adverse effects from additional prednisolone, the absence of infection and also the possibility of spontaneous resolution of granulomatous lesions, the patient was followed up for 2 months without escalating dose of prednisolone or additional immunosuppressant. Celecoxib, a cox-2 inhibitor, was additionally administered for arthralgia of the knees and wrists, and arthralgia was alleviated. Cough gradually decreased spontaneously subsequent two months (X+2M), and chest X-ray also showed a slight improving. However, after four months form bronchoscopic examination (X+4M), right knee and right wrist, proximal interphalangeal (PIP) joint pain and metacarpophalangeal (MP) joint pain were aggravated again. Since chief complaint of the patient was joint pain and prednisolone and methotrexate (MTX) and/or azathioprine were recommended for pulmonary sarcoidosis (5), MTX 4mg/2weeks was started for the arthralgia. The dose was subsequently increased, and pain was under control. No adverse effects due to MTX have appeared. Despite worsening arthralgia on the day X+4, cough and the lung lesions have remained without recurrence, and those were no subsequent deterioration. Changes in serum angiotensin converting enzyme (ACE) and soluble interleukin-2 receptor (sIL-2R) levels appeared to reflect well the manifestation of cough and lung lesions and their subsequent resolution (Figure 1).

Discussion

Blau syndrome is characterized by dermatitis, arthritis, and uveitis related to *NOD2* mutation, but in recent years, granulomatous lesions other than the triad of BS have also been considered as a phenotype of BS (3). The background of the manifestation of lung lesions in this patient was speculated from three aspects. The first was whether the frequency of pulmonary lesions differed depending on the type of NOD2 mutations, the second was whether there was a trigger for enhancing *NOD2* pathway activation, and the third was whether there were triggers for pulmonary lesion formation observed in adult sarcoidosis. First, BS patients who have been reported to having pulmonary lesions with *NOD2* mutation were a 23-years-old male with amino acid substitution Glu498Gly (not R334Q, R334W and L489F) (6), a six-teen-years-old male with R334 Q (3), a two-years-old and 7 months boy with pulmonary hemorrhage due to bronchial granuloma with the R334Q, a two-years-old boy with R334W and a nineteen-year-old male of this presenting with M513T. R334W is most common in BS and R334Q is also frequent but M513T is less frequent in BS (7). The activation levels of NF-κb by NOD2 mutations are similar among R334Q, R334W and M513T (7). In terms of these, it is not possible to determine the mutation that predispose

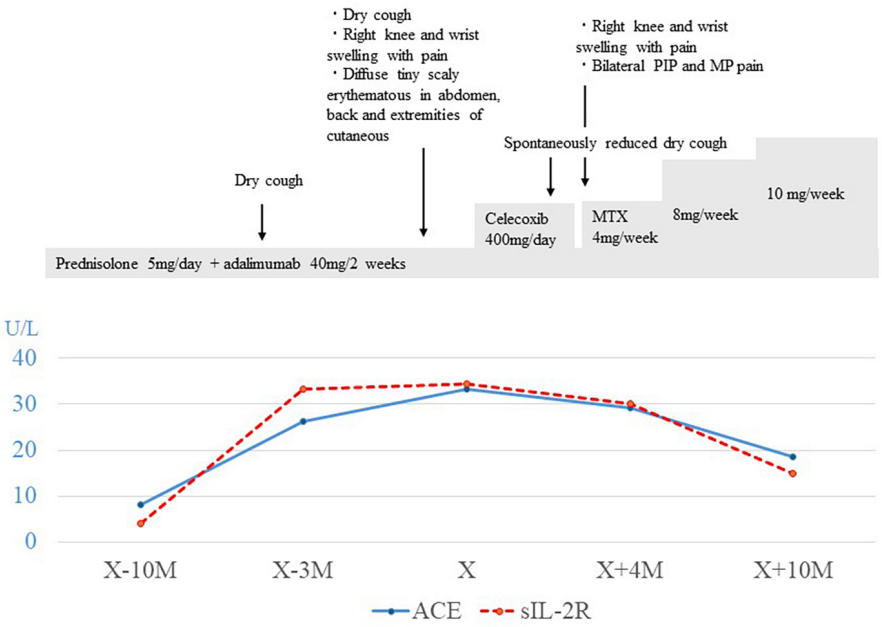

FIGURE 1
Clinical and treatment course. X indicated the day of bronchoscopic examination was performed, and X-10M indicated the day of 10 month (M) before the day of bronchoscopic examination was performed. Changes in serum levels of angiotensin converting enzyme (ACE) and soluble interleukin-2 receptor (sIL-2R) were in blue line and red-dot line, each. PIP, proximal interphalangeal; MP, metacarpophalangeal; MTX, Methotrexate.

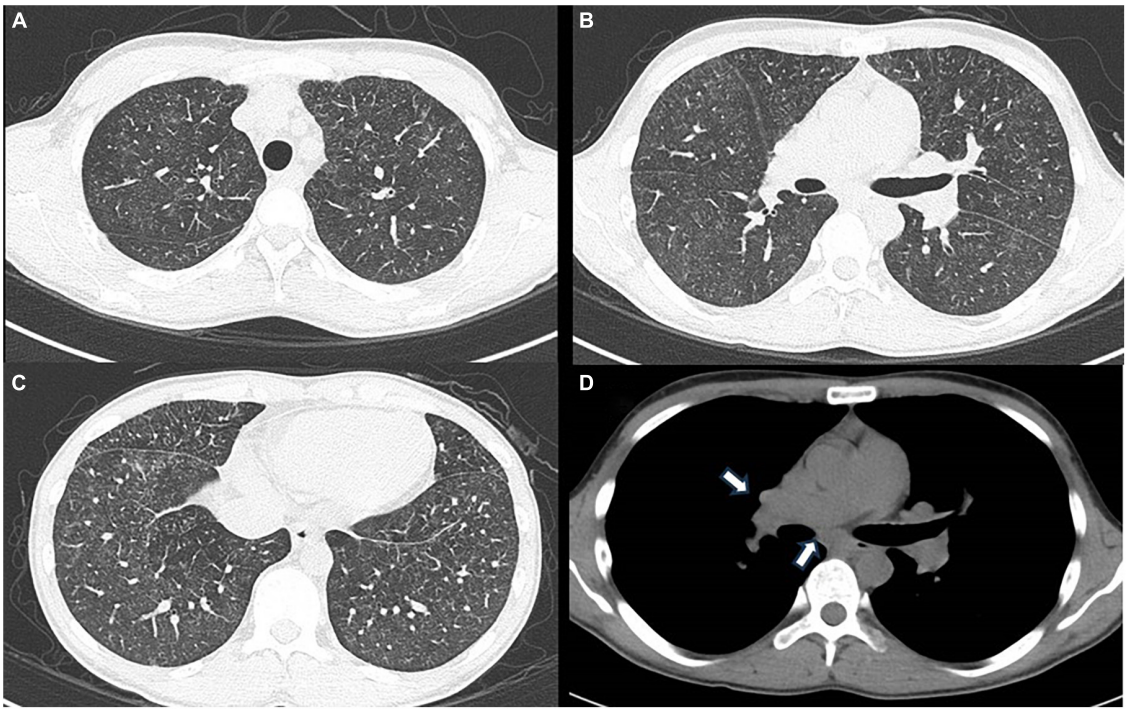

FIGURE 2
(A) Chest computed tomography using the lung window setting shows diffuse ground-glass shadows presumed to be fine nodules in the bilateral upper lobes, **(B)** middle and lingular lobes, **(C)** and bilateral lower lobes. **(D)** Chest computed tomography using the mediastinum window setting shows minor swelling of mediastinal lymph nodes, indicated by white arrows.

to pulmonary lesions in BS. Second, NOD2 mutation leads to autoactivation of NF-κb, but external factors might further amplify the activation of the pathway from *NOD2* to NF-κb. *NOD2* is activated by muramyl-dipeptide MurNAc-L-Ala-D-isoGln (MDP), a conserved proteoglycan (PGN) found in almost all bacteria and also mycobacterium tuberculosis activates via MDP. Single

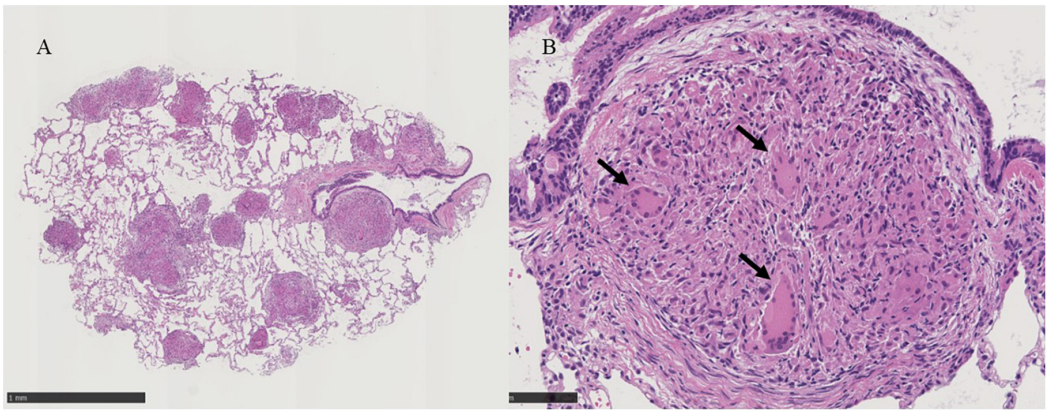

FIGURE 3
(A) Histological examinations of the lung tissue obtained by transbronchial lung cryobiopsy show non-caseating epithelioid granulomas scattered around the alveolar septum, bronchi, vessels and large complex of granulomas without inter granulomatous sclerosis at X30 magnification, black scale bar = 1mm. **(B)** Prominent epithelioid cells and multinucleated giant cells around bronchioles are indicated by black arrows in the panel at X200 magnification, black scale bar = 100 μm.

strand RNA virus including influenza A or RS virus induce NOD2 expression (8). In the presenting patient, there was no tuberculosis or influenza infection at the emergence of the pulmonary lesions, but RS virus infection was not examined, so the involvement of RS virus infection could not be ruled out as a trigger for developing lung lesions in present case. BCG vaccination also activates NOD2 (7), but there was no BCG vaccination in this patient. There is a report that propionibacterium acnes (*P. acnes*) had been detected on the skin specimen of a patient with BS (9), but whether *P. acnes* was involved in pulmonary lesion was unknown because staining using anti-propionibacterium acnes monoclonal antibody (PAB) was not performed on specimens of present patient. Third, Mycobacterium tuberculosis, cutibacterium acnes, metals, carbon, silicon inorganic antigens could be antigen for sarcoidosis (10), but there was no history of inhalation of these antigens in present case. Examination with polarized light to rule out foreign body was not done on specimens.

In an *ex vivo* study using pluripotent stem cells from BS patients with the *NOD2* R334W mutation, abnormal cytokine expressions in monocytes were induced by interferon-γ stimulation, and those expressions were inhibited by anti-TNF-α antibody or pan Janus kinase inhibitor, tofacitinib (11, 12). In the present case, despite the therapy with prednisolone and adalimumab, lung lesions appeared accompanied with worsening arthralgia and skin rash, but at the time of recurrence of worsening arthralgia, cough and lung lesion did not appear. MTX administration was started at the time of recurrence of arthralgia and MTX has been continued since then, and there has been no recurrence of lung lesions. It was unclear whether MTX contributed to the suppression of recurrence of pulmonary symptoms and lesions. In two previous case reports of pulmonary involvement in adolescent (16-years-old) and adult (23-years-old) BS, one case report of adult BS recommended the use of prednisolone and immunosuppressive agents (6). In another 16-years-old BS case, disease control was achieved with prednisolone 10 mg/day combined with anti-TNF-α (infiliximab) 10 mg/kg every 8 weeks (3). In that case report, biopsy of the lung lesion was not performed, but a biopsy was performed on the posterior auricular lymph node. The pathological findings demonstrated discrete non-necrotizing granulomas with a multinucleated cell, but large granulomatous complexes without inter-granulomatous sclerosis, which could be found in present case by TBLC were difficult to determine from the literature (3). In presented case, when pulmonary symptoms and granulomas appear again, it may be useful to monitor the changes in ACE and sIL-2R levels and consider the use of immunosuppressive agents if the pulmonary lesions worsen.

Unlike sarcoidosis, the spontaneous remission of BS is rare, and the syndrome eventually leads to sequelae such as blindness and joint contractures. Thus, early diagnosis are considered necessary, even in the lungs. The diagnostic rate was reported to be 37–90% for transbronchial lung biopsy (TBLB) and 80–92% for TBLC in sarcoidosis, a major disease presenting with granulomatous lesions of the lungs (13, 14). The similarities and differences between pulmonary granulomatous lesions in BS and sarcoidosis remain unresolved.

Accordingly, accumulating knowledge from pathological examination on TBLC specimens would be useful in determining the timing of therapeutic intervention for lung lesion and that can contribute to improving management for BS in the future.

Data availability statement

The original contributions presented in the study are included in the article/supplementary material, further inquiries can be directed to the corresponding author.

Ethics statement

Written informed consent was obtained from the patient for the publication of any potentially identifiable images or data included in this article.

Author contributions

YS: Writing—review and editing, Writing—original draft, Visualization, Project administration, Investigation, Formal analysis, Data curation, Conceptualization. YK: Writing—review and editing, Writing—original draft, Investigation, Data curation. AyT: Writing—review and editing, Writing—original draft, Data curation. AkT: Writing—review and editing, Writing—original draft, Methodology. KI: Investigation, Writing—review and editing, Writing—original draft, Visualization, Validation. SN: Writing—review and editing, Writing—original draft, Supervision.

Funding

The author(s) declare that no financial support was received for the research, authorship, and/or publication of this article.

Conflict of interest

The authors declare that the research was conducted in the absence of any commercial or financial relationships that could be construed as a potential conflict of interest.

The author(s) declared that they were an editorial board member of Frontiers, at the time of submission. This had no impact on the peer review process and the final decision.

Publisher's note

References

1. Blau E. Familial granulomatous arthritis, iritis, and rash. *J Pediatr*. (1985) 107:689–93. doi: 10.1016/s0022-3476(85)80394-2

2. Matsuda T, Kambe N, Ueki Y, Kanazawa N, Izawa K, Honda Y, et al. Clinical characteristics and treatment of 50 cases of Blau syndrome in Japan confirmed by genetic analysis of the *NOD2* mutation. *Ann Rheum Dis*. (2020) 79:1492–9. doi: 10.1136/annrheumdis-2020-217320

3. Becker M, Martin T, Doyle T, Rosé C. Interstitial pneumonitis in Blau syndrome with documented mutation in CARD15. *Arthritis Rheum*. (2007) 56:1292–4. doi: 10.1002/art.22509

4. Janssen C, Rose C, De Hertogh G, Martin T, Bader Meunier B, Cimaz R, et al. Morphologic and immunohistochemical characterization of granulomas in the nucleotide oligomerization domain 2-related disorders Blau syndrome and Crohn disease. *J Allergy Clin Immunol*. (2012) 129:1076–84. doi: 10.1016/j.jaci.2012.02.004

5. Japan Society of Sarcoidosis and other Granulomatous Disorders. *Guide to Sarcoidosis Clinical Practice*. (2020). Available online at. https://www.jssog.com/wp/wp-content/themes/jssog/images/system/guidance/1-3-1.pdf

6. Chauhan K, Michet C. A case of blau syndrome. *Case Rep Rheumatol*. (2014) 2014:216056. doi: 10.1155/2014/216056

7. Okafuji I, Nishikomori R, Kanazawa N, Kambe N, Fujisawa A, Yamazaki S, et al. Role of the NOD2 genotype in the clinical phenotype of Blau syndrome and early-onset sarcoidosis. *Arthritis Rheum*. (2009) 60:242–50. doi: 10.1002/art.24134

8. Wiese K, Coates B, Ridge K. The role of nucleotide-binding oligomerization domain-like receptors in pulmonary infection. *Am J Respir Cell Mol Biol*. (2017) 57(2):151–61. doi: 10.1165/rcmb.2016-0375TR

9. Okazaki F, Wakiguchi H, Korenaga Y, Nakamura T, Yasudo H, Uchi S, et al. A novel mutation in early-onset sarcoidosis/Blau syndrome: an association with Propionibacterium acnes. *Pediatr Rheumatol Online J*. (2021) 19:18. doi: 10.1186/s12969-021-00505-5

10. Chen C, Luo N, Dai F, Zhou W, Wu X, Zhang J. Advance in pathogenesis of sarcoidosis: triggers and progression. *Heliyon*. (2024) 10:e27612. doi: 10.1016/j.heliyon.2024.e27612

11. Matsuda T, Kambe N, Takimoto-Ito R, Ueki Y, Nakamizo S, Saito M, et al. Potential Benefits of TNF targeting therapy in Blau syndrome, a NOD2-associated systemic autoinflammatory granulomatosis. *Front Immunol*. (2022) 13:895765. doi: 10.3389/fimmu.2022.895765

12. Ueki Y, Takimoto-Ito R, Saito M, Tanizaki H, Kambe N. Tofacitinib, a suppressor of NOD2 expression, is a potential treatment for Blau syndrome. *Front Immunol*. (2023) 14:1211240. doi: 10.3389/fimmu.2023.1211240

13. Pedro C, Melo N, Bastos H, Magalhães A, Fernandes G, Martins N. Role of bronchoscopic techniques in the diagnosis of thoracic sarcoidosis. *J Clin Med*. (2019) 8:1327. doi: 10.3390/jcm8091327

14. Jacob M, Bastos H, Mota P, Melo N, Cunha R, Pereira J, et al. Diagnostic yield and safety of transbronchial cryobiopsy in sarcoidosis. *ERJ Open Res*. (2019) 5:00203–2019. doi: 10.1183/23120541.00203-2019

frontiers | Frontiers in Medicine

TYPE Case Report
PUBLISHED 25 September 2024
DOI 10.3389/fmed.2024.1361372

OPEN ACCESS

EDITED BY
Dawei Yang,
Fudan University, China

REVIEWED BY
Giuseppe Fiorentino,
Colli Hospital, Italy
Meng Dai,
Fourth Military Medical University, China
Habib Md Reazaul Karim,
All India Institute of Medical Sciences, Guwahati, India

*CORRESPONDENCE
Filippo Luca Fimognari
✉ filippofimognari@gmail.com

RECEIVED 25 December 2023
ACCEPTED 02 September 2024
PUBLISHED 25 September 2024

CITATION
Fimognari FL, Baffa Bellucci F, Fedele F, Scarlata S, Armentaro G and Sciacqua A (2024) Combining high-flow nasal cannula oxygen therapy with repeated toilet bronchoscopies for respiratory failure due to excessive infected airway secretions: a case report and series from a non-intensive hospital ward.
Front. Med. 11:1361372.
doi: 10.3389/fmed.2024.1361372

Combining high-flow nasal cannula oxygen therapy with repeated toilet bronchoscopies for respiratory failure due to excessive infected airway secretions: a case report and series from a non-intensive hospital ward

Filippo Luca Fimognari[1]*, Francesco Baffa Bellucci[1], Flavio Fedele[2], Simone Scarlata[3], Giuseppe Armentaro[4] and Angela Sciacqua[4,5]

[1]Unit of Geriatrics, Department of Medicine, Azienda Ospedaliera Annunziata-Mariano Santo-S. Barbara, Cosenza, Italy, [2]Unit of Bronchology, Azienda Ospedaliera Annunziata-Mariano Santo-S. Barbara, Cosenza, Italy, [3]Unit of Internal Medicine, Fondazione Policlinico Universitario Campus Biomedico, Rome, Italy, [4]Unit of Geriatrics, Azienda Ospedaliero-Universitaria Renato Dulbecco, Catanzaro, Italy, [5]Department of Medical and Surgical Sciences, University Magna Graecia, Catanzaro, Italy

Fiberoptic bronchoscopy (FBO) has diagnostic or therapeutic purposes but can cause respiratory deterioration, particularly in patients with pre-existing acute respiratory failure (ARF). Non-invasive ventilation (NIV) and high-flow nasal cannula oxygen therapy (HFNC) are used as respiratory support for ARF as well as to prevent significant oxygen deterioration during FBO. The combined use of NIV and early therapeutic FBO to clear retained abundant infected secretions from the airways may be an alternative to intubation and invasive mechanical ventilation (IMV), but no data exist on the combined use of FBO and HFNC. A 78-year-old male patient with ARF secondary to chronic obstructive pulmonary disease (COPD) exacerbation and pneumonia was admitted to our non-intensive geriatric ward. After an initial improvement, his respiratory conditions worsened. While continuing HFNC, he underwent a series of eight FBOs over 9 days, each performed in response to significant decreases in peripheral oxygen saturation (SpO_2). The goal was to remove copious and occlusive infected secretions from the airways, with each procedure resulting in good SpO_2 recovery. After etiological targeted antibiotic therapy based on bronchial aspirate, the patient improved and was discharged. Next, six consecutive similar ARF patients were treated using the same strategy of combining HFNC with repeated toilet FBO performed within the ward to clear secretions. All patients showed improvement and were discharged. The combination of HFNC and repeated toilet FBO could be a safe and effective intervention in non-intensive wards to prevent intubation and IMV in frail and elderly patients with ARF secondary to copious and occlusive infected secretions in the airways.

KEYWORDS

fiberoptic bronchoscopy, toilet fiberoptic bronchoscopy, acute respiratory failure, high-flow nasal cannula oxygen therapy, geriatric hospital ward

1 Introduction

Acute respiratory failure (ARF) is a complex syndrome diagnosed on the basis of a low level of partial pressure of oxygen (pO_2) in the arterial blood, often resulting from acute illnesses or exacerbations of chronic cardio-pulmonary disorders (1). ARF is a very frequent reason for hospital admission in older patients. In an Italian national survey including patients admitted to hospital after evaluation in the emergency department (ED), it was documented that ARF was the most frequent discharge diagnosis from hospital wards for persons aged ≥75 years (2). In a recent prospective study, ARF predicted short-term death of older patients hospitalized in medical wards after accounting for the severity of critical illness, frailty, delirium, and other confounders (3). Underlying causes that may trigger ARF in elderly patients include congestive heart failure, pneumonia, exacerbation of chronic obstructive pulmonary disease (COPD), sepsis, pulmonary embolism, acute bronchitis, and other conditions. These causes frequently occur in combination due to the patients' clinical vulnerability (1).

In addition to the prompt identification and treatment of causative illnesses, ARF management requests respiratory support to correct hypoxia and improve respiratory dynamics, such as conventional oxygen therapy (COT), non-invasive mechanical ventilation (NIV), or high-flow nasal cannula oxygen therapy (HFNC). These non-invasive respiratory treatments aim at avoiding escalation to endotracheal intubation and invasive mechanical ventilation (IMV) in the intensive care units (ICU) (4).

High-flow nasal cannula oxygen therapy (HFNC) is strongly indicated for the treatment of type 1 ARF, i.e., hypoxia without hypercapnia (5). A very high flow of heated and humidified gas mixture (oxygen and room air) is administered through soft nasal prongs. The high flow generates a continuous positive pressure in the airways (approximately 5 cmH_2O at a flow of 60 L/min with a closed patient's mouth), and a flow-dependent washout of expired gas in the dead space reduces carbon dioxide (CO_2) (4). Furthermore, due to ease of use and high tolerability, HFNC is particularly suitable for older patients hospitalized in non-intensive settings (4). In addition, it is more effective than COT in preventing adverse events (desaturation, worsening of ARF, and hemodynamic instability) that may sometimes complicate flexible fiberoptic bronchoscopy (FBO) performed for diagnostic or therapeutic purposes (6, 7).

In case of failure of non-invasive respiratory supports, the clinical decision to subject frail elderly patients to IMV may be controversial due to difficulties in predicting prognosis, limited availability of beds in ICUs, and concerns regarding intubation-related complications (1). Thus, combined non-invasive therapeutic strategies should be developed within non-intensive hospital settings to prevent IMV in severe older ARF patients without compromising clinical outcomes (8). For instance, NIV associated with early therapeutic FBO for removing copious occlusive secretions in the airways was found to be a valid alternative to IMV (9).

In this case report and subsequent case series, we describe a strategy combining HFNC with repeated therapeutic FBO, which successfully prevented intubation in ARF secondary to copious infected secretions in the airways.

2 Case report and case series

A 78-year-old man presented to the ED because of acute-onset (less than 1 day) worsening of dyspnea and severe ARF on 14 September 2022. The patient's chronic diseases included type 2 diabetes mellitus (metformin 500 mg *bis in die*), chronic atrial fibrillation (rivaroxaban 20 mg per day and digoxin 0.125 mg per day), COPD (inhaled fluticasone furoate/vilanterol 92/22 µg plus inhaled umeclidinium bromide 55 µg, both once per day), and hypertension (amlodipine 5 mg and enalapril 10 mg). His baseline functional status, before the acute worsening, was normal. On admission to our ward, the patient was afebrile and tachypneic (approximately 22 breaths per minute). Peripheral oxygen saturation (SpO_2) was 82% with a fraction of inspired oxygen (FiO_2) of 50%, and arterial blood analysis (ABG) showed type 1 ARF. His heart rate was 135 beats per minute and his blood pressure was 140/70 mmHg. His mental status was normal, vesicular breath sounds were diminished, and a right-sided hemiparesis, mostly involving the upper extremity, was detected. N-terminal pro-brain natriuretic peptide (NT-proBNP) and troponin measurements showed values of 11.296 pg./mL and 5.6 ng/mL, respectively.

Based on chest X-rays (bilateral hilar interstitial and alveolar edema) and head computed tomography (CT, pre-Rolandic left ischemic stroke) previously performed in the ED, an initial diagnosis of ARF secondary to acute congestive heart failure, COPD exacerbation, and possible pneumonia, associated with a left ischemic stroke, was made. NIV support was continued (face mask, bi-level pressure support with expiratory pressure of 6 cmH_2O, inspiratory pressure of 16 cmH_2O, and 10 L/min of oxygen flow), but the patient's respiratory conditions worsened, and he was transferred to the ICU after only 5 h of stay in our ward. In the ICU, NIV was replaced by HFNC (60 L/min, FiO_2 60%, and temperature 34°C), and empiric intravenous (IV) piperacillin/tazobactam 4.5 g three times daily was continued. Following overall and respiratory improvement, he was shifted back to our ward 2 days later. Here, clinical improvement continued, and HFNC was replaced by low-flow COT on day 5 of hospital admission. In the subsequent days, he suffered repeated episodes of rectorrhagia with post-hemorrhagic anemia. A contrast-enhanced total-body CT performed on day 11 showed pneumonia (consolidation) in the left lower lobe and, to a lesser extent, in the lateral and posterior segments of the right lower lobe. Piperacillin/tazobactam was stopped, and an empiric antibiotic therapy of IV meropenem 1 g three times per day plus tigecycline 50 mg (after loading dose of 100 mg) twice per day was started. The same CT also highlighted sigmoid wall thickening, suggestive of cancer.

TABLE 1 Sequence of FBO and oxygenation values before and after each procedure.

	Before FBO			After FBO			
Day of FBO	SpO_2	FiO_2	SpO_2/FiO_2	SpO_2	FiO_2	SpO_2/FiO_2	Notes
13	92	88	1.04	98	74	1.32	
14	88	80	1.1	95	50	1.9	
15	92	91	1.01	99	75	1.32	
17	88	75	1.17	97	70	1.38	
18	78	80	0.97	96	80	1.20	
19	84	85	0.98	96	80	1.17	Removal of mucus plug in the right inferior lobar bronchus.
19	83	80	1.03	98	67	1.46	Removal of mucus plug in the right inferior lobar bronchus.
22	93	60	1.55	98	60	1.63	

FBO, fiberoptic bronchoscopy; SpO_2, peripheral oxygen saturation by pulse oximetry; FiO_2, fraction of inspired oxygen. Day of FBO is the day during hospital stay on which FBO was performed (the day of admission to the ward from the emergency department is day 0).

On day 12, his respiratory status seriously worsened (tachypnea and decreased SpO_2/FiO_2 ratio), and HFNC (FiO_2 60%, 50 L/min) was reintroduced. The day after (day 13), because of further worsened respiratory status, a CT was repeated, which displayed worsening multifocal pneumonia, with increased involvement of the right lower lobe, extension to the middle lobe, and mucoid obstruction of the right lower lobe bronchus. On the same day, he underwent toilet FBO (performed in the bronchoscopy laboratory while continuing HFNC) that removed abundant retained secretions from the airways of both lungs. After this first FBO, the SpO_2/FiO_2 ratio immediately increased (Table 1). Rapid polymerase chain reaction testing of the bronchial samples detected *Acinetobacter baumannii* positive for extended-spectrum beta-lactamase (ESBL) and *Klebsiella pneumoniae* carbapenemase (KPC) producing, with results later confirmed by culture. Meropenem and tigecycline were interrupted. Based on antibiotic sensitivity tests, a treatment of IV ceftazidime/avibactam 2.5 g three times per day, IV colistin 4.5 million International Units (IU) twice per day (after 9 million loading dose), and aerosolized colistin (1 million IU with saline three times per day) was started.

In the following days, however, frequent measurements of the SpO_2/FiO_2 ratio identified further episodes of respiratory deterioration due to the accumulation of infected secretions in the airways of both lungs, mainly in the right inferior lobar bronchus. In each of such respiratory deteriorations, FBO was immediately performed during HFNC and always obtained significant recovery of acceptable arterial oxygenation parameters by clearing secretions in the airways (Table 1). On two occasions, a plug in the right inferior lobar bronchus was removed by FBO (Table 1). Overall, he was submitted to eight FBOs during 9 days, and, except for the first, FBO was always performed at the patient's bedside. Afterward, the patient's clinical, laboratory, and respiratory conditions improved; he was switched to COT and discharged after 20 days of targeted etiological antibiotic therapy and a 35-day hospital stay. He subsequently underwent surgery for colon cancer.

After this clinical experience, the non-invasive strategy combining HFNC treatment with repeated FBO—performed in response to episodes of oxygen desaturation with the aim of removing abundant infected occlusive secretions from the airways—was applied in our ward to the other six consecutive patients already in treatment with HFNC for severe ARF (Table 2). In all cases, FBO was performed to treat episodes of oxygen desaturation that were refractory to increases in flow and FiO_2 up to 60 L/min and 80%, respectively. FBO was undertaken within the ward at the patient's bedside by experienced pulmonologists inserting the flexible bronchoscope through one nostril after removing the ipsilateral soft nasal HFNC prong. During the procedure, HFNC was continued through the other nostril, and flow and FiO_2 were adjusted in order to maintain a SpO_2 value of ≥93%. Bronchial aspirates were sent to the microbiology laboratory for etiological determinations. Complications related to the procedure were never observed, and all patients were discharged alive after clinical improvement (Table 2). The patients, or their proxies for those with severe cognitive impairment, signed an informed consent to undergo FBO.

3 Discussion

FBO has diagnostic and therapeutic purposes, such as removing abundant and infected secretions occluding the airways (8). On the other hand, since FBO can cause acute dynamic narrowing of the airways with worsening hypoxia and secondary cardiovascular distress, concerns exist regarding its use and safety in patients with severe ARF, in whom many clinicians would not undertake FBO without intubation and IMV (10). However, in our patient with severe ARF, recurrent episodes of desaturation were successfully managed without intubation, removing infected secretions by means of repeated FBO. This strategy also allowed the microbiological identification in the cleared secretions of bacteria responsible for the multifocal pneumonia and COPD exacerbation and the subsequent choice of a targeted etiological antibiotic therapy. Even though a community-onset exacerbated COPD was one of the reasons for initial hospital

TABLE 2 Case series of patients submitted to HFNC for severe respiratory failure combined with repeated therapeutic (removal of infected secretions) and diagnostic (bronchial aspirate) FBO.

Age (years)	Sex	Diagnosis	Number of FBO (days of FBO)	Outcome	Isolated pathogen(s) (bronchial aspirate)	Comorbidities	Mean SpO_2 before FBO*	Mean SpO_2 after FBO*
79	M	Aspiration pneumonia	9 (4, 5, 7, 8, 11, 13, 15, 16, and 17)	Hospice	Respiratory syncytial virus, *Candida albicans*, and *Candida glabrata*.	HHF, AKI, and vascular dementia.	89	94.3
87	M	AB	3 (3, 4, and 6)	Nursing home	*Candida glabrata*.	PD with dementia and obesity.	88.6	93.3
96	F	AB	2 (3, 4)	Home	Nothing.	AF, BRS, and carotid atherosclerotic disease.	92	98
65	F	Exacerbated COPD	2 (1, 2)	Rehabilitation facility	*Acinetobacter baumannii*.	HHF and BRS secondary to previous stroke.	84	96.5
84	M	AB	3 (6, 21, 23)	Rehabilitation facility	*Candida glabrata*, Influenza A, and *Aspergillus*.	AF, decompensated valvular heart disease, BRS, and type 2 DM.	86.3	93.4
74	M	Pneumonia	2 (8, 12)	Hospice	*Pseudomonas Aeruginosa*.	Metastatic lung cancer, PE, and BRS.	88.5	95

HFNC, high-flow nasal cannula oxygen therapy; FBO, fiberoptic bronchoscopy; SpO_2, peripheral oxygen saturation by pulse oximetry; M, male; F, female; HHF, hypertensive heart failure; AKI, acute kidney injury; AB, acute bronchitis; PD, Parkinson's disease; AF, atrial fibrillation; BRS, bed rest syndrome; COPD, chronic obstructive pulmonary disease; DM, diabetes mellitus, PE, pulmonary embolism. Days of FBO are the days of hospital stay on which FBO was performed (the day of admission to the ward from the emergency department is day 0). *Means of values recorded before and after each FBO.

admission, the following hospital stay was presumably complicated by the development of hospital-acquired pneumonia and severe bronchial infection caused by antibiotic-resistant bacteria (*Acinetobacter Baumannii* and *Klebsiella Pneumoniae*).

COT administered through nasal cannula is used during FBO to counteract the risk of respiratory complications related to the procedure, but it may be insufficient to prevent the worsening of hypoxia and hypercapnia in older patients with comorbidities and severe ARF (11). Because this category of individuals is growing worldwide due to population aging, an increasing number of patients is expected to be excluded from FBO and conclusive diagnosis, owing to safety concerns, particularly in those with pO_2/FiO_2 below 100 (12). In addition, such critical patients are often hospitalized in non-intensive wards, and FBO could cause further respiratory compromise that could require unintended intubation and ICU transfer (13).

NIV performed during FBO has been extensively studied as a method capable of preventing such FBO-related respiratory derangement (14). HFNC has also been demonstrated to maintain adequate oxygenation levels better than COT (6, 7) and to avoid the loss of end-expiratory lung volume (6) during diagnostic FBO. NIV seems to be superior to HFNC in preventing oxygenation deterioration during FBO in patients with moderate-to-severe ARF (15, 16), particularly when heart failure contributes to ARF and the application of a positive airway pressure is necessary to determine an adequate positive intrathoracic pressure that cannot be assured by HFNC (10). It is unknown, however, whether the benefit-to-risk ratio of FBO, "assisted" by NIV or HFNC, in patients with ARF may increase when an oxygenation improvement is expected as a therapeutic result of the procedure *per se*, for instance when there is the need to remove mucus plugs and infected secretions from the airways (8). Furthermore, comparative studies of NIV and HFNC are lacking in this specific subgroup of patients who require a "therapeutic" FBO for unclogging the airways.

Indeed, a therapeutic combination of NIV and therapeutic FBO may be effective in COPD patients with abundant obstructive secretions (9, 17). In a case–control study, Scala et al. showed that a strategy based on the combination of early FBO for clearing secretions from the airways and NIV was comparable to a strategy based on FBO after IMV in terms of oxygenation values, hospital mortality, duration of hospitalization, and ventilation (9). In a prospective cohort study, NIV combined with a non-invasive strategy to aspirate and clear secretions from the trachea in the first 2 h was at least as effective as IMV and was also associated with lower hospital mortality (17). These combined strategies aim at avoiding intubation and IMV but can be applied only in expert units, not being within the reach of non-intensive medical hospital settings (8). With this regard, our clinical experience seems to be the first ever reported on the combined use of HFNC and repeated toilet FBO in patients with severe ARF sustained by abundant retained bronchial secretions in a non-intensive setting (8). FBO is easier to perform and better tolerated if "assisted" by HFNC compared to NIV, particularly in frail and uncooperative patients hospitalized in non-intensive medical wards (8, 18). HFNC assures several beneficial physiological effects: flow-dependent washout of expired gas in the dead space (reducing CO_2), generation of a flow-dependent continuous positive pressure in the airways with alveolar recruitment, improved mucociliary clearance by the heated and humidified gas, adequate matching between ventilation and the patient's inspiratory effort, reduction of airway resistance that could balance the increase that is possibly caused by FBO (4, 10), and augmented end-respiratory lung volume reflecting alveolar recruitment (6). In addition, the fact that, unlike NIV, HFNC can be provided continuously without interruptions—before, during, and after the procedure—could theoretically emphasize the synergy with FBO (4, 8).

In our patients, the removal of secretions from the airways—together with the above-mentioned physiological effects of HFNC—may have accounted for the increased oxygenation obtained after each toilet FBO

performed for episodes of significant oxygen desaturation. The peculiarities of these observations are the high number (up to 9) of FBO, the fact that such procedures were performed within the non-intensive ward, and that no procedure-related complications were reported. Furthermore, although our elderly patients were frail and burdened with significant comorbidities, intubation and ICU transfer were avoided, and they all were discharged alive. Another not negligible aspect is the diagnostic value of repeated FBO, which provided occasions to identify in the bronchial aspirate the pathogen(s) responsible for the acute respiratory infection.

This study has limitations. Since this is a real-life clinical observation, no firm conclusion can be drawn, and the combination of HFNC/repeated toilet FBO needs to be tested in a randomized controlled trial to verify whether it may really be superior to other strategies, mostly intubation and IMV, in improving outcomes of frail patients with severe ARF due to abundant retained infected secretions in the airways. We did not measure cough peak flow and did not use a mechanically assisted cough device that would have reduced the need for endoscopic toilets. In our busy hospital setting, arterial oxygenation trajectories were carefully and non-invasively tracked by SpO_2 /FiO_2 rather than obtaining a comparable number of partial pressure of oxygen (PaO_2) measurements by arterial blood analysis. In addition, ROX or modified ROX indexes (19), both incorporating high respiratory rate and poor arterial oxygenation values (SpO_2 /FiO_2 or PaO_2 /FiO_2, respectively) for the prediction of HFNC failure, were not routinely used to capture the need for therapeutic FBO as an alternative to intubation. It should be mentioned, however, that the reported post-FBO improvements in SpO_2 /FiO_2 inevitably resulted in an increase of ROX/modified ROX indexes, and poor arterial oxygenation was found to be a better predictor of failure than a high respiratory rate in patients supported with non-invasive oxygenation strategies (20).

In conclusion, the combination of continuous HFNC treatment and repeated therapeutic FBO could be a safe and effective intervention to apply in non-intensive wards for preventing ICU transfer of older and frail patients with ARF secondary to obstructive infected secretions in the airways.

Data availability statement

The raw data supporting the conclusions of this article will be made available by the authors, without undue reservation.

Ethics statement

The requirement of ethical approval was waived because of the retrospective observational nature of the study. The study was conducted in accordance with local legislation and institutional requirements. The participants (or their close relatives) provided written informed consents, contained in the medical record, to participate in this study, as well as for the publication of any potentially identifiable data.

Author contributions

FFi: Conceptualization, Data curation, Formal analysis, Writing – original draft, Writing – review & editing. FBB: Data curation, Writing – review & editing. FFe: Methodology, Supervision, Writing – review & editing. SS: Supervision, Validation, Writing – review & editing. GA: Data curation, Writing – review & editing. AS: Supervision, Validation, Writing – review & editing.

Funding

The author(s) declare that no financial support was received for the research, authorship, and/or publication of this article.

Conflict of interest

The authors declare that the research was conducted in the absence of any commercial or financial relationships that could be construed as a potential conflict of interest.

Publisher's note

References

1. Ray P, Birolleau S, Lefort Y, Becquemin MH, Beigelman C, Isnard R, et al. Acute respiratory failure in the elderly: etiology, emergency diagnosis and prognosis. *Crit Care*. (2006) 10:R82. doi: 10.1186/cc4926

2. Fimognari FL, Lelli D, Landi F, Antonelli Incalzi R. Association of age with emergency department visits and hospital admissions: a nationwide study. *Geriatr Gerontol Int*. (2022) 22:917–23. doi: 10.1111/ggi.14481

3. Fimognari FL, Tassistro E, Rossi E, Bambara V, Valsecchi MG, Cherubini A, et al. The interplay among respiratory failure, delirium, frailty and severity of illness in hospitalized older medical patients: a nationwide multicenter observational study. *J Frailty Aging*. (2024) (In press). doi: 10.14283/jfa.2024.12

4. Frat JP, Le Pape S, Coudroy R, Thille AW. Noninvasive oxygenation in patients with acute respiratory failure: current perspectives. *Int J Gen Med*. (2022) 15:3121–32. doi: 10.2147/IJGM.S294906

5. Oczkowski S, Ergan B, Bos L, Chatwin M, Ferrer M, Gregoretti C, et al. ERS clinical practice guidelines: high-flow nasal cannula in acute respiratory failure. *Eur Respir J*. (2022) 59:2101574. doi: 10.1183/13993003.01574-2021

6. Longhini F, Pelaia C, Garofalo E, Bruni A, Placida R, Iaquinta C, et al. High-flow nasal cannula oxygen therapy for outpatients undergoing flexible bronchoscopy: a randomised controlled trial. *Thorax*. (2022) 77:58–64. doi: 10.1136/thoraxjnl-2021-217116

7. Arias-Sanchez PP, Ledesma G, Cobos J, Tirape H, Jaramillo B, Ruiz J, et al. Changes in oxygen saturation during Fiberoptic bronchoscopy: high-flow nasal cannula versus standard oxygen therapy. *Respir Care*. (2023) 68:727–33. doi: 10.4187/respcare.10598

8. Scala R, Guidelli L. Clinical value of bronchoscopy in acute respiratory failure. *Diagnostics*. (2021) 11:1755. doi: 10.3390/diagnostics11101755

9. Scala R, Naldi M, Maccari U. Early fiberoptic bronchoscopy during non-invasive ventilation in patients with decompensated chronic obstructive pulmonary disease due to community-acquired-pneumonia. *Crit Care*. (2010) 14:R80. doi: 10.1186/cc8993

10. Longhini F, Bruni A, Saraco G, Garofalo E, Conti G. Should high-flow through nasal cannula be used during bronchoscopy in critically ill patients with hypoxemic acute respiratory failure? *J Anesth Analg Crit Care*. (2021) 1:4. doi: 10.1186/s44158-021-00001-y

11. Choi JS, Lee EH, Lee SH, Leem AY, Chung KS, Kim SY, et al. Risk factors for predicting hypoxia in adult patients undergoing bronchoscopy under sedation. *Tuberc Respir Dis*. (2020) 83:276–82. doi: 10.4046/trd.2020.0002

12. Oraczewska A, Cofta S, Warcholiński A, Trejnowska E, Brożek G, Swinarew A, et al. The use of non-invasive respiratory assistance to facilitate bronchofiberoscopy performance in patients with hypoxemic (type one) respiratory failure - study protocol. *Adv Med Sci*. (2023) 68:474–81. doi: 10.1016/j.advms.2023.10.011

13. Kamel T, Helms J, Janssen-Langenstein R, Kouatchet A, Guillon A, Bourenne J, et al. Clinical research in intensive care Sepsis group (CRICS-TRIGGERSEP). Benefit-to-risk balance of bronchoalveolar lavage in the critically ill. A prospective, multicenter cohort study. *Intensive Care Med*. (2020) 46:463–74. doi: 10.1007/s00134-019-05896-4

14. Esquinas A, Zuil M, Scala R, Chiner E. Bronchoscopy during non-invasive mechanical ventilation: a review of techniques and procedures. *Arch Bronconeumol*. (2013) 49:105–12. doi: 10.1016/j.arbres.2012.05.008

15. Simon M, Braune S, Frings D, Wiontzek AK, Klose H, Kluge S. High-flow nasal cannula oxygen versus non-invasive ventilation in patients with acute hypoxaemic respiratory failure undergoing flexible bronchoscopy--a prospective randomised trial. *Crit Care*. (2014) 18:712. doi: 10.1186/s13054-014-0712-9

16. Saksitthichok B, Petnak T, So-Ngern A, Boonsarngsuk V. A prospective randomized comparative study of high-flow nasal cannula oxygen and non-invasive ventilation in hypoxemic patients undergoing diagnostic flexible bronchoscopy. *J Thorac Dis*. (2019) 11:1929–39. doi: 10.21037/jtd.2019.05.02

17. Wang J, Cui Z, Liu S, Gao X, Gao P, Shi Y, et al. Early use of noninvasive techniques for clearing respiratory secretions during noninvasive positive-pressure ventilation in patients with acute exacerbation of chronic obstructive pulmonary disease and hypercapnic encephalopathy: a prospective cohort study. *Medicine (Baltimore)*. (2017) 96:e6371. doi: 10.1097/MD.0000000000006371

18. Fimognari FL, Rizzo M, Cuccurullo O, Cristiano G, Ricchio R, Ricci C, et al. High-flow nasal cannula oxygen therapy for acute respiratory failure in a non-intensive geriatric setting. *Geriatr Gerontol Int*. (2018) 18:1652–3. doi: 10.1111/ggi.13557

19. Karim HMR, Esquinas AM. Success or failure of high-flow nasal oxygen therapy: the ROX index is good, but a modified ROX index may be better. *Am J Respir Crit Care Med*. (2019) 200:116–7. doi: 10.1164/rccm.201902-0419LE

20. Frat JP, Ragot S, Coudroy R, Constantin JM, Girault C, Prat G, et al. REVA network. Predictors of intubation in patients with acute hypoxemic respiratory failure treated with a noninvasive oxygenation strategy. *Crit Care Med*. (2018) 46:208–15. doi: 10.1097/CCM.0000000000002818

Frontiers in Medicine

Translating medical research and innovation into improved patient care

A multidisciplinary journal which advances our medical knowledge. It supports the translation of scientific advances into new therapies and diagnostic tools that will improve patient care.

Discover the latest Research Topics

See more →

Frontiers

Avenue du Tribunal-Fédéral 34
1005 Lausanne, Switzerland
frontiersin.org

Contact us

+41 (0)21 510 17 00
frontiersin.org/about/contact